ISSN 1997-1389 (Print)
ISSN 2313-5530 (Online)

Журнал Сибирского федерального университета

Биология

Journal of Siberian Federal University

Biology

2021 14 (4)

ISSN 1997-1389 (Print)
ISSN 2313-5530 (Online)

Журнал Сибирского федерального университета Биология

2021 14(4)

Journal of Siberian Federal University Biology

Издание индексируется Scopus (Elsevier), «Russian Science Citation Index» и «Zoological Record» на платформе «Web of Science» (Clarivate Analytics), Российским индексом научного цитирования (НЭБ), представлено в международных и российских информационных базах: Ulrich's periodicals directiory, ProQuest, EBSCO (США), Google Scholar, Centre for Agriculture and Biosciences International (CABI), DOAJ, КиберЛенинка.
Включено в список Высшей аттестационной комиссии «Рецензируемые научные издания, входящие в международные реферативные базы данных и системы цитирования».

Журнал Сибирского федерального университета. Биология.
Journal of Siberian Federal University. Biology.

Учредитель: Федеральное государственное автономное образовательное учреждение высшего образования «Сибирский федеральный университет» (СФУ)

Главный редактор: *Е.С.Кравчук*. Редактор *И.А.Вейсиг*. Корректор *С.В.Хазаржан*. Компьютерная верстка *Е.В. Гревцовой*

№ 4. 30.12.2021. Индекс: 42325. Тираж: 1000 экз.

Свободная цена

Адрес редакции и издательства: 660041 г. Красноярск, пр. Свободный, 79, оф. 32-03.

Отпечатано в типографии Издательства БИК СФУ
660041 г. Красноярск, пр. Свободный, 82а.

Свидетельство о регистрации СМИ ПИ № ФС 77-28725 от 29.06.2007 г., выданное Федеральной службой по надзору в сфере массовых коммуникаций, связи и охраны культурного наследия.

http://journal.sfu-kras.ru

Подписано в печать 15.12.2021. Формат 84x108/16. Усл. печ. л. 13,6.
Уч.-изд. л. 13,1. Бумага тип. Печать офсетная. Тираж 1000 экз. Заказ № 15452.

Возрастная маркировка в соответствии с Федеральным законом № 436-ФЗ: 16+

CONTENTS

СОДЕРЖАНИЕ

Preface to the Special Issue

Special Issue of the «Journal of the Siberian Federal University. Biology» is devoted to the currently important and principal areas of biotechnology, biomedicine, and bioecology with an emphasis on the characteristics and role of new biomaterials and composites of «green» chemistry, which are of major interest and contribute to the development of the sustainable economy. As the population of the planet is growing, the production and consumption of chemicals, primarily synthetic plastics and xenobiotics, is increasing on an ever-larger scale. The pollution of the planet destroys the self-regulation mechanisms of the biosphere, leading to unpredictable consequences. To maintain the stability of the biosphere, it is necessary to switch to new forms of management, including new materials, drugs, and technologies for their use. Biotechnology has enormous potential, capable of satisfying all human needs without negatively affecting the environment.

The articles included in this special issue are based on the presentations of the participants the IV International Scientific Conference «Biotechnology of New Materials – Environment – Quality of Life» and the School for Young Scientists, which were held at the School of Fundamental Biology and Biotechnology of the Siberian Federal University (Krasnoyarsk) in October 2021.

Dr. Prof. Sabu Thomas
Symposium Co-Chair,
Vice Chancellor of Mahatma Gandhi University (India)
Head of the Laboratory for Innovative Preparations and Materials,
Siberian Federal University (Russia)

Dr. Prof. T. G. Volova
Special Editor
Head of Biotechnology Chair, Siberian Federal University (Russia)

Journal of Siberian Federal University. Biology 2021 14(4): 398–421
~ ~ ~

DOI 10.17516/1997-1389-0361

УДК 577.11:612.06

Biopolymers as Multiplatform Materials to Improve Quality of Life and Well-Being

Fernando Gomes de Souza Jr[a]*, Sergio Thode Filho[a, b], Emiliane Daher[a], Fernanda Diva[a], Nathali Ricardo[a], Rafael Moraes[a], Marcio Nogueira[a], Johny Chantre[a] and Priscila Soares[a]

[a]*Federal University of Rio de Janeiro*
Rio de Janeiro, Brazil
[b]*Federal Institute of Education, Science and Technology of Rio de Janeiro*
Rio de Janeiro, Brazil

Received 16.06.2021, received in revised form 20.07.2021, accepted 14.08.2021

Abstract. Biopolymers are all the macromolecular materials formed in nature or produced using biomonomers. Biopolymers are extremely diverse materials, which have unique properties. Unfortunately, the general cost of biopolymers production is about 25 % higher compared to similar materials from petrochemical sources. Therefore, scientists must continuously pursue the search for differentiated applications for these materials. These new applications, especially those with enhanced added value, are essential for extending the use of these unique materials. In this context, the Biopolymers & Sensors Lab. (LaBioS) of the Federal University of Rio de Janeiro has been operating since 2008 in research related to the production of biopolymers. LaBioS works on the chemical modification and the nanomodification of these biopolymers. These were the strategies found by the group to increase the added value of these systems, allowing their use in several applications that positively impact human well-being. Therefore, we dedicate this work to describing the state of the art in biopolymers via text mining study of the content produced on this great subject from the year 2008 to the year 2021. In addition, we present here short case studies developed by the team that currently composes LaBioS. These cases cover several areas, ranging from drug release, through environmental recovery, to food security.

* Corresponding author E-mail address: fernando_gomes@ima.ufrj.br
ORCID: 0000-0002-8332-4953 (Souza F.G. Jr.); 0000-0001-6669-2677 (Thode Filho S.); 0000-0002-4857-9512 (Daher E.); 0000-0003-2960-9197 (Diva F.); 0000-0002-1553-9469 (Ricardo N.); 0000-0003-3476-4511 (Moraes R.); 0000-0003-4762-2395 (Nogueira M.); 0000-0002-9727-714X (Chantre J.); 0000-0001-8923-6834 (Soares P.)

Keywords: data analysis, statistical analysis, data mining, biopolymers.

Acknowledgements. This work was supported by Conselho Nacional de Desenvolvimento Científico e Tecnológico (CNPq-304500/2019–4), Coordenação de Aperfeiçoamento de Pessoal de Nível Superior (CAPES – Finance Code 001), Financiadora de Estudos e Projetos (FINEP PRESAL Ref.1889/10) and Fundação Carlos Chagas Filho de Amparo à Pesquisa do Estado do Rio de Janeiro (FAPERJ – CNE2020).

Citation: Souza F.G. Jr., Thode Filho S., Daher E., Diva F., Ricardo N., Moraes R., Nogueira M., Chantre J., Soares P. Biopolymers as multiplatform materials to improve quality of life and well-being. J. Sib. Fed. Univ. Biol., 2021, 14(4), 398–421. DOI: 10.17516/1997-1389-0361

Биополимеры как многоплатформенные материалы для улучшения качества жизни и благополучия населения

Ф. Г. де Соуза мл.[а], С. Т. Филью[а, б], Э. Дахер[а], Ф. Дива[а], Н. Рикардо[а], Р. Мораес[а], М. Ногейра[а], Дж. Шантр[а], П. Соарес[а]

[а] Федеральный университет Рио-де-Жанейро Бразилия, Рио-де-Жанейро

[б] Федеральный институт образования, науки и технологий Рио-де-Жанейро Бразилия, Рио-де-Жанейро

Аннотация. Биополимеры – это природные или созданные искусственно с использованием биомономеров макромолекулярные материалы. Биополимерные материалы чрезвычайно разнообразны и обладают уникальными свойствами. К сожалению, общая стоимость производства биополимеров примерно на 25 % выше стоимости аналогичных материалов из нефтехимических источников. Поэтому ученые должны постоянно продолжать поиск различных вариантов применения биополимерных материалов. Эти новые области применения, особенно позволяющие получить продукцию с более высокой добавленной стоимостью, необходимы для более широкого распространения данных уникальных материалов. В этом контексте лаборатория биополимеров и сенсоров (LaBioS) Федерального университета Рио-де-Жанейро с 2008 г. занимается исследованиями, связанными с производством биополимеров. Сотрудники LaBioS работают над химической модификацией и наномодификацией биополимеров. Эта стратегия, применяемая данной группой исследователей для увеличения добавленной стоимости полимерных продуктов, позволяет использовать их в ряде областей, способствующих повышению благополучия населения. Данная статья посвящена описанию современного состояния исследований в области биополимеров, основанному

на интеллектуальном анализе текстов статей, опубликованных по этой важной теме в период с 2008 по 2021 г. Мы представляем также краткую информацию о результатах исследований группы ученых, в настоящее время работающих в LaBioS, которые охватывают несколько областей – от получения лекарственных средств и технологий восстановления окружающей среды до обеспечения продовольственной безопасности.

Ключевые слова: анализ данных, статистический анализ, интеллектуальный анализ данных, биополимеры.

Благодарности. Эта работа была поддержана Национальным советом по техническому и технологическому развитию (G-304500/2019–4), Координатором квалификационных работ в Пессоаль–де-Нивель-Супериор (M - Финансовый код 001), Отделом финансов и проектов (ПРЕДВАРИТЕЛЬНАЯ заявка FINEP.1889/10) и Фондом Карлоса Шагаса Фильо де Ампаро Пескиса в Рио-де-Жанейро (FAPERJ-CNE2020).

Цитирование: де Соуза мл. Ф.Г. Биополимеры как многоплатформенные материалы для улучшения качества жизни и благополучия населения / Ф. Г. де Соуза мл., С.Т. Филью, Э. Дахер, Ф. Дива, Н. Рикардо, Р. Мораес, М. Ногейра, Дж. Шантр, П. Соарес // Журн. Сиб. федер. ун-та. Биология, 2021. 14(4). С. 398–421. DOI: 10.17516/1997-1389-0361

Introduction

Polymers are materials that are widespread in our society (Souza et al., 2008). Due to their versatility, they increasingly replace traditional materials, such as metals and ceramics, in various applications (Ferreira et al., 2017; Grance et al., 2016). It is easy to identify a myriad of polymeric artifacts that surround us, leading to the realization that polymers will be increasingly present in every aspect of our lives, from our birth to our last moments on this planet. However, a side effect generated by polymers on a large scale is the immense amount of waste produced (Maranhão et al., 2018), whose persistence time in the environment, given the exceptional chemical stability of the polymers, is in the order of hundreds of years. In addition, obtaining conventional polymers is a polluting activity since most conventional monomers are obtained from a petrochemical source (Marques et al., 2016) via fractional distillation of oil. Thus, the use of materials from renewable sources should be increasingly encouraged (Marinho et al., 2018). These materials have the potential to maintain our lifestyle, but with an infinitely less environmental impact than what we currently produce.

Biopolymers (Péres et al., 2017) are polymers produced by living organisms or obtained from renewable sources (Buono et al., 2018; Fertahi et al., 2021; Jensen et al., 2016; Kanehashi et al., 2015; Khan et al., 2016; Roguszewska et al., 2020; Sotoudeh et al., 2021; Techawinyutham et al., 2019; Zubkiewicz et al., 2021). Among them, the ones commercially called «green polymers» are synthetic polymers obtained using monomers from renewable sources (Costa et al., 2017). This class of polymers allows the production of new artifact products that are highly beneficial to nature because they are biodegradable or, when they are not, because they can store carbon from CO_2 in the form of macrostructures of biological origin.

Despite the numerous advantages presented by biopolymers, the cost factor is still an

impediment to the large-scale use of these materials. In recent years, the emergence and improvement of several biotechnological routes have allowed the increasingly competitive production of several biopolymers, such as polyhydroxyalkanoates (PHAs) and many monomers, such as lactic, glycolic, and succinic acids, as well as the 1,4-butanediol (Satam et al., 2019). These new processes and the derived chemical species have significantly increased the availability of biopolymers for the most diverse markets, including the automotive, textile, and packaging sectors for quick disposal items (Babu et al., 2013). Increasing the value added by these materials must be a constant concern for the entire scientific community. In this context, the Biopolymers and Sensors Laboratory (LaBioS) of the Federal University of Rio de Janeiro has been seeking, since 2008, to boost the use of biopolymers by modifying their properties by chemical modification or by preparing nanocomposites.

The extension of the use of these materials in each of these areas is a driver for increasing the quality of life of human beings, helping to preserve our planet, and this is our research group's ultimate mission. Thus, this work provides an overview of the scientific work in biopolymers from 2008 to 2021. This information was collected at the Scopus base and mined using various free and open-source tools. In addition, this paper briefly presents some studies developed by the team that currently runs the LaBioS. Besides, the retrieved information allows us to foresee the perspectives referring to biopolymers in the near future.

Text mining methodology

Scientific articles containing the word biopolymer in the titles or abstracts were collected using the Scopus database. The Scopus search was restricted to the broad term biopolymer only among the articles published between 2008 and 2021. The used search key was: *TITLE-ABS-KEY (Biopolymer) AND (LIMIT-TO (DOCTYPE,»ar»)) AND (LIMIT-TO (PUBYEAR,2020) OR LIMIT-TO (PUBYEAR,2019) OR LIMIT-TO (PUBYEAR,2018) OR LIMIT-TO (PUBYEAR,2017) OR LIMIT-TO (PUBYEAR,2016) OR LIMIT-TO (PUBYEAR,2015) OR LIMIT-TO (PUBYEAR,2014) OR LIMIT-TO (PUBYEAR,2013) OR LIMIT-TO (PUBYEAR,2012) OR LIMIT-TO (PUBYEAR,2011) OR LIMIT-TO (PUBYEAR,2010) OR LIMIT-TO (PUBYEAR,2009) OR LIMIT-TO (PUBYEAR,2008))*. The results were gathered using Zotero 5.0.95 and finally saved in a single RIS file. The data of these articles were separated into (i) titles and (ii) abstracts. The tools were LibreOffice Calc and LibreOffice Writer (both version: 7.0.4.2 Build ID: dcf040e67528d9187c66b2379df5ea4407429775). The online Voyant Tools (Hetenyi et al., 2019; Miller, 2018) (https://voyant-tools.org/) was used in the text mining of the most relevant words in the texts, which were cleaned by removing all the numbers and editors' names from them. Then, the set conditions in the Voyant Tools were (a) Fixed term *biopolymer* and (b) minimum coverage of 5 %. The second Text Mining tool used was the VOSviewer (van Eck & Waltman, 2010) (https://www.vosviewer.com/), which allows obtaining the main clusters from the titles and abstracts. The last cleaning step is unnecessary for the VOSviewer analysis, and the raw RIS file was used as produced by Zotero. The set conditions used in VOSviewer were: (a) Create a map based on text data, (b) Read data from reference manage files (RIS), Fields from which terms will be extracted ((c) Title and abstracts separately and (d) ignore structures abstracts labels and (e) ignore copyright statements both turned on). The counting method was set to Binary (f). To the titles and abstracts, the minimum numbers of occurrences (g) were set to 50 and 500, respectively.

Results of text mining

The data mining variation focused on text analysis is named text mining (Abramo et al., 2019; Lehmann & Wohlrabe, 2017; Martín-Martín et al., 2018; Panagopoulos et al., 2017). Text mining allows the data extraction from text documents (Jeong et al., 2019; Ma et al., 2019; Robinson et al., 2019; Zhou et al., 2019), being a handy tool in areas as diverse as medicine, engineering, and customer service (Lucini et al., 2020; Pezzini, 2017; Sun et al., 2018). The chosen time span, between 2008 and 2021 (May 29), is the period in which the LaBioS has been working on the subject of biopolymers. Specifically about the term biopolymer, the scenario between the years 2008 and 2021 is complex because of the myriad of papers collected, which was equal to 18,277 scientific documents. Of course, these numbers can vary depending on the database used. According to the Voyant Tools (VT), the titles returned 256,702 total words and 18,212 unique word forms. In turn, the abstracts returned 3,416,625 total words and 57,689 unique word forms. These numbers make clear that the ordinary analysis of these data is humanly impossible.

Therefore, the analysis of this complex scenario demands the computer assistance offered by text mining tools. Then, the first approach was performed using the Wordcloud tool from Voyant Tools. The results are shown in Figure 1. Besides, the Titles and Abstracts corpus can be inspected through these links:

Titles: https://voyant-tools.org/?corpus=91168bf881a70c7a8fbf0d31fc2c640d&lang=en

Abstracts: https://voyant-tools.org/?corpus=4c21860a0981330a26179bb37eac123a&lang=en

Among the texts, the most frequent words in the titles are *biopolymer* (2969); *based* (2348); *chitosan* (2085); *properties* (1713); and *using* (1327). In turn, the most frequent words in the abstracts are *biopolymer* (13834); *properties* (11658); *using* (9980); *chitosan* (8992); and *study* (8440). Voyant Tools also allows the calculation of the correlations between the terms. In both titles and abstracts cases, the fixed term was *biopol**. Among the most cited words into Titles and Abstracts, only *based* (among titles) and *chitosan* (among abstracts) presented significant (95 % of probability) determination coefficients equal to 0.69 and 0.16, respectively. The R2 values are small in both cases, indicating that a different methodology must be performed, allowing further explanations. One possible way to deal with these data is subdividing them by years, as performed elsewhere (Gomes, 2021). This approach is advantageous to understanding how the concepts or keywords evolve during research time. On the other hand, understanding how data are correlated in a massive amount of information is crucial to see how the investigations are being conducted. Therefore, another tool, such as VOSviewer, should be used.

Fig. 2 shows the clustering maps from the studied titles and abstracts between 2008 and 2021, while Table 1 shows the top trending inside the five most relevant clusters in the Titles and Abstracts (data obtained from VOSviewer).

These clusters are created according to the probability or level at which the words are grouped together and indicate how each word is connected to its neighborhood. Among the Titles, the most relevant cluster allows inferring the relevant concerning polymer and blends based on lactic acid or PHAs. The next cluster focuses on using these materials in environmental recovery applications, mainly related to removing heavy metals from the water. In turn, the third cluster deals with the production of PHAs by biosynthesis. The next cluster mainly focuses on biopolymers in medicine, highlighting the terms scaffold, delivery system, and tissue engineering. Finally, the fifth cluster deals with the green synthesis of these biomaterials, highlighting catalyst and

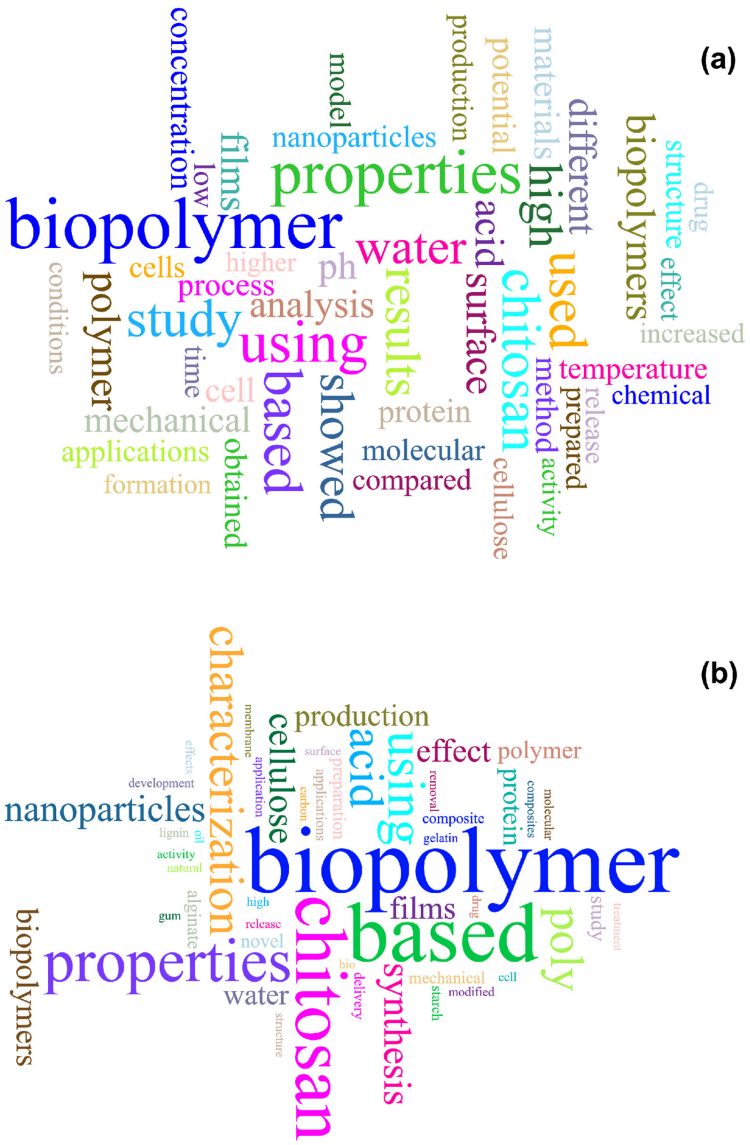

Fig. 1. Word clouds from studied titles (a) and abstracts (b) between 2008 and 2021

ionic liquid. In turn, among the Abstracts, the first cluster deals with the characterization of biopolymers used in environmental recovery applications. Among the top trending words, XRD (X-ray diffraction) and TGA (thermogravimetric analysis) are highlighted. The next cluster deals with medicine, and the highlighted words are drug, delivery, scaffold, and tissue engineering. The third cluster reveals the primary concern regarding the characterization of these materials, while the next one is focused on the preparation of biopolymers, evolving the terms gene, culture, glucose, and accumulation. Finally, the last cluster is probably concerned with silicon chemistry, which is relevant to the further developments in this field.

Therefore, data gathered from literature allowed inferring that relevant drivers in the biopolymers field focus on preparing and characterizing biomaterials useful to

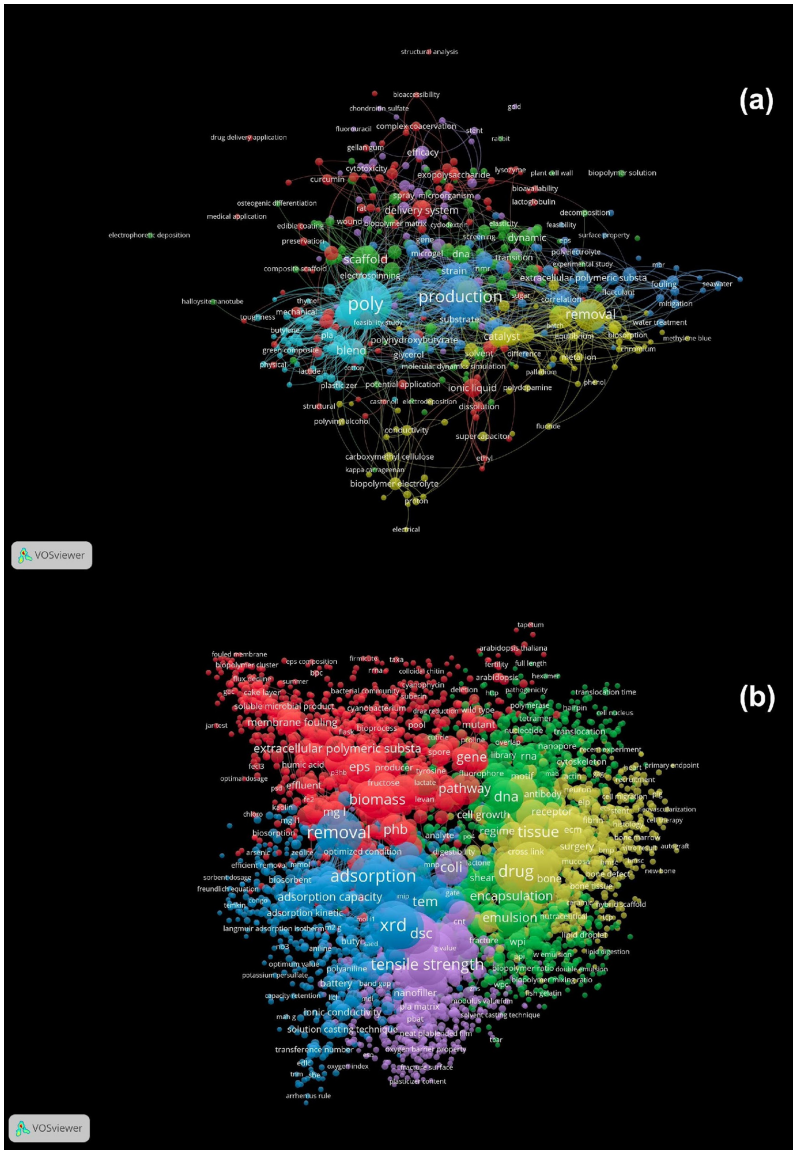

Fig. 2. Clustering maps from studied titles (a) and abstracts (b) between 2008 and 2021

environmental recovery and bio-medicine applications. In the contexts regarding biopolymer synthesis (Almeida et al., 2020; Araujo et al., 2015; Bedor et al., 2021; Costa et al., 2017; Daher Pereira et al., 2021; de Araújo Segura et al., 2018; Elias et al., 2021; Ferreira et al., 2012a, 2012b, 2015, 2017; Figueiredo et al., 2019; França et al., 2019; Gomes et al., 2018; Icart et al., 2018; Middea et al., 2017; Moraes et al., 2018a, 2018b; Neto et al., 2021; Pereira et al., 2013, 2014; Péres et al., 2014, 2017; Picciani et al., 2007; Ramon et al., 2018; Sá et al., 2017; Yusoff et al., 2021), environmental recovery (Aboelkheir et al., 2019a, 2019b; Bedor et al., 2020, 2021; Ferreira et al., 2012b; Figueiredo et al., 2019; Gomes et al., 2018; Grance et al., 2012; Nogueira et al., 2020; Si et al., 2020; Souza et al., 2012; Varela et al., 2012), medicine (Costa et al., 2018; Daher et al., 2021; Daher Pereira et al., 2021; Lange et al., 2016; Pereira et al., 2013, 2014; Ramon et al.,

Table 1. Top trending inside the five most relevant clusters obtained from VOSviewer

Cluster	Label in Titles	Occurrences	Label in Abstracts	Occurrences
1	poly	988	xrd	968
1	blend	236	removal	895
1	lactic acid	185	adsorption	872
1	hydroxybutyrate	145	x ray diffraction	782
1	hydroxybutyrate co	96	aqueous solution	761
1	hydroxyvalerate	77	ion	707
1	nanocomposite film	73	tga	600
2	removal	374	drug	787
2	aqueous solution	193	delivery	726
2	ion	139	scaffold	657
2	wastewater	130	tissue	589
2	sludge	111	vitro	555
2	dye	107	disease	417
2	extracellular polymeric substance	92	tissue engineering	398
3	production	684	thermal stability	721
3	strain	115	tensile strength	668
3	bacterium	110	nanocomposite	649
3	polyhydroxyalkanoate	105	blend	588
3	biosynthesis	94	pla	586
3	culture	92	dsc	538
3	substrate	92	elongation	484
4	scaffold	278	biomass	535
4	delivery system	144	gene	430
4	tissue engineering	90	g l	404
4	adhesion	75	pathway	404
4	efficacy	75	phb	380
4	tissue	56	culture	364
4	cancer	50	glucose	360
4	conjugate	50	accumulation	339
5	catalyst	146	dna	459
5	reaction	136	dynamic	382
5	ionic liquid	127	simulation	299
5	conversion	71	theory	269
5	solvent	59	regime	207
5	degree	50	deformation	189
5	green synthesis	50	regulation	184

2018; Sá et al., 2017; Souza et al., 2013; Vargas & Souza, 2011), and even nanotechnology (Araujo et al., 2015; Asthana et al., 2021; Costa & Souza, 2014; de Araújo Segura et al., 2018; Elias et al., 2015, 2016, 2021; Elkodous et al., 2019; Ferreira et al., 2014; Grance et al., 2012; Lopes et al.,

2018; Maranhão et al., 2021; Marques et al., 2016, 2017; Neto et al., 2018, 2021; Pal et al., 2019, 2021; Pereira et al., 2013; Péres et al., 2017; Pérez et al., 2020; Santos et al., 2021; Si et al., 2021; Siddaramaiah et al., 2012; Soares et al., 2017; Souza et al., 2007, 2009a, 2009b, 2010a, 2010b, 2012, 2013; V et al., 2020; Varela et al., 2013; Vargas & Souza, 2011) or Civil Engineering (Aboelkheir et al., 2018a, 2018b, 2021; Rocha Ferreira et al., 2020; Santos et al., 2018, 2021; Veloso de Carvalho et al., 2021) applications, LaBioS has presented several contributions in the last years, helping to boost and spread these relevant subjects. Thus, the following paragraphs are reserved for a brief description of some of the latest research activities under development at LaBioS and associated groups.

Case studies carried out in the LaBioS

Reduction of enzymatic browning of chunkey banana from the application of cassava biofilms by Sergio Thode

Between 2010 and 2019, the generation of solid municipal waste (MSW) in Brazil registered a considerable increase, going from 67 million to 79 million tons per year. In addition, per capita generation increased from 348 kg/year to 379 kg/year. However, the study of the gravimetric composition reveals that organic material remains the main component of MSW, constituting 45.3 %. On the other hand, dry recyclable waste totals 35 %, being mainly composed of plastics (16.8 %), paper and cardboard (10.4 %), in addition to glass (2.7 %) and metals (2.3 %), among others (Panorama dos Resíduos …, 2020). In Brazil, the banana (*Musa* spp.) stands out because it is the most widespread and because it is the most consumed by all social classes. Brazil is now the world's fourth-largest banana producer globally, with 6,953,747 tons per year (FAO…, 2018; https://www.embrapa.br/mandioca-e-fruticultura/cultivos/banana). Numerous initiatives are under development to minimize losses within this production chain, deserving highlight to the biodegradable packaging, also known as biofilms, from natural sources. These biofilms are microorganisms degraded in weeks or months under favorable conditions (Assis & Britto, 2014).

In the search to develop more sustainable materials, cassava starch biofilms have already been developed to mitigate these losses (Veiga-Santos et al., 2008). The mean values of fresh mass loss as a function of time are shown in Fig. 3. The mass loss increased in the two treatments during storage, meaning that the starch biofilms produced of cassava starch are semi-permeable, allowing the fruits to continue breathing and losing mass. At the end of the analysis period, the control group had a 41.88 % loss, followed by T1 (23.77 %) and T2 (25.41 %). There are no statistically significant differences between biofilm treatments. The mass loss occurs through the outlet in the form of water vapor to the environment (Assis & Britto, 2014), so the results obtained demonstrated that the biofilms protected fruits by minimizing water loss through perspiration, avoiding fruit shrinkage and shriveling as a natural indication of ripeness.

This study revealed the efficiency of biofilm coating with and without gelatin to reduce the rate of enzymatic browning and increase the shelf life of bananas. Furthermore, it was possible to verify a reduction in fresh weight loss in the treatments. Besides, no significant difference was observed in the addition of gelatin to the parameters evaluated in the fruit. Moreover, slowing the deterioration of healthy foods is necessary for a reality where nutritional deficiencies are increasingly common, whether due to lack of proper nutrition education or unfavorable economic situations.

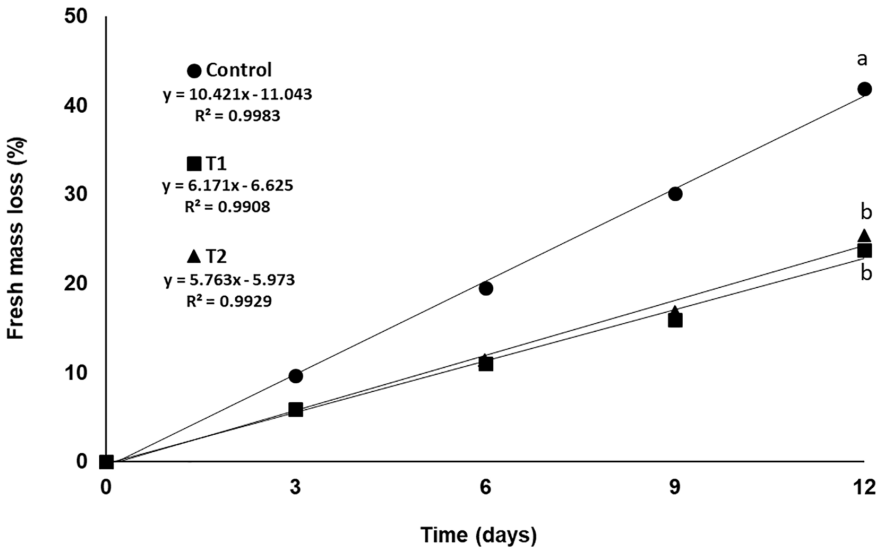

Fig. 3. Fresh mass loss as a function of the two biofilms during 12 days of the experiment. T1 (2.6 % starch / 500 mL of distilled water); T2 (2.6 % starch / 500 mL of distilled water + 1 g of gelatin). Mean values followed by the same lower-case letter do not differ statistically by Tukey's test at 5 % probability test

Polymeric microsystems for use in the controlled release of antibiotics by Emiliane Daher

One of the most significant problems to contemporary public health worldwide is resistance to treatment with antibiotics. It is estimated that antimicrobial resistance causes about 700 thousand deaths every year (Estrela, 2018; Santos, 2004). The forecast is that, by 2050, 10 million deaths annually will be attributed to antimicrobial resistance, which means more deaths than cancer deaths, and the effect on the global economy will be around $100 trillion (Estrela, 2018; https://www.gov.br/anvisa/pt-br/assuntos/noticias-anvisa/2019/resistencia-antimicrobiana-e-ameaca-global-diz-oms). In order to maintain the plasma concentration of the antibiotic and decrease the risk of bacterial resistance using the conventional delivery system, the patient must administer successive doses of the medication at the correct time, which often does not occur (Smith, 2005). For this reason, to improve conventional therapies is crucial in the case of antibiotics. Controlled drug release systems often use synthetically biocompatible and biodegradable polymers, such as poly(lactic acid) – PLA, as carriers for drugs (Uhrich et al., 1999). For this work, the drug cephalexin was chosen, and to improve its encapsulation into the polymer matrix, it was decided to graft a more hydrophilic polymer, polyethylene glycol-PEG, to PLA. In addition, it was decided to add the drug through microemulsion, to try to avoid the initial explosive release, known as «burst release» (Kim et al., 2008). Fig. 4 (a) shows the system used for polymer synthesis, and Fig. 4 (b) the emulsion process used in the production of polymer spheres containing the drug.

The PLA-g-PEG polymer was synthesized, characterized, and the drug was inserted in the microspheres by the emulsion method.

Influence of chemical similarity on the sorption capacity of lignocellulosic fibers by Fernanda Diva

Oil is an essential material and because it is preferably transported by sea, spills frequently occur in the ocean. Several alternatives have

Fig. 4. System used for polymer synthesis (a) and emulsion process used in the production of polymer spheres containing the drug (b)

already been investigated to combat these disasters. A work conducted during the Master Degree studies of Fernanda Diva / LaBioS proved by data mining that the sorption of the material is related to the chemical similarity between the sorber and the sorbent. Fernanda Diva's study is derived from our chemical similarity hypothesis presented elsewhere (Ferreira et al., 2012b). The data mining allowed the gathering of eleven pieces of research developed in the sorption of toluene using vegetable fibers. The extracted data allowed for comparing spectral data reduced to root-mean-square error (RMSE) values and oil sorption capability for every lignocellulosic fiber material from the eleven scientific works. Data analysis proved that the greater the chemical similarity (related to the lowest RMSE obtained values – See Fig. 5), the greater the sorption of the oil by the tested material.

The extraction of data, despite the difficulties caused by the authors' different approaches, proves that the chemical similarity is a critical factor for the sorption of petroleum derivatives in natural polymers. Based on this study, more efficient sorbents may be developed for the sorption of toluene and other components present in oil using vegetable materials that would often be discarded.

Synthesis of thiol-PEG-PBS copolymer by Nathali Ricardo

Cancer is a worldwide public health problem. Therefore, new technologies to combat this disease more efficiently and with fewer side effects attract the attention of the scientific community (Bray et al., 2018; Ferlay et al., 2015). In this context, gold nanoparticles have been shown to be extremely promising. The critical point in using these particles is their stability (Yue et al., 2016). One way to get around this problem is through their coating; one of the coatings most used with AuNPs in pharmacological research is polyethylene glycol (PEG) (Kodiyan et al., 2012; Li et al., 2013). Several studies also proved that PEG conferred prolonged circulation of gold nanoparticles in the blood and, therefore, could show the «Enhanced Permeability and Retention (EPR)» effect, which means more significant accumulation of nanoparticles in tumor tissue (Singh et al., 2018). Additionally, in this study, poly (butylene succinate) (PBS) was used. This polymer is very useful for immobilizing various

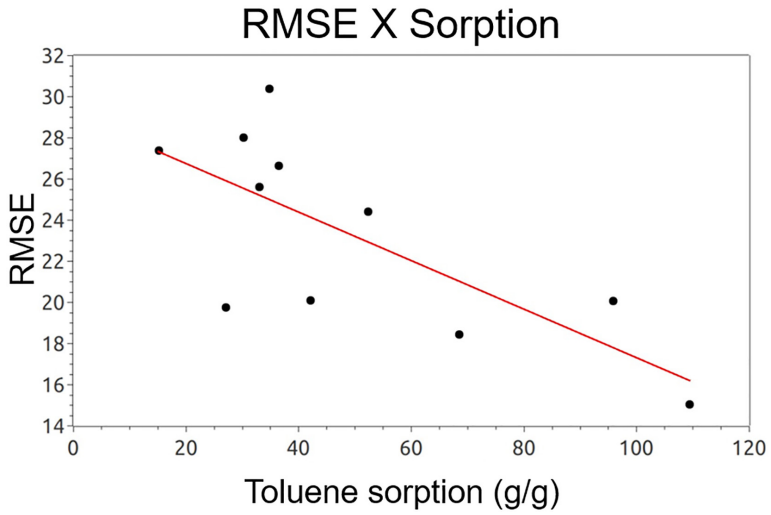

Fig. 5. RMSE ratio and sorption of all analyzed sorption materials

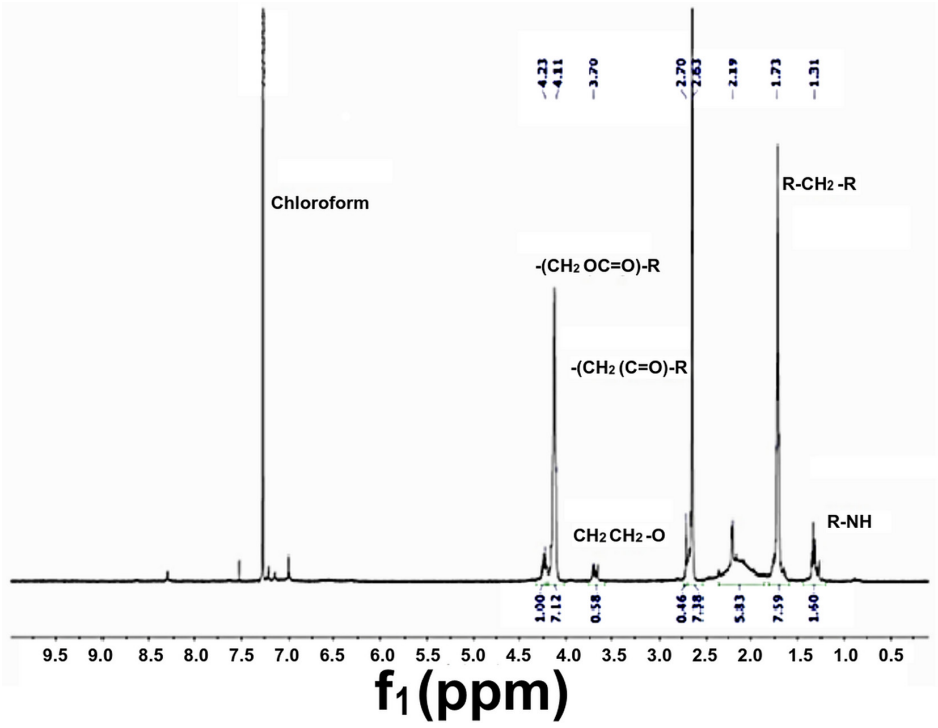

Fig. 6. ^{1}H Nuclear Magnetic Resonance of PBS-PEG

substances, such as medicines, besides having accessible handling capacity (Baldanza et al., 2018; Ferreira et al., 2014).

The nuclear magnetic resonance technique was used to prove whether there was a chemical bond between PEG and PBS and, consequently, the copolymer's formation. The spectrum, shown in Fig. 6, presents chemical shifts located at 1.73 ppm (R-CH_2-R) and 4.11 ppm (–CH_2O(C=O)-R), which correspond to methylene protons in

1,4-butanediol units. The spectrum also shows the chemical shift located at 3.70 ppm referring to methylene protons in ether grouping units (CH_2-CH_2-O) characteristic of polyethylene glycol. In the FTIR spectrum, it is possible to notice that the main expected chemical structures are present in the spectrum, which is another strong indication of obtaining the copolymer.

Therefore, it is possible to see that the proposed interfacial reaction between HS-PEG and PBS modified with TDI was successful; this was proven by the characteristic chemistries of a polyether and polyester in the NMR, and the same was observed in the FTIR spectrum with the presence of characteristic bands of both classes of polymers. It is essential to point out that the purification process allows us to infer that it is a copolymer and not a mixture of polymers. The results of the thermal analysis were within the expected ones and consistent with the data obtained by other authors.

Nanostructured hybrid of magnetite and poly(butylene succinate) with potential application for controlled drug release, magneto hyperthermia, and imaging diagnostics by Rafael Moraes

Nanomedicine is one of the most promising areas of current research in the medical field (Mirza & Siddiqui, 2014). It is the medical application of the unique technologies and properties obtained through manipulating the nanometric scale of materials. The present work aims to build a nanostructured system made of poly (butylene succinate) and magnetite capable of carrying a drug (drug delivery) and releasing it in a controlled manner through specific magnetic stimuli. This technique can reduce side effects mainly in drugs with low bioavailability, such as chemotherapy. Furthermore, this system also aims at the use of magnetohyperthermia, through the use of oscillating magnetic fields, which can heat the magnetite, promoting, for example, the death of tumor cells and sensitizing the cancerous tissue to the action of the drug, resulting in a synergistic effect of the two techniques (Colombo et al., 2012).

Poly(butylene succinate) was synthesized using a 1:1 ratio of succinic acid and 1,4-butanediol (Ferreira et al., 2015). Magnetite was synthesized using the alkaline precipitation method (Moraes et al., 2018a). The hybrid material was synthesized using lactic acid, which forms bonds with the iron hydroxide surface of the magnetite, and later added toluene diisocyanate, which forms urethane bonds with the lactic acid and the polymer. The model drug chosen was ketoconazole due to its properties and the ease of identification during the characterizations. First, the drug and the polymer were dissolved using dichloromethane. Then, water was added to the system under stirring, producing an emulsion where the polymer chains trapped the drug.

The dynamic light scattering results allowed inferring that magnetite presents an average size of 100 nm. Besides, these particles were modified by the polymer chains, and the drug was effectively encapsulated. Fig. 7 shows the SEM micrograph, from which the morphology of the dried hybrid can be observed. The micro-agglomerates retain the drug in the chains, as proved by energy dispersive spectroscopy, which presents chlorine from the drug. The successful synthesis of the hybrid nanostructures and their ability to encapsulate drugs was concluded. The potential to combine different treatments drives all the medicine to a new frontier, where reduced side effects and increased effectiveness of the treatment could come true in a few years. In addition, treatment and diagnosis could be allied in an unprecedented way, as the capacity of the ferromagnetic material to remain in specific tissues, such as tumors, for a time can be used to monitor the effects of medical intervention.

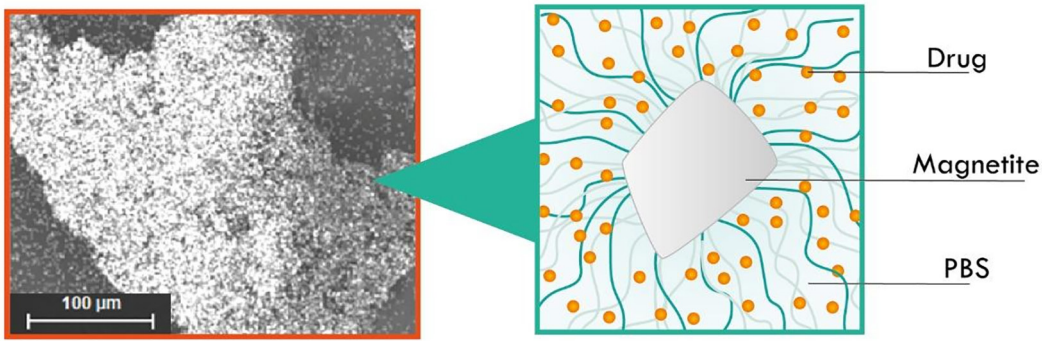

Fig. 7. Micrograph taken by a scanning electron microscope, on the right, energy dispersive spectroscopy showing the element chlorine in emphasis

Heavy metal removal from wastewater using modified biomass
by Marcio Nogueira

Water is an essential asset for the survival of all species of life on planet Earth. Large quantities of industrial wastewater generated in industries such as galvanoplasty, metallurgy, and leather production, in which there are many heavy metals, including chromium, copper, zinc, nickel, lead, and others, are harmful to the environment and living organisms. Numerous studies report the application of biosorption to treat effluents from various sources, with very satisfactory results. Submerged macrophytes have significant potential for bioconcentration of heavy metals due to their larger surface area compared to non-submerged plants (Nogueira et al., 2020). The present work is based on the chemical modification of biological materials to evaluate their efficiency in removing cations of toxic metals, in particular chromium and nickel, present in aquatic environments. The biomass mainly used is of the species *Eichhornia crassipes*, with the chemical modification from the application of an organic anhydride (succinic anhydride). The tests show satisfactory results, with metallic removal rates of around 80 % efficiency. Table 2 shows exciting results for removing chromium and nickel, present in synthetic effluents, using modified biomasses. From the results obtained, it is possible to conclude that the use of chemically modified biomaterials is based on the biocompatibility and stability of these compounds. Moreover, the combination of biosorption with magnetic particles represents an alternative of enormous potential in the treatment of industrial effluents, at the same time representing a non-toxic and low-cost technology.

Table 2. Metal removal efficiency

Biosorbent	Initial concentration					
	Cr^{+6}	Ni^{+2}	Cr^{+6}	Ni^{+2}	Cr^{+6}	Ni^{+2}
Modified biomass with succinic anhydride	10 mg·L^{-1}		50 mg·L^{-1}		100 mg·L^{-1}	
	Metal maximum removal (%)					
	79.1	85.2	80.9	82.4	81.7	83.6

Modification of plant fibers and their applications by Johny Chantre

Vegetable materials have gained space in science and industry because they are less abrasive, biodegradable, have low commercial value, and excellent thermo-mechanical properties. However, chemical modifications are usually necessary for better compatibility with polymeric matrices. Thus, part of Johny Chantre's M. Sc. studies address the main treatments applied to vegetable fibers and their possible applications. The most commonly used treatments for the modification of vegetable substrates are acetylation, sodium bicarbonate, and hornification. These treatments allow the use of waste materials reinforcing polymeric matrices by improving adhesion and compatibility between phases. During the synthesis of polymeric composites from glycerin, castor oil, and maghemite as oil absorbers, milled coffee grounds were added as a filler to lower the costs and improve the final buoyancy of the composite. The results showed that the buoyancy of the composite was improved. However, the addition of vegetable waste as an additive significantly increased water absorption by the composite, increasing its hydrophilic character, thus constituting a competition problem since the objective was the recovery of oil through absorption by the composite. Thus, the acetylation treatment reduced the hydrophilic character of the coffee grounds powder. After the acetylation treatment, the coffee grounds were washed with deionized water and dried at 70 ºC for 24 h. Then, the modified substrate was characterized by Fourier transform infrared spectroscopy (see Fig. 8). The results showed a considerable reduction in the bands around 3500 cm^{-1} of the hydroxyl group, proving that the coffee grounds powder is more hydrophobic than the non-modified analog. For the oil spill cleanup tests, 0.1 g of the composites filled with different amounts of virgin and acetylated coffee grounds (2.5 %, 5 %, and 10 %) were used to remove one gram of oil spilled on seawater. Tests were performed in triplicate. Every time, all the oil was removed from the water. On the other hand, the materials filled with modified coffee grounds powder, compared to the similar non-modified materials, presented an average reduction in the amount of sorbed water equal to (55±39)%, with a confidence limit of 95 %. Therefore, the use of the acetylated filler improved the characteristics of the sorber by

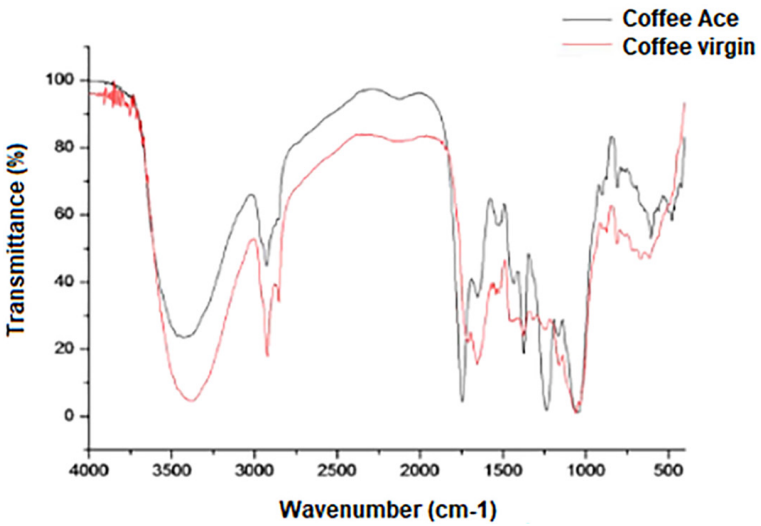

Fig. 8. Fourier transform infrared spectroscopy of non-modified and acetylated (Ace) coffee grounds powder

reducing the water removed and, for this reason, making more straightforward the oil spill cleanup process.

Conclusions and perspectives

Thus, the bibliometric survey presented in this work and the LaBioS' specific contributions to the topic of biopolymers make clear the use of these materials should be encouraged. From our perspective, one of the best ways to spread biopolymers is by modifying their properties. Thus, chemical modifications and nanomodifications via nanoparticles, used as nanofillers or nanosubstrates, must be increasingly researched by the scientific community. So, the use of these new biomaterials will lead us to a healthier relationship with our planet, additionally providing us with real gains in the quality of life and well-being, which are fundamental for our continuous prospering as a civilization.

The data collected here through text mining tools leads us to conclude that the study of the biopolymers is far from being complete. More than that, the correlations shown throughout this research indicate an evolution of the systems studied, proceeding from different clusters, such as the ones dealing with green polymers and biosynthesis of biopolymers, medicine and environmental recovery. Besides that, silicon chemistry possesses crucial relevance to the subsequent developments in this field. In these contexts, LaBioS has contributed by raising a new generation of scientists dealing with the pressure from the short time our planet has to being saved from ourselves and keeping in mind that quality of life must be a premise driving our scientific contributions to the future!

References

Aboelkheir M. G., Bedor P. B., Leite S. G., Pal K., Toledo Filho R. D., Gomes De Souza F. (2019a) Biodegradation of vulcanized SBR: a comparison between Bacillus subtilis, Pseudomonas aeruginosa and Streptomyces sp. *Scientific Reports*, 9(1): 19304

Aboelkheir M. G., Thomas S., Gomes de Souza F. Jr., Dias Toledo Filho R., Celestino R., Thode Filho S., Veloso de Carvalho F., da Silveira Maranhão F., Daher Pereira E., Corrêa da Costa V., Ricardo Barbosa de Lima N. (2021) Influence of UV-modified GTR on the properties of interlocking concrete paving units. *Journal of Molecular Structure*, 1234: 130110

Aboelkheir M. G., Visconte L. Y., Oliveira G. E., Toledo Filho R. D., Souza F. G. (2019b) The biodegradative effect of Tenebrio molitor Linnaeus larvae on vulcanized SBR and tire crumb. *Science of the Total Environment*, 649: 1075–1082

Aboelkheir M., Siqueira C. Y.S., Souza F. G. Jr., Toledo Filho R. D. (2018a) Influence of styrene-butadiene co-polymer on the hydration kinetics of SBR-modified well cement slurries. *Macromolecular Symposia*, 380(1): 1800131

Aboelkheir M., Siqueira C., Souza F. Jr., Toledo R. (2018b) Macromolecular and aromatic character influence of SBR on the rheological properties of well cement slurries. *Journal of Urban Technology and Sustainability*, 1(1): 21–27

Abramo G., D'Angelo C.A., Felici G. (2019) Predicting publication long-term impact through a combination of early citations and journal impact factor. *Journal of Informetrics*, 13(1): 32–49

Almeida T., Pal K., Souza F. G. Jr. (2020) Bibliometric analysis of the hot theme «Phytosynthesized nanoparticles». *Archives in Biomedical Engineering & Biotechnology*, 4(1): 5

Araujo R. T., Ferreira G. R., Segura T., Souza F. G. Jr., Machado F. (2015) An experimental study on the synthesis of poly(vinyl pivalate)-based magnetic nanocomposites through suspension polymerization process. *European Polymer Journal*, 68: 441–459

Assis O. B.G., Britto D. (2014) Review: edible protective coatings for fruits: fundamentals and applications. *Brazilian Journal of Food Technology*, 17(2): 87–97

Asthana N., Pal K., Aljabali A. A.A., Tambuwala M. M., Souza F. G. Jr., Pandey K. (2021) Polyvinyl alcohol (PVA) mixed green–clay and aloe vera based polymeric membrane optimization: Peel-off mask formulation for skin care cosmeceuticals in green nanotechnology. *Journal of Molecular Structure*, 1229: 129592

Babu R. P., O'Connor K., Seeram R. (2013) Current progress on bio-based polymers and their future trends. *Progress in Biomaterials*, 2(1): 8

Baldanza V. A.R., Souza F. G. Jr., Filho S. T., Franco H. A., Oliveira G. E., Caetano R. M.J., Hernandez J. A.R., Ferreira Leite S. G., Furtado Sousa A. M., Nazareth Silva A. L. (2018) Controlled-release fertilizer based on poly(butylene succinate)/urea/clay and its effect on lettuce growth. *Journal of Applied Polymer Science*, 135(47): 46858

Bedor P. B.A., Caetano R. M.J., De Souza F. G., Leite S. G.F. (2020) Advances and perspectives in the use of polymers in the environmental area: a specific case of PBS in bioremediation. *Polimeros*, 30(2): e2020023

Bedor P. B.A., Rondelli P., Filho S. T., Souza F. G. Jr., Leite S. G.F. (2021) Production and toxicological evaluation of poly(butylene succinate)–urea microspheres targeting bioremediation. *Journal of Chemical Technology & Biotechnology*, 96(7): 1842–1853

Bray F., Ferlay J., Soerjomataram I., Siegel R. L., Torre L. A., Jemal A. (2018) Global cancer statistics 2018: GLOBOCAN estimates of incidence and mortality worldwide for 36 cancers in 185 countries. *CA Cancer Journal for Clinicians*, 68(6): 394–424

Buono P., Averous L., Duval A., Habibi Y. (2018) Clicking biobased polyphenols: A sustainable platform for aromatic polymeric materials. *ChemSusChem*, 11(15): 2472–2491

Colombo M., Carregal-Romero S., Casula M. F., Gutiérrez L., Morales M. P., Böhm I. B., Heverhagen J. T., Prosperi D., Parak W. J. (2012) Biological applications of magnetic nanoparticles. *Chemical Society Reviews*, 41(11): 4306–4334

Costa R. C. da, Souza F. G. Jr. (2014) Preparation of maghemite and polyaniline nanocomposites assisted by ultrasound. *Polimeros*, 24(2): 243–249

Costa R. M.D. da, Hungerbühler G., Saraiva T., De Jong G., Moraes R. S., Furtado E. G., Silva F. M., De Oliveira G. E., Ferreira L. S., Souza F. G. Jr. (2017) Green polyurethane synthesis by emulsion technique: a magnetic composite for oil spill removal. *Polimeros*, 27(4): 273–279

Costa R. C.D., Pereira E. D., Silva F. M., Jesus E. O.D., Souza F. G. (2018) Drug micro-carriers based on polymers and their sterilization. *Chemistry and Chemical Technology*, 12(4): 473–487

Daher E., Souza F. G., Carelo J., Brandão V. (2021) Drug delivery polymers: an analysis based on literature text mining. *Brazilian Journal of Experimental Design, Data Analysis and Inferential Statistics*, 1(1): 40–55

Daher Pereira E., Thomas S., Souza F. G. Jr., da Silva Cardoso J., Thode Filho S., Corrêa da Costa V., da Silveira Maranhão F., Ricardo Barbosa de Lima N., Veloso de Carvalho F., Galal Aboelkheir M. (2021) Study of controlled release of ibuprofen magnetic nanocomposites. *Journal of Molecular Structure*, 1232: 130067

de Araújo Segura T.C., Pereira E.D., Icart L.P., Fernandes E., Esperandio de Oliveira G., Souza F.G. Jr. (2018) Hyperthermic agent prepared by one-pot modification of maghemite using an aliphatic polyester model. *Polymer Science, Series B*, 60(6): 806–815

Elias E., Chandran S., Zachariah A.K., Vineesh Kumar V.K., Sunil M.A., Bose S., Souza F.G., Thomas S. (2016) Percolated network formation in biocidal 3D porous PCL/clay nanocomposite scaffolds: effect of organic modifier on interfacial and water sorption properties. *RSC Advances*, 6(88): 85107–85116

Elias E., Costa R., Marques F., Oliveira G., Guo Q., Thomas S., Souza F.G. Jr. (2015) Oil-spill cleanup: The influence of acetylated curaua fibers on the oil-removal capability of magnetic composites. *Journal of Applied Polymer Science*, 132(13): 41732

Elias E., Sarathchandran C., Joseph S., Zachariah A.K., Thomas J., Devadasan D., Souza F.G. Jr., Thomas S. (2021) Photoassisted degradation of rhodamine B using poly(ε-caprolactone) based nanocomposites: Mechanistic and kinetic features. *Journal of Applied Polymer Science*, 138(26): e50612

Elkodous M.A., El-Sayyad G.S., Mohamed A.E.E., Pal K., Asthana N., de Souza F.G. Jr., Mosallam F.M., Gobara M., El-Batal A.I. (2019) Layer-by-layer preparation and characterization of recyclable nanocomposite (CoxNi1–xFe2O4; X = 0.9/SiO2/TiO2). *Journal of Materials Science: Materials in Electronics*, 30(9): 8312–8328

Estrela T.S. (2018) Resistência antimicrobiana: enfoque multilateral e resposta brasileira. *Saúde e política externa: os 20 anos da Assessoria de Assuntos Internacionais de Saúde (1998–2018)*. Brasília, Ministério da Saúde, p. 307–327

FAO, IFAD, UNICEF, WFP and WHO (2018) *The state of food security and nutrition in the world 2018. Building climate resilience for food security and nutrition*. Rome, FAO, 181 p.

Ferlay J., Soerjomataram I., Dikshit R., Eser S., Mathers C., Rebelo M., Parkin D.M., Forman D., Bray F. (2015) Cancer incidence and mortality worldwide: sources, methods and major patterns in GLOBOCAN2012. *International Journal of Cancer*, 136(5): E359- E386

Ferreira G.R., Segura T., Souza F.G. Jr., Umpierre A.P., Machado F. (2012a) Synthesis of poly(vinyl acetate)-based magnetic polymer microparticles. *European Polymer Journal*, 48(12): 2050–2069

Ferreira L.P., da Cunha B.P., Kuster R.M., Pinto J.C., Souza M.N., Souza F.G. Jr. (2017) Synthesis and chemical modification of poly(butylene succinate) with rutin useful to the release of silybin. *Industrial Crops and Products*, 97: 599–611

Ferreira L.P., Moreira A.N., Delazare T., Oliveira G.E., Souza F.G. Jr. (2012b) Petroleum absorbers based on CNSL, furfural and lignin – the effect of the chemical similarity on the interactions among petroleum and bioresins. *Macromolecular Symposia*, 319(1): 210–221

Ferreira L.P., Moreira A.N., Pinto J.C., Souza F.G. Jr. (2015) Synthesis of poly(butylene succinate) using metal catalysts. *Polymer Engineering & Science*, 55(8): 1889–1896

Ferreira L.P., Moreira A.N., Souza F.G. Jr., Pinto J.C.C. da S. (2014) Preparation of nanocomposites based on poly(butylene succinate) and montmorillonite organoclay via in situ polymerization. *Polimeros*, 24(5): 604–611

Fertahi S., Ilsouk M., Zeroual Y., Oukarroum A., Barakat A. (2021) Recent trends in organic coating based on biopolymers and biomass for controlled and slow release fertilizers. *Journal of Controlled Release*, 330: 341–361

Figueiredo A. S., Icart L. P., Marques F. D., Fernandes E. R., Ferreira L. P., Oliveira G. E., Souza F. G. (2019) Extrinsically magnetic poly(butylene succinate): An up-and-coming petroleum cleanup tool. *Science of the Total Environment*, 647: 88–98

França D., Rebessi A. C., Camilo F. F., Souza F. G. Jr., Faez R. (2019) Pressure sensibility of conductive rubber based on NBR- and polypyrrole-designed materials. *Frontiers in Materials*, 6: 189

Gomes F. (2021) Polyaniline: Trends and perspectives from text mining analysis. *Brazilian Journal of Experimental Design, Data Analysis and Inferential Statistics*, 1(1): 9–39

Gomes F. W., Lima R. C., Piombini C. R., Sinfitele J. F., Souza F. G. Jr., Coutinho P. L. A., Pinto J. C. (2018) Comparative analyses of poly(ethylene 2,5-furandicarboxylate) – PEF – and poly(ethylene terephthalate) – PET – resins and production processes. *Macromolecular Symposia*, 381(1): 1800129

Grance E. G. O., Souza F. G. Jr., Varela A., Pereira E. D., Oliveira G. E., Rodrigues C. H. M. (2012) New petroleum absorbers based on lignin-CNSL-formol magnetic nanocomposites. *Journal of Applied Polymer Science*, 126(Suppl. 1): E305-E312

Grance E. O., dos Santos E. R. F., Andrade C., Oliveira G. E., Pinto J. C., Nele M., Souza F. G. (2016) Smart composite useful to acid release. *Journal of Applied Polymer Science*, 133(10): 43071

Hetenyi G., Lengyel A., Szilasi M. (2019) Quantitative analysis of qualitative data: Using voyant tools to investigate the sales-marketing interface. *Journal of Industrial Engineering and Management*, 12(3): 393–404

Icart L. P., Fernandes E., Agüero L., Cuesta M. Z., Silva D. Z., Rodríguez-Fernández D. E., Souza F. G., Lima L. M. T. R., Dias M. L. (2018) End functionalization by ring opening polymerization: influence of reaction conditions on the synthesis of end functionalized poly(lactic acid). *Journal of the Brazilian Chemical Society*, 29(1): 99–108

Jensen A. T., de Oliveira A. C. C., Gonçalves S. B., Gambetta R., Machado F. (2016) Evaluation of the emulsion copolymerization of vinyl pivalate and methacrylated methyl oleate. *Journal of Applied Polymer Science*, 133(45): 44129

Jeong Y., Park I., Yoon B. (2019) Identifying emerging Research and Business Development (R&BD) areas based on topic modeling and visualization with intellectual property right data. *Technological Forecasting and Social Change*, 146: 655–672

Kanehashi S., Masuda R., Yokoyama K., Kanamoto T., Nakashima H., Miyakoshi T. (2015) Development of a cashew nut shell liquid (CNSL)-based polymer for antibacterial activity. *Journal of Applied Polymer Science*, 132(45): 42725

Khan A., Abas Z., Kim H. S., Kim J. (2016) Recent progress on cellulose-based electro-active paper, its hybrid nanocomposites and applications. *Sensors*, 16(8): 1172

Kim B.-S., Park S. W., Hammond P. T. (2008) Hydrogen-bonding layer-by-layer-assembled biodegradable polymeric micelles as drug delivery vehicles from surfaces. *ACS Nano*, 2(2): 386–392

Kodiyan A., Silva E. A., Kim J., Aizenberg M., Mooney D. J. (2012) Surface modification with alginate-derived polymers for stable, protein-repellent, long-circulating gold nanoparticles. *ACS Nano*, 6(6): 4796–4805

Lange J., Souza F. G. Jr., Nele M., Tavares F. W., Segtovich I. S. V., da Silva G. C. Q., Pinto J. C. (2016) Molecular dynamic simulation of oxaliplatin diffusion in poly(lactic acid-co-glycolic acid). Part A: parameterization and validation of the force-field CVFF. *Macromolecular Theory and Simulations*, 25(1): 45–62

Lehmann R., Wohlrabe K. (2017) Who is the 'Journal Grand Master'? A new ranking based on the Elo rating system. *Journal of Informetrics*, 11(3): 800–809

Li G., Qi R., Lu J., Hu X., Luo Y., Jiang P. (2013) Rheological properties and foam preparation of biodegradable poly(butylene succinate). *Journal of Applied Polymer Science*, 127(5): 3586–3594

Lopes M. C., Marques F., Souza F. G. Jr., Oliveira G. E. (2018) Experimental design optimization of castor oil, phthalic anhydride, and glycerin magnetic nanocomposites useful as oil spill cleanup tool. *Macromolecular Symposia*, 380(1): 1800085

Lucini F. R., Tonetto L. M., Fogliatto F. S., Anzanello M. J. (2020) Text mining approach to explore dimensions of airline customer satisfaction using online customer reviews. *Journal of Air Transport Management*, 83: 101760

Ma J., Abrams N. F., Porter A. L., Zhu D., Farrell D. (2019) Identifying translational indicators and technology opportunities for nanomedical research using tech mining: The case of gold nanostructures. *Technological Forecasting and Social Change*, 146: 767–775

Maranhão F. da S., Oliveira C. P. de, Filho S. T., Das D. B., Souza F. G. de (2021) Synthesis and characterization of modified magnetic nanoparticles for removal of dispersed oil in water. *Brazilian Journal of Experimental Design, Data Analysis and Inferential Statistics*, 1(1): 148–156

Maranhão F. S., Marques D., Visconte L. Y., Souza F. G. Jr. (2018) Chewing gum degradation as an environmental awakening tool. *MOJ Polymer Science*, 2(2): 71–73

Marinho V., Lima N., Neves M. A., Souza F. G. Jr. (2018) Petroleum sorbers based on renewable alkyd resin and lignin. *Macromolecular Symposia*, 380(1): 1800116

Marques F. D., Nele de Souza M., Souza F. G. Jr. (2017) Sealing system activated by magnetic induction polymerization. *Journal of Applied Polymer Science*, 134(47): 45549

Marques F. D., Souza F. G. Jr., Oliveira G. E. (2016) Oil sorbers based on renewable sources and coffee grounds. *Journal of Applied Polymer Science*, 133(11): 43127

Martín-Martín A., Orduna-Malea E., Thelwall M., Delgado López-Cózar E. (2018) Google Scholar, Web of Science, and Scopus: A systematic comparison of citations in 252 subject categories. *Journal of Informetrics*, 12(4): 1160–1177

Middea A., Spinelli L. S., Souza F. G. Jr., Neumann R., Fernandes T. L.A.P., Gomes O. da F.M. (2017) Preparation and characterization of an organo-palygorskite-Fe3O4 nanomaterial for removal of anionic dyes from wastewater. *Applied Clay Science*, 139: 45–53

Miller A. (2018) Text mining digital humanities projects: assessing content analysis capabilities of voyant tools. *Journal of Web Librarianship*, 12(3): 169–197

Mirza A. Z., Siddiqui F. A. (2014) Nanomedicine and drug delivery: a mini review. *International Nano Letters*, 4(1): 94

Moraes R. S., Ricardo N. S., Saez V., Souza F. G. Jr. (2018a) Synthesis of magnetic composite of poly (butylene succinate) and magnetite for the controlled release of meloxicam. *MOJ Polymer Science*, 2(1): 39–42

Moraes R. S., Saez V., Hernandez J. A.R., Souza F. G. Jr. (2018b) Hyperthermia system based on extrinsically magnetic poly (butylene succinate). *Macromolecular Symposia*, 381(1): 1800108

Neto W. S., Dutra G. V.S., Jensen A. T., Araújo O. A., Garg V., de Oliveira A. C., Valadares L. F., de Souza F. G. Jr., Machado F. (2018) Superparamagnetic nanoparticles stabilized with free-radical polymerizable oleic acid-based coating. *Journal of Alloys and Compounds*, 739: 1025–1036

Neto W. S., Simões Dutra G. V., de Sousa Brito Neta M., Chaves S. B., Valadares L. F., Souza F. G. Jr., Machado F. (2021) Nanodispersions of magnetic poly(vinyl pivalate) for biomedical applications: Synthesis and in vitro evaluation of its cytotoxicity in cancer cells. *Materials Today Communications*, 27: 102333

Nogueira M. da C., Santos E. R.F. dos, Pal K., Souza F. G. Jr. de (2020) Removal of chromium VI and others metals from wastewater treatment by modification of macrophytes and magnetite: A review. *Revista Brasileira de Gestao Ambiental e Sustentabilidade*, 7(17): 1439–1453

Pal K., Aljabali A. A., Kralj S., Thomas S., Gomes de Souza F. (2021) Graphene-assembly liquid crystalline and nanopolymer hybridization: A review on switchable device implementations. *Chemosphere*, 263: 128104

Pal K., Sajjadifar S., Abd Elkodous M., Alli Y. A., Gomes F., Jeevanandam J., Thomas S., Sigov A. (2019) Soft, self-assembly liquid crystalline nanocomposite for superior switching. *Electronic Materials Letters*, 15(1): 84–101

Panagopoulos G., Tsatsaronis G., Varlamis I. (2017) Detecting rising stars in dynamic collaborative networks. *Journal of Informetrics*, 11(1): 198–222

Panorama dos Resíduos Sólidos no Brasil 2020 (2020) ABRELPE, 52 p.

Pereira E. D., Souza F. G., Santana C. I., Soares D. Q., Lemos A. S., Menezes L. R. (2013) Influence of magnetic field on the dissolution profile of cotrimoxazole inserted into poly(lactic acid-co-glycolic acid) and maghemite nanocomposites. *Polymer Engineering & Science*, 53(11): 2308–2317

Pereira E. D., Souza F. G. Jr., Pinto J. C.C.S., Cerruti R., Santana C. (2014) Synthesis, characterization and drug delivery profile of magnetic PLGA-PEG-PLGA/maghemite nanocomposite. *Macromolecular Symposia*, 343(1): 18–25

Péres E. U.X., Sousa M. H., Souza F. G. Jr., Machado F., Suarez P. A.Z. (2017) Synthesis and characterization of a new biobased poly(urethane-ester) from ricinoleic acid and its use as biopolymeric matrix for magnetic nanocomposites. *European Journal of Lipid Science and Technology*, 119(10): 1600451

Péres E. U.X., Souza F. G. Jr., Silva F. M., Chaker J. A., Suarez P. A.Z. (2014) Biopolyester from ricinoleic acid: Synthesis, characterization and its use as biopolymeric matrix for magnetic nanocomposites. *Industrial Crops and Products*, 59: 260–267

Pérez A. I., Materón E. M., Zanoni M. V.B., Moreira J. C., Farias P. A.M., Souza F. G. Jr. (2020) Electrochemical detection of sotalol on a magnetographite-epoxy electrode using magnetite nanoparticles. *Pramana – Journal of Physics*, 94(1): 114

Pezzini A. (2017) Text mining: concept, process and applications. *Revista Eletrônica do Alto Vale do itajaí*, 5(8): 058–061

Picciani P. H.S., Souza F. G. Jr., Comerlato N. M., Soares B. G. (2007) A novel material based on polyaniline doped with [Cs][In(dmit)2], (cesium) [bis(1,3-dithiole-2-thione-4,5-dithiolato)indium (III)]. *Synthetic Metals*, 157(24): 1074–1079

Ramon J., Saez V., Souza F. G. Jr., Pinto J., Nele M. (2018) Synthesis and characterization of PEG-PBS copolymers to obtain microspheres with different naproxen release profiles. *Macromolecular Symposia*, 380(1): 1800065

Robinson D. K.R., Lagnau A., Boon W. P.C. (2019) Innovation pathways in additive manufacturing: Methods for tracing emerging and branching paths from rapid prototyping to alternative applications. *Technological Forecasting and Social Change*, 146: 733–750

Rocha Ferreira S., Rodrigues Sena Neto A., de Andrade Silva F., Gomes de Souza F., Dias Toledo Filho R. (2020) The influence of carboxylated styrene butadiene rubber coating on the mechanical performance of vegetable fibers and on their interface with a cement matrix. *Construction and Building Materials*, 262: 120770

Roguszewska M., Parzuchowski P., Rokicki G. (2020) Biopolyol synthesis from ricinoleic acid and epoxy resin. *Przemysł Chemiczny*, 99(1): 78–80

Sá L., Viçosa A., Rocha S., Souza F. G. Jr. (2017) Synthesis and characterization of poly (butylene succinate) -g- poly (vinyl acetate) as ibuprofen drug delivery system. *Current Applied Polymer Science*, 1(2): 159–169

Santos N. de Q. (2004) Bacterial resistence in the context of hospital infection. *Texto & Contexto – Enfermagem*, 13: 64–70

Santos R. D., Ferreira S. R., Oliveira G. E., Silva F. A., Souza F. G. Jr., Filho R. D.T. (2018) Influence of alkaline hornification treatment cycles on the mechanical behavior in curaua fibers. *Macromolecular Symposia*, 381(1): 1800096

Santos R. D., Thomas S., Ferreira S. R., Silva F. A., Combariza M. Y., Blanco-Tirado C., Ovalle-Serrano S.A., Souza F. G. Jr., Oliveira G. E., Toledo Filho R. D. (2021) Molecular grafting of nanoparticles onto sisal fibers – adhesion to cementitious matrices and novel functionalities. *Journal of Molecular Structure*, 1234: 130171

Satam C. C., Daub M., Realff M. J. (2019) Techno-economic analysis of 1,4-butanediol production by a single-step bioconversion process. *Biofuels, Bioproducts and Biorefining*, 13(5): 1261–1273

Si A., Kyzas G. Z., Pal K., Souza F. G. Jr. (2021) Graphene functionalized hybrid nanomaterials for industrial-scale applications: A systematic review. *Journal of Molecular Structure*, 1239: 130518

Si A., Pal K., Kralj S., El-Sayyad G.S., de Souza F. G., Narayanan T. (2020) Sustainable preparation of gold nanoparticles via green chemistry approach for biogenic applications. *Materials Today Chemistry*, 17: 100327

Siddaramaiah, Souza F. G. Jr., Soares B. G., Somashekar R. (2012) Investigation on microstructural behavior of styroflex/polyaniline blends by WAXS. *Journal of Applied Polymer Science*, 124(6): 5097–5105

Singh P., Pandit S., Mokkapati V. R.S.S., Garg A., Ravikumar V., Mijakovic I. (2018) Gold nanoparticles in diagnostics and therapeutics for human cancer. *International Journal of Molecular Sciences*, 19(7): 1979

Smith A. (2005) Biofilms and antibiotic therapy: Is there a role for combating bacterial resistance by the use of novel drug delivery systems? *Advanced Drug Delivery Reviews*, 57(10): 1539–1550

Soares D., Souza F. G. Jr., Freitas R., Soares V., Ferreira L., Ramon J., Oliveira G. E. (2017) Praziquantel release systems based on poly(butylene succinate) / polyethylene glycol nanocomposites. *Current Applied Polymer Science*, 1: 45–51

Sotoudeh A., Darbemamieh G., Goodarzi V., Shojaei S., Asefnejad A. (2021) Tissue engineering needs new biomaterials: Poly(xylitol-dodecanedioic acid)–co-polylactic acid (PXDDA-co-PLA) and its nanocomposites. *European Polymer Journal*, 152: 110469

Souza F. G. Jr., Ferreira A. C., Varela A., Oliveira G. E., Machado F., Pereira E. D., Fernandes E., Pinto J. C., Nele M. (2013) Methodology for determination of magnetic force of polymeric nanocomposites. *Polymer Testing*, 32(8): 1466–1471

Souza F. G. Jr., Marins J. A., Rodrigues C. H.M., Pinto J. C. (2010a) A magnetic composite for cleaning of oil spills on water. *Macromolecular Materials and Engineering*, 295(10): 942–948

Souza F. G. Jr., Marins J., Pinto J., de Oliveira G., Rodrigues C., Lima L. (2010b) Magnetic field sensor based on a maghemite/polyaniline hybrid material. *Journal of Materials Science*, 45(18): 5012–5021

Souza F. G. Jr., Oliveira G. E., Anzai T., Richa P., Cosme T., Nele M., Rodrigues C. H.M., Soares B. G., Pinto J. C. (2009a) A sensor for acid concentration based on cellulose paper sheets modified with polyaniline nanoparticles. *Macromolecular Materials and Engineering*, 294(11): 739–748

Souza F. G. Jr., Oliveira G. E., Lopes M. C. (2012) Environmental recovery by magnetic nanocomposites based on castor oil. *Natural polymers, biopolymers, biomaterials, and their composites, blends, and IPNs. Volume 2*. Thomas S., Ninan N., Mohan S., Francis E. (Eds.) New York, Apple Academic Press, p. 247–262

Souza F. G. Jr., Oliveira G. E., Rodrigues C. H.M., Soares B. G., Nele M., Pinto J. C. (2009b) Natural Brazilian amazonic (curauá) fibers modified with polyaniline nanoparticles. *Macromolecular Materials and Engineering*, 294(8): 484–491

Souza F. G. Jr., Pinto J. C., Rodrigues M. V., Anzai T. K., Richa P., Melo P. A., Nele M., Oliveira G. E., Soares B. G. (2008) New polyaniline/polycardanol conductive blends characterized by FTIR, NIR, and XPS. *Polymer Engineering & Science*, 48(10): 1947–1952

Souza F. G. Jr., Soares B. G., Dahmouche K. (2007) Effect of preparation method on nanoscopic structure of conductive SBS/PANI blends: Study using small-angle X-ray scattering. *Journal of Polymer Science Part B: Polymer Physics*, 45(22): 3069–3077

Sun W., Cai Z., Li Y., Liu F., Fang S., Wang G. (2018) Data processing and text mining technologies on electronic medical records: a review. *Journal of Healthcare Engineering*, 2018: 4302425

Techawinyutham L., Siengchin S., Parameswaranpillai J., Dangtungee R. (2019) Antibacterial and thermomechanical properties of composites of polylactic acid modified with capsicum oleoresin-impregnated nanoporous silica. *Journal of Applied Polymer Science*, 136(31): 47825

Uhrich K. E., Cannizzaro S. M., Langer R. S., Shakesheff K. M. (1999) Polymeric systems for controlled drug release. *Chemical Reviews*, 99(11): 3181–3198

V R., Pal K., Zaheer T., Kalarikkal N., Thomas S., Souza F. G. Jr., Si A. (2020) Gold nanoparticles against respiratory diseases: oncogenic and viral pathogens review. *Therapeutic Delivery*, 11(8): 521–534

Van Eck N. J., Waltman L. (2010) Software survey: VOSviewer, a computer program for bibliometric mapping. *Scientometrics*, 84(2): 523–538

Varela A., Lopes M. C., Delazare T., Oliveira G. E., Souza F. G. Jr. (2012) Magnetic and green resins useful to oil spill cleanup. *Oil: production, consumption and environmental impact*. Xiu S. (ed.) Nova Science Publishers, Inc., p. 1–18

Varela A., Oliveira G., Souza F. G. Jr., Rodrigues C. H.M., Costa M. A.S. (2013) New petroleum absorbers based on cardanol-furfuraldehyde magnetic nanocomposites. *Polymer Engineering & Science*, 53(1): 44–51

Vargas A., Souza F. G. Jr. (2011) Nanocomposites of poly(l-lactic acid) and maghemite for drug delivery of caffeine. *Ceramic Transactions. Volume 228. Biomaterials science – processing, properties,*

and applications. Narayan R., Bandyopadhyay A., Bose S. (eds.) John Wiley & Sons, Inc., Hoboken, NJ, USA, p. 95–105

Veiga-Santos P., Suzuki C. K., Nery K. F., Cereda M. P., Scamparini A. R.P. (2008) Evaluation of optical microscopy efficacy in evaluating cassava starch biofilms microstructure. *LWT – Food Science and Technology*, 41(8): 1506–1513

Veloso de Carvalho F., Pal K., Souza F. G. Jr., Dias Toledo Filho R., Moraes de Almeida T., Daher Pereira E., Thode Filho S., Galal Aboelkheir M., Corrêa Costa V., Ricardo Barbosa de Lima N., da Silveira Maranhão F. (2021) Polyaniline and magnetite on curaua fibers for molecular interface improvement with a cement matrix. *Journal of Molecular Structure*, 1233: 130101

Yue G., Su S., Li N., Shuai M., Lai X., Astruc D., Zhao P. (2016) Gold nanoparticles as sensors in the colorimetric and fluorescence detection of chemical warfare agents. *Coordination Chemistry Reviews*, 311: 75–84

Yusoff N. H., Pal K., Narayanan T., Souza F. G. Jr. (2021) Recent trends on bioplastics synthesis and characterizations: Polylactic acid (PLA) incorporated with tapioca starch for packaging applications. *Journal of Molecular Structure*, 1232: 129954

Zhou X., Huang L., Porter A., Vicente-Gomila J.M. (2019) Tracing the system transformations and innovation pathways of an emerging technology: Solid lipid nanoparticles. *Technological Forecasting and Social Change*, 146: 785–794

Zubkiewicz A., Paszkiewicz S., Szymczyk A. (2021) The effect of annealing on tensile properties of injection molded biopolyesters based on 2,5-furandicarboxylic acid. *Polymer Engineering & Science*, 61(5): 1536–1545

Journal of Siberian Federal University. Biology 2021 14(4): 422–441
~ ~ ~

DOI 10.17516/1997-1389-0362

УДК 577.32:677.46–022.532

Preparation and Properties of Cellulosic Nanomaterials

Alain Dufresne*
Univ. Grenoble Alpes, CNRS, Grenoble INP, LGP2
Grenoble, France

Received 14.06.2021, received in revised form 22.07.2021, accepted 23.08.2021

Abstract. What are the reasons for the effervescence and explosion of the scientific literature during the last decade in the field of cellulosic and other polysaccharide nanomaterials? First, the raw materials are abundant, available in a variety of forms, renewable, non-toxic, low density, and biodegradable. In addition, it is well known that unexpected and attractive properties can be observed when decreasing the size of a material down to the nanoscale. Different forms of cellulose nanomaterials, resulting from a top-down deconstructing strategy (cellulose nanocrystals – CNCs, cellulose nanofibrils – CNFs) or bottom-up strategy (bacterial cellulose – BC), can be prepared. Multiple mechanical shearing actions applied to cellulosic fibers release more or less individually the nanofibrils. A controlled strong acid hydrolysis treatment can be applied to cellulosic fibers allowing the selective dissolution of non-crystalline domains and disengagement of nanocrystalline cellulose regions. The mechanical modulus of crystalline cellulose is the basis of many potential applications. With a Young's modulus of the order of 100–130 GPa and a specific surface of several hundred $m^2 \cdot g^{-1}$, these cellulosic nanomaterials have a significant capacity of reinforcement at low filler content. Several properties reviewed in this article are impacted by the nanoscaling process.

Keywords: cellulose nanocrystals, cellulose nanofibrils, cellulose nanomaterials, production, properties.

Acknowledgements. LGP2 is part of the LabEx Tec 21 (Investissementsd'Avenir – grant agreement No. ANR-11-LABX-0030) and of the PolyNat Carnot Institut (Investissementsd'Avenir – grant agreement No. ANR-11-CARN-030–01).

Citation: Dufresne A. Preparation and properties of cellulosic nanomaterials. J. Sib. Fed. Univ. Biol., 2021, 14(4), 422–441. DOI: 10.17516/1997-1389-0362

* Corresponding author E-mail address: alain.dufresne@pagora.grenoble-inp.fr
ORCID: 0000-0001-8181-1849

Получение и свойства целлюлозных наноматериалов

А. Дюфрен
Университет Гренобль – Альпы
Франция, Гренобль

Аннотация. Каковы причины резкого роста в последнее десятилетие научной литературы в области целлюлозных и других полисахаридных наноматериалов? Во-первых, сырье для получения этих материалов в изобилии, доступно в различных формах и из возобновляемых источников, нетоксично, обладает биоразлагаемостью и низкой плотностью. Кроме того, хорошо известно, что при уменьшении материала до наноразмера могут появляться необычные и привлекательные свойства. С использованием природной целлюлозы можно создавать различные формы целлюлозных наноматериалов: в результате применения стратегии деконструкции «сверху вниз» (нанокристаллы целлюлозы – CNC, нанофибриллы целлюлозы – CNF) или стратегии «снизу вверх» (бактериальная целлюлоза – BC). Многократные механические сдвиговые воздействия на целлюлозные волокна приводят к высвобождению отдельных нанофибрилл. Контролируемый кислотный гидролиз целлюлозы обеспечивает селективное растворение некристаллических доменов и разъединение областей нанокристаллической целлюлозы. Высокие механические свойства кристаллической целлюлозы открывают потенциал для ее использования во многих областях. Благодаря модулю Юнга порядка 100–130 ГПа и высокой удельной поверхности в несколько сотен $м^{2}·г^{-1}$ целлюлозные наноматериалы обладают значительной способностью к армированию при низком содержании наполнителя. В статье рассматриваются свойства целлюлозы, изменяющиеся в процессе наномасштабирования.

Ключевые слова: нанокристаллы целлюлозы, нанофибриллы целлюлозы, целлюлозные наноматериалы, производство, характеристики.

Благодарности. LGP2 является частью LabEx Tec 21 (Investissementsd'Avenir – соглашение о гранте № ANR-11-LABX-0030) и Института Карно PolyNat (Investissementsd'Avenir – соглашение о гранте № ANR-11-CARN-030-01).

Цитирование: Дюфрен, А. Получение и свойства целлюлозных наноматериалов / А. Дюфрен // Журн. Сиб. федер. ун-та. Биология, 2021. 14(4). С. 422–441. DOI: 10.17516/1997-1389-0362

Introduction

Cellulose is an organic compound belonging to the category of polysaccharides. It is the most important material of the plant cell wall. It is also biosynthesized by a number of living organisms including some amoebae, sea animals, bacteria, and fungi. Its chemistry and its structure determine its properties. The cellulose molecule is a monotone polymer made of glucose units linked in β-1,4 (Fig. 1). As a result of the β-1,4 glycosidic bond, the homologous functions of the monomers are alternately above and below

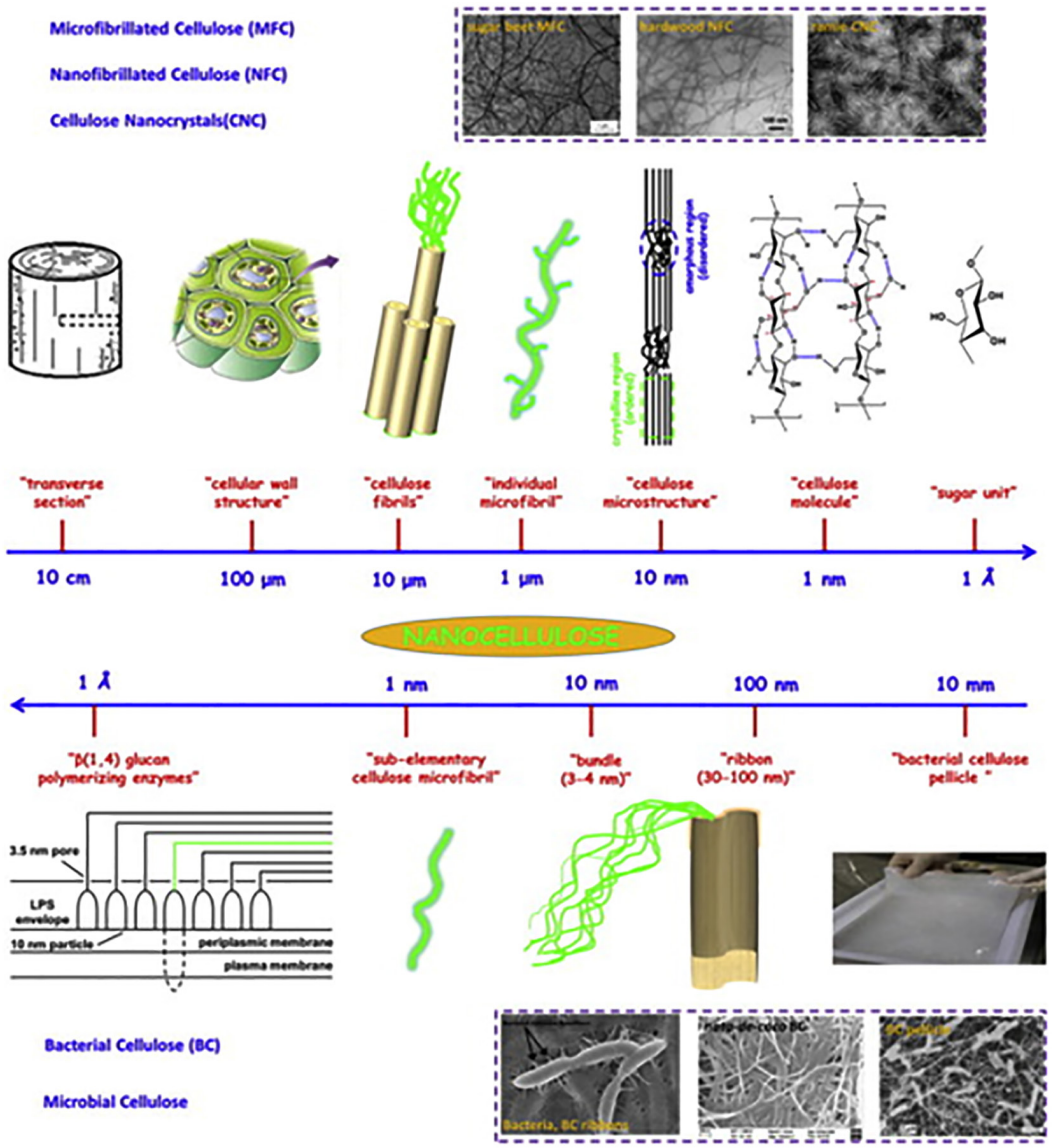

Fig. 1. Hierarchical structure and multi-level organization of cellulose; top image (from large unit to small unit): cellulose nanocrystals (CNC), micro/nanofibrillated cellulose (MFC and CNF/NFC); bottom image (from tiny unit to small unit): bacterial cellulose (BC) (Lin, Dufresne, 2014a)

the plane. The molecule is thus linear and its flexibility comes from the degree of freedom at each bond. Each glucose bears three hydroxyl groups, and their ability to form hydrogen bonds plays a major role in directing the crystalline packing and governing the physical properties of cellulose. The flexibility of the cellulose molecule is therefore limited by the regular formation of intramolecular H-bonds, and this linear molecule then becomes more rigid and resistant. Intermolecular H-bonds can also develop and allow the formation of numerous molecular assemblies (microfibrils) with diameters ranging from 2 to 20 nm, which are even more rigid and resistant. These intermolecular H-bonds are so strong that the glass transition and melting points of dry cellulose usually observed for semi-crystalline polymers occur at temperatures

higher than the degradation temperature. The degradation of cellulose occurs around 220 °C but its color already starts to become yellow-brown at 180 °C under ambient conditions because of a loss of chemical stability.

Cellulose acts as a structural element and provides rigidity to the plant cells. The high tensile strength of cellulose fibers present in the plant cell wall is responsible for maintaining the shape and rigidity of plant cells. It is due to such strong cellulose fibers in the cell wall that plant cells do not burst like animal cells when placed in a hypotonic solution. The purest form of plant cellulose is cotton, which contains around 98 % cellulose. Besides, cellulose is also present in wood obtained from the trees, which is approximately 40–50 wt% cellulose with about half in nanocrystalline form and half in non-crystalline form. Wood and plants are cellular hierarchical biocomposites designed by nature, basically consisting of an amorphous matrix composed of hemicellulose, lignin, waxes, extractives, and trace elements reinforced by semicrystalline cellulose microfibrils. Lignocellulosic fibers consist therefore of a cemented microfibril aggregate. The hierarchical struture and multi-level organization of cellulose is reported in Figure 1. The structure of plants spans many length scales, in order to provide maximum strength with a minimum of material. Cellulose has been used for centuries in different industries for the welfare of mankind. It is used to make paper, cardboards, and other paper products. In the textile industry, different clothes are made using cotton and other plant fibers. It is also used to make electrical insulation paper in the electric industry, bio-fuel, gunpowder. Cellulose can be used as a stabilizer in different drugs and as a stationary phase for chromatography in biological labs. More recently, the recognition that, by suitable chemical and mechanical treatments, it is possible to produce fibrous materials with at least one dimension in the nanometer range from any naturally occurring source of cellulose has been emphasized and it opens the door to new applications because of specific properties in the nanoscale.

Preparation of cellulosic nanomaterials

Nanomaterials describe materials for which a size (in at least one dimension) ranges between 1 and 100 nm according to the usual definition of nanoscale. Biological systems often feature natural, functional nanomaterials. Accordingly, the synthesis method should allow controlling the size of the material within this range. These methods are usually divided into two main types, «bottom up» and «top down». Nanocellulose is often used as an umbrella and general term for the different types of nano- and micro-sized cellulosic particles (Lavoine et al., 2012). Based on their dimensions and preparation methods, nanocelluloses may be classified in three main subcategories (Table 1).

Top-down approach

In this approach, the starting material consists of micrometer lignocellulosic fibers. As for most cellulosic sources this material is intimately tied to other materials, removal of most of the non-cellulosic components from the natural fiber is generally performed. It usually involves an alkali extraction, during which soluble polysaccharides such as low molecular weight hemicelluloses and other extractives are dissolved in what is called the black liquor. Bleaching with sodium chlorite ($NaClO_2$) solution in a buffer medium under mechanical stirring generally follows to remove most of the residual phenolic molecules like lignin or polyphenols and proteins. This process converts the brown pulp to a white material. It is associated with a decrease

Table 1. The family of cellulose nanomaterials (adapted from (Klemm et al., 2011)

Type of nanocellulose	Synonyms	Typical sources	Formation and average dimensions
Cellulose nanofibrils (CNF)	Microfibrillated cellulose (MFC), cellulose nanofibers, nanofibrillar cellulose (NFC), nanofibrillated cellulose	Wood, sugar beet, potato tuber, hemp, flax	Delamination of the pulp by mechanical treatment after chemical or enzymatic treatment Diameter: 5–100 nm Length: several μm
Cellulose nanocrystals (CNC)	Cellulose crystallites, nanocrystalline cellulose, rod-like cellulose microcrystals	Wood, cotton, hemp, flax, wheat straw ramie, microcrystalline cellulose, tunicate, bacterial cellulose	Acid hydrolysis Diameter: 5–70 nm Length: 100–1000 nm
Bacterial cellulose (BC)	Bacterial nanocellulose, microbial cellulose, biocellulose	Low molecular weight sugars, alcohols	Bacterial synthesis Diameter: 20–100 nm

in the diameter of the fiber due to the removal of the cementing materials, an increase in the crystallinity index, and an increase in thermal stability due to the removal of poorly thermally stable hemicelluloses. This purified material can be subsequently submitted to a mechanically- or chemically-induced deconstructing treatment to decrease its size to the nanoscale.

Mechanically-induced deconstructing strategy. After the purification step, the cellulose fibers consist of fibril aggregates made of strongly interacting bundles of parallel glucan chains, which are the smallest discernable building blocks of cellulose I (native cellulose) as shown in Figure 1. A mechanically-induced deconstructing treatment involving strong multiple mechanical shearing actions can be applied to diluted aqueous dispersions of cellulose fibers in order to release more or less individually these fibrils. Different terminologies are used to describe the material resulting from the cellulose fiber fibrillation process, sometimes leading to misunderstanding and ambiguities. The resulting material was denoted microfibrillated cellulose (MFC) in the pioneering work reported in 1983 (Herrick et al., 1983; Turbak et al., 1983). This terminology is now usually limited to materials with a broad size distribution of the fibers, from the nanoscale to bigger fibers, forming a network structure and interconnected to each other. Other terms, such as cellulose nanofibers, nanofibrillar cellulose, cellulose nanofibrils (CNFs), and nanofibrillated cellulose are used when the material is more in the nanoscale than in the microscale and exhibits a narrow size distribution.

Different equipment can be used to induce the fibrillation of cellulose fibers including homogenizing (Dufresne et al., 2000; Malainine et al., 2005; Zuluaga et al., 2007; Ferrer et al., 2012), grinding (Taniguchi, Okamura, 1998; Iwamoto et al., 2007), cryocrushing (Chakraborty et al., 2005), high-intensity ultrasonication (Cheng et al., 2007; Chen et al., 2011), aqueous counter collision (Kondo et al., 2014; Tsuboi et al., 2014), ball milling (Zhang et al., 2015; Nuruddin et al., 2016), and twin-screw extrusion (Cobut et al., 2014; Ho et al., 2015). A detailed description of these different techniques can be found elsewhere (Dufresne, 2017a). Among these different methods, homogenizing and grinding are the most commonly used for the preparation

of CNFs and the most effective for the scaling production of CNFs at present.

The yield of these processes is close to 100 %, but this production route through mechanically-induced deconstruction is normally connected to high energy consumptions associated with the fiber delamination. A renewed interest has emerged when different pretreatments were proposed to obtain fibers that are less stiff and cohesive, thus decreasing the energy needed for fibrillation, as detailed in (Lavoine et al., 2012). Three different strategies were basically proposed: (i) limiting the hydrogen bonding in the system, and/or (ii) adding a repulsive charge, and/or (iii) decreasing the degree of polymerization (DP) or the non-crystalline link between individual fibrils. The most popular pretreatments are enzymatic hydrolysis, 2,2,6,6-tetramethylpiperidine-1-oxyl (TEMPO)-mediated oxidation, and carboxymethylation/acetylation. For the enzymatic hydrolysis pretreatment, it was reported that monocomponent endoglucanase is more efficient to facilitate the fibrillation of the pulp (Rosgaard et al., 2007). TEMPO-oxidation and carboxymethylation pretreatments induce negatively charged groups into cellulosic fibers, improving their delamination. The typical oxidation system for cellulose is TEMPO/NaBr/NaClO (Saito et al., 2006), which has been extensively used for the pretreatment of raw cellulose materials before mechanical disintegration. During the reaction, the primary alcohol groups are first oxidized to aldehydes and further converted to carboxyl groups. At the same time, the depolymerization phenomenon of cellulose occurs. TEMPO/$NaClO/NaClO_2$ system was also applied, which overcame the depolymerization (Saito et al., 2009). For carboxymethylation, it was shown that a pH higher than 10 is required to dissociate all the charges of the microfibrils (Wågberg et al., 2008). Other pretreatments such as periodate-chlorite oxidation (Liimatainen et al., 2012), oxidative sulfonation (Liimatainen et al., 2013), cationization (Aulin et al., 2010; Olszewska et al., 2011; Ho et al., 2011), ionic liquids (Li et al., 2012; Ninomiya et al., 2018), and deep eutectic solvent (Li et al., 2017) have been reported.

Morphologically, CNF occurs as a highly viscous suspension (Fig. 2a) and consists of long entangled filaments made of both individual nanofibrils and microfibril bundles as shown in Figure 2b. The particle diameter is generally in the range 5–30 nm, and the length, which is more difficult to determine, is supposed to be in the range 1–10 μm. MFC prepared without pretreatment of the initial pulp consists of coarser nanofibers with a diameter ranging from 10 to 100 nm forming a 3D network (Fig. 2c).

Chemically-induced deconstructing strategy. Cellulose nanomaterials can also be prepared through acid hydrolysis or enzymatic treatment of cellulose under controlled conditions. The acid hydrolysis process is based on the difference in accessibility of hydronium ions in the crystallized and non-crystallized zones of cellulose. It induces the dissolution of non-crystalline domains, due to the easier penetration of hydronium ions within the non-crystalline cellulosic regions, promoting the hydrolytic cleavage of the glycosidic bonds and release of individual crystallites (Nickerson, Habrle, 1947). Different descriptors are used to describe the material resulting from this process. It includes cellulose whiskers, cellulose nanowhiskers, nanocrystalline cellulose, and cellulose nanocrystals (CNCs), the latter being the most commonly used.

CNCs are generally obtained through mineral acid hydrolysis of cellulose pulp under very harsh reaction conditions, which usually require concentrated acid. Sulfuric acid is generally preferred as it produces negatively charged sulfate ester groups at the surface of released crystals,

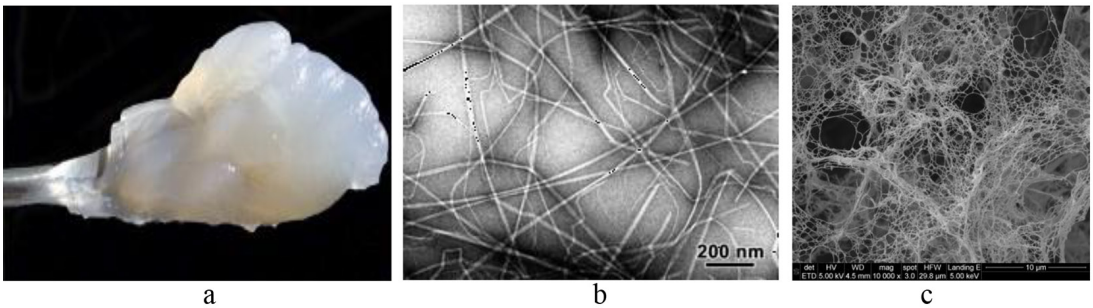

Fig. 2. CNF morphologically: (a) Appearance of a 2 wt% CNF suspension obtained from enzymatically pretreated eucalyptus showing its gel-like behavior (Lavoine et al., 2012); (b) TEM for CNF obtained by fibrillation of TEMPO-oxidized tunicin fibers (Saito et al., 2006); (c) SEM for MFC mechanically isolated from oat straw cellulose powder (Tingaut et al., 2011)

resulting in improved electrostatic stabilization of the suspension. At the same time, it decreases the thermal stability of the nanoparticles. In general, the hydrolysis process is performed at sulfuric acid concentration of 60–65 %, reaction temperature of 40–50 °C, and reaction time in the range 30–60 min. CNCs with increased thermal stability but a higher tendency to flocculation can be prepared using hydrochloric acid. Phosphoric (Camarero Espinosa et al., 2013), hydrobromic (Lee et al., 2009), nitric (Liu et al., 2010), phosphotungstic (Liu et al., 2014), and formic acids (Li et al., 2015) have also been reported for the preparation of CNCs. Using the mineral acid hydrolysis strategy to produce CNCs is a simple method that has been used at pilot scale and even in a demonstration plant. It has some drawbacks, such as the problem of corrosion of the equipment resulting in high production cost, and the generation of a large amount of residual acid and other pollutants during the acid hydrolysis process, which are very difficult to dispose of and recover. The enzymatic hydrolysis process for obtaining CNCs requires longer time. Other processes have been proposed for the preparation of CNCs. These include TEMPO oxidation (Hirota et al., 2010), hydrolysis with gaseous acid (Pääkkönen et al., 2018), ionic liquid (Man et al., 2011), ammonium persulfate oxidation (Leung et al., 2011), periodate oxidation (Yang et al., 2013), ultrasonication-assisted $FeCl_3$-catalyzed hydrolysis (Lu et al., 2014), liquefaction (Kunaver et al., 2016), and acid deep eutectic solvents (Sirviö et al., 2016). The yield of CNCs prepared via acid hydrolysis is generally quite lower, in the order of 30 % (Dufresne, 2017a). Morphologically, CNC occurs as a suspension that exhibits the formation of birefringent domains when observed in polarized light between cross-nicols (Fig. 3a). This behavior results from two origins: (i) a structural form anisotropy of cellulose (anisotropic refractive index, $\Delta n \sim 0.05$) and (ii) a flow anisotropy resulting from the alignment of the nanorods under flow generally operated before observation. Each nanocrystal consists of straight rod-like or needle-like nanoparticles (Fig. 3b). The dimensions of these nanorods are governed by the source of cellulose, hydrolysis conditions, and ionic strength. The length is typically of the order of a few hundreds of nanometers and the width is of the order of a few nanometers.

Bottom-up approach

The bottom-up, or self-assembly, approach to nanofabrication uses chemical or physical forces operating at the nanoscale to assemble basic units into more complex and larger structures. For the production of nanocellulose,

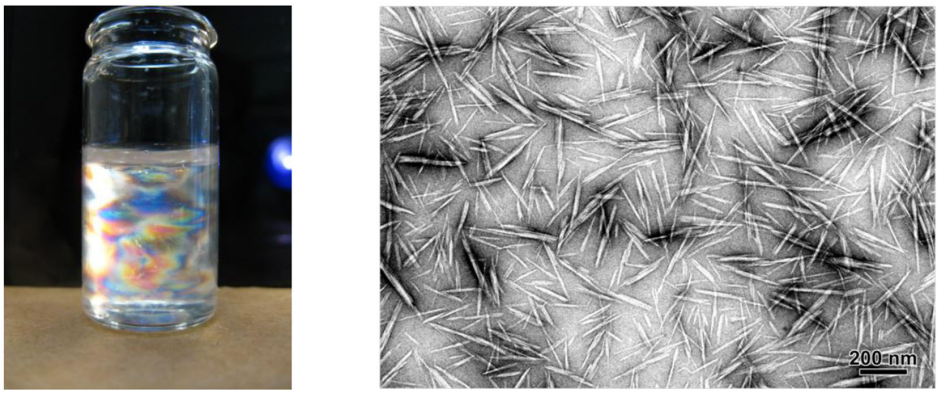

a b

Fig. 3. (a) Photograph of a diluted aqueous suspension of CNC (0.50 wt%) obtained by H_2SO_4 hydrolysis of capim dourado fibers observed between cross-nicols showing the formation of birefringent domains (Siqueira et al., 2010); (b) TEM from a dilute suspension of CNC obtained by H_2SO_4 hydrolysis of ramie fibers showing both individual and laterally associated crystallites (Habibi et al., 2008)

it utilizes the ability of some bacteria to produce cellulose from a wide range of carbon and nitrogen sources. These include Gram-negative species such as *Acetobacter*, *Azotobacter*, *Rhizobium*, *Pseudomonas*, *Salmonella*, and *Alcaligenes* and Gram-positive species such as *Sarcina ventriculi*. The most effective producer of cellulose is *Acetobacter xylinum*. Historically, bacterial cellulose (BC) has been limited to the manufacture of Nata de coco, a South-East Asian food product (Iguchi et al., 2000).

The production of BC is based on a process involving dual couple steps, *viz.* polymerization and crystallization. Glucose residues polymerize to β-1,4 glucan linear chains in the bacterial cytoplasm and are extracellularly secreted. The developed chains crystallize into microfibrils, and then some microfibrils consolidate to materialize a highly pure 3D porous network of entangled nanoribbons 20–60 nm wide (Fig. 1). Compared to plant cellulose, BC is produced in a pure form, free of lignin, pectin, and hemicelluloses, and no purification treatment is needed. Under static culture conditions, these ribbons and associated cells form a 3D-nanofibrilar floating pellicle that allows the non-mobile, strictly aerobic bacteria to grow in the top oxygen-rich interface of the growth medium. Under agitated and/or aerated conditions, BC is obtained in the form of fleeces with variable size.

Properties of cellulose in the nanoscale

When decreasing the size of a material down to the nanoscale, some properties are altered compared to its microscale form. These modifications can strengthen the use of cellulose and broaden its applications to new markets. The main properties of cellulose that are amended in the nanoscale are collected in Table 2 and detailed in the following sections.

Specific surface area

The specific surface area of a solid material refers to the total surface area of a material per unit of mass. When decreasing the size of a material, it obviously increases due to the increase in the surface-to-volume ratio. It is usually measured by gas adsorption using the BET (Brunauer-Emmett-Teller) isotherm with nitrogen as adsorbate. However, this method requires completely dried samples, resulting in the collapse of the

Table 2. Properties of cellulose in the nanoscale

Property	Modification compared to microscale	Reason	Market
Specific surface area	Huge increase	Nanosize, high surface-to-volume ratio	Paper and cardboard, composites, packaging, pharmaceutics, membranes, hydrogels, aerogels
Stiffness	Improvement	Reduction of defects	Paper and cardboard, composites, packaging
Aspect ratio	Broad range	Different preparation techniques	Composites
Thermal properties	Lower coefficient of thermal expansion	Crystallinity, ability to form a dense network	Electronics, sensors
Rheological properties	High viscosity of the suspension, shear-thinning behavior	High specific surface area, high density of surface hydroxyl groups	Food, cosmetics, oil, construction, paper & cardboards, paints, coatings, inks
Optical properties	Transparency, iridescence	Nanosize, rod-like morphology, birefringence	Electronics, packaging, paper, cultural heritage, inks, coatings, cosmetics
Barrier properties	Improvement in dry conditions	Nanosize, crystallinity, ability to form a dense network	Packaging
Functionalization	Wide range	High density of surface hydroxyl groups	Composites, filtration, biomedical, hygiene

pores, irreversible hydrogen bonding, and hornification, leading to an underestimation of the specific surface area. Nuclear magnetic resonance (NMR) approach provides a good first approximation for the specific surface area of cellulose nanomaterials and overcomes the limitations of BET measurements for highly aggregated samples (Brinkmann et al., 2016). A method based on xyloglucan adsorption was also proposed (Moser et al., 2018). The specific surface area of cellulose nanomaterials can be estimated from the average geometrical dimensions of the nanoparticles, assuming a rod-like geometry and a density ρ of 1.5 $g \cdot cm^{-3}$ for crystalline cellulose. Figure 4 shows the evolution of the specific surface area as a function of the diameter of rod-like nanoparticles. A sharp increase is observed when the diameter drops below a value of 20 nm, which corresponds to the diameter range of most cellulose nanomaterials.

The specific surface area of cellulose nanomaterials plays a crucial role in determining the fiber-fiber interaction, which is an important parameter for the tensile strength of paper and for stress transfer from the matrix to the reinforcement in composite applications. It also affects the chemical reactivity and promotes an efficient surface functionalization. Active packaging where cellulose nanomaterials can serve as carriers of active substances such as antioxidants and antimicrobials can be developed.

This high specific surface area coupled with the low concentration of the suspensions allows the preparation of hydrogels and highly porous aerogels (by removal of the aqueous phase by e. g. freeze-drying), which can be used as porous templates. The aerogel network can be chemically modified to tune its wetting properties towards non-polar liquids/oils. It can also be impregnated with different precursors, which can readily

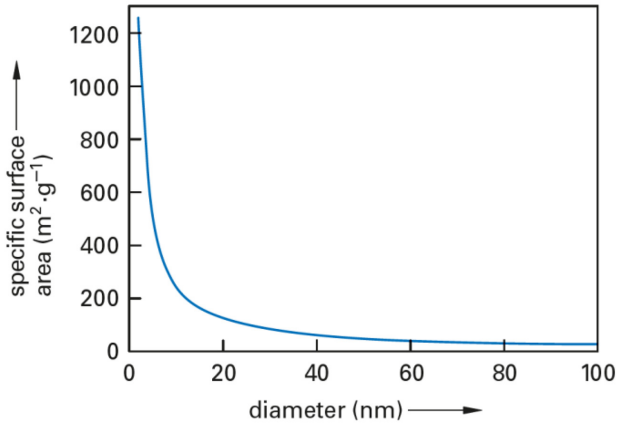

Fig. 4. Evolution of the specific surface area for cellulose rod-like nanoparticles as a function of their diameter, assuming a density of 1.5 g·cm^{-3} for crystalline cellulose (Dufresne, 2017a)

be transformed into functional nanoparticles. Nanopapers fabricated by filtration or casting-evaporation can be used in the sensors sector since they can maintain their 3D structure in water. They can also be used for the development of high capacity retention filters and membranes for the removal of contaminants.

Stiffness and strength

Cellulose serves as structural element in nature and confers mechanical properties to higher plant cells. Plant fibers have a length ranging from few mm to several cm and their diameter is in the order of 20–40 μm. The formation of defects in a material adversely affects its mechanical properties, but the probability of their occurrence decreases when the size of the material is reduced. The extraction of cellulose at the nanoscale is therefore beneficial to improving the stiffness and strength of the fiber. The mechanical modulus of cellulose nanomaterials is probably their main asset, and it is the basis of many potential applications, including the reinforcement of polymer composites and improvement of the durability and scratch resistance of water-based paints and varnishes. The tensile modulus and strength of single cellulose I crystal has been estimated both experimentally and theoretically. Average values of 130 GPa and 10 GPa, respectively, were reported (Dufresne, 2017b). The tensile modulus is slightly lower (100 GPa) for CNF because of its lower crystallinity. Enhanced mechanical properties and fracture characteristics of concrete were reported, with the ability of cellulose nanomaterials to arrest micro-cracks formed during hydration and to prevent their further growth. In composite applications, density is also an important parameter to consider. It can be reflected through the specific tensile modulus, which is the ratio between the tensile modulus and the density. Considering a density around 1.5–1.6 g·cm^{-3} for crystalline cellulose, the specific modulus for CNC and CNF was found around 85 and 65 J·g^{-1}, respectively, much higher than for steel (25 J·g^{-1}) or glass (27 J·g^{-1}) (Dufresne, 2013).

Aspect ratio

The aspect ratio of rod-like particles is defined as the length-to-diameter ratio. This parameter is difficult to precisely determine for CNF due to its flexibility and difficulties associated with the determination of its length, but it is considered to be very high. It is easier to quantify for CNC, and its value is found to mainly depend on both the source of cellulose

and hydrolysis conditions. Low values around 10 are reported for cotton, and for most cellulosic sources, it ranges between 10 and 30 (Dufresne, 2017a). For specific sources of cellulose, higher aspect ratio CNCs have been obtained, e. g. close to 70 for tunicin (Anglès, Dufresne, 2000) or capimdourado (golden grass) (Siqueira et al., 2010). The value of the aspect ratio determines the anisotropic phase formation and reinforcing properties of CNC.

In composite science, the concept of critical aspect ratio is well-known and is an indicator of the amount of stress transferred to the fiber. Below this critical aspect ratio, insufficient stress is transferred and the reinforcement is inefficient. For cellulose nanomaterial reinforced nanocomposites, the impact of aspect ratio is even more relevant. It was shown in the pioneering work in this research area (Favier et al., 1995) that the mechanical behavior of these materials is linked to the formation of a rigid continuous network of H-bonded nanoparticles. Above a critical volume fraction, defined as the percolation threshold, whose value decreases as the aspect ratio of the nano-rods increases, an unusual and exceptional strengthening effect was reported. A high value of the aspect ratio is therefore necessary to decrease the percolation threshold, which guarantees a high reinforcing effect for lower nanofiller contents. Moreover, it was shown that when increasing the aspect ratio of individual CNC, the stiffness of the percolating network increases (Bras et al., 2011), further increasing the mechanical reinforcement effect. These effects are illustrated in Figure 5, which shows the evolution of the storage modulus in the rubbery state of the matrix as a function of CNC content for nanocomposites obtained by mixing poly(styrene-co-butyl acrylate) (poly(S-co-BuA)) with CNCs extracted from *Posidonia oceanica* balls and leaves, with an aspect ratio of 35 and 75, respectively (Bettaieb et al., 2015).

Thermal properties

Compared to inorganic materials, organic compounds have limited thermal stability, due to the low polar character of C–C and C–H bonds. This can restrict the use of cellulose and manufacturing conditions of its composites at

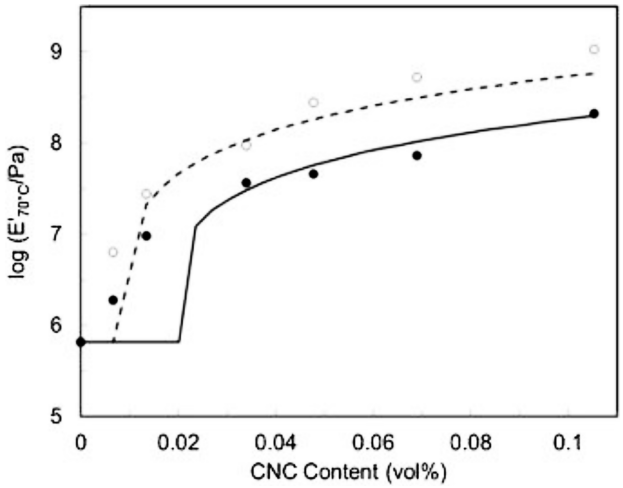

Fig. 5. Evolution of the logarithm of the tensile storage modulus at 70 °C (Tg + 40 °C) for poly(S-co-BuA) versus CNC content: experimental data for CNC extracted from *Posidonia oceanica* balls (●, aspect ratio 35) and leaves (○, aspect ratio 75), and predicted data from the percolation approach for CNC extracted from *Posidonia oceanica* balls (solid line) and leaves (dashed line) (Bettaieb et al., 2015)

high temperatures. This issue is even more critical for H_2SO_4-hydrolyzed CNC, for which some of the surface hydroxyl groups are substituted with charged sulfate groups ($–OSO_3^-$) that lower its thermal stability (Lin, Dufresne, 2014b). The amount of charged sulfate groups on the crystal surface can be controlled or changed in different ways, either during the sulfuric acid hydrolysis or afterwards.

An interesting thermal property benefiting from the size reduction of cellulose to the nanoscale is its very low coefficient of thermal expansion (CTE) when in film form. This is attributed to both the enhanced crystallinity and strength of the cellulose nanomaterial network interactions (Sheltami et al., 2017). This feature can be used to reduce the CTE of polymer nanocomposite sheets assuming that the strength of the network is strong enough to restrict the thermal expansion of the matrix (Yang et al., 2015).

This low CTE value of cellulose nanomaterial films associated with transparency, lightweight, resistance, and flexibility make them potentially useful in electronics and sensors applications to replace plastic of glass for flexible display panels and electronic devices, e. g. mobile phones, computers, TVs, touch sensors, solar cells, and paper-based generators.

Rheological properties

Cellulose nanomaterials are produced and commonly used in the form of aqueous dispersions, and highly viscous suspensions are obtained as shown in Figure 2a for CNF. This highly viscous behavior results from the high specific surface area of cellulose nanomaterials and ensuing huge amount of surface hydroxyl groups that can interact with the surrounding medium. In addition, the fibrils tend to form a continuous and strong network that resists flow effectively. A gel-like behavior of cellulose nanomaterial suspensions at low solid content is observed. It has been found that the higher the concentration, the higher the viscosity. Cellulose nanomaterial suspensions can therefore be good stabilizing agents for emulsions or suspensions since they can trap particles or droplets in the network, preventing them from settling or floating.

The shear rheology flow curve for CNC suspensions is concentration-dependent and usually exhibits three distinct zones (Bercea, Navard, 2000; Ureña-Benavides et al., 2011; Shafiei-Sabet et al., 2012) as shown in Figure 6. At low concentrations, the viscosity is mostly constant, indicating a Newtonian behavior, and a slight shear-thinning behavior is observed when increasing the shear rate. At higher concentrations, where the suspensions become lyotropic, a typical behavior of liquid crystalline polymers in solutions is generally reported. Shear-thinning is first observed at the lowest shear rates, followed by a viscosity plateau region and then another shear thinning region at higher shear rates. The first shear thinning region has been attributed to the breaking of aggregated domains or clusters. The plateau region indicates that the microstructure of the CNC suspension remains unchanged until a sufficiently high shear flow is applied allowing the alignment of individual particles, which corresponds to the second shear thinning region. At higher concentrations (corresponding to a gel), the viscosity depends on the shear rate according to a power-law relation across the entire shear rate range, a typical gel behavior. Ultrasound treatment severely affects the viscosity of CNC suspensions as shown in Figure 6. Increasing the amount of applied ultrasound energy significantly decreases the viscosity of the sample.

The rheological behavior of CNF suspensions has also been studied, but since it consists of

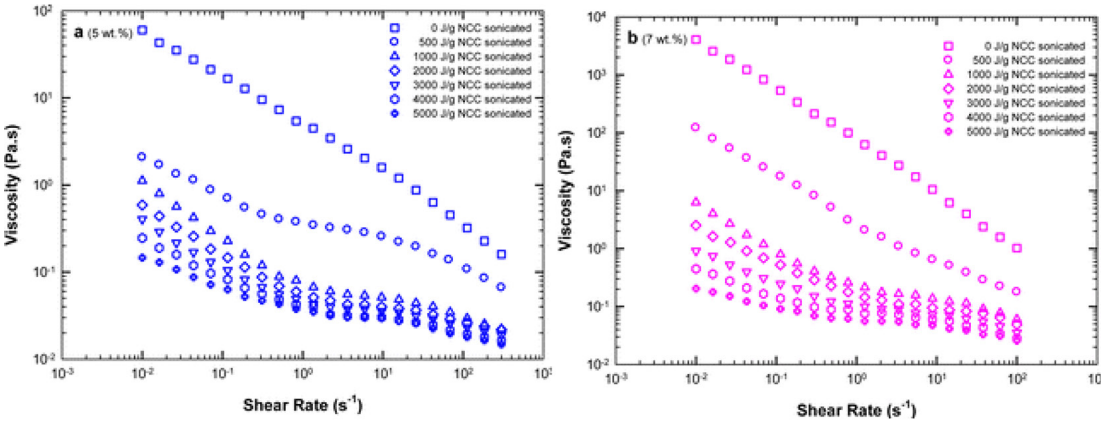

Fig. 6. Effect of ultrasound energy input (level of sonication) on the viscosity for (a) 5 wt% and (b) 7 wt% CNC suspensions prepared from black spruce kraft pulp (Shafiei-Sabet et al., 2012)

aggregated fibril bundles and long fibers of large size variations, it is therefore difficult to perform accurate and reproducible rheological studies (Pääkkö et al., 2007; Iotti et al., 2011; Schenker et al., 2019). Wall slip, heterogeneous flow, and flocculation may occur during the measurement process, which impacts the reproducibility and the reliability of the results (Nazari et al., 2016). The rheological behavior of cellulose nanomaterial suspensions associated with their natural origin opens up potential applications in various sectors. These include the food industry, where they can be used as rheological modifier and fat replacer and low-calorie substitute for carbohydrate additives used as gelling agents, flavor carrier, or stabilizer. In the cosmetics industry, they can be a valuable ingredient providing texture that improves a product's feel in facial and body applications. The rheological properties of cellulose nanomaterial dispersions can find potential applications in cosmetic products for hair, eyelashes, eyebrows, or nails. The paper and cardboard or coating industries can benefit from their ability to stabilize fillers and adsorb dyes. The addition of cellulose nanomaterials to cement and concrete mixes can accelerate the hydration process of cement cure and alter the rheology.

Optical properties

Due to the nanoscale of cellulose nanomaterials, transparent films (nanopapers) or coatings can be obtained if the nanoparticles are densely packed, and the interstices between the fibers are small enough to avoid light scattering. These optically transparent films can find applications in packaging, for flexible device substrates, or for conservation and restoration of cultural heritage serving for filling paper losses on cultural objects and a stabilizing agent for paper. Transparent composite films can also be obtained by impregnating the CNF/CNC film with a transparent resin or mixing if the difference in refractive index between both components is small and/or the domain sizes in the different phases are smaller than the wavelength of visible light. Examples of transparent composite films consisting of poly(lactide) (PLA) and CNC prepared from microcrystalline cellulose (MCC) are shown in Figure 7.

At sufficiently high concentrations, CNC suspensions self-organize into a chiral nematic (cholesteric) liquid crystal phase with a helical arrangement. After slow evaporation of the suspension, semi-translucent films that retain this self-assembled chiral nematic liquid crystalline order formed in the suspension can be produced,

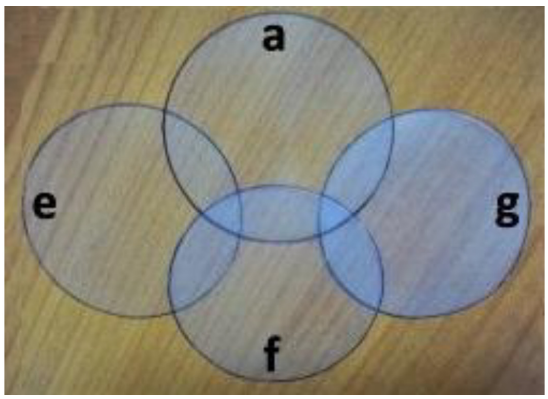

Fig. 7. Optically transparent composite films made of neat poly(lactide) (PLA) (a) and PLA reinforced with 2.5wt% (e), 7.5 wt% (f) and 15 wt% (g) CNC grafted by n-octadecyl-isocyanate (Espino-Pérez et al., 2013)

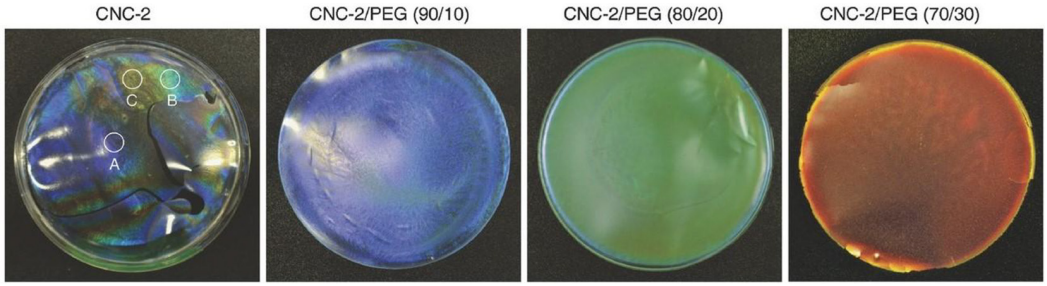

Fig. 8. Photographs of neat CNC and CNC/PEG (PEG content varying from 10 to 30 wt%) composite films showing various structural colors under white light illumination (Yao et al., 2017)

and then CNCs can form chiral nematic, iridescent, colored films. This chiral nematic organization of CNCs is always left-handed and thus, chiral nematic CNC films selectively reflect left-handed light and appear colorful when the helicoidal pitch is of the order of magnitude of the wavelength of visible light, giving a photonic band gap. The pitch can be controlled through ionic strength, temperature, concentration, relative humidity, sulfur content, and exposure to magnetic field or ultrasonic treatment, allowing modulating the film color. Photonic composite films with uniform brilliant structure colors from blue to red were also prepared by assembly of poly(ethylene glycol) (PEG) (Fig. 8). These iridescence properties can be exploited in security papers, birefringent inks, coatings, and cosmetics.

Barrier properties

Nanoscale dimensions and high specific surface area of cellulose nanomaterials can impart improved barrier properties when used as self-standing films, coating for polymers and paper, or reinforcement in polymer composites due to a tortuosity effect towards diffusing gazes. Their high crystallinity and ability to form a dense percolating network strengthen this effect. However, because of their inherent hydrophilic nature, they are generally poor moisture barrier. When exposed to water vapor, the water molecules adsorb in the material and increase the fractional free volume of the film serving as a moving carrier for gases. Under dry conditions (below 70 % RH), good oxygen barrier is observed. Improved performance of such materials can be optimized by tailoring the morphology and

surface chemistry of cellulose nanomaterials or sandwiching them with high moisture-resistant polymers (Wang et al., 2018). The edibility, flexibility, biodegradability, transparency, and possibility to develop active packaging, as cellulose nanomaterials can serve as carriers of some active substances such as antioxidants and antimicrobials, are additional motivations for their use in the packaging field. However, a key need is the achievement of an adequate resistance of cellulose nanomaterial-based packaging films to water vapor and moisture.

Functionalization

Since the cellulose molecule contains many reactive hydroxyl groups, it can be easily chemically modified to impart it specific properties. As a carbohydrate, the chemistry of cellulose is primarily the chemistry of alcohols, and it forms many of the common derivatives of alcohols, such as esters, ethers, etc. It is well-known that the hydroxyl group at the 6 position can react ten times faster than the other OH groups. In order to keep the structural integrity of cellulose nanomaterials, their functionalization needs to be limited to their surface. It is therefore necessary to perform the chemical grafting process in mild conditions, avoiding swelling media and peeling effect of surface-grafted chains inducing their dissolution in the reaction medium.

Because of the nanoscale dimensions of cellulose nanomaterials, the impact of surface functionalization is intensified by the prevalence of surface OH groups. A broad range of opportunities to develop new functional nanomaterials via a chemical reaction strategy, but also through physical methods may be considered (Lin et al., 2012). The surface of charged cellulose nanomaterials, e. g. H_2SO_4-hydrolyzed CNC, can also be tuned profitably using the charged groups through ionic adsorption. A broad range of functionalization methods, including coupling of hydrophobic small molecules, grafting of polymers and oligomers, and adsorption of hydrophobic compounds onto the surface hydroxyl groups of cellulosic nanomaterials, can be used. The most common surface covalent functionalization strategies of CNCs are reported in Figure 9.

The objective of these modifications is to make available cellulose nanomaterials that can be used as reinforcing agents in composite materials or can contribute to specific functions for the development of new nanomaterials, with the target of expanding their applications in the field of functional nanomaterials. Impacted sectors include filtration, biomedicine, and hygiene.

Conclusions

Cellulose is the most abundant polymer on Earth, and it has been widely used for centuries in industries such as paper, textile, chemical, and biomedical among others. The applications of this abundant and renewable bioresource can be further broadened by transforming it into a nanomaterial. Both mechanical and chemical methods can be used to prepare cellulose nanomaterials using a top-down strategy. A bottom-up strategy can also be applied. Cellulose nanomaterials exhibit specific properties, which are described in this manuscript, such as improved mechanical, thermal, and barrier properties, increased specific surface and aspect ratio, special rheological and optical properties, and magnification of the impact of surface functionalization. Individually or together, these distinguishable properties have the potential to provide new applications for cellulose. The industrial production and commercialization of cellulose nanomaterials are increasing rapidly, and several companies are already producing them at the scale of tons per day. Nevertheless, extraction of cellulosic nanomaterials remains

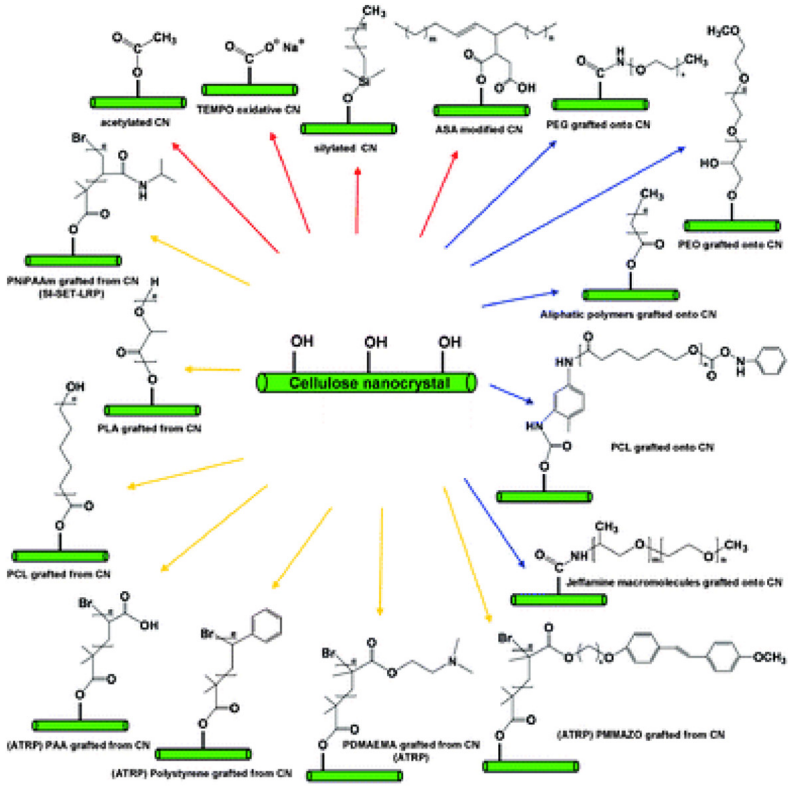

Fig. 9. Common surface covalent chemical modifications of cellulose nanocrystals. PEG: poly(ethylene glycol); PEO: poly(ethylene oxide); PLA: poly(lactic acid); PAA: poly(acrylic acid); PNiPAAm: poly(*N*-isopropylacrylamide); PDMAEMA: poly(*N*, *N*-dimethylaminoethyl methacrylate) (Lin et al., 2012)

an expensive and energy-consuming process. The challenges are mainly related to affordable large-scale production and cost-effective surface modification pathways.

References

Anglès M. N., Dufresne A. (2000) Plasticized starch/tunicin whiskers nanocomposites. 1. Structural analysis. *Macromolecules*, 33(22): 8344–8353

Aulin C., Johansson E., Wågberg L., Lindström T. (2010) Self-organized films from cellulose I nanofibrils using the layer-by-layer technique. *Biomacromolecules*, 11(4): 872–882

Bettaieb F., Khiari R., Dufresne A., Mhenni M. F., Belgacem M. N. (2015) Mechanical and thermal properties of *Posidonia oceanica* cellulose nanocrystal reinforced polymer. *Carbohydrate Polymers*, 123: 99–104

Bercea M., Navard P. (2000) Shear dynamics of aqueous suspensions of cellulose whiskers. *Macromolecules*, 33(16): 6011–6016

Bras J., Viet D., Bruzzese C., Dufresne A. (2011) Correlation between stiffness of sheets prepared from cellulose whiskers and nanoparticles dimensions. *Carbohydrate Polymers*, 84(1): 211–215

Brinkmann A., Chen M., Couillard M., Jakubek Z. J., Leng T., Johnston L. J. (2016) Correlating cellulose nanocrystal particle size and surface area. *Langmuir*, 32(24): 6105–6114

Camarero Espinosa S., Kuhnt T., Foster E. J., Weder C. (2013) Isolation of thermally stable cellulose nanocrystals by phosphoric acid hydrolysis. *Biomacromolecules*, 14(4): 1223–1230

Chakraborty A., Sain M., Kortschot M. (2005) Cellulose microfibrils: A novel method of preparation using high shear refining and cryocrushing. *Holzforschung*, 59(1): 102–107

Chen W., Yu H., Liu Y., Hai Y., Zhang M., Chen P. (2011) Isolation and characterization of cellulose nanofibers from four plant cellulose fibers using a chemical-ultrasonic process. *Cellulose*, 18(2): 433–442

Cheng Q., Wang S., Rials T. G., Lee S. H. (2007) Physical and mechanical properties of polyvinyl alcohol and polypropylene composite materials reinforced with fibril aggregates isolated from regenerated cellulose fibers. *Cellulose*, 14(6): 593–602

Cobut A., Sehaqui H., Berglund L. A. (2014) Cellulose nanocomposites by melt compounding of TEMPO-treated wood fibers in thermoplastic starch matrix. *BioResources*, 9(2): 3276–3289

Dufresne A., Dupeyre D., Vignon M. R. (2000) Cellulose microfibrils from potato tuber cells: processing and characterization of starch-cellulose microfibril composites. *Journal of Applied Polymer Science*, 76(14): 2080–2092

Dufresne A. (2013) Nanocellulose: A new ageless bionanomaterial. *Materials Today*, 16(6): 220–227

Dufresne A. (2017a) *Nanocellulose: from nature to high performance tailored materials. 2nd edition*. Berlin/Boston, Walter de Gruyter GmbH & Co KG, 632 p.

Dufresne A. (2017b) Cellulose nanomaterial reinforced polymer nanocomposites. *Current Opinion in Colloid & Interface Science*, 29: 1–8

Espino-Pérez E., Bras J., Ducruet V., Guinault A., Dufresne A., Domenek S. (2013) Influence of chemical surface modification of cellulose nanowhiskers on thermal, mechanical, and barrier properties of poly(lactide) based bionanocomposites. *European Polymer Journal*, 49(10): 3144–3154

Favier V., Canova G. R., Cavaillé J.-Y., Chanzy H., Dufresne A., Gauthier C. (1995) Nanocomposite materials from latex and cellulose whiskers. *Polymers for Advanced Technologies*, 6(5): 351–355

Ferrer A., Filpponen I., Rodríguez A., Laine J., Rojas O. J. (2012) Valorization of residual Empty Palm Fruit Bunch Fibers(EPFBF) by microfluidization: production of nanofibrillated cellulose and EPFBF nanopaper. *Bioresource Technology*, 125: 249–255

Habibi Y., Goffin A.-L., Schiltz N., Duquesne E., Dubois P., Dufresne A. (2008) Bionanocomposites based on poly(ε-caprolactone)-grafted cellulose nanocrystals by ring opening polymerization. *Journal of Materials Chemistry*, 18(41): 5002–5010

Herrick F. W., Casebier R. L., Hamilton J. K., Sandberg K. R. (1983) Microfibrillated cellulose: morphology and accessibility. *Journal of Applied Polymer Science Polymer Symposium*, 37: 797–813

Hirota M., Tamura N., Saito T., Isogai A. (2010) Water dispersion of cellulose II nanocrystals prepared by TEMPO-mediated oxidation of mercerized cellulose at pH 4.8. *Cellulose*, 17(2): 279–288

Ho T. T.T., Zimmermann T., Hauert R., Caseri W. (2011) Preparation and characterization of cationic nanofibrillated cellulose from etherification and high-shear disintegration processes. *Cellulose*, 18(6): 1391–1406

Ho T. T.T., Abe K., Zimmermann T., Yano H. (2015) Nanofibrillation of pulp fibers by twin-screw extrusion. *Cellulose*, 22(1): 421–433

Iguchi M., Yamanaka S., Budhiono A. (2000) Bacterial cellulose' a masterpiece of nature's arts. *Journal of Materials Science*, 35(2): 261–270

Iotti M., Gregersen Ø. W., Moe S., Lenes M. (2011) Rheological studies of microfibrillar cellulose water dispersions. *Journal of Polymers and the Environment*, 19(1): 137–145

Iwamoto S., Nakagaito A. N., Yano H. (2007) Nano-fibrillation of pulp fibers for the processing of transparent nanocomposites. *Applied Physics A-Materials Science & Processing*, 89(2): 461–466

Klemm D., Kramer F., Moritz S., Lindström T., Ankerfors M., Gray D., Dorris A. (2011) Nanocelluloses: a new family of nature-based materials. *Angewandte Chemie – International Edition*, 50(24): 5438–5466

Kondo T., Kose R., Naito H., Kasai W. (2014) Aqueous counter collision using paired water jets as a novel means of preparing bio-nanofibers. *Carbohydrate Polymers*, 112: 284–290

Kunaver M., Anžlovar A., Žagar E. (2016) The fast and effective isolation of nanocellulose from selected cellulosic feedstocks. *Carbohydrate Polymers*, 148: 251–258

Lavoine N., Desloges I., Dufresne A., Bras J. (2012) Microfibrillated cellulose – Its barrier properties and applications in cellulosic materials: a review. *Carbohydrate Polymers*, 90(2): 735–764

Lee S. Y., Mohan D. J., Kang I. A., Doh G. H., Lee S., Han S. O. (2009) Nanocellulose reinforced PVA composite films: Effects of acid treatment and filler loading. *Fibers and Polymers*, 10(1): 77–82

Leung A. C.W., Hrapovic S., Lam E., Liu Y., Male K. B., Mahmoud K. A., Luong J. H.T. (2011) Characteristics and properties of carboxylated cellulose nanocrystals prepared from a novel one-step procedure. *Small*, 7(3): 302–305

Li J., Wei X., Wang Q., Chen J., Chang G., Kong L., Su J., Liu Y. (2012) Homogeneous isolation of nanocellulose from sugarcane bagasse by high pressure homogenization. *Carbohydrate Polymers*, 90(4): 1609–1613

Li B., Xu W., Kronlund D., Määttänen A., Liu J., Smått J.-H., Peltonen J., Willför S., Mu X., Xu C. (2015) Cellulose nanocrystals prepared via formic acid hydrolysis followed by TEMPO-mediated oxidation. *Carbohydrate Polymers*, 133: 605–612

Li P., Sirviö J. A., Haapala A., Liimatainen H. (2017) Cellulose nanofibrils from nonderivatizing urea-based deep eutectic solvent pretreatments. *ACS Applied Materials & Interfaces*, 9(3): 2846–2855

Liimatainen H., Visanko M., Sirviö J. A., Hormi O. E.O., Niinimaki J. (2012) Enhancement of the nanofibrillation of wood cellulose through sequential periodate-chlorite oxidation. *Biomacromolecules*, 13(5): 1592–1597

Liimatainen H., Visanko M., Sirviö J., Hormi O., Niinimäki J. (2013) Sulfonated cellulose nanofibrils obtained from wood pulp through regioselective oxidative bisulfite pre-treatment. *Cellulose*, 20(2): 741–749

Lin N., Huang J., Dufresne A. (2012) Preparations, properties and applications of polysaccharide nanocrystals in advanced functional nanomaterials: A review. *Nanoscale*, 4(11): 3274–3294

Lin N., Dufresne A. (2014a) Nanocellulose in biomedicine: Current status and future prospect. *European Polymer Journal*, 59: 302–325

Lin N., Dufresne A. (2014b) Surface chemistry, morphological analysis and properties of cellulose nanocrystals with gradiented sulfation degrees. *Nanoscale*, 6(10): 5384–5393

Liu D., Zhong T., Chang P. R., Li K., Wu Q. (2010) Starch composites reinforced by bamboo cellulosic crystals. *Bioresource Technology*, 101(7): 2529–2536

Liu Y., Wang H., Yu G., Yu Q., Li B., Mu X. (2014) A novel approach for the preparation of nanocrystalline cellulose by using phosphotungstic acid. *Carbohydrate Polymers*, 110: 415–422

Lu Q., Tang L., Lin F., Wang S., Chen Y., Chen X., Huang B. (2014) Preparation and characterization of cellulose nanocrystals via ultrasonication-assisted $FeCl_3$-catalyzed hydrolysis. *Cellulose*, 21(5): 3497–3506

Malainine M. E., Mahrouz M., Dufresne A. (2005) Thermoplastic nanocomposites based on cellulose microfibrils from Opuntia ficus-indica parenchyma cell. *Composites Science and Technology*, 65(10): 1520–1526

Man Z., Muhammad N., Sarwono A., Bustam M. A., Kumar M. V., Rafiq S. (2011) Preparation of cellulose nanocrystals using an ionic liquid. *Journal of Polymers and the Environment*, 19(3): 726–731

Moser C., Backlund H., Drenth L., Henriksson G., Lindström M. E. (2018) Xyloglucan adsorption for measuring the specific surface area on various never-dried cellulose nanofibers. *Nordic Pulp & Paper Research Journal*, 33(2): 186–193

Nazari B., Kumar V., Bousfield D. W., Toivakka M. (2016) Rheology of cellulose nanofibers suspensions: Boundary driven flow. *Journal of Rheology*, 60(6): 1151–1159

Nickerson R. F., Habrle J. A. (1947) Cellulose intercrystalline structure. *Industrial & Engineering Chemistry*, 39(11): 1507–1512

Ninomiya K., Abe M., Tsukegi T., Kuroda K., Tsuge Y., Ogino C., Taki K., Taima T., Saito J., Kimizu M., Uzawa K., Takahashi K. (2018) Lignocellulose nanofibers prepared by ionic liquid pretreatment and subsequent mechanical nanofibrillation of bagasse powder: Application to esterified bagasse/polypropylene composites. *Carbohydrate Polymers*, 182: 8–14

Nuruddin Md., Hosur M., Uddin Md.J., Baah D., Jeelani S. (2016) A novel approach for extracting cellulose nanofibers from lignocellulosic biomass by ball milling combined with chemical treatment. *Journal of Applied Polymer Science*, 133(9): 42990

Olszewska A., Eronen P., Johansson L.-S., Malho J.-M., Ankerfors M., Lindström T., Ruokolainen J., Laine J., Österberg M. (2011) The behaviour of cationic nanofibrillar cellulose in aqueous media. *Cellulose*, 18(5): 1213–1226

Pääkkö M., Ankerfors M., Kosonen H., Nykänen A., Ahola S., Österberg M., Ruokolainen J., Laine J., Larsson P. T., Ikkala O., Lindström T. (2007) Enzymatic hydrolysis combined with mechanical shearing and high-pressure homogenization for nanoscale cellulose fibrils and strong gels. *Biomacromolecules*, 8(6): 1934–1941

Pääkkönen T., Spiliopoulos P., Knuts A., Nieminen K., Johansson L.-S., Enqvist E., Kontturi E. (2018) From vapour to gas: optimising cellulose degradation with gaseous HCl. *Reaction Chemistry & Engineering*, 3(3): 312–318

Rosgaard L., Pedersen S., Langston J., Akerhielm D., Cherry J. R., Meyer A. S. (2007) Evaluation of minimal *Trichoderma reesei* cellulase mixtures on differently pretreated barley straw substrates. *Biotechnology Progress*, 23(6): 1270–1276

Saito T., Nishiyama Y., Putaux J. L., Vignon M., Isogai A. (2006) Homogeneous suspensions of individualized microfibrils from TEMPO-catalyzed oxidation of native cellulose. *Biomacromolecules*, 7(6): 1687–1691

Saito T., Hirota M., Tamura N., Kimura S., Fukuzumi H., Heux L., Isogai A. (2009) Individualization of nano-sized plant cellulose fibrils by direct surface carboxylation using TEMPO catalyst under neutral condition. *Biomacromolecules*, 10(7): 1992–1996

Schenker M., Schoelkopf J., Gane P., Mangin P. (2019) Rheology of microfibrillated cellulose (MFC) suspensions: influence of the degree of fibrillation and residual fibre content on flow and viscoelastic properties. *Cellulose*, 26(2): 845–860

Shafiei-Sabet S., Hamad W. Y., Hatzikiriakos S. G. (2012) Rheology of nanocrystalline cellulose aqueous suspensions. *Langmuir*, 28(49): 17124–17133

Sheltami R. M., Kargarzadeh H., Abdullah I., Ahmad I. (2017) Thermal properties of cellulose nanocomposites. *Handbook of nanocellulose and cellulose nanocomposites. Vol. 2*. Kargarzadeh H., Ahmad I., Thomas S., Dufresne A. (eds.) Weinheim, Wiley VCH Verlag GmbH & Co. KGaA, p. 523–552

Siqueira G., Abdillahi H., Bras J., Dufresne A. (2010) High reinforcing capability cellulose nanocrystals extracted from *Syngonanthus nitens* (Capim Dourado). *Cellulose*, 17(2): 289–298

Sirviö J. A., Visanko M., Liimatainen H. (2016) Acidic deep eutectic solvents as hydrolytic media for cellulose nanocrystal production. *Biomacromolecules*, 17(9): 3025–3032

Taniguchi T., Okamura K. (1998) New films produced from microfibrillated natural fibres. *Polymer International*, 47(3): 291–294

Tingaut P., Eyholzer C., Zimmermann T. (2011) Functional polymer nanocomposite materials from microfibrillated cellulose. *Advances in nanocomposite technology*. Hashim A. (ed.) InTech, p. 319–334

Tsuboi K., Yokota S., Kondo T. (2014) Difference between bamboo- and wood-derived cellulose nanofibers prepared by the aqueous counter collision method. *Nordic Pulp & Paper Research Journal*, 29(1): 69–76

Turbak A. F., Snyder F. W., Sandberg K. R. (1983) Microfibrillated cellulose, a new cellulose product: properties, uses, and commercial potential. *Journal of Applied Polymer Science: Applied Polymer Symposium*, 37: 815–827

Ureña-Benavides E.E., Ao G., Davis V. A., Kitchens C. L. (2011) Rheology and phase behavior of lyotropic cellulose nanocrystal suspensions. *Macromolecules*, 44(22): 8990–8998

Wågberg L., Decher G., Norgren M., Lindström T., Ankerfors M., Axnäs K. (2008) The build-up of polyelectrolyte multilayers of microfibrillated cellulose and cationic polyelectrolytes. *Langmuir*, 24(3): 784–795

Wang J., Gardner D. J., Stark N. M., Bousfield D. W., Tajvidi M., Cai Z. (2018) Moisture and oxygen barrier properties of cellulose nanomaterial-based films. *ACS Sustainable Chemistry & Engineering,* 6(1): 49–70

Yang H., Alam M. N., van de Ven T. G.M. (2013) Highly charged nanocrystalline cellulose and dicarboxylated cellulose from periodate and chlorite oxidized cellulose fibers. *Cellulose*, 20(4): 1865–1875

Yang Q., Saito T., Berglund L. A., Isogai A. (2015) Cellulose nanofibrils improve the properties of all-cellulose composites by the nano-reinforcement mechanism and nanofibril-induced crystallization. *Nanoscale*, 7(42): 17957–17963

Yao K., Meng Q., Bulone V., Zhou Q. (2017) Flexible and responsive chiral nematic cellulose nanocrystal/poly(ethylene glycol) composite films with uniform and tunable structural color. *Advanced Materials*, 29(28): 1701323

Zhang L., Tsuzuki T., Wang X. (2015) Preparation of cellulose nanofiber from softwood pulp by ball milling. *Cellulose*, 22(3): 1729–1741

Zuluaga R., Putaux J.-L., Restrepo A., Mondragon I., Gañán P. (2007) Cellulose microfibrils from banana farming residues: isolation and characterization. *Cellulose*, 14(6): 585–592

Journal of Siberian Federal University. Biology 2021 14(4): 442–453
~ ~ ~

DOI 10.17516/1997-1389-0363

УДК 577.12

Biosynthesis of Poly(3-Hydroxybutyrate-*co*-3-Hydroxyhexanoate) with a High 3-Hydroxyhexanoate Fraction and Low Molecular Weight for Polymer Blending

Fakhrul Ikhma Mohd Fadzil, Makoto Kobayashi, Yuki Miyahara, Manami Ishii-Hyakutake and Takeharu Tsuge*
Tokyo Institute of Technology
Yokohama, Japan

Received 14.06.2021, received in revised form 23.07.2021, accepted 23.08.2021

Abstract. Polyhydroxyalkanoates (PHAs) are aliphatic polyesters that are biosynthesized and accumulate in bacterial cells. Among PHAs, poly(3-hydroxybutyrate-*co*-3-hydroxyhexanoate)s [P(3HB-*co*-3HHx)s] are known to be practical PHA copolymers with an appropriate degree of flexibility. In the biosynthesis of PHA, ethanol induces chain transfer (CT) reaction, resulting in the biosynthesis of low-molecular-weight PHA. In this study, P(3HB-*co*-3HHx)s were biosynthesized using recombinant *Escherichia coli* by feeding fatty acid(s) and ethanol as the 3HHx precursor and CT agent, respectively, to obtain polymers with high 3HHx fractions and low molecular weights. Two biosynthesized P(3HB-*co*-3HHx)s, whose 3HHx fractions were 49 and 86 mol% and weight average molecular weights were 1.5×10^4 and 2.8×10^4, respectively, were blended with P(3HB-*co*-5 mol% 3HHx) (PHBH5) as the base material. The blending properties were investigated to explore how the thermal properties can be modified. Thermal analysis by differential scanning calorimetry (DSC) showed that blends prepared by solution casting were obviously immiscible when 30 wt.% or more of biosynthesized polymer was added, even if its molecular weight was low. In the blended polymers, a lower crystallization effect compared to neat PHBH5 was observed without changing the melting temperature. However, crystallization was promoted in the blended material under specific blending conditions. Thus, blending is a simple method for producing polymer materials with altered thermal and microstructural properties.

Keywords: recombinant *E. coli*, poly(3-hydroxybutyrate-*co*-3-hydroxyhexanoate), low molecular weight, polymer blending, polyhydroxyalkanoate, miscibility, crystallization.

* Corresponding author E-mail address: tsuge.t.aa@m.titech.ac.jp
ORCID: 0000-0002-6296-6500 (Tsuge T.); 0000-0003-4781-5760 (Miyahara Y.)

Acknowledgements. We would like to thank Dr. Shunsuke Sato (Kaneka Corporation) and Prof. Christopher T. Nomura (University of Idaho) for kindly gifting PHBH5 and *E. coli* LSBJ, respectively. This research was supported by the Adaptable and Seamless Technology Transfer Program through Target-driven R&D (AStep), JST, Japan.

Citation: Mohd Fadzil F. I., Kobayashi M., Miyahara Y., Ishii-Hyakutake M., Tsuge T. Biosynthesis of poly(3-hydroxybutyrate-*co*-3-hydroxyhexanoate) with a high 3-hydroxyhexanoate fraction and low molecular weight for polymer blending. J. Sib. Fed. Univ. Biol., 2021, 14(4), 442–453. DOI: 10.17516/1997-1389-0363

Биосинтез поли(3-гидроксибутирата-со-3-гидроксигексаноата) с высоким содержанием 3-гидроксигексаноата и низкой молекулярной массой для смешения полимеров

Ф. И. Мохд Фадзил, М. Кобаяши, Ю. Мияхара, М. Исии-Хякутаке, Т. Тсуге
Токийский технологический институт
Япония, Йокогама

Аннотация. Полигидроксиалканоаты (ПГА) представляют собой алифатические полиэфиры, которые синтезируются и накапливаются в бактериальных клетках. Среди множества ПГА большой интерес представляет сополимер поли(3-гидроксибутират-со-3-гидроксигексаноат) [П(3ГБ-со-3ГГ)], характеризующийся высокой эластичностью. В реакциях биосинтеза ПГА этанол индуцирует реакцию переноса цепи, в результате чего происходит биосинтез низкомолекулярных ПГА. В этом исследовании для получения низкомолекулярного сополимера П(3ГБ-со-3ГГ) с высоким содержанием мономеров 3ГГ рекомбинантный штамм *Escherichia coli* культивировали с подачей в среду жирных кислот и этанола в качестве предшественников мономеров 3ГГ и агента переноса цепи соответственно. Получены два образца П(3ГБ-со-3ГГ) с содержанием мономеров 3ГГ 49 и 86 мол.% и средневесовой молекулярной массой $1{,}5 \times 10^4$ и $2{,}8 \times 10^4$ соответственно. Были исследованы термические свойства смесей полученных сополимеров с П(3ГБ-со-5 мол.% 3ГГ) (PHBH5). Термический анализ с помощью дифференциальной сканирующей калориметрии показал, что смеси, приготовленные литьем из раствора, очевидно, были несмешиваемыми при добавлении биосинтезированного полимера 30 мас.% или более, даже при его низкой молекулярной массе. В смешанных полимерах наблюдался более низкий эффект кристаллизации по сравнению с чистым PHBH5 без изменения температуры плавления. Однако некоторые условия смешивания способствовали ускорению кристаллизации смешанного материала. Таким образом, смешивание представляет собой простой метод получения полимерных материалов с измененными термическими и микроструктурными свойствами.

Ключевые слова: рекомбинантная *E. coli*, поли (3-гидроксибутират-со-3-гидроксигексаноат), низкая молекулярная масса, смешение полимеров, полигидроксиалканоат, смешиваемость, кристаллизация.

Благодарности. Мы хотели бы поблагодарить доктора Сюнсукэ Сато (корпорация Канека) и проф. Кристофера Т. Номура (Университет Айдахо) за любезно предоставленные PHBH5 и E. coli LSBJ соответственно. Это исследование было поддержано Программой адаптивной и беспрепятственной передачи технологий в рамках целевых исследований и разработок (A Step), JST, Япония.

Цитирование: Мохд Фадзил, Ф. И. Биосинтез поли(3-гидроксибутирата-со-3-гидроксигексаноата) с высоким содержанием 3-гидроксигексаноата и низкой молекулярной массой для смешения полимеров / Ф. И. Мохд Фадзил, М. Кобаяши, Ю. Мияхара, М. Исии-Хякутаке, Т. Тсуге // Журн. Сиб. федер. ун-та. Биология, 2021. 14(4). С. 442–453. DOI: 10.17516/1997-1389-0363

Introduction

The use of petroleum-based polymer materials in daily life has led to various environmental problems. Hence, the development of eco-friendly materials has become a topic of major interest. Polyhydroxyalkanoates (PHAs) are a family of polyesters produced by many prokaryotes as energy storage molecules under conditions of stress or unbalanced nutrient supply (Tsuge, 2002; Tsuge et al., 2015). These microbial polyesters have attracted global interest because they are completely biodegradable and environmentally benign and have thermal properties comparable to those of fossil-based plastics. Among the various PHAs, poly(3-hydroxybutyrate-*co*-3-hydroxyhexanoate) [P(3HB-*co*-3HHx)] has numerous potential applications, particularly in nanomedicine (Kılıçay et al., 2011) and tissue engineering (Qu et al., 2006; Zhang et al., 2018). Since P(3HB-*co*-3HHx) contains 3-hydroxyhexanoate (3HHx), a medium-chain monomer, the copolymer exhibits flexibility unlike highly crystalline poly(3-hydroxybutyrate) [P(3HB)] and poly(3HB-*co*-3-hydroxyvalerate) [P(3HB-*co*-3HV)] (Doi et al., 1995; Volova et al., 2021). However, the 3HHx fraction in currently available P(3HB-*co*-3HHx) is insufficient, which limits its potential applications. Therefore, to expand the applications of P(3HB-*co*-3HHx), further research is required on diversifying the 3HHx fraction and altering its microchemical structure (Xu et al., 2018).

The properties of PHA have been improved by copolymerization (Cespedes et al., 2018), increasing the molecular weight (Kahar et al., 2005), chain chemical modification (Levine et al., 2016), polymer processing (Iwata et al., 2004), and blending (Basnett et al., 2013). Among these, blending, which involves mixing two kinds of polymers with different microstructures, is the simplest way to produce polymer materials with new properties. The blend performance can be easily modified by adjusting the mixing ratio and mixing state. There are many reports on the blending of PHAs with other bioplastics (Luo et al., 2009; Martelli et al., 2012; Zembouai et al., 2014; Botta et al., 2015). These polymers can be processed by solution casting or melt pressing (Nerkar et al., 2014; Zembouai et al., 2014), thereby enabling the modification of physical properties at low cost. P(3HB-*co*-3HHx) blends have been studied extensively in recent years owing to their ability to reduce crystallinity (Cai et al., 2012).

Escherichia coli is a bacterium that does not biosynthesize PHA naturally; however, expressing PHA biosynthetic genes from other bacteria confers PHA-producing-ability to *E. coli*.

Generally, PHA synthesized by recombinant *E. coli* has a higher molecular weight than that synthesized by natural PHA producers. This is probably because, unlike natural bacteria, *E. coli* does not have PHA depolymerase. On the other hand, the molecular weight of biosynthesized PHA can be lowered by using the chain transfer (CT) reaction, in which PHA synthase transfers the elongating polymer chain to an alcoholic compound that acts as a CT agent (Hiroe et al., 2013; Tsuge, 2016). Therefore, the higher the frequency of CT reactions, the lower the molecular weight of the biosynthesized PHA. The frequency of CT reactions can be controlled by adjusting the concentration of alcoholic compounds added to the culture medium. Low-molecular-weight polymers can be effectively utilized in polymer blends because they exhibit relatively high miscibility with other polymers (Blumm, Owen, 1995; Ohkoshi et al., 2000).

In this paper, we report the biosynthesis of P(3HB-*co*-3HHx) with a high 3HHx fraction and low molecular weight using recombinant *E. coli* by feeding fatty acid(s) and ethanol as the 3HHx precursor and CT agent, respectively. This study aimed to investigate how the thermal properties can be modified by blending biosynthesized P(3HB-*co*-3HHx)s using P(3HB-*co*-5 mol% 3HHx) (PHBH5) as the base material.

Materials and methods

Materials

Commercial grade PHBH5 was provided by Kaneka Corporation (Osaka, Japan), while P(3HB-*co*-3HHx) copolymers with higher 3HHx fractions and lower molecular weights were synthesized using recombinant *E. coli* strains.

Biosynthesis of P(3HB-co-3HHx) using recombinant E. coli strains

Recombinant *E. coli* strains were cultivated in 100 mL M9 medium (Sambrook, Russell, 2011) on a reciprocal shaker (130 strokes min^{-1}) in a 500-mL flask at 37 °C for 72 h. When required, kanamycin (50 mg/L) was added to the medium.

E. coli strain LS5218 [*fadR601*, *atoC512*(Const)] (Spratt et al., 1981) harboring the plasmid pBBR1*phaPCJ*$_{Ac}$*AB*$_{Re}$ (Ushimaru et al., 2015), which carried the genes *phaP*$_{Ac}$(D4N) (*Aeromonas caviae* phasin gene with D4N mutation), *phaC*$_{Ac}$(NSDG) (*A. caviae* PHA synthase gene with N149S and D171G mutations), *phaJ*$_{Ac}$ (*A. caviae R*-specific enoyl-CoA hydratase gene), *phaA*$_{Re}$ (*Ralstonia eutropha* 3-ketothiolase gene), and *phaB*$_{Re}$ (*R. eutropha* acetoacetyl-CoA reductase gene) (Fig. 1), was cultured in M9 medium supplemented with dodecanoic acid (2.5 g/L) and 0.4 vol.% Brij35. Ethanol (5 g/L) was also added as a CT agent to produce a low-molecular-weight polymer. The sample obtained under these conditions is referred to as sPHBH49.

The *E. coli* strain LSBJ [*fadB:: Cm*, ΔfadJ, *atoC512* (Const), *fadR601*] (Tappel et al., 2012; Mohd Fadzil et al., 2018) harboring pBBR1*phaPCJ*$_{Ac}$*AB*$_{Re}$ (Ushimaru et al., 2015) was cultured in M9 medium supplemented with yeast extract (2.5 g/L) and ethanol (10 g/L). Glucose (2.5 g/L) and two fatty acids, namely hexanoic acid (0.4 g/L) and butyric acid (0.1 g/L), were fed to the medium three times every 24 h (0, 24, and 48 h after cultivation was started). The sample obtained under these conditions is referred to as sPHBH86.

Polymer extraction

The bacterial cultures were harvested by centrifugation. The harvested cells were washed with hexane followed by distilled water twice. The cell pellets were then lyophilized for 72 h. Subsequently, the dried cells were placed in chloroform to extract intracellular PHA from the cells. After filtration, the PHA polymers were recovered from the filtrate by precipitation with hexane, and dried in vacuum dryer for 3 days to ensure complete solvent removal.

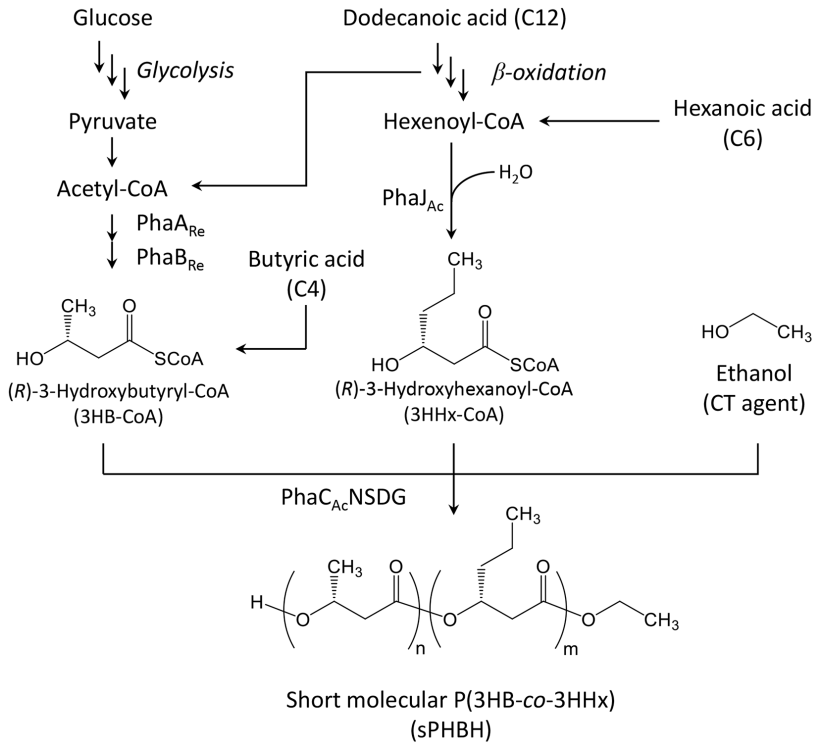

Fig. 1. The main biosynthetic pathway constructed in recombinant *E. coli* and enzymes involved in the synthesis of ethanol-capped P(3HB-*co*-3HHx). PhaA$_{Re}$, *Ralstonia eutropha* 3-ketothiolase; PhaB$_{Re}$, *R. eutropha* acetoacetyl-CoA reductase; PhaC$_{Ac}$NSDG, N149S and D171G (NSDG)-mutated *Aeromonas caviae* PHA synthase; PhaJ$_{Ac}$, *A. caviae* (*R*)-specific enoyl-CoA hydratase

Preparation of blended materials

Blended samples were prepared by mixing the base polymer PHBH5 with 10, 20, 30, and 50 wt.% of biosynthesized P(3HB-*co*-3HHx) samples in chloroform solution for 3 days. The blended films were obtained by evaporating the solvent at room temperature for 3 days. Then, the materials were dried in a vacuum dryer for 1 day to completely evaporate the remaining solvent.

Gas chromatography (GC) analysis

The content of biosynthesized P(3HB-*co*-3HHx) in the cells was determined using a Shimadzu 2014S GC system with a flame ionization detector. Intracellular PHA in the freeze-dried cells was subjected to methanolysis by adding 15 vol.% sulfuric acid in methanol prior to analysis, as described previously (Huang et al., 2018).

Nuclear magnetic resonance (NMR) analysis

Monomer fraction estimation and structural analysis of the P(3HB-*co*-3HHx) copolyesters were carried out using ^{1}H-NMR and ^{13}C-NMR, respectively. Samples (50 mg) were dissolved in chloroform-*d*, and tetramethylsilane (TMS) was used as an internal reference. NMR spectra were recorded using a Bruker Biospin AVANCE III spectrometer (Furutate et al., 2021).

Gel permeation chromatography (GPC) analysis

The molecular weights of P(3HB-*co*-3HHx) samples were characterized using a Shimadzu 10A GPC system with a 10A refractive index detector

equipped with two Shodex K-806M joint columns. Chloroform was used as the eluent at a flow rate of 0.8 mL/min, and calibration was performed using polystyrene standards with low polydispersity.

Differential scanning calorimetry (DSC) analysis

Thermal analysis of the P(3HB-*co*-3HHx) and blended samples was carried out using a Perkin Elmer Pyris 1 system under nitrogen flow. The samples (6–10 mg) were encapsulated in an aluminum pan and heated to 200 °C at 20 °C/min, quenched to –50 °C, and heated again at 20 °C/min. The glass transition temperature (T_g) was determined as the midpoint of the heat capacity change in the second heating scan of the DSC thermogram (Furutate et al., 2021).

Results

Biosynthesis of P(3HB-co-3HHx)s with ethanol feeding

Previously, we demonstrated the biosynthesis of P(3HB-*co*-3HHx) with 40 mol% 3HHx from dodecanoic acid (C12 fatty acid) using recombinant *E. coli* LS5218 harboring pBBR1*phaPCJ*$_{Ac}$*AB*$_{Re}$ (Table 1) (Ushimaru et al., 2015). This polymer had a weight average molecular weight (M_w) and polydispersity of 1.8×10^6 and 4.8, respectively. In this study, to lower the molecular weight of biosynthesized P(3HB-*co*-3HHx), the culture medium was supplemented with ethanol (5 g/L) to induce CT reaction. As a result, the dry cell weight and PHA content reached 1.1±0.1 g/L and 58±1 wt.%, respectively after 72 h of cultivation (Table 1), and P(3HB-*co*-3HHx) with a 3HHx fraction of 49 mol% and a M_w of 1.5×10^4 (Table 2) was obtained. The M_w of the polymer obtained using an ethanol-supplemented culture was two orders of magnitude lower than that of the polymer obtained using a non-ethanol-supplemented culture (Ushimaru et al., 2015). In addition, the M_w was one order of magnitude lower than that of the PHBH5 base material (Table 2). This low-molecular-weight P(3HB-*co*-49 mol% 3HHx) is referred to as sPHBH49.

To further increase the 3HHx fraction, instead of using dodecanoic acid, the culture medium was supplemented with hexanoic acid, a C6 fatty acid, as a direct precursor for 3HHx. A small amount of butyric acid, a C4 fatty acid, was also added to allow the incorporation of small amounts of 3HB into the polymer (Fig. 1). Additionally, ethanol (10 g/L) was added to the culture medium to lower the molecular weight of the biosynthesized PHA. After 72 h of cultivation, the dry cell weight and PHA content reached 1.7±0.1 g/L and 25±1 wt.%, respectively (Table 1). The obtained P(3HB-*co*-3HHx) exhibited a high 3HHx fraction (86 mol%) and relatively low molecular weight (M_w, 2.8×10^4) (Table 2); it is referred to as sPHBH86.

Characterization of P(3HB-co-3HHx)s by NMR

From the ^{1}H- and ^{13}C-NMR spectra, the molecular structures of the P(3HB-*co*-3HHx) samples were investigated. From the ^{1}H-NMR spectra, the copolymer compositions were determined as listed in Tables 1 and 2. As in the ^{13}C-NMR spectra, the presence of the 3HHx comonomer caused a carbonyl peak to split into multiplets. The carbonyl resonances around 168–170 ppm were identified as belonging to 3HB*-3HB, 3HB*-3HHx and 3HHx*-3HB, and 3HHx*-3HHx, which are structures possibly existing in the copolymer chain (Abe et al., 1994). The randomness of the copolymer samples, described by parameter *D*, was calculated as follows (Kamiya et al., 1989):

$$D = (F_{3HHx\text{-}3HHx}F_{3HB\text{-}3HB})/(F_{3HHx\text{-}3HB}F_{3HB\text{-}3HHx}) \quad (1)$$

where $F_{3HHx\text{-}3HHx}$, $F_{3HB\text{-}3HB}$, $F_{3HHx\text{-}3HB}$, and $F_{3HB\text{-}3HHx}$ represent the fractions of 3HHx-3HHx, 3HB-3HB,

3HHx-3HB, and 3HB-3HHx diads, respectively. The diad sequence distributions derived from the carbonyl carbon were used to calculate *D* values, shown in Table 3.

Altogether, the observed values were consistently comparable with the calculated Bernoullian statistics applicable to statistically random copolymerization. Based on the observed *D* values, it is suggested that PHBH5 is a slightly blocky copolymer, while sPHBH49 and sPHBH86 resemble random copolymers.

Blends of sPHBH49 and the base material

Using sPHBH49, polymer blending was conducted with PHBH5 as the base material. Figure 2A shows the DSC results of the PHBH5 blends and the neat sPHBH49 sample. Neat sPHBH49 showed a weak T_g peak at –12 °C, which is in good agreement with the reported T_g (–9 °C) for the closest 3HHx fraction (53 mol%) copolymer (Feng et al., 2003). On the other hand, sPHBH49 did not show a T_m peak, suggesting that it is an amorphous polymer. As for the PHBH5 blends, the T_m peaks were observed at 142–144 °C and were almost unchanged regardless of the blending ratio. Meanwhile, the enthalpy of fusion (area of the melting peak) tended to decrease as the sPHBH49 content increased. Interestingly, the cold crystallization temperature (T_{cc}) of PHBH5 in the second heating scan decreased from 63 °C to 56 °C with the addition of 10 wt.% sPHBH49, and the crystallization peak became sharper. This implies that crystallization of the blended sample became easier and faster,

Table 1. PHA biosynthesis by recombinant *E. coli*

E. coli strain	Fatty acid added	Ethanol (g/L)	Dry cell wt. (g/L)	PHA content (wt.%)	PHA composition (mol%)		Reference
					3HB	3HHx	
LS5218	Dodecanoic acid (C12)	-	1.2±0.1	62±4	60	40	Ushimaru et al., 2015
LS5218	Dodecanoic acid (C12)	5	1.1±0.1	58±1	51	49	This study
LSBJ	Hexanoic acid (C6), butyric acid (C4)	10	1.7±0.1	25±1	14	86	This study

Cells were cultured in 100 mL M9 medium containing fatty acid(s) at 37 °C for 72 h. For the culture of LSBJ strain, glucose was supplemented to support cell growth. The PHA content and composition were determined by GC and ^{1}H-NMR, respectively, in this study. 3HB, 3-hydroxyburyrate; 3HHx, 3-hydroxyhexanoate. Results are expressed as mean ± standard deviation (n = 3).

Table 2. Thermal properties and molecular weights of PHA samples used in this study

Polymer sample	Sample name	Thermal property [a]		Molecular weight		Source
		T_g (°C)	T_m (°C)	M_w (×10^4)	M_w/M_n	
P(3HB-*co*-5 mol% 3HHx)	PHBH5	–3.3	143	51	2.4	Kaneka Co., Osaka, Japan
P(3HB-*co*-49 mol% 3HHx)	sPHBH49	–12	-[b]	1.5	1.5	This study
P(3HB-*co*-86 mol% 3HHx)	sPHBH86	–13	-[b]	2.8	1.7	

T_g, glass transition temperature; T_m, melting temperature; M_w, weight average molecular weight; M_n, number average molecular weight.
[a]Determined from DSC second heating scan.
[b] Not detectable.

Table 3. Diad sequence distributions and *D* values of P(3HB-*co*-3HHx) samples

Sample name	PHA composition (mol%)		Diad sequence distribution				*D* value
	3HB	3HHx		3HB*-3HB	3HB*-3HHx + 3HHx*-3HB	3HHx*-3HHx	
PHBH5	95	5	(observed)	0.89	0.10	<0.01	3.56
			(calculated)	0.90	0.10	<0.01	-
sPHBH49	51	49	(observed)	0.32	0.49	0.19	1.01
			(calculated)	0.26	0.50	0.24	-
sPHBH86	14	86	(observed)	0.25	0.45	0.30	1.53
			(calculated)	0.02	0.24	0.74	-

PHA compositions were determined by ^{1}H-NMR. 3HB, 3-hydroxyburyrate; 3HHx, 3-hydroxyhexanoate. The observed relative intensities were determined from the relative peak areas of the carbonyl carbon resonances in the ^{13}C-NMR spectra. The calculated values were obtained using Bernoullian statistics.

probably because of the promotion of primary nucleation. When more sPHBH49 was added, T_{cc} shifted to the higher temperature side and the crystallization peak became broader, implying that crystallization became more difficult. With the addition of up to 30 wt.% sPHBH49, a single T_g was observed in the –2 to –4 °C range. These blends appeared to be miscible in the amorphous phase. However, when more sPHBH49 was added, two T_g derived from each polymer were detected. Thus, the blended state was partially immiscible.

Blends of sPHBH86 and the base material

Using sPHBH86, polymer blending was also conducted with PHBH5 as the base material. Figure 2B shows the second scan DSC thermograms of the PHBH5 blends and the neat sPHBH86 sample. Neat sPHBH86 showed a weak T_g peak at –13 °C but did not show a T_m peak, suggesting that it is an amorphous polymer. For the blends with 30 wt.% or more sPHBH86, two distinct T_g peaks appeared. Thus, it is apparent that PHBH5 and sPHBH86 are immiscible. Despite this, crystallization occurred in all blended samples regardless of the blend ratio without changing T_m. The crystallization of PHBH5 occurred even after blending with amorphous PHBH86, but crystallization in the presence of sPHBH86 was harder than that in the presence of sPHBH49.

Discussion

For the P(3HB-*co*-3HHx) blends, the two polymers are reported to be miscible in the amorphous phase when the difference in the 3HHx fraction between these polymers is less than 20 mol%, but are immiscible when the difference is larger than 30 mol% (Feng et al., 2003). On the other hand, as mentioned earlier, low-molecular-weight polymers are known to exhibit relatively high miscibility with other polymers (Blumm, Owen, 1995; Ohkoshi et al., 2000). Therefore, to modify the material properties with a small amount of additive, P(3HB-*co*-3HHx) with a low molecular weight and a high 3HHx fraction may be effective for polymer blending. This study investigated how the thermal properties can be changed by blending polymers with a low molecular weight and high 3HHx fraction P(3HB-*co*-3HHx), which were biosynthesized in this study.

The crystallization behavior of the P(3HB-*co*-3HHx) blends was evaluated using DSC. The shift and unification of T_g is an

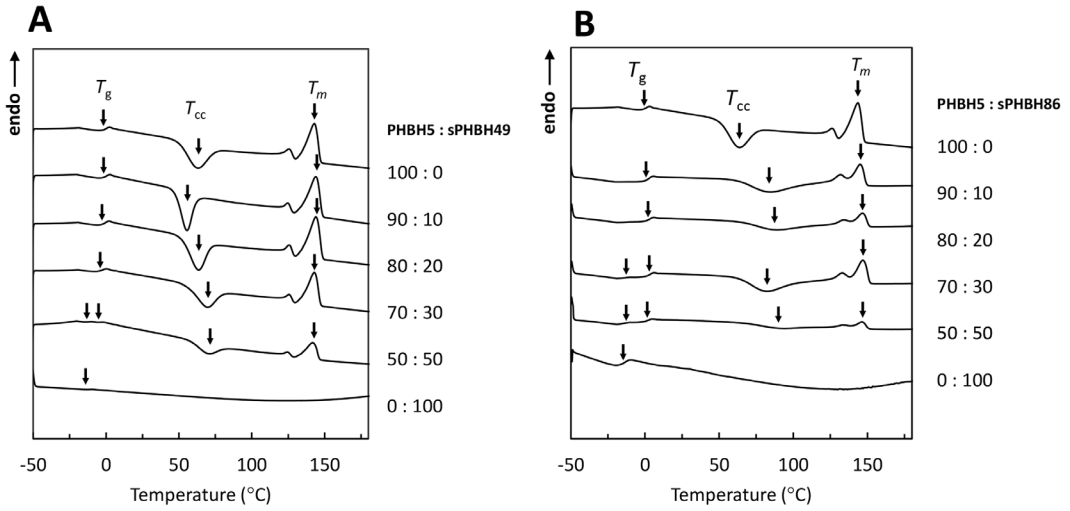

Fig. 2. DSC thermograms (second heating scan) of (A) PHBH5, sPHBH49, and its blends and (B) PHBH5, sPHBH86, and its blends. The samples were heated to 200 °C at 20 °C/min, quenched to –50 °C, and heated again at 20 °C/min during the second scan

important indicator for understanding whether the blended polymers are completely miscible with each other in the amorphous phase. When 30 wt.% or more of sPHBH49/86 was added to PHBH5, two distinct T_g peaks appeared in the second scan thermograms (Fig. 2). These blends were immiscible because of the large gap in their copolymer compositions, as previously demonstrated by Feng et al. (2003), even though one of them is a low-molecular-weight polymer. Initially, we expected miscibility between PHBH5 and the low-molecular-weight polymers; however, poor miscibility was observed with P(3HB-*co*-3HHx) biosynthesized using the CT reaction.

DSC analysis revealed that crystallization occurred on the lower temperature side in the 10 wt.% sPHBH49 blends. This implies that crystallization of the blended sample was promoted, probably because of easier primary nucleation. Low-molecular-weight polymers tend to form crystal nuclei, and it has also been reported that low-molecular-weight P(3HB) has a nucleating effect (Dong et al., 2010; Tsuge et al., 2017). However, it is surprising that even a non-crystalline polymer like sPHBH49 showed a nucleating effect in the PHBH5 blend. Further research is required to elucidate the mechanism of crystallization.

Conclusions

This study demonstrated that the crystallinity of blends of P(3HB-*co*-3HHx) could be tuned without changing the melting temperature. Additionally, the crystallization of the blended samples became easier and faster with the addition of 10 wt.% sPHBH49. Such a simple blending method provides an alternative way to produce materials with better performance.

References

Abe H., Doi Y., Fukushima T., Eya H. (1994) Biosynthesis from gluconate of a random copolyester consisting of 3-hydroxybutyrate and medium-chain-length 3-hydroxyalkanoates by *Pseudomonas* sp. 61–3. *International Journal of Biological Macromolecules*, 16(3): 115–119

Basnett P., Ching K. Y., Stolz M., Knowles J. C., Boccaccini A. R., Smith C., Locke I. C., Keshavarz T., Roy I. (2013) Novel poly (3-hydroxyoctanoate)/poly (3-hydroxybutyrate) blends for medical applications. *Reactive and Functional Polymers*, 73(10): 1340–1348

Blümm E., Owen A. J. (1995) Miscibility, crystallization and melting of poly(3-hydroxybutyrate)/poly(L-lactide) blends. *Polymer*, 36(21): 4077–4081

Botta L., Mistretta M. C., Palermo S., Fragalà M., Pappalardo F. (2015) Characterization and processability of blends of polylactide acid with a new biodegradable medium-chain-length polyhydroxyalkanoate. *Journal of Polymers and the Environment*, 23(4): 478–486

Cai H., Yu J., Qiu Z. (2012) Miscibility and crystallization of biodegradable poly(3-hydroxybutyrate-*co*-3-hydroxyhexanoate)/poly(vinyl phenol) blends. *Polymer Engineering & Science*, 52(2): 233–241

Cespedes L. G., Nahat R. A.T.P.S., Mendonça T. T., Tavares R. R., Oliveira-Filho E.R., Silva L. F., Taciro M. K., Sánchez R. J., Gomez J. G.C. (2018) A non-naturally-occurring P(3HB-*co*-3HA$_{MCL}$) is produced by recombinant *Pseudomonas* sp. from an unrelated carbon source. *International Journal of Biological Macromolecules*, 114: 512–519

Doi Y., Kitamura S., Abe H. (1995) Microbial synthesis and characterization of poly(3-hydroxybutyrate-*co*-3-hydroxyhexanoate). *Macromolecules*, 28(14): 4822–4828

Dong T., Mori T., Aoyama T., Inoue Y. (2010) Rapid crystallization of poly(3-hydroxybutyrate-*co*-3-hydroxyhexanoate) copolymer accelerated by cyclodextrin-complex as nucleating agent. *Carbohydrate Polymers*, 80(2): 387–393

Feng L., Watanabe T., He Y., Wang Y., Kichise T., Fukuchi T., Chen G. Q., Doi Y., Inoue Y. (2003) Phase behavior and thermal properties for binary blends of bacterial poly(3-hydroxybutyrate-*co*-3-hydroxyhexanoate)s with narrow-comonomer-unit compositional distribution. *Macromolecular Bioscience*, 3(6): 310–319

Furutate S., Kamoi J., Nomura C. T., Taguchi S., Abe H., Tsuge T. (2021) Superior thermal stability and fast crystallization behavior of a novel, biodegradable α-methylated bacterial polyester. *NPG Asia Materials*, 13(1): 31

Hiroe A., Hyakutake M., Thomson N. M., Sivaniah E., Tsuge T. (2013) Endogenous ethanol affects biopolyester molecular weight in recombinant *Escherichia coli*. *ACS Chemical Biology*, 8(11): 2568–2576

Huang P., Okoshi T., Mizuno S., Hiroe A., Tsuge T. (2018) Gas chromatography-mass spectrometry-based monomer composition analysis of medium-chain-length polyhydroxyalkanoates biosynthesized by *Pseudomonas* spp. *Bioscience, Biotechnology, and Biochemistry*, 82(9): 1615–1623

Iwata T., Aoyagi Y., Fujita M., Yamane H., Doi Y., Suzuki Y., Takeuchi A., Uesugi K. (2004) Processing of a strong biodegradable poly[(*R*)-3-hydroxybutyrate] fiber and a new fiber structure revealed by micro-beam X-ray diffraction with synchrotron radiation. *Macromolecular Rapid Communications*, 25(11): 1100–1104

Kahar P., Agus J., Kikkawa Y., Taguchi K., Doi Y., Tsuge T. (2005) Effective production and kinetic characterization of ultra-high-molecular-weight poly[(*R*)-3-hydroxybutyrate] in recombinant *Escherichia coli*. *Polymer Degradation and Stability*, 87(1): 161–169

Kamiya N., Yamamoto Y., Inoue Y., Chujo R., Doi Y. (1989) Microstructure of bacterially synthesized poly(3-hydroxybutyrate-*co*-3-hydroxyvalerate). *Macromolecules*, 22(4): 1676–1682

Kılıçay E., Demirbilek M., Türk M., Güven E., Hazer B., Denkbas E. B. (2011) Preparation and characterization of poly(3-hydroxybutyrate-*co*-3-hydroxyhexanoate) (PHBHHX) based nanoparticles for targeted cancer therapy. *European Journal of Pharmaceutical Sciences*, 44(3): 310–320

Levine A. C., Heberlig G. W., Nomura C. T. (2016) Use of thiol-ene click chemistry to modify mechanical and thermal properties of polyhydroxyalkanoates (PHAs). *International Journal of Biological Macromolecules*, 83: 358–365

Luo L., Wei X., Chen G. Q. (2009) Physical properties and biocompatibility of poly(3-hydroxybutyrate-*co*-3-hydroxyhexanoate) blended with poly(3-hydroxybutyrate-*co*-4-hydroxybutyrate). *Journal of Biomaterials Science, Polymer Edition*, 20(11): 1537–1553

Martelli S. M., Sabirova J., Fakhouri F. M., Dyzma A., De Meyer B., Soetaert W. (2012) Obtention and characterization of poly(3-hydroxybutyricacid-*co*-hydroxyvaleric acid)/mcl-PHA based blends. *LWT – Food Science and Technology*, 47(2): 386–392

Mohd Fadzil F. I., Mizuno S., Hiroe A., Nomura C. T., Tsuge T. (2018) Low carbon concentration feeding improves medium-chain-length polyhydroxyalkanoate production in *Escherichia coli* strains with defective β-oxidation. *Frontiers in Bioengineering and Biotechnology*, 6: 178

Nerkar M., Ramsay J. A., Ramsay B. A., Kontopoulou M. (2014) Melt compounded blends of short and medium chain-length poly-3-hydroxyalkanoates. *Journal of Polymers and the Environment*, 22(2): 236–243

Ohkoshi I., Abe H., Doi Y. (2000) Miscibility and solid-state structures for blends of poly[(*S*)-lactide] with atactic poly[(*R, S*)-3-hydroxybutyrate]. *Polymer*, 41(15): 5985–5992

Qu X. H., Wu Q., Liang J., Zou B., Chen G. Q. (2006) Effect of 3-hydroxyhexanoate content in poly(3-hydroxybutyrate-*co*-3-hydroxyhexanoate) on *in vitro* growth and differentiation of smooth muscle cells. *Biomaterials*, 27(15): 2944–2950

Sambrook J., Russell D. W. (2011) *Molecular cloning: a laboratory manual cold spring harbor laboratory*. New York, USA

Spratt S. K., Ginsburgh C. L., Nunn W. D. (1981) Isolation and genetic characterization of *Escherichia coli* mutants defective in propionate metabolism. *Journal of Bacteriology*, 146(3): 1166–1169

Tappel R. C., Wang Q., Nomura C. T. (2012) Precise control of repeating unit composition in biodegradable poly(3-hydroxyalkanoate) polymers synthesized by *Escherichia coli*. *Journal of Bioscience and Bioengineering*, 113(4): 480–486

Tsuge T. (2002) Metabolic improvements and use of inexpensive carbon sources in microbial production of polyhydroxyalkanoates. *Journal of Bioscience and Bioengineering*, 94(6): 579–584

Tsuge T. (2016) Fundamental factors determining the molecular weight of polyhydroxyalkanoate during biosynthesis. *Polymer Journal*, 48(11): 1051–1057

Tsuge T., Hyakutake M., Mizuno K. (2015) Class IV polyhydroxyalkanoate (PHA) synthases and PHA-producing *Bacillus*. *Applied Microbiology and Biotechnology*, 99(15): 6231–6240

Tsuge T., Hyakutake M., Tomizawa S., Suzuki N., Matsumoto K. (2017) Japan patent P6195296

Ushimaru K., Watanabe Y., Hiroe A., Tsuge T. (2015) A single-nucleotide substitution in phasin gene leads to enhanced accumulation of polyhydroxyalkanoate (PHA) in *Escherichia coli* harboring *Aeromonas caviae* PHA biosynthetic operon. *Journal of General and Applied Microbiology*, 61(2): 63–66

Volova T., Kiselev E., Nemtsev I., Lukyanenko A., Sukovatyi A., Kuzmin A., Ryltseva G., Shishatskaya E. (2021) Properties of degradable polyhydroxyalkanoates with different monomer compositions. *International Journal of Biological Macromolecules*, 182: 98–114

Xu P., Cao Y., Lv P., Ma P., Dong W., Bai H., Wang W., Du M., Chen M. (2018) Enhanced crystallization kinetics of bacterially synthesized poly(3-hydroxybutyrate-*co*-3-hydroxyhexanate) with structural optimization of oxalamide compounds as nucleators. *Polymer Degradation and Stability*, 154: 170–176

Zembouai I., Bruzaud S., Kaci M., Benhamida A., Corre Y. M., Grohens Y., Taguet A., Lopez-Cuesta J.M. (2014) Poly(3-hydroxybutyrate-*co*-3-hydroxyvalerate)/polylactide blends: Thermal stability, flammability and thermo-mechanical behavior. *Journal of Polymers and the Environment*, 22(1): 131–139

Zhang J., Shishatskaya E. I., Volova T. G., da Silva L. F., Chen G. Q. (2018) Polyhydroxyalkanoates (PHA) for therapeutic applications. *Materials Science and Engineering C*, 86: 144–150

Journal of Siberian Federal University. Biology 2021 14(4): 454–464
~ ~ ~

DOI 10.17516/1997-1389-0364

УДК 542.61–036.7

Scale-Up of the Downstream Process for Polyhydroxyalkanoate Copolymer P(HB-co-HHx) Extraction with Nonhalogenated Solvents

Isabel Thiele[a], Jan Hendrik Rose[b], Björn Gutschmann[a], Samantha Tofaily[b], Julie Schöttel[b], Torsten Widmer[b], Peter Neubauer[a], Thomas Grimm[b] and Sebastian L. Riedel*[a]

[a]Technische Universität Berlin
Berlin, Germany
[b]ANiMOX GmbH
Berlin, Germany

Received 22.06.2021, received in revised form 23.07.2021, accepted 14.08.2021

Abstract. Biobased and biodegradable polyhydroxyalkanoates (PHAs) are promising alternatives to common plastics. Due to their high production costs, only a minimal share of global plastic production is composed of PHA. A major contributor to the high costs minimizing the potential to occupy a larger market share is the downstream process. To obtain high recovery yields and pure products, most approaches rely on large amounts of solvents. While short-chain-length PHA (*scl*-PHA) is poorly soluble in nonhalogenated solvents, medium-chain-length PHA (*mcl*-PHA) was shown to be soluble in nonhalogenated solvents. In this study, an approach to recover poly(hydroxybutyrate-*co*-hydroxyhexanoate) with acetone and 2-propanol was scaled up 30-fold to 300 g of lyophilized cells per recovery cycle. High PHA purities of 90–100 % were reached from extractions at moderate temperatures from 30–58 °C. In two-stage extractions, up to 100 % PHA was recovered, while the molecular weight was not reduced. Solvents were recovered by distillation in a concentration step and after precipitation. Furthermore, the material properties were analyzed. PHA recovered from the distillation bottom had an increased HHx content compared to the first and second extractions using recovered solvents and was of low purity, indicating efficient and pure precipitation of the recovered PHA during the 2-stage extractions.

Keywords: P(HB-*co*-HHx), *mcl*-PHA, nonhalogenated solvents, PHA recovery.

* Corresponding author E-mail address: riedel@tu-berlin.de
ORCID: 0000-0003-2871-7399 (Thiele I.); 0000-0003-0166-8734 (Gutschmann B.); 0000-0002-1214-9713 (Neubauer P.); 0000-0003-1373-417X (Riedel S.L.)

Acknowledgements. This research was funded by the German Federal Ministry of Education and Research (grant numbers: 031B0798A and 031B0798C).

Citation: Thiele I., Rose J. H., Gutschmann B., Tofaily S., Schöttel J., Widmer T., Neubauer P., Grimm T., Riedel S. L. Scale-up of the downstream process for polyhydroxyalkanoate copolymer P(HB-*co*-HHx) extraction with nonhalogenated solvents. J. Sib. Fed. Univ. Biol., 2021, 14(4), 454–464. DOI: 10.17516/1997-1389-0364

Масштабирование процесса экстракции сополимера П(ГБ-со-ГГ) негалогенированными растворителями

И. Тиле[а], Я. Х. Роуз[б], Б. Гутчманн[а], С. Тофайли[б], Д. Шеттель[б], Т. Видмер[б], П. Нойбауэр[а], Т. Гримм[б], С. Л. Ридель[а]
[а]Берлинский технический университет
Германия, Берлин
[б]ANiMOX GmbH
Германия, Берлин

Аннотация. Синтезируемые микроорганизмами биоразлагаемые полигидроксиалканоаты (ПГА) являются многообещающей альтернативой обычным пластмассам. Однако высокая стоимость ПГА ограничивает объемы их мирового производства. Одной из основных причин высоких затрат, сводящих к минимуму возможность занять большую долю рынка, является сложный и дорогостоящий процесс извлечения полимеров из клеточной биомассы. Для получения высоких выходов извлечения и чистых образцов полимеров используются большие количества растворителей. При этом известно, что короткоцепочечные ПГА плохо растворяются в негалогенированных растворителях, в то время как среднецепочечные – растворяются. В этом исследовании процесс извлечения сополимера гидроксибутирата и гидроксигексаноата с использованием ацетона и 2-пропанола масштабирован в 30 раз (до 300 г лиофилизированной клеточной массы на один цикл извлечения). Высокая чистота ПГА (90–100 %) достигнута при проведении экстракции при умеренных температурах от 30 до 58 °С. При двукратной экстракции полнота извлечения полимера достигала 100 % без снижения значений молекулярной массы. Растворители возвращали для повторных циклов перегонкой на стадии концентрирования и после осаждения извлеченного полимера. Проанализированы свойства полученных образцов ПГА. Полимер, извлеченный из остаточной от дистилляции фракции, по сравнению с полимером, полученным в результате двукратной экстракции с повторным использованием растворителей, имел повышенное содержание фракции мономеров гексаноата и низкую степень чистоты. Это свидетельствует об эффективности осаждения полимера, извлеченного в процессе двукратной экстракции.

Ключевые слова: П(ГБ-со-ГГ), среднецепочечные ПГА, негалогенированные растворители, извлечение ПГА.

Благодарности. Это исследование финансировалось Федеральным министерством образования и научных исследований Германии (номера грантов: 031B0798A и 031B0798C).

Цитирование: Тиле, И. Масштабирование процесса экстракции сополимера П(ГБ-со-ГГ) негалогенированными растворителями / И. Тиле, Я.Х. Роуз, Б. Гутчманн, С. Тофайли, Д. Шеттель, Т. Видмер, П. Нойбауэр, Т. Гримм, С.Л. Ридель //Журн. Сиб. федер. ун-та. Биология, 2021. 14(4). С. 454–464. DOI: 10.17516/1997-1389-0364

Introduction

Plastic pollution is a worldwide problem, yet global plastic production is still increasing and reached 359 million t per year in 2018, and with it, the need for environmentally friendly alternatives has increased. One of these alternatives is biobased and biodegradable polyhydroxyalkanoates (PHAs), which can be produced from low-cost feedstocks with microorganisms (Riedel and Brigham, 2019, 2020). During downstream processing, PHA is either extracted from the cells or the surrounding non-PHA cell material is removed, which was recently comprehensively reviewed (Koller et al., 2013b; Gahlawat et al., 2020). In this context, solvent-based PHA downstream processing often relies on large amounts of halogenated, mostly chlorinated, solvents, which cause a very negative ecological footprint (Pérez-Rivero et al., 2019; Saavedra del Oso et al., 2021).

PHAs are categorized based on the number of carbon atoms of their monomer building blocks. Monomers consisting of 3–5 carbon atoms are termed *short-chain-length* (*scl*), and monomers of 6–l4 carbon atoms are termed *medium-chain-length* (*mcl*) (Steinbüchel et al., 1992). Various *scl-mcl*-copolymers can be produced to obtain PHAs with tailored properties, making them promising alternatives to conventional plastics for various applications (Chen, 2010). Specifically, the *scl-mcl*-copolymer poly(hydroxybutyrate-*co*-hydroxyhexanoate) (P(HB-*co*-HHx)) shows reduced crystallinity, reduced melting temperature and higher elasticity compared to polyhydroxybutyrate (PHB) and thus makes it suitable for further processing (Noda et al., 2010). In seawater or soil, P(HB-*co*-HHx) degrades easily within months without pretreatment (Chen, 2012; Shang et al., 2012). Regarding downstream processing, *mcl*-PHA and copolymers thereof are more soluble in nonhalogenated solvents than *scl*-PHA (Jiang et al., 2006; Furrer et al., 2007; Cerrone et al., 2019). Methyl isobutyl ketone, methyl ethyl ketone, ethyl acetate and acetone were mainly reported in combinations with precipitation solvents such as ethanol, n-hexane or 2-propanol to precipitate the extracted PHA that was recovered from dried cells or wet biomass (Furrer et al., 2007; Riedel et al., 2013; Bartels et al., 2020; Saavedra del Oso et al., 2021).

Recently, a recovery method was developed by Bartels et al. using acetone and 2-propanol to achieve recovery yields up to 100% with the possibility of separating and recycling the solvents due to their zeotropic nature (Bartels et al., 2020). In this work, the approach by Bartels et al. (2020) was scaled up to process 300 g of dried cells, and the recycling of the solvents was assessed.

Material and Methods

Biomass for P(HB-co-HHx) recovery

Engineered *Ralstonia eutropha* Re2058/pCB113 cells (Budde et al., 2011) containing the copolymer P(HB-*co*-HHx) were produced in a 150 L bioreactor utilizing waste fats of porcine origin (ANiMOX GmbH, Berlin, Germany) as the main carbon source adapting the cultivation

strategy performed by Riedel et al. (Riedel et al., 2015).

Extraction and precipitation with acetone and 2-propanol

Bartels et al. (2020) recently identified acetone and 2-propanol as a suitable solvent and nonsolvent pair for the *scl-mcl*-copolymer P(HB-*co*-HHx). The established volume to weight ratio of 10:1 (acetone: freeze-dried cells) was scaled up to a larger volume (Fig. 1). Cells (300 g) and 3 L of solvent were added to a 5 L round-bottom flask and rotated in a water bath at 30–58 °C for 1 h in a rotary evaporator to extract the PHA. Separation of the extract from cell debris was performed by centrifugation (4000 rpm, 10 min, room temperature) and subsequent decantation. The separated extract was concentrated using a rotary evaporator and precipitated with 4 °C cold 2-propanol overnight. PHA was recovered by centrifugation at 4000 rpm for 10 min and dried either at 50 °C, in a vacuum pot or in a freeze dryer.

Two-stage extraction

Extraction was performed as described above. Residual cells were dried at 50 °C and pooled with similar residual cells, if necessary, prior to the next extraction. The remaining PHA from the residual cell material was extracted under the same conditions as the first extraction.

Extraction conditions

Different temperatures from 30 to 58 °C as well as different solvent evaporations (40–68 % of the initial volume of acetone) from the PHA extract were tested. Different 2-propanol concentrations occurring either due to the evaporation of acetone and subsequent addition of 6 L of 2-propanol or varying addition of 2-propanol were investigated. The final concentrations of each solvent per recovery cycle are given for the respective results.

Recovery yield determination

The recovery yield was calculated according to Equation 1:

$$RecoveryYield[\%] = = \frac{extractedmaterial[g]}{lyophilzedcells[g] \times PHAcontent} \times 100 \quad (1)$$

Molecular weight characteristics

Molecular weight characteristics were determined by gel permeation chromatography (GPC) equipped with a differential refractive index detector (Merck-Hitachi, RI-Detector L-7490) using two sequentially coupled columns (Agilent PLgel 5 µm MIXED-C300 × 7.5 mm, 50 × 7.5 mm Guard). Polystyrene standards in the range of 9.6–3187 kDa were used for calibration (Agilent Polystyrol PS-1). PHA samples were

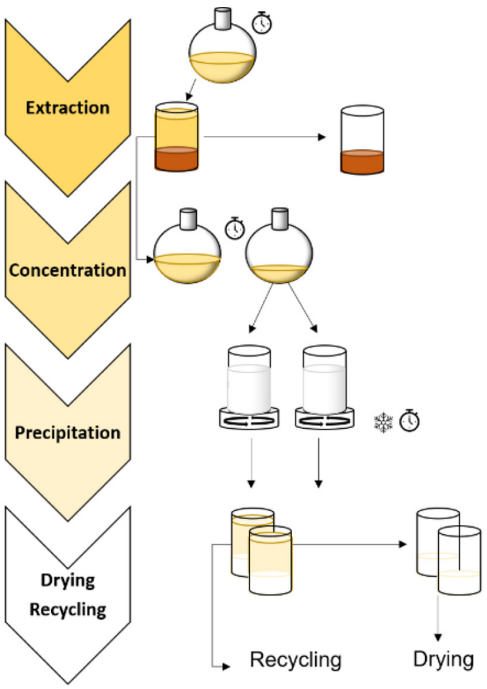

Fig. 1. Schematic description of the workflow to recover *scl-co-mcl*-PHA from lyophilized cells using acetone and 2-propanol

weighed to obtain a concentration of 5 mg mL^{-1} in 2 mL of chloroform containing 2-butanone at a concentration of 1 mg mL^{-1} in a borosilicate tube (Borosilicate Screw Thread Culture Tube with PTFE-Faced Rubber Lined Caps, Ø16 mm x 100 mm, KIMAX®) and incubated at 55 °C for 24 h (Hettich Lab Technology). After cooling to room temperature, the samples were filtered into an amber HPLC vial through 0.2 µm PTFE syringe filters. Analysis of 15 µL samples was performed at 30 °C and a flow rate of 0.8 mL min^{-1} chloroform. Signal data points (n_i) and respective MW (M_i) calculated by the calibration data were used to calculate the number average (M_n), weight average (M_w), and dispersity values ($Đ$) according to Equations 2–4 (Bartels et al., 2020):

$$M_n = \frac{\sum_{i=1}^{k}(n_i \cdot M_i)}{\sum_{i=1}^{k} n_i} \quad (2)$$

$$M_w \frac{\sum(n_i \cdot M_i^2)}{\sum(n_i \cdot M_i)} \quad (3)$$

$$Đ = \frac{M_w}{M_n} \quad (4)$$

Determination of PHA content, molar HHx content and purity

The determination of PHA content by gas chromatography (GC) was previously described by Bartels et al. (2020) and performed accordingly.

Dry substance and ash content determination

To check whether the PHA was fully dried after precipitation and to ensure that no residual solvent might interfere with further processing or impact the melting temperature, dry substance was calculated by balancing the weight of the sample (0.6 g) that was dried as described in this procedure and the weight after drying in an oven at 105 °C. Samples were weighed every 2 h until a constant weight was reached. Ashing was performed by heating recovered PHA samples in a muffle furnace (Phoenix Black Muffelofen, CEM) for 5 h at 550 °C. After cooling to room temperature, the ash content was determined by weighing.

Results

In this study, *scl-co-mcl*-PHA recovery using acetone as a solvent and 2-propanol as a nonsolvent was scaled up by a factor of 30 to 300 g of lyophilized cells. The nonhalogenated solvents were separated and recovered by distillation and utilized for further recovery cycles to increase the sustainability of the process by reducing the overall solvent usage. Recovery was performed on different lyophilized cell materials (Batch 1 and Batch 2). The batches from different cultivations had different PHA contents of 76.1 or 81.1 % with either 16.1 or 19.2 mol% HHx content, respectively.

P(HB-co-HHx) extraction at moderate temperatures and impact of solubilized PHA concentration and variation of 2-propanol concentration

As shorter extraction times were reported to result in lower molecular weight reduction at 21 and 70 °C (Bartels et al., 2020), PHA was extracted for 1 h at 30–58 °C with different subsequent extract concentrations and precipitation conditions (Fig. 2A). The solubility is temperature dependent. At lower temperatures of 30 °C, the recovery yield was 49 %, while an extraction temperature of 58 °C resulted in a 1.5-fold higher recovery yield of 78 %. The largest increase in recovery yield was observed in a temperature range from 30–40 °C (Fig. 2B). After extraction at 40 °C, the PHA was concentrated by 40 to 68 % of the initial volume of the extract (Fig. 2C). When the extract was concentrated by

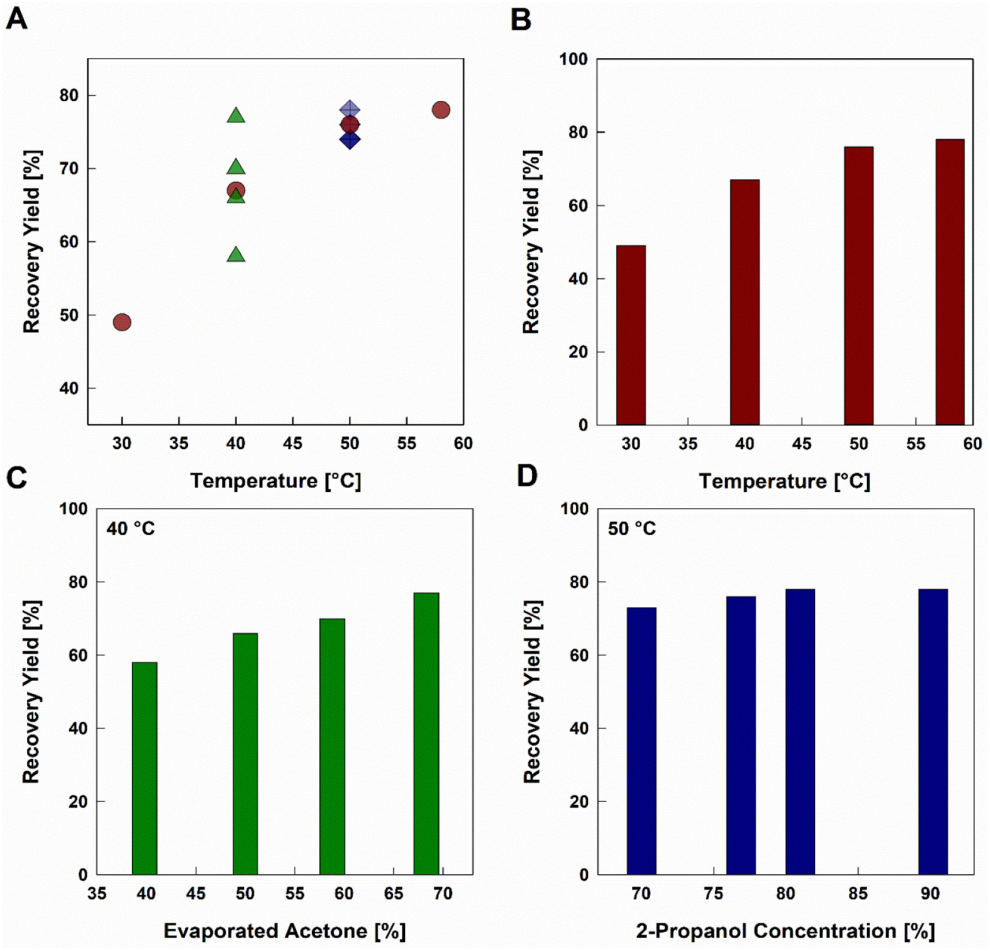

Fig. 2. P(HB-*co*-HHx) extraction at moderate temperatures (A). Recovery yields depending on different extraction, concentration and precipitation conditions; (B) extraction at 30–58 °C for 1 h; concentration by evaporation of 58.3 ± 0.6 % acetone and precipitation with 2-propanol at 4 °C (82.1 ± 1.3 % 2-propanol content in the solvent mixture); (C) extraction at 40 °C for 1 h, increasing the concentration of solubilized P(HB-*co*-HHx) in acetone by evaporation of 40–68 % acetone and precipitation with 58–77 % 2-propanol; (D) extraction at 50 °C for 1 h with evaporation of 50 ± 0.6 % acetone and varying 2-propanol concentration from 70–90 %

40 %, less 2-propanol was added for precipitation (17 % less, approximately 5 L instead of 6 L, resulting in a concentration of 74 %). The most concentrated extract was supplied with more 2-propanol (17 % more, 88 % (i. e., approximately 7 L)). Due to the higher concentration of the PHA extract, precipitation becomes more efficient. By realizing higher concentrations of PHA extract (68 %), the recovery yields at 40 °C increased up to a recovery yield of 77 %, which is comparable to yields at 50 or 58 °C, where the PHA extract was concentrated by approximately 58 %. Moreover, by concentration of the solution in a rotary evaporator, pure acetone is recovered before the precipitation step, leading to a lower demand of 2-propanol to achieve a large volumetric excess. To investigate whether the extracted PHA was successfully precipitated, less acetone (50 %) was evaporated after extraction at 50 °C with subsequent addition of cold 2-propanol to achieve 70–90 % acetone in the mixture (Fig. 2D). With increasing concentrations of 2-propanol, only slightly improved recovery yields by 5 % were achieved. The recovery yields were comparable

to those of the extraction at 50 °C in the previous section.

Two-stage extraction

Two to three batches of residual cells from extractions at the same temperature were pooled for a second extraction cycle. The results were analyzed regarding purity, HHx content, recovery yield and molecular weight characteristics.

PHA purity and HHx content

High PHA purities in the range of 87.9–100 % were reached in all experiments (Fig. 3A, 3C, Supplementary Table 1). No drastic changes regarding the HHx content of the recycled material in the first or second extraction cycle were observed, nor were they observed in the residual cells (Fig. 3B). On the other hand, a slight decrease in the molecular weight was noticeable (Table 1). This might be due to the longer duration of PHA exposure to higher temperatures and solvents or the lower solubility of higher molecular weight polymers.

Recovery yield from two-stage extraction at different temperatures

The recovery yields were obtained from 62 % at 30 °C up to 100 % at 50 or 55 °C (Fig. 3D).

Generally, Batch 2 (19.2 % HHx; 81.1 % PHA; higher MW) gave lower total recovery yields after the second extraction compared to Batch 1. This might be due to the temperature dependency shown in the previous section and to a smaller part the different starting material properties, as the differences are minor. The recovered product was clustered in two different ranges of molecular weights depending on the batch from which they were recovered. The molecular weight and dispersity index were shown to depend on the amount of PHA synthase (Sim et al., 1997) and are therefore cultivation- and strain-dependent.

Table 1. Molecular weight characteristics of the recovered PHA after the first and second extraction

PHA	M_w [Da] × 10^5	M_n [Da] × 10^5	Đ [–]	
B1.1	1.88 ± 0.02	0.79 ± 0.01	3.39 ± 0.07	1. Extraction
B1.2	2.06 ± 0.03	0.87 ± 0.03	2.36 ± 0.05	
B1.1+2	1.89 ± 0.01	0.94 ± 0.03	2.01 ± 0.05	2. Extraction
B1.3	1.90 ± 0.01	0.84 ± 0.01	2.26 ± 0.03	1. Extraction
B1.4	2.07 ± 0.01	0.93 ± 0.14	2.27 ± 0.26	
B1.3+4	1.79 ± 0.01	0.94 ± 0.03	1.91 ± 0.04	2. Extraction
B1.5	1.99 ± 0.001	0.89 ± 0.02	2.24 ± 0.06	1. Extraction
B1.6	2.08 ± 0.05	0.82 ± 0.03	2.54 ± 0.04	
B1.7	2.09 ± 0.02	0.87 ± 0.04	2.42 ± 0.08	
B1.5+6+7	1.75 ± 0.01	0.86 ± 0.005	2.04 ± 0.02	2. Extraction
B2.1	2.68 ± 0.04	1.12 ± 0.05	2.39 ± 0.07	1. Extraction
B2.2	2.70 ± 0.04	1.20 ± 0.01	2.25 ± 0.01	
B2.1+2	2.52 ± 0.03	1.08 ± 0.01	2.32 ± 0.01	2. Extraction
B2.3	2.77 ± 0.02	1.26 ± 0.02	2.19 ± 0.01	1. Extraction
B2.4	2.75 ± 0.01	1.14 ± 0.04	2.42 ± 0.07	
B2.5	2.70 ± 0.05	1.26 ± 0.02	2.15 ± 0.06	
B2.3+4+5	2.50 ± 0.07	1.34 ± 0.03	1.86 ± 0.10	2. Extraction

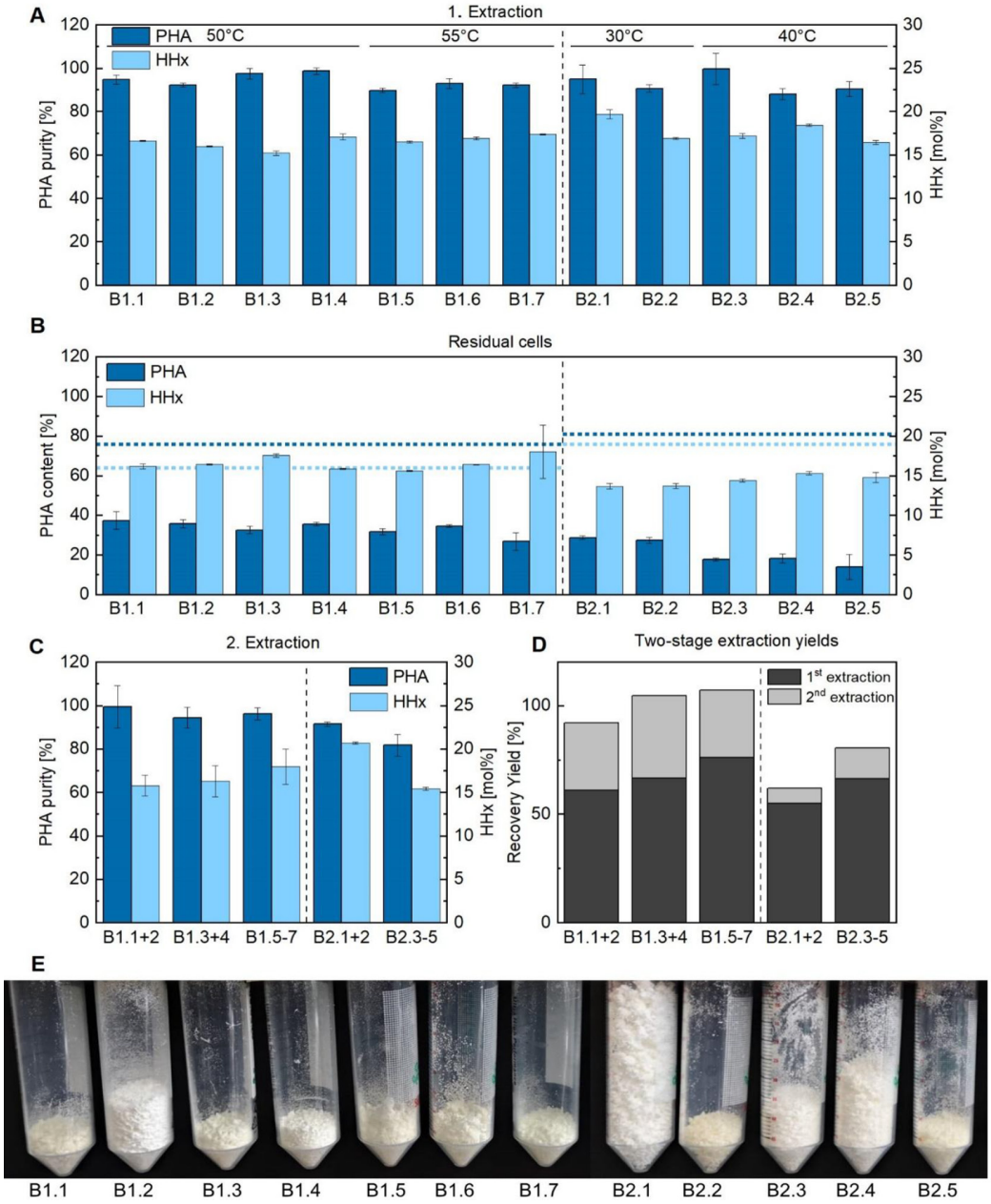

Fig. 3. Two-stage extraction of P(HB-*co*-HHx) from lyophilized cells at 50, 55, 30 and 40 °C. PHA purity and HHx content (Batch 1: 76.1 % PHA content, 16.1 mol% HHx; Batch 2: 81.1 % PHA content, 19.2 mol% HHx), Batch 1, 50 °C, B1.1, B1.2: 43.3 % evaporated acetone, final 2-propanol concentration: 77.9 %; Batch 1, 50 °C, B1.3, B1.4: 50 % evaporated acetone, final 2-propanol concentration: 80 %; Batch 1, 55 °C, B1.5, B1.6, B1.7: 49.7–50 % evaporated acetone, final 2-propanol concentration: 80–81.7 %; Batch 2, 30 °C, B2.1, B2.2: 54.5–60.7 % evaporated acetone, final 2-propanol concentration: 81.4–83.6 %; Batch 2, 40 °C, B2.3, B2.4, B2.5: 50–59 % evaporated acetone, final 2-propanol concentration: 81.4–83.6 % (A). PHA and HHx contents in the residual cells after extraction (B). PHA purity and HHx content after the second extraction (C). Recovery yields after two-stage extraction under different conditions (D). Properties of the recovered material (E). Error bars indicate technical triplicates of GC samples. Dashed lines indicate the initial PHA and HHx contents of the respective starting cell material

Coloration and bulk density

The bulk density, texture and coloration of the recovered polymer were investigated. Three grams of each recovery cycle (1 stage extractions) is shown (Fig. 3E). More granular material appeared more yellow in color and had a lower bulk density. The material properties seem to vary throughout all experiments without a connection to purity or solvents and their content in the mixture (Supplementary Tables 1, 2, and 3; Supplementary Figures 1, 2, and 3). Materials with lower bulk densities are preferable because they are more convenient to package, transport and further process.

Moisture content before drying

After extraction and precipitation of the PHA, the solvent mixture was decanted. The wet PHA was dried using a freeze dryer or a vacuum pot or was dried at 50 °C. The recovered PHA was regularly (approximately every 30 minutes) mixed and manually broken up into smaller pieces. The drying process was done for 6 hours. The solvent content of the wet mass was determined. All samples contained 81–92 % moisture before drying regardless of the extraction conditions (Supplementary Table 4).

Product recovery from the distillation bottom

After various recovery cycles, PHA was recovered from the distillation bottom. Interestingly, PHA showed a higher molar content of hydroxy hexanoate as well as a comparably high molecular weight (Table 2).

Dry substance and ash content

Solvent residues might hamper further processability of PHA. Because of the high moisture content prior to drying, dry substance and ash content were determined to ensure a pure and dry polymer. As the material is recovered from biological material, the inorganic content remaining after ashing should be near zero. The dry substance determination gave > 99 % dry substance and < 1 % ash content for all recovery cycles (Supplementary Table 4).

Discussion

The recovery method developed by Bartels et al. (2020) was scaled up by a factor of 30 from 10 to 300 g of lyophilized cells as the starting material. The concentration of the PHA extract and 2-propanol excess was further investigated. While it was previously reported that acetone is evaporated until the viscosity increases, the concentration of PHA in the extract impacts the efficiency of the precipitation step. However, increased temperatures or pressure contribute largely to higher recovery yields in short extraction times (Koller et al., 2013a; Bartels et al., 2020). However, high recovery yields might be obtained at moderate temperatures due to PHA extract concentration by acetone evaporation and recovery after extraction. Therefore, the energy demand is reduced, leading to a more sustainable process: heating the water bath and acetone to 55 or 58 °C has a 1.5- and 1.8-fold energy demand compared to extraction at 40 °C, respectively. A major drawback of solvent-based downstream processing is the large amounts of

Table 2. Properties of the material recovered from the distillation bottom

PHA	Purity [%]	HHx [mol%]	M_w [Da]	M_n [Da]	Đ [–]
Distillation Bottom	69.03±8.36	25.63±1.24	$2.97±0.03×10^5$	$1.1±0.001×10^5$	2.71±0.02

often halogenated solvents (Saavedra del Oso et al., 2021). Evaporation and recovery of acetone during the concentration step leads to a lower demand for 2-propanol to obtain a large nonsolvent excess to precipitate PHA. The concentration of the extract was also shown to result in higher recovery yields. Given the zeotropic nature of the solvent mixture, acetone and 2-propanol were separated and reused for multiple recovery cycles. Fractions of up to 30% 2-propanol in acetone were reported to still recover PHA adequately, and even pure 2-propanol was able to extract 14.5% of P(HB-*co*-HHx) (Bartels et al., 2020). Moreover, acetone extraction and 2-propanol precipitation are suitable to obtain PHA with low endotoxin content, making it utilizable for medical applications (Furrer et al., 2007).

In this study, no significant molecular weight or purity reduction depending on temperature was observed. Even though polymer solubility is expected to decrease with higher molecular weight (Terada and Marchessault, 1999) interaction between polar groups and hydrogen bonding. For polar polymers such as poly(3-hydroxyalkanoates, the minor differences in the molecular weight of the different cell batches did not impact the recovery yield. The appearance of the recovered product varies regarding granularity and color as well as bulk volume, but for commercial use, a consistent product is desired. Most likely, the differences occur due to handling at the lab scale by mixing and breaking the polymer mass into smaller pieces while drying, which might be overcome with a less manual drying process. Losses of solvent due to drying on a lab scale can be easily avoided on larger scales by dryers that collect the withdrawn solvent.

Conclusion

P(HB-*co*-HHx) extraction from freeze-dried *R. eutropha* cells using a combination of acetone and 2-propanol was scaled up to 300 g of lyophilized cells as the starting material. The process was adapted to mild process conditions. The solvents were recycled over the course of the experiments, reducing the costs and making the process greener by using nonhalogenated solvents. This might contribute to further research on the PHA production process.

References

Bartels M., Gutschmann B., Widmer T., Grimm T., Neubauer P., Riedel S. L. (2020) Recovery of the PHA copolymer P(HB-co-HHx) with non-halogenated solvents: influences on molecular weight and HHx-content. *Frontiers in Bioengineering and Biotechnology*, 8: 944

Budde C. F., Riedel S. L., Willis L. B., Rha C., Sinskey A. J. (2011) Production of poly(3-hydroxybutyrate-co-3-hydroxyhexanoate) from plant oil by engineered Ralstonia eutropha strains. *Applied and Environmental Microbiology*, 77(9): 2847–2854

Cerrone F., Radivojevic J., Nikodinovic-Runic J., Walsh M., Kenny S. T., Babu R., O'Connor K.E. (2019) Novel sodium alkyl-1,3-disulfates, anionic biosurfactants produced from microbial polyesters. *Colloids and Surfaces B: Biointerfaces*, 182: 110333

Chen G.-Q. (2010) Industrial production of PHA. *Plastics from bacteria: natural functions and applications*. Chen G. G.-Q. (ed) Springer Berlin Heidelberg, Berlin, Heidelberg, p. 121–132

Chen H. (2012) *Assessment of biodegradation in different environmental compartments of blends and composites based on microbial poly(hydroxyalkanoate)s*. 185 p.

Furrer P., Panke S., Zinn M. (2007) Efficient recovery of low endotoxin medium-chain-length poly([R]-3-hydroxyalkanoate) from bacterial biomass. *Journal of Microbiological Methods*, 69(1): 206–213

Gahlawat G., Kumari P., Bhagat N. R. (2020) Technological advances in the production of polyhydroxyalkanoate biopolymers. *Current Sustainable/Renewable Energy Reports*, 7(3): 73–83

Jiang X., Ramsay J. A., Ramsay B. A. (2006) Acetone extraction of mcl-PHA from Pseudomonas putida KT2440. *Journal of Microbiological Methods*, 67(2): 212–219

Koller M., Bona R., Chiellini E., Braunegg G. (2013a) Extraction of short-chain-length poly-[(R)-hydroxyalkanoates] (scl-PHA) by the «anti-solvent» acetone under elevated temperature and pressure. *Biotechnology Letters*, 35(7): 1023–1028

Koller M., Niebelschütz H., Braunegg G. (2013b) Strategies for recovery and purification of poly[(R)-3-hydroxyalkanoates] (PHA) biopolyesters from surrounding biomass. *Engineering in Life Sciences*, 13(6): 549–562

Noda I., Lindsey S. B., Caraway D. (2010) Nodax™ class PHA copolymers: their properties and applications. *Plastics from bacteria: natural functions and applications*. Chen G. G.-Q. (ed.) Springer Berlin Heidelberg, Berlin, Heidelberg, p. 237–255

Pérez-Rivero C., López-Gómez J.P., Roy I. (2019) A sustainable approach for the downstream processing of bacterial polyhydroxyalkanoates: State-of-the-art and latest developments. *Biochemical Engineering Journal*, 150: 107283

Riedel S. L., Brigham C. J. (2019) Polymers and adsorbents from agricultural waste. *Byproducts from agriculture and fisheries*. Simpson B. K., Aryee A. N.A., Toldrá (eds.) John Wiley & Sons Ltd, Chichester UK, p. 523–544

Riedel S. L., Brigham C. J. (2020) Inexpensive and waste raw materials for PHA production. *The handbook of polyhydroxyalkanoates*. Koller M. (ed.) CRC Press Taylor & Francis Group, Boca Raton, p. 203–221

Riedel S. L., Brigham C. J., Budde C. F., Bader J., Rha C., Stahl U., Sinskey A. J. (2013) Recovery of poly(3-hydroxybutyrate-co-3-hydroxyhexanoate) from Ralstonia eutropha cultures with non-halogenated solvents. *Biotechnology and Bioengineering*, 110(2): 461–470

Riedel S. L., Jahns S., Koenig S., Bock M. C.E., Brigham C. J., Bader J., Stahl U. (2015) Polyhydroxyalkanoates production with Ralstonia eutropha from low quality waste animal fats. *Journal of Biotechnology*, 214: 119–127

Saavedra del Oso M., Mauricio-Iglesias M., Hospido A. (2021) Evaluation and optimization of the environmental performance of PHA downstream processing. *Chemical Engineering Journal*, 412: 127687

Shang L., Fei Q., Zhang Y. H., Wang X. Z., Fan D.-D., Chang H. N. (2012) Thermal properties and biodegradability studies of poly(3-hydroxybutyrate-co-3-hydroxyvalerate). *Journal of Polymers and the Environment*, 20(1): 23–28

Sim S. J., Snell K. D., Hogan S. A., Stubbe J., Rha C., Sinskey A. J. (1997) PHA synthase activity controls the molecular weight and polydispersity of polyhydroxybutyrate in vivo. *Nature Biotechnology*, 15(1): 63–67

Steinbüchel A., Hustede E., Liebergesell M., Pieper U., Timm A., Valentin H. (1992) Molecular basis for biosynthesis and accumulation of polyhydroxyalkanoic acids in bacteria. *FEMS Microbiology Letters*, 103(2–4): 217–230

Terada M., Marchessault R. H. (1999) Determination of solubility parameters for poly(3-hydroxyalkanoates). *International Journal of Biological Macromolecules*, 25(1–3): 207–215

Journal of Siberian Federal University. Biology 2021 14(4): 465–474
~ ~ ~

DOI 10.17516/1997-1389-0365

УДК 677.021.127-022.532:547.992:66.086

A Brief Review on Electrospun Lignin Nanofibres

Akhila Raman[a], B.D.S. Deeraj[b], Jitha S. Jayan[a], Appukuttan Saritha[a] and Kuruvilla Joseph[b]*

[a]Amrita Vishwa Vidyapeetham
Kollam, India
[b]Indian Institute of Space Science and Technology
Trivandrum, India

Received 12.06.2021, received in revised form 20.07.2021, accepted 14.08.2021

Abstract. Application of bio-based materials in various fields is currently gaining momentum; and lignin occupies a prominent place among such materials. Integrating lignin with synthetic plastics is an innovative approach in the development of sustainable polymers. However, blending lignin with other polymers is not an easy process because of its brittleness and low dispersibility. Grafting of lignin with poly(methyl methacrylate) via atom transfer radical polymerisation enhances the miscibility of lignin with other polymers. A number of publications describe the applications of electrospun lignin nanofibres in various fields. Often discarded as an unwanted component this material has a vast potential for various applications. With the advent of electrospinning technique, lignin-based nanofibres used as an alternative to conventional lignin due to its exceptional property and thus find use in various biomedical as well as electronic applications. Antimicrobial properties of these nanofibres could be exploited effectively in the current pandemic situation. Numerous reviews have been lately published on lignin and lignin-based materials. Most of them focus on the applications of lignin, that is why the idea of the present review is to concentrate entirely on lignin-based nanofibres prepared by the electrospinning process and consolidate the applications of these electrospun lignin nanofibres.

Keywords: electrospinning, lignin nanofibres, carbon nanofibres, kraft lignin, organosolv lignin, alkali lignin.

* Corresponding author E-mail address: kuruvilla@iist.ac.in
ORCID: 0000-0001-9772-6905 (Deeraj B.D.S.); 0000-0001-7858-6919 (Jayan J.S.); 0000-0002-2253-8050 (Saritha A.); 0000-0002-2866-9713 (Joseph K.)

Citation: Raman A., Deeraj B.D.S., Jayan J.S., Saritha A., Joseph K. A brief review on electrospun lignin nanofibres. J. Sib. Fed. Univ. Biol., 2021, 14(4), 465–474. DOI: 10.17516/1997-1389-0365

Краткий обзор по применению нановолокон лигнина, полученных электроспиннингом

А. Раман[а], Б.Д.С. Дирэдж[б], Д. С. Джаян[а], А. Саритха[а], К. Джозеф[б]
[а]Университет Амрита
Индия, Коллам
[б]Индийский институт космической науки и технологии
Индия, Тривандрум

Аннотация. В настоящее время стремительно возрастает использование в различных областях материалов на биологической основе, лигнин занимает важное место среди таких материалов. Создание соединений лигнина с синтетическими пластиками можно рассматривать как инновационный подход в разработке экологически безопасных полимеров. Однако соединение лигнина с другими полимерами – это не простой процесс из-за его хрупкости и неспособности к хорошей дисперсии. Сополимер лигнина с полиметилметакрилатом, полученный посредством радикальной полимеризации с переносом атома, может обладать лучшей смешиваемостью. В ряде недавно опубликованных работ описаны перспективы применения в различных областях нановолокон лигнина, полученных электроспиннингом. Этот многообещающий материал часто выбрасывают как нежелательный компонент, хотя он имеет огромный потенциал для использования в различных сферах. С появлением технологии электроспиннинга получаемые с его помощью нановолокна на основе лигнина благодаря исключительным свойствам стали находить применение в различных областях биомедицины и электроники. Нановолокна, обладающие антимикробными свойствами, могут быть эффективно использованы в нынешней ситуации пандемии. В настоящее время опубликовано множество обзоров, посвященных применению лигнина и материалов на его основе. Идея настоящего обзора состоит в том, чтобы полностью сконцентрироваться на нановолокнах на основе лигнина, полученных в процессе электроспиннинга, и охарактеризовать области их применения.

Ключевые слова: электроспиннинг, лигниновые нановолокна, углеродные нановолокна, крафт-лигнин, органосольвентный лигнин, щелочной лигнин.

Цитирование: Раман, А. Краткий обзор по применению нановолокон лигнина, полученных электроспиннингом / А. Раман, Б.Д.С. Дирэдж, Д.С. Джаян, А. Саритха, К. Джозеф // Журн. Сиб. федер. ун-та. Биология, 2021. 14(4). С. 465–474. DOI: 10.17516/1997-1389-0365

Introduction

Lignins are aromatic polymers that occur mainly in secondarily thickened plant cell walls. Lignin is the second most abundant organic polymer on earth after cellulose. It accounts for approximately 30 % of the organic carbon existing in the biosphere and is the main biorenewable source of aromatic structures. It is the major constituent of the plant body responsible for inhibition of diffusion of enzymes into wood and creates strong cell walls in plants. Lignin is a complex amorphous highly branched polymer. It consists of three phenylpropane monomers, coniferyl, sinapyl, and p-coumaryl alcohols which are termed as lignols. These monolignols generate guaiacyl, syringyl and p-hydroxyphenyl residues respectively in the lignin polymer. The composition and ratio of lignols in the structure of lignin is largely influenced by both the nature of a plant and the environment in which the plant dwells. Industrial lignins are mainly classified as kraft lignin, lignosulfonates, organosolv lignin and steam-exploded lignin based on the preparation methods (Calvo-Flores, Dobado, 2010). Following the go green trend, researchers are keenly interested in replacing synthetic materials with bio-based materials, such as cellulose, lignin, tannin etc. (Domínguez-Robles et al., 2020). Due to their high porosity and large surface area, nanofibres have various applications such as air filters (Chang, Chang, 2016), protective clothes (Baji et al., 2020), drug delivering agents (Li et al., 2021), scaffolds (Wang et al., 2018a), supercapacitors (Zhu et al., 2020), catalists (García-Mateos et al., 2018), solar cell electrodes (Zhao et al., 2018) etc. Electrospun lignin nanofibres deserve special attention because of their biocompatibility, biodegradability and magnificent selectivity (Gupta et al., 2015). The nature of electrospun fibres crucially depends on the attributes of the spinning solution, namely its viscosity, electrical conductivity and surface tension. If viscosity values are higher or lower than the required value, bead formation will occur instead of fibre formation (Kumar et al., 2019). Using a suitable spinning solution with required properties, electrospun nanofibres are produced, then stabilised thermally and carbonised.

MiJung Cho et al. (2020) used flax lignin to fabricate high performance electrospun carbon nanofibre mats. Their work opens a new avenue for utilisation of agricultural residue rich in flax fibre as a source for production of electrospun carbon nanofibres. Jose Francisco Vivo-Vilches et al. (2019) used three different types of lignin to make carbon nanofibres and analysed its ability as an electrode material. All fabricated fibres were subjected to electrochemical reactions and the samples prepared from kraft and phosphorus lignin exhibited superior properties.

Integrating lignin with synthetic plastics can be considered a promising approach in the development of sustainable polymers. However, blending lignin with other polymers is not an easy process because of its brittleness and low dispersion in many composites. Grafting lignin with poly(methyl methacrylate) via atom transfer radical polymerisation improves the miscibility of lignin with other polymers (Kai et al., 2015). Ying Zhao et al. (2018) used lignin as the precursor to develop flexible carbon nanofibre mats which are used as a counter electrode for solar cells. The outstanding features of the electrode are credited to the exceptionally high surface area and low charge transfer resistance of carbon nanofibre mats made of lignin.

Numerous reviews on lignin and lignin-based materials have been lately published. Most of them focus on lignin applications. The present review aims to concentrate entirely on lignin-based nanofibres prepared by the electrospinning process and consolidate the information on the applications of electrospun lignin nanofibres.

Parameters involved in electrospinning of lignin

As mentioned above, creation of the appropriate spinning solution is very important for production of nanoscale fibres using the electrospinning technique. In 2007, Manuel Lallave et al. (2007) published the first research on the application of this technology to virgin lignin devoid of any binders. In their work, a lignin: ethanol solution of 1:1 w/w ratio with a viscosity of 350 to 400 cPs was used to make lignin fibres by following the coaxial electrospinning technique. The diameter of the fabricated fibre ranged between 400 nm and 2 μm. The scanning electron microscopy (SEM) image of the fabricated nanofibres is shown in Figure 1. In addition, coaxial electrospinning method in a triaxial configuration was used by these authors to produce lignin hollow nanofibers (nanotubes). The flow rates for ethanol sheath: lignin solution: glycerine varied from 0.05/0.5/0.01 to 0.1/1/0.25 mL h^{-1}, respectively. The tip-to-collector distance was maintained at 20–25 cm, and an electrical voltage of 12 kV was applied.

The common practice for producing lignin nanofibres with enhanced properties is adding binder polymers along with lignin. It was observed that water soluble polymers, such as polyethylene oxide (PEO) (Wang et al., 2020) and polyvinyl alcohol (PVA) (Camiré et al., 2020), were ideal as binders in the process of electrospinning of lignin. Lignin-polyacrylonitrile (PAN) solutions in the N, N-dimethylformamide (DMF) solvent improve the electrospinning of lignin (Seo et al., 2011). Seo et al. (2011) observed that upon increasing the lignin content the viscosity of the solution changed, which led to the formation of beads and thicker fibres. R. Ruiz-Rosas et al. (2010) fabricated lignin-derived carbon fibres using platinum (Pt)-doped lignin: ethanol solution for electrospinning. The tip-collector distance was set as 20–25 cm, and the applied electrical voltage was 12 kV. Maintaining such conditions prevented the fibres from reaching places other than the collector, thus facilitating the collection of electrospun fibres. The obtained lignin fibres were thermostabilised in an oxidising environment. Then, the fibres were heated to 200 °C maintaining a heating rate of 0.05 °C/min for about 36 hours. The obtained fibres exhibited high resistance to oxidation because of the lack of surface defects and fairly regular structure. Oxidation resistance of lignin-derived carbon fibres was slightly reduced due to the presence of platinum.

Formation of uniform fibres by addition of poly(ethylene oxide) (PEO) was studied by Ian Dallmeyer et al. (2014). The process

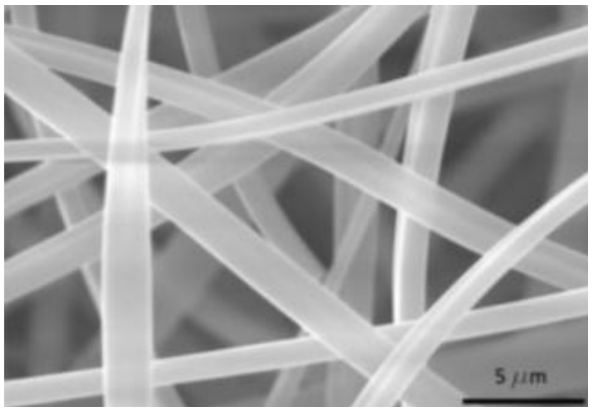

Fig. 1. SEM image of fabricated Alcell lignin electrospun nanofibres (Lallave et al., 2007)

occurred at the tip-collector distance of 14 to 20 cm, the potential difference between 9 and 14 kV, and the continuous flow rate of 0.03 mL/min. The fabricated electrospun fibres were thermostabilised under oxidative condition: they were heated at a constant heating rate to a temperature of 250 °C and held isothermally for 1 hour. The properties of the fabricated sample suggested that lignin polymers have potential applications as precursors for flexible carbon electrodes. Figure 2 illustrates the process of electrospinning of lignin and shows the SEM images of the sample prepared by this method.

Applications of electrospun lignin nanofibres

Applications of lignin fibres can be significantly improved by converting them to nanofibre structures. Electrospinning is a charge-assisted technique that allows to do it. Lignin nanofibre production is challenging because of the complex lignin's structure, but electrospun lignin nanofibres can be prepared using proper solvent combinations and incorporating secondary supporting polymers. These nanofibres find applications in various fields of material chemistry (Deeraj et al., 2021) (Table).

Camire et al. (2020) prepared electrospun fibres of alkali lignin with the addition of PVA polymer and investigated the adsorption of fluoxetine (pharmaceutical contaminant) in an aqueous solution. They used different combinations of lignin and PVA and tested their performance. The researchers observed that nanofibres with a diameter of 156 nm adsorbed 70 % of fluoxetine in the tested solution. This accounts for the removal of 32 ppm of contaminants in water.

Salami et al. (2017) obtained polycaprolactone (PCL)/lignin nanofibres by changing the weight percentage of lignin and used them to produce scaffolds for biomedical applications. They observed that the mechanical properties of lignin-loaded samples were better than those of pure PCL samples. The introduction of lignin to PCL scaffolds enhanced their hydrophobicity and porosity. The authors determined that 10 % lignin-loaded samples had better physical, morphological and mechanical properties and were ideal for cell tests. They concluded that these

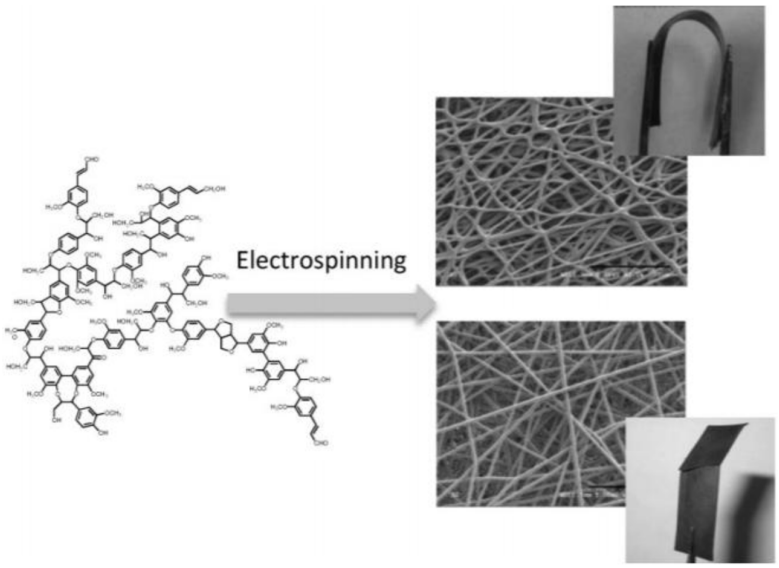

Fig. 2. Images of electrospun lignin derived carbon fibres and their SEM images (Dallmeyer et al., 2014)

Table. Elecrospun lignin nanofibres and their applications (PVA – Polyvinyl alcohol, PAN – Polyacrylonitrile, PEO – Poly(ethylene oxide))

Elecrospinning material	Solvent	Applications	Reference
PVA-alkali lignin	Aqueous solution of NaOH	Adsorption of pharmaceutical contaminants in wastewater	Camiré et al., 2020
PVA-lignin	Dimethyl sulfoxide (DMSO)	Microelectrodes	Roman et al., 2019
PAN-lignin	N, N-dimethylformamide (DMF)	Supercapacitor electrodes	Zhu et al., 2020
PVA-lignin	Water	Absorbent for water purification	Roman et al., 2019
Silver nanoparticles loaded PVA-lignin	Methanol: Water (60: 40)	Antimicrobial agents	Aadil et al., 2018
PAN-enzyme hydrolysis lignin (EHL)	N, N-dimethylformamide (DMF)	Binder-free supercapacitor electrodes	Wang et al., 2018b
PCL-lignin	1,1,1,3,3,3-hexafluoro-2-propanol (HFP)	Healthcare	Kai et al., 2017
PAN-lignin	N, N-dimethylformamide (DMF)	Supercapacitors	Jayawickramage et al., 2019
PVA-alkali lignin	Water	Counter electrodes of dye-sensitized solar cells	Ma et al., 2016
Kraft lignin-cellulose acetate	Acetone: N, N-dimethylcyclohexylamine (2:1 volume ratio)	Anode for high-performance sodium-ion batteries	Jia et al., 2018
PAN-lignin	N, N-dimethylformamide (DMF)	Electrodes for sodium ion batteries	Jin et al., 2014
PEO-lignin / N-doped (urea)	N, N-dimethylformamide (DMF)	Anode materials for lithium ion batteries	Wang et al., 2013
PEO-kraft lignin	N, N-dimethylformamide (DMF)	Piezoresistive sensors	Wang et al., 2020
Kraft lignin	N, N-dimethylformamide (DMF)	Supercapacitor	Schlee et al., 2019
H_3PO_4-lignin	Ethanol	Catalysis	García-Mateos et al., 2018

PCL/lignin composites have excellent potential for medical applications. Aadil et al. (2018) used electrospinning to prepare silver nanoparticle loaded PVA-acacia lignin fibre mats. Examining morphological characteristics of the resultant fibres showed that their average diameter was at nanoscale. The presence of silver nanoparticles was confirmed by XRD. The antimicrobial activity of these fibres against *Bacillus circulans* (MTCC7906) and *Escherichia coli* (MTCC739) was investigated. In both cases, significant antimicrobial activity was observed. The authors concluded that these silver nanoparticle-loaded fibres are potential materials for wound dressing, membrane filtration, and antimicrobial fabrics. Joo-Hyun Hong et al. (2019) prepared lignin/PCL electrospun mats for antifungal treatment of wood. Pathogenic fungi can deteriorate wood and are responsible for timber loss, whereas prevention of fungal attacks is costly. In their work, lignin/PCL mats were investigated for their anti-fungal properties against the sapstain fungi, *Grosmannia koreana*, and *Ophiostoma floccosum*. The authors report that mat-covered pin sapwood showed better resistance to fungal infection than unprotected sapwood. They also

observed that these mats performed as good mechanical protection against moisture. That is why these environmentally friendly mats can enhance wood trade globally. C.-Y. Chang and F.-C. Chang (2016) focused on studying the performance of lignin fibres as filter media. They produced electrospun mats from lignin and lignin/PEO combinations and investigated the filtration efficiency of these mats. They determined that composite filters created of lignin/PEO mats and surgical mask filter layers had filtration efficiency comparable to that of N95 respirators that filter 95 % of airborne particles. This allowed them to conclude that these lignin/PEO mats have a potential for air filtration applications.

Applications of lignin-derived electrospun carbon nanofibres

Lignin is a low-cost biosource for preparation of carbon nanofibres (Svinterikos et al., 2020). Carbon materials derived from lignin have multi-functional applications, especially in material electronics (Zhu et al., 2020). Roman et al. (2019) prepared lignin nanofibres from lignin, PVA, and dimethylsulfoxide (DMSO) combinations employing the electrospinning technique. The obtained lignin fibre mats were carbonised, and electrochemical measurements were carried out. They also prepared lignin-based twisted carbon nanofibres by twisting lignin nanofibres precursor mats. The twisting level influenced the electrochemical capacitance (from 330 $mF \cdot g^{-1}$ to a few $mF \cdot g^{-1}$) and conductivity (from 11 to 22 $S \cdot cm^{-1}$) of the twisted carbon fibres. They concluded that these twisted carbon nanofibres could be promising candidates as microelectrodes.

Beck et al. (2017) prepared porous lignin carbon nanofibre membranes for applications in adsorptive water treatment. They determined that the prepared nanofibre membranes had the surface area of 583 m^2/g, pore diameter of 3.5 nm and pore volume of 0.29 cm^3/g which enhanced their adsorptive performance. They estimated that energy consumption in water treatment could be reduced by 87 % by using these nanofibre membranes. Zhang et al. (2020) functionalised lignin-derived carbon fibres with air plasma. Prepared by this technique oxygen/nitrogen co-doped lignin fibre electrodes exhibited good specific capacitance (344.6 F/g). In addition, the water contact angle was observed to decrease by 64 %. Thus, these materials display excellent electrochemical performance. Dai et al. (2019) prepared electrospun lignin/polyacrylonitrile derived carbon fibres with nitrogen-sulphur and graphene by electrospinning, carbonisation, and subsequent activation. They found the exceptional supercapacitor performance of the resultant material. They also observed that doped carbon fibres increased the energy density (4.12 to 9.28 Wh kg^{-1}) and barely reduced power density of the obtained supercapacitor. Kai et al. (2015) obtained lignin– poly(methyl methacrylate) (PMMA) copolymers using the atom transfer radical polymerisation technique, then blended it with poly(ε-caprolactone) and prepared nanofibres employing the electrospinning technique. Mechanical performance of lignin–PMMA copolymer loaded samples were observed to have improved mechanical properties. The cell culture studies on electrospun nanofibre mats showed that they were biocompatible and helped in the proliferation of cells. The authors concluded that these materials have a potential in biomedical applications. Zhang et al. (2019) investigated the Safranine T (dye) adsorption of alkali lignin/PVA composite membranes. The results indicate that there are strong intermolecular hydrogen bonds between lignin and PVA. The results also show that the capacity of adsorption is improved with an increase in pH and temperature of the dye. Moreover, the absorption exhibited a close proximity to Langmuir isotherm. The kinetics was in accordance with pseudo second order type

models. They also observed excellent desorption behavior and concluded that these results indicate that the prepared composite fibre membrane can be used for dye removal.

Conclusion and prospects

The review clearly shows a number of ways for effective utilisation of a biowaste material, such as lignin, after its transformation into nanofibres using electrospinning. Through careful choice of the solvent and processing parameters lignin can be converted into nanoscale fibres. Electrospun lignin can also be used as a precursor of carbon nanofibres. Carbonised as well as non-carbonised electrospun lignin nanofibres are effectively used for various industrial, medical, textile and biomedical applications. The combination of lignin with suitable polymeric substrates often makes the process easier. However, only a few polymers, such as PVA, PAN, PEO etc. are mostly used. There is a vast potential for replacing these polymers with novel biomedical polymers. Fabrication of hybrid fibres using lignin along with other nanofillers is another area that is less explored. The development of these novel lignin derived nanofibres using electrospinning as a tool could definitely increase the applications of lignin nanofibres.

References

Aadil K. R., Mussatto S. I., Jha H. (2018) Synthesis and characterization of silver nanoparticles loaded poly (vinyl alcohol)-lignin electrospun nanofibers and their antimicrobial activity. *International Journal of Biological Macromolecules*, 120: 763–767

Baji A., Agarwal K., Oopath S. V. (2020) Emerging developments in the use of electrospun fibers and membranes for protective clothing applications. *Polymers*, 12(2): 492

Beck R. J., Zhao Y., Fong H., Menkhaus T. J. (2017) Electrospun lignin carbon nanofiber membranes with large pores for highly efficient adsorptive water treatment applications. *Journal of Water Process Engineering*, 16: 240–248

Calvo-Flores F.G., Dobado J. A. (2010) Lignin as renewable raw material. *ChemSusChem*, 3(11): 1227–1235

Camiré A., Espinasse J., Chabot B., Lajeunesse A. (2020) Development of electrospun lignin nanofibers for the adsorption of pharmaceutical contaminants in wastewater. *Environmental Science and Pollution Research*, 27(4): 3560–3573

Chang C.-Y., Chang F.-C. (2016) Development of electrospun lignin-based fibrous materials for filtration applications. *BioResources*, 11(1): 2202–2213

Cho M., Ji L., Liu L. Y., Johnson A. M., Potter S., Mansfield S. D., Renneckar S. (2020) High performance electrospun carbon nanofiber mats derived from flax lignin. *Industrial Crops and Products*, 155: 112833

Dai Z., Ren P.-G., JinY.-L., Zhang H., Ren F., Zhang Q. (2019) Nitrogen-sulphur Co-doped graphenes modified electrospun lignin/polyacrylonitrile-based carbon nanofiber as high performance supercapacitor. *Journal of Power Sources*, 437: 226937

Dallmeyer I., Lin L. T., Li Y., Ko F., Kadla J. F. (2014) Preparation and characterization of interconnected, kraft lignin-based carbon fibrous materials by electrospinning. *Macromolecular Materials and Engineering*, 299(5): 540–551

Deeraj B. D.S., Jayan J. S., Saritha A., Joseph K. (2021) Electrospun biopolymer-based hybrid composites. *Hybrid natural fiber composites: material formulations, processing, characterization, properties, and engineering applications*. Elsevier, p. 225–252

Domínguez-Robles J., Cárcamo-Martínez Á., Stewart S. A., Donnelly R. F., Larrañeta E., Borrega M. (2020) Lignin for pharmaceutical and biomedical applications – Could this become a reality? *Sustainable Chemistry and Pharmacy*, 18: 100320

García-Mateos F.J., Berenguer R., Valero-Romero M.J., Rodríguez-Mirasol J., Cordero T. (2018) Phosphorus functionalization for the rapid preparation of highly nanoporous submicron-diameter carbon fibers by electrospinning of lignin solutions. *Journal of Materials Chemistry A*, 6(3): 1219–1233

Gupta A. K., Mohanty S., Nayak S. K. (2015) Preparation and characterization of lignin nanofibre by electrospinnig technique. *International Journal of Scientific Engineering and Applied Science*, 1(3): 184–190

Hong J. H., An S., Song K. Y., Kim Y. I., Yarin A. L., Kim J. J., Yoon S. S. (2019) Eco-friendly lignin nanofiber mat for protection of wood against attacks by environmentally hazardous fungi. *Polymer Testing*, 74: 113–118

Jayawickramage R. A. P., Balkus K. J., Ferraris J. P. (2019) Binder free carbon nanofiber electrodes derived from polyacrylonitrile-lignin blends for high performance supercapacitors. *Nanotechnology*, 30(35): 355402

Jia H., Sun N., Dirican M., Li Y., Chen C., Zhu P., Yan C., Zang J., Guo J., Tao J., Wang J., Tang F., Zhang X. (2018) Electrospun kraft lignin/cellulose acetate-derived nanocarbon network as an anode for high-performance sodium-ion batteries. *ACS Applied Materials & Interfaces*, 10(51): 44368–44375

Jin J., Yu B.-J., Shi Z.-Q., Wang C.-Y., Chong C.-B. (2014) Lignin-based electrospun carbon nanofibrous webs as free-standing and binder-free electrodes for sodium ion batteries. *Journal of Power Sources*, 272: 800–807

Kai D., Jiang S., Low Z. W., Loh X. J. (2015) Engineering highly stretchable lignin-based electrospun nanofibers for potential biomedical applications. *Journal of Materials Chemistry B*, 3(30): 6194–6204

Kai D., Zhang K., Jiang L., Wong H. Z., Li Z., Zhang Z., Loh X. J. (2017) Sustainable and antioxidant lignin–polyester copolymers and nanofibers for potential healthcare applications. *ACS Sustainable Chemistry & Engineering*, 5(7): 6016–6025

Kumar M., Hietala M., Oksman K. (2019) Lignin-based electrospun carbon nanofibers. *Frontiers in Materials*, 6: 62

Lallave M., Bedia J., Ruiz-Rosas R., Rodriguez-Mirasol J., Cordero T., Otero J. C., Marquez M., Barrero A., Loscertales I. G. (2007) Filled and hollow carbon nanofibers by coaxial electrospinning of alcell lignin without binder polymers. *Advanced Materials*, 19(23): 4292–4296

Li B., Xia X., Chen J., Xia D., Xu R., Zou X., Wang H., Liang C. (2021) Paclitaxel-loaded lignin particle encapsulated into electrospun PVA/PVP composite nanofiber for effective cervical cancer cell inhibition. *Nanotechnology*, 32(1): 015101

Ma X., Elbohy H., Sigdel S., Lai C., Qiao Q., Fong H. (2016) Electrospun carbon nano-felt derived from alkali lignin for cost-effective counter electrodes of dye-sensitized solar cells. *RSC Advances*, 6(14): 11481–11487

Roman J., Neri W., Derré A., Poulin P. (2019) Electrospun lignin-based twisted carbon nanofibers for potential microelectrodes applications. *Carbon*, 145: 556–564

Ruiz-Rosas R., Bedia J., Lallave M., Loscertales I. G., Barrero A., Rodriguez-Mirasol J., Cordero T. (2010) The production of submicron diameter carbon fibers by the electrospinning of lignin. *Carbon*, 48(3): 696–705

Salami M. A., Kaveian F., Rafienia M., Saber-Samandari S., Khandan A., Naeimi M. (2017) Electrospun polycaprolactone/lignin-based nanocomposite as a novel tissue scaffold for biomedical applications. *Journal of Medical Signals and Sensors*, 7(4): 228–238

Schlee P., Hosseinaei O., Baker D., Landmer A., Tomani P., Mostazo-Lopez M.J., Cazorla-Amoros D., Herou S., Titirici M. M. (2019) From waste to wealth: from kraft lignin to free-standing supercapacitors. *Carbon*, 145: 470–480

Seo D. K., Jeun J. P., Kim H. B., Kang P. H. (2011) Preparation and characterization of the carbon nanofiber mat produced from electrospun PAN/lignin precursors by electron beam irradiation. *Reviews on Advanced Materials Science*, 28(1): 31–34

Svinterikos E., Zuburtikudis I., Al-Marzouqi M. (2020) Electrospun lignin-derived carbon micro- and nanofibers: a review on precursors, properties, and applications. *ACS Sustainable Chemistry & Engineering*, 8(37): 13868–13893

Vivo-Vilches J.F., Celzard A., Fierro V., Devin-Ziegler I., Brosse N., Dufour A., Etienne M. (2019) Lignin-based carbon nanofibers as electrodes for vanadium redox couple electrochemistry. *Nanomaterials*, 9(1): 106

Wang J., Tian L., Luo B., Ramakrishna S., Kai D., Loh X. J., Yang I. H., Deen G. R., Mo X. (2018a) Engineering PCL/lignin nanofibers as an antioxidant scaffold for the growth of neuron and Schwann cell. *Colloids and Surfaces B-Biointerfaces*, 169: 356–365

Wang S.-X., Yang L., Stubbs L. P., Li X., He C. (2013) Lignin-derived fused electrospun carbon fibrous mats as high performance anode materials for lithium ion batteries. *ACS Applied Materials & Interfaces*, 5(23): 12275–12282

Wang S., Innocent M. T., Wang Q., Xiang H., Tang J., Zhu M. (2020) Kraft lignin-based piezoresistive sensors: Effect of chemical structure on the microstructure of ultrathin carbon fibers. *International Journal of Biological Macromolecules*, 151: 730–739

Wang X., Zhang W., Chen M., Zhou X. (2018b) Electrospun enzymatic hydrolysis lignin-based carbon nanofibers as binder-free supercapacitor electrodes with high performance. *Polymers*, 10(12): 1306

Zhang W., Yang P., Li X., Zhu Z., Chen M., Zhou X. (2019) Electrospun lignin-based composite nanofiber membrane as high-performance absorbent for water purification. *International Journal of Biological Macromolecules*, 141: 747–755

Zhang W., Yang P., Luo M., Wang X., Zhang T., Chen W., Zhou X. (2020) Fast oxygen, nitrogen co-functionalization on electrospun lignin-based carbon nanofibers membrane via air plasma for energy storage application. *International Journal of Biological Macromolecules*, 143: 434–442

Zhao Y., Liu Y., Tong C., Ru J., Geng B., Ma Z., Liu H., Wang L. (2018) Flexible lignin-derived electrospun carbon nanofiber mats as a highly efficient and binder-free counter electrode for dye-sensitized solar cells. *Journal of Materials Science*, 53(10): 7637–7647

Zhu M., Liu H., Cao Q., Zheng H., Xu D., Guo H., Wang S., Li Y., Zhou J. (2020) Electrospun lignin-based carbon nanofibers as supercapacitor electrodes. *ACS Sustainable Chemistry & Engineering*, 8(34): 12831–12841

Journal of Siberian Federal University. Biology 2021 14(4): 475–497
~ ~ ~

DOI 10.17516/1997-1389-0366

УДК 577.114.4:664

Aloe vera Incorporated Chitosan/Nanocellulose Hybrid Nanocomposites as Potential Edible Coating Material under Humid Conditions

Anjumol Kidangayil Sali[a, b], Aiswarya Payyapilly Ravi[b], Shabna Pazhavoorkonath Shamsudeen[c], Sneha Sabu Mathew[b], Blessy Joseph[b], Abhimanyu Tharayil[b], Raji Vijayamma[c], Hanna J. Maria[b, d], Petr Spatenka[a], Nandakumar Kalarikkal[c] and Sabu Thomas[b, d]*

[a]Czech Technical University
Prague, Czech Republic
[b]Mahatma Gandhi University
Kottayam, India
[c]Center for Professional and Advanced Studies
Kottayam, India
[d]University of Johannesburg
Johannesburg, South Africa

Received 13.06.2021, received in revised form 23.07.2021, accepted 23.08.2021

Abstract. Innovative post-harvest technologies are in demand to meet the requirements of farmers and agricultural industries to ensure global food security and to avoid food wastage. Edible coatings that can prevent food spoilage and/or enhance shelf life have taken on increasing importance. This work involves the development of edible coatings based on easily available bio resources, chitosan and nanocellulose, and utilizing their unique properties as an effective coating material. *Aloe vera*, known for its antioxidant and antimicrobial properties, has been proposed as an active ingredient that can be incorporated into the biodegradable film. Varying volumes of *Aloe vera* (0.25 ml, 0.35 ml, 0.5 ml, and 2.5 ml) were added to fabricate nanocomposite films by solvent casting. Transparent films were obtained, and their morphology was analysed using scanning electron microscope (SEM). The incorporation

* Corresponding author E-mail address: sabuthomas@mgu.ac.in
ORCID: 0000-0002-5442-0540 (Sali A.K.); 0000-0002-0650-9831 (Mathew S.S.); 0000-0003-2846-3296 (Joseph B.); 0000-0003-2879-6656 (Maria H.J.); 0000-0003-4726-5746 (Thomas S.)

of *Aloe vera* was confirmed in various spectroscopic studies, which clearly show reduction in light transmittance for the nanocomposite films containing *Aloe vera*. The contact angle study showed an increase in hydrophobicity initially. Maximum tensile strength was obtained with 0.25 ml of *Aloe vera*. The potential use of nanocomposite solution as edible films was demonstrated in green chillies, which showed lower weight loss after 3 days when compared with uncoated chillies. In the first phase of this study, chitosan/nanocellulose nanocomposites enriched with *Aloe vera* have been proposed as a potential edible food coating material.

Keywords: edible coating, chitosan, nanocellulose, bio nanocomposite, *Aloe vera*.

Acknowledgements. Authors acknowledge support from School of Energy Materials and IIUCNN (Mahatma Gandhi University), Jaivam project (Mahatma Gandhi University) and School of Environmental Sciences (Mahatma Gandhi University).

Citation: Sali A.K., Ravi A.P., Shamsudeen S.P., Mathew S.S., Joseph B., Tharayil A., Vijayamma R., Maria H.J., Spatenka P., Kalarikkal N., Thomas S. *Aloe vera* incorporated chitosan/nanocellulose hybrid nanocomposites as potential edible coating material under humid conditions. J. Sib. Fed. Univ. Biol., 2021, 14(4), 475–497. DOI: 10.17516/1997-1389-0366

Гибридные нанокомпозиты хитозан/наноцеллюлоза с включением *Aloe vera* как потенциальный материал для изготовления съедобных покрытий, применяемых в условиях повышенной влажности

А.К. Сали[а, б], А.П. Рави[б], Ш.П. Шамсудин[в], С.С. Мэтью[б], Б. Джозеф[б], А. Тараил[б], Р. Виджаямма[в], Х. Дж. Мария[б, г], П. Спатенка[а], Н. Каларикал[в], С. Томас[б, г]

[а]Чешский технический университет
Чешская Республика, Прага
[б]Университет Махатмы Ганди
Индия, Коттаям
[в]Центр профессиональных и перспективных исследований
Индия, Коттаям
[г]Университет Йоханнесбурга
Южная Африка, Йоханнесбург

Аннотация. Инновационные технологии переработки и хранения сельскохозяйственной продукции широко востребованы в сельскохозяйственной отрасли и нацелены на обеспечение глобальной продовольственной безопасности и снижение потерь продуктов питания. Все большую значимость приобретает разработка съедобных пищевых покрытий, которые могут

предотвратить порчу пищевых продуктов и / или продлить срок их хранения. Это исследование посвящено созданию эффективного материала для изготовления съедобных покрытий на основе легкодоступных биоресурсов с уникальными свойствами – хитозана и наноцеллюлозы. *Aloe vera*, известный своими антиоксидантными и антимикробными свойствами, предложен в качестве активного ингредиента, который может быть включен в биоразлагаемую пленку. Различные объемы экстракта *Aloe vera* (0,25 мл, 0,35 мл, 0,5 мл и 2,5 мл) добавляли при изготовлении нанокомпозитных пленок методом литья из раствора. Морфология полученных прозрачных пленок изучена с помощью сканирующей электронной микроскопии. Включение *Aloe vera* в композит подтверждено различными спектроскопическими исследованиями, которые показали снижение светопропускания пленок нанокомпозитов, содержащих *Aloe vera*. Исследования краевого угла выявили увеличение гидрофобности композита. Максимальное значение прочности на разрыв получено при включении в состав композита 0,25 мл *Aloe vera*. Возможность использования полученного нанокомпозита в качестве съедобной пленки оценена в эксперименте с зеленым перцем чили. Покрытые пленкой образцы перца показали более низкую потерю веса через 3 дня по сравнению с образцами без покрытия. Исследование продемонстрировало потенциал разработанного нанокомпозита хитозан/наноцеллюлоза, обогащенного добавками экстракта *Aloe vera*, в качестве материала для изготовления съедобных пищевых покрытий.

Ключевые слова: съедобное покрытие, хитозан, наноцеллюлоза, бионанокомпозит, *Aloe vera*.

Благодарности. Авторы выражают благодарность за поддержку Институту энергетических материалов и IIUCNN (Университет Махатмы Ганди), проекту Java (Университет Махатмы Ганди) и Институту наук об окружающей среде (Университет Махатмы Ганди).

Цитирование: Сали, А. К. Гибридные нанокомпозиты хитозан/наноцеллюлоза с включением *Aloe vera* как потенциальный материал для изготовления съедобных покрытий, применяемых в условиях повышенной влажности / А. К. Сали, А. П. Рави, Ш. П. Шамсудин, С. С. Мэтью, Б. Джозеф, А. Тараил, Р. Виджаямма, Х. Дж. Мария, П. Спатенка, Н. Каларикал, С. Томас // Журн. Сиб. федер. ун-та. Биология, 2021. 14(4). С. 475–497. DOI: 10.17516/1997-1389-0366

Introduction

Consumer demands for high quality food are increasing day by day. Different kinds of synthetic materials or preservatives are used to enhance the food quality, which in turn improves the shelf life of the fresh food products by incorporating substances that have strong antimicrobial and antibacterial properties (Arvanitoyannis, 1999). Food products are vulnerable to the attack of microbial and bacterial microorganisms that will reduce the nutritional value of food commodities. There are many synthetic materials available in the market like fungicides or insecticides that protect the food commodities from harmful microorganisms. As a major constituent of food coatings, chemicals are potential sources of food adulteration. Chemicals usually enter into the food supply chain in the form of antioxidants, stabilizers, preservatives, and so on. It should be emphasized that such chemicals can be malicious in the long run. Nowadays most of the research is aimed at developing bio based antibacterial coatings that can be consumed without any side effects (Geueke et al., 2018; Aloui, Khwaldia, 2016). Significance of edible coatings increased due to their environment friendly nature and their potential use in the food industry. Edible films or coatings based on natural polymers or

biopolymers cause no environmental issues, as they are biocompatible and obtained from agricultural and animal products like proteins, gums, lipids, etc. They improve the quality of food by limiting the migration of moisture, lipids, flavours /aromas, and colours between food components, carrying active ingredients (e. g., antioxidants, antimicrobials, flavour), and improving the mechanical integrity or handling characteristics (Khwaldia et al., 2004; Joshy et al., 2020b). Bioactive compounds such as essential oils (EOs) are added into such coatings to improve shelf life, prevent the growth of microorganisms, and preserve nutritional value of food. EOs have been found to exhibit excellent antimicrobial and antifungal properties, which makes them a natural alternative to fight against foodborne pathogens and normal food decay caused by bacterial and mould growth. The immobilization of the active compounds in polymer can result in their high concentrations on the surface of food in order to achieve a longer storage time (Ju et al., 2019; Vu et al., 2011). The prepared film coating should be non-toxic and possess high barrier properties to moisture, antibacterial properties, and high transparency. Bio polymers such as chitosan are easily available and are well known for their antimicrobial, biodegradable, biocompatible, and cost-effective properties (Joseph et al., 2020b; Ramadan et al., 2020; Dutta et al., 2019). Chitosan based films were produced by blending with biopolymers such as polysaccharides or proteins, by adopting solution-casting, layer-by-layer, extrusion, and other techniques (Kumar et al., 2020; Mohammadi et al., 2018; Fitch-Vargas et al., 2016; Ribeiro et al., 2020).

Nanocellulose has gained increasing interest for a wide range of applications in different fields of engineering due to its renewability, anisotropic nature, excellent mechanical properties, good biocompatibility, tailorable surface chemistry, and interesting optical properties (Iwamoto et al., 2009; Joseph et al., 2019); moreover, nanocellulose based edible coatings have been found to have anticancer properties (Joshy et al., 2020a). The most beneficial attributes of nanocellulose are the green nature of the particles, their physical and chemical properties, and the diversity of applications that can be derived from this material (Sultana et al., 2020; Joseph et al., 2020a). It is a natural nanoscale product, and it also possesses characteristics like special morphology and geometrical dimensions, crystallinity, high specific surface area, rheological properties, liquid crystalline behaviour, alignment and orientation, mechanical reinforcement, barrier properties, surface chemical reactivity, biocompatibility, biodegradability, lack of toxicity, etc. (Lin, Dufresne, 2014). Nanocellulose can be extracted from natural sources and has antimicrobial properties. Paper coatings with cellulose nanofibrils have been shown to have resistance to air permeance and enhanced tensile properties (Azeredo et al., 2017). Films made of cellulose nanofibrils (CNF) and cellulose nanocrystals (CNC) have high mechanical strength and outstanding oxygen barrier properties (Cherpinski et al., 2018). Poor water barrier properties of biopolymers like nanocellulose can be controlled by combining with edible oils or essential oils (Joshy et al., 2020b).

Aloe vera is well known for its medicinal and therapeutic properties (Valverde et al., 2005). The predominant medical uses of the orally ingested gel juice are against ulcerous, gastrointestinal, kidney, and cardiovascular problems and also to reduce the cholesterol and triglyceride levels in blood. Due to its other properties like anti-inflammatory and antibiotic activities, it is also used against some diseases (diabetes, cancer, allergy, AIDS) (Eshun, He, 2004). *Aloe vera* extract is tasteless, odourless, and colourless, and, therefore, it can be used in edible coating as an additive. *Aloe vera* contains

many constituents, which results in anti-microbial properties. Due to the presence of carbohydrates, saccharides, etc., *Aloe vera* can form a barrier on the fruit surface, which will considerably reduce the respiration rate, decay rate, and water loss (Misir et al., 2014). *Aloe vera* based coating was used for enhancement of storage life and quality maintenance of papaya fruits due to its antifungal activity (Marpudi et al., 2011). Inner gel extract of *Aloe vera* was shown to be effective against Gram positive and Gram negative bacteria (Habeeb et al., 2007; Sánchez et al., 2020b). A study by Hazrati et al. (2017) showed that *Aloe vera* gel was an effective coating material for peach fruits during cold storage period. The coating was effective against weight loss and colour change (Hazrati et al., 2017). Strawberries coated with banana starch-chitosan and *Aloe vera* gel showed decreased decay rates under commercial refrigerated conditions and shelf life was found to increase up to 15 days (Pinzon et al., 2020).

Films based on chitosan and nanocellulose crystals have shown superior antimicrobial characteristics (Amirabad et al., 2018; Naseri et al., 2015). It is also reported that reinforcing nanocellulose with other long-chain polymers, such as chitosan, improves the quality of the packaging material as well as ensures long storage life (Sundaram et al., 2016). Chitosan/polycaprolactone based bilayer films containing grape seed extract and nanocellulose were used to enhance the quality of chicken breast fillets. The modified films showed antioxidant activity and higher antimicrobial effect and further restricted the growth of mesophilic aerobic and coliform bacteria in fresh chicken breast fillets (Sogut, Seydim, 2019). The effect of chitosan based edible coating on post harvested fruit quality of strawberry fruits showed that chitosan treatment could inhibit oxidative enzyme activity in strawberries during storage, and decay did not begin in chitosan treated fruit 9 days longer than in untreated fruit (Wang, Gao, 2013). A recent study on chitosan/*Aloe vera* combination for extending shelf life of blueberries demonstrated that addition of chitosan and *Aloe vera* enhanced the shelf life of the fruits and showed the potential to fight against fungi (Vieira et al., 2016). To the best of our knowledge, rather few studies reported the effectiveness of chitosan based nanocellulose films as edible coatings incorporating *Aloe vera* as an additive.

The right combination of new bio-materials and preparation methods is significant for improving the effectiveness of coating material to preserve fruit and vegetables. This study details the preparation of chitosan/nanocellulose based films containing *Aloe vera* by solvent casting method. The study was focused in this initial phase on investigating the physicochemical characteristics of the coating material along with its effectiveness as an edible coating material for vegetables stored in humid conditions.

Materials

Chitosan (Sigma Aldrich), nanocellulose suspension (extracted from 1000 g of pineapple leaf fibres and processed using an autoclave), glycerol (Sigma Aldrich), *Aloe vera* oil (AL KAMIL Factory for Natural Products), glacial acetic acid (Emplura 99–100 %).

Preparation of chitosan based nanocellulose film

Synthesis of nanocellulose suspension

Cellulose is obtained from raw material taken for alkali treatment and bleaching, as this will break the intermolecular and intramolecular hydrogen bonding between the hydroxyl group of cellulose and hemicellulose and can increase the hydrophilicity of fibres (Abraham et al., 2011).

Nanocellulose was extracted from pineapple leaves using the following procedures.

(a) Alkaline treatment of pineapple fibre: About 1000 g pineapple leaf fibres were collected and processed using an autoclave set at 100 °C for 1 hour (Mahardika et al., 2018; Cherian et al., 2011). After that, steam explosion was done and then the alkali treated fibres were exposed to water until it reached neutral pH. The alkali treatment process was repeated five more times and then the treated fibres were completely neutralized by washing with water and were subjected to bleaching process (Cherian et al., 2010).

(b) Bleaching process: For bleaching process, 1:1 mixture of the two solutions was used. The solution A (1000 ml) consisted of sodium hydroxide, acetic acid, and water (26.5 g, 73.3 ml, and 900 ml, respectively) and solution B (1000 ml) consisted of 1:3 mixture of sodium hypochlorite and water (250 ml and 750 ml, respectively). The bleaching was carried out in an autoclave at a pressure of 1.5 kg/cm^2 at 100 °C for 1 hour. Fibres were subjected to washing after the steam explosion and the process was continued until the fibres became clear white (the process was repeated four times). Finally, the bleached fibres were thoroughly washed using distilled water until the odour of the bleaching agent had been removed completely. The bleached fibres were then subjected to oxalic acid treatment (Cherian et al., 2011; Asrofi et al., 2017).

(c) Oxalic acid treatment: Acid hydrolysis treatment was found to increase the crystallinity and reduce the diameter of the fibres. 11 % oxalic acid was used, and the bleached fibres were treated with oxalic acid in an autoclave (1.5 kg/cm^2, 100 °C). The process was repeated six times, and the treated fibres were washed with distilled water. After neutralization, the fibres were subjected to homogenization (Asrofi et al., 2017; Fahma et al., 2011).

(d) Mechanical treatment: The extracted fibres were suspended in distilled water and stirred using homogenizer (10000 rpm for 5 hours), which resulted in 3.33 wt.% nanocellulose suspension formation. The obtained nanocellulose was analysed using FTIR, SEM, and TEM (Chandra et al., 2016; Santos et al., 2013).

Preparation of solution for edible coating film

For preparing nanocellulose/chitosan solution (Sample 1, presented as NC/CH), varied compositions of chitosan were weighed (0.5 g, 1.0 g, 1.5 g, 2.0 g) and kept in a beaker. Weighed chitosan was dissolved in 3 % acetic acid solution and kept overnight to get maximum solubility. Nanocellulose suspension containing 3.2 g solids in 100 ml water was added to the chitosan solution at a 1:1 ratio. Then, around 30 ml of water was added to the mix along with 2 drops of glycerine. Water and glycerol acted as plasticizer. The mixture was then stirred for 1 hour using a magnetic stirrer. After that, the mixture was homogenized for 10 minutes using a probe homogenizer at 10,000 rpm. The homogenized mix was sonicated in a probe sonicator for 10 minutes. After sonication, solution was cast. Sample 2 (presented as NC/CH/V) was prepared at a 1:0.25 ratio of chitosan and nanocellulose. The procedure described above was used to prepare Sample 2 except that different volumes of *Aloe vera* extract (0.25 ml, 0.35 ml, 0.5 ml, and 2.5 ml) were also added to the solution as an additive before homogenization.

Characterization techniques

Scanning electron microscopy (SEM)

The morphology of the nanocellulose/chitosan composite surface was examined at 15 kV under high vacuum conditions. A small part of the sample was cut and kept on the aluminium stage covered by carbon tapes, and then the samples were coated with an ultrathin gold layer (Au) using an ion sputtering machine.

Fourier transform infrared spectrometry (FTIR)

FTIR spectra were collected using a Nicolet 6700 Fourier Transform infrared spectrometer and measured over a 4000–650 cm^{-1} range. Both sets of samples (Samples 1 and 2) were examined. For each sample, 200 scans were averaged with a spectral resolution of 4 cm^{-1}.

Contact angle measurement

The hydrophilicity of edible coating films before and after adding *Aloe vera* was measured using digital contact angle analyser equipped with a CCD camera (Pheonix-KGV-5000) at room temperature. The films were placed on the stage of the machine. The contact angle was measured after carefully adding a water droplet (Milling-Q-Water) on the surface of the scaffold by using the software-controlled system. A series of images of the solution droplet was taken and the contact angle was measured accordingly. The measurements were taken at 3 different portions of the sample.

Tensile properties

Tensile measurements were done on a universal testing machine (Tinius Oslen H50K) by setting a crosshead speed of 50 mm/min and gauge length of 50 mm. Measurements were performed at ASTMD882 standard by using rectangular specimens. Average values were obtained from at least three successful determinations. The testing was conducted at 23±2 °C and 50±5 % relative humidity.

UV-visible spectroscopy

UV–Vis spectroscopic studies of the samples were carried out using a Shimadzu UV-2600 UV–Vis spectrophotometer. For the study, 1 ml solution of each sample was taken in a sample vial.

Weight loss study

The nanocomposite solution was applied on green chillies purchased at a local market with the objective of prolonging their shelf life during storage. The assessment was based on weight loss. The weight loss was measured for three days with a three decimal precision weighing balance. The value was expressed as a relative percentage and calculated as weight loss (%) = (Wi – Wt)/Wi *100 (where Wi is the initial weight and Wt is the weight measured during storage).

Results and discussion

Solvent casting method was used for fabrication of films (Saldanha, Kyu, 1987; Suh et al., 2002; Kuila, Nandi, 2004). It included solubilizing polymer in a suitable solvent followed by casting the solution in a Petri dish and then drying (Rhim et al., 2006). Suitable filler materials like plasticizers, cross linking agents, etc. were added prior to casting. Furthermore, solution filtration, sonication, or centrifugation for removing insoluble particles and air bubbles were also performed. Solution casting method is mainly used at laboratory scale to prepare films, and further research is needed in order to analyse its feasibility on commercial scale. The protocol for preparation of Sample 2 is given in Fig. 1.

The films were dried at 40 °C for about 24 hours. The films were transparent and exhibited uniform appearance and plastic-like properties (Fig. 2, 3). All films were easily peeled off from Teflon covered Petri dish. Increase in the plasticiser amount made the films stickier. Transparency of the prepared film will depend on the amount of nanocellulose, as an increase in nanocellulose content decreases the transparency of the film (Xu et al., 2019; Cazón et al., 2018). It can be safely assumed that chitosan is the material that is responsible for better film forming property.

SEM images of chitosan-nanocellulose composite films with 0.5 g, 1 g, 1.5 g, and 2 g chitosan, respectively, are shown in Fig. 4 (a-d). The nanocellulose fibres are clearly visible and

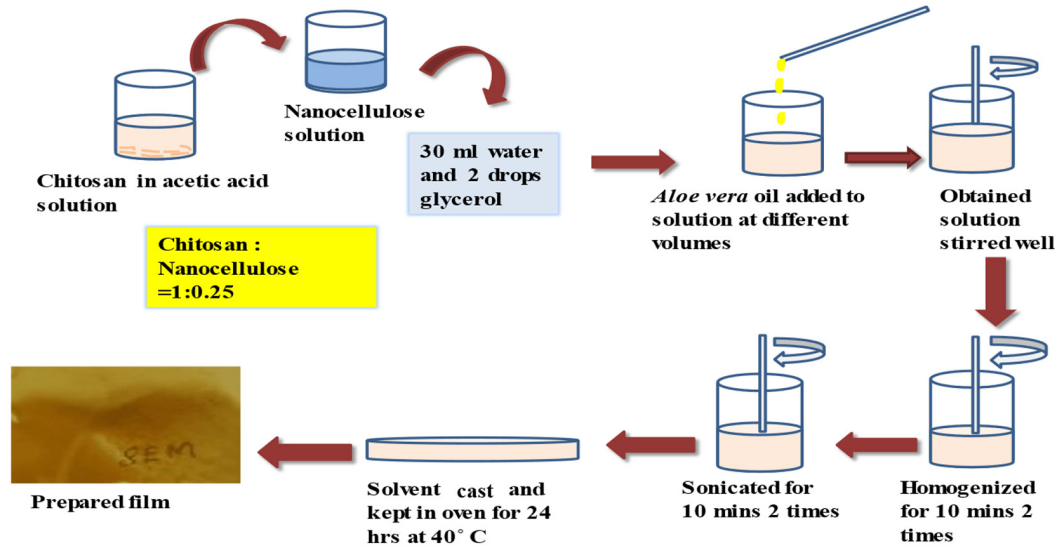

Fig. 1. Flowchart for the preparation of edible coating films of sample NC/CH/V (sample 2)

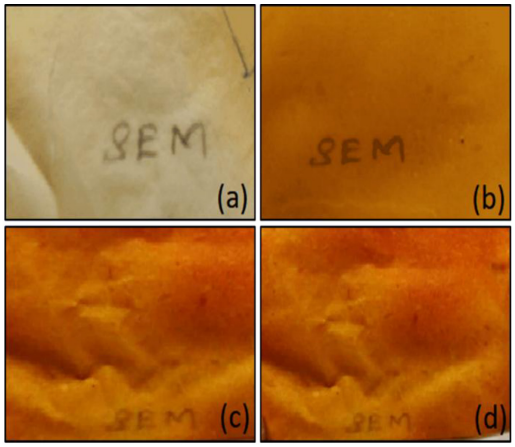

Fig. 2. Transparency of (a) NC/0.5 CH, (b) NC/1CH, (c) NC/1.5 CH, and (d) NC/2CH films

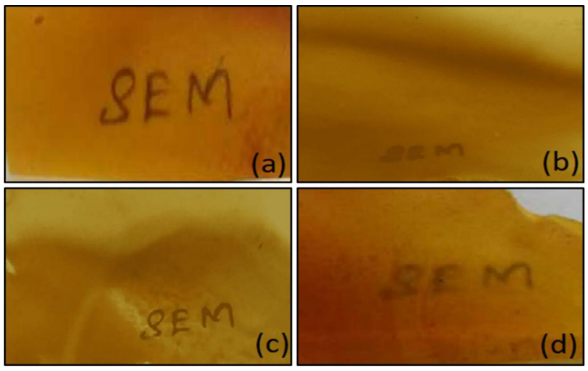

Fig. 3. Transparency of (a) NC/CH/0.25V, (b) NC/CH/0.35V, (c) NC/CH/0.5V, and (d) NC/CH/2.5V films

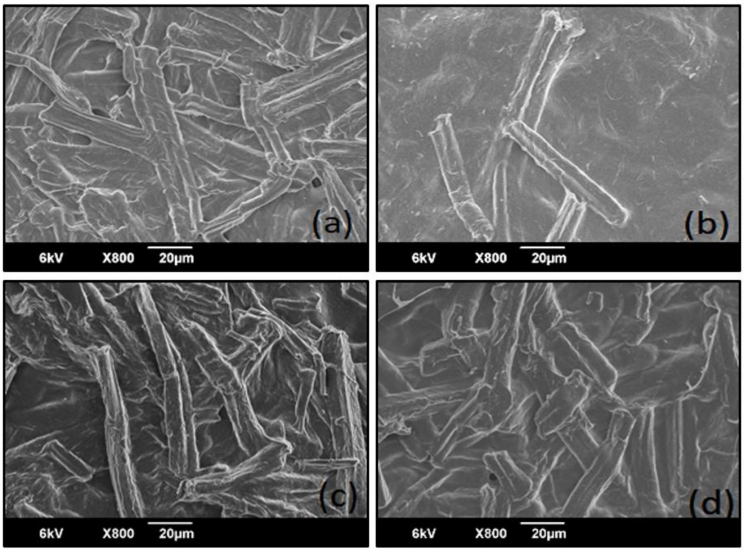

Fig. 4. SEM images of films of sample NC/CH with (a) 0.5 g, (b) 1 g, (c) 1.5 g, and (d) 2 g chitosan, respectively

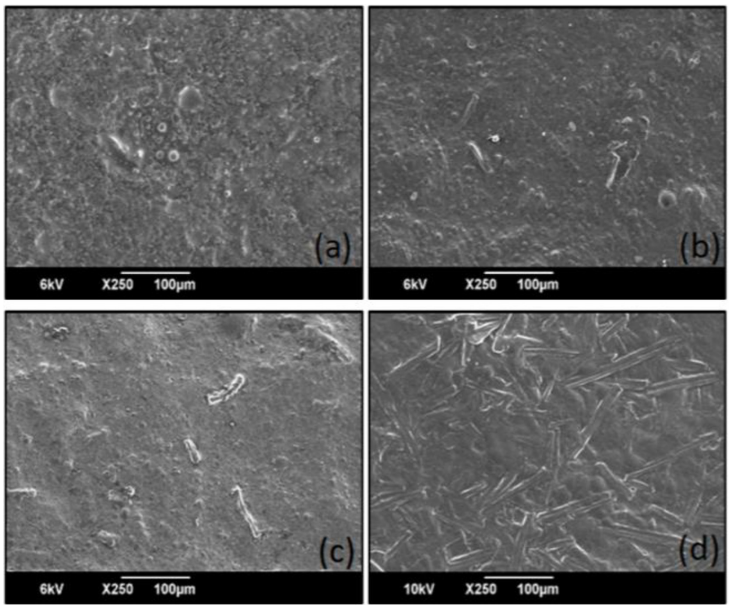

Fig. 5. SEM images of films of sample NC/CH/V with (a) 0.25 ml, (b) 0.35 ml, (c) 0.5 ml, and (d) 2.5 ml *Aloe vera*

are distributed throughout the chitosan matrix, and the fibre diameter varies from 3.96 µm to 7.26 µm. These images clearly show that the amount of nanocellulose fibre as filler is very high in these compositions. Fillers are dispersed in the matrix as multilayers and these contribute to the high strength of the film and its stiffness. It can be seen that the length of the fibres varies in the nanocellulose suspension. Mechanical properties of the film completely depend on the amount of filler (Corsello et al., 2017; Khan et al., 2012; Rubentheren et al., 2015). Fig. 5 shows SEM images of films with varied compositions of *Aloe vera*. The incorporation of *Aloe vera* made the

film surface smooth. A coating-like appearance is also seen on the substrate.

The FTIR spectra were recorded to characterise the specific chemical groups present in each one of the materials and to analyse the effect of chitosan addition on nanocellulose films. The spectra of pure nanocellulose and chitosan were used as the reference. Fig. 6A shows the FTIR spectra of chitosan nanocellulose composite films with 0.5 g, 1 g, 1.5 g, and 2 g chitosan. The nanocellulose spectra contain typical bands for cellulose. The region between 3600 and 3200 cm^{-1} is assigned to OH stretching vibrations with the maximum at 3343 cm^{-1}, which is related to OH vibration due to hydrogen intramolecular bonding (Salari et al., 2018). Absorption peak in this range shows an increasing trend with the molecular weight of chitosan. This increase is due to the increase in hydrogen bonding between chitosan and nanocellulose. The 3000–2800 cm^{-1} region is related to CH and C-H_2 stretching vibrations. This peak also shows an increase in intensity with increased molecular weight of chitosan (Balti et al., 2017). The 1500–1250 cm^{-1} region is related to CH deformation and OH out-of-plane bending vibrations. The 1180–800 cm^{-1} region has the same pattern for the nanocellulose and chitosan samples due to their similar structure. This region is also sensitive to the C-O and C-H stretching vibrations. Moreover, there was a drastic increase in the intensity of the absorption bands at 1054 and 1032 cm^{-1} with increasing molecular weight of chitosan (Khan et al., 2012). This is due to the increased interaction of nanocellulose with chitosan. However, other changes, which occurred due to the increased molecular weight of chitosan, were minor at 1538 and 1340 cm^{-1}, and their intensity increased with increasing molecular weight of chitosan. The main characteristic feature is the presence of bands at 1610 cm^{-1}, which is related to stretching of carbonyl group, while bands at 1740 cm^{-1} are related to ester-stretching (Salari et al., 2018).

Fig. 6B shows the FTIR spectra of chitosan-nanocellulose composite films with different amounts of *Aloe vera*. For comparative study, spectra of neat chitosan (1 g) and chitosan-nanocellulose (1 g chitosan) without *Aloe vera* are also included. Except chitosan-nanocellulose film without *Aloe vera*, all other films show a band at 3000–3600 cm^{-1}, which is attributed to the hydroxyl groups of the adsorbed water (Bajer et al., 2020). This band is broad in the case of plain chitosan film. In composites with

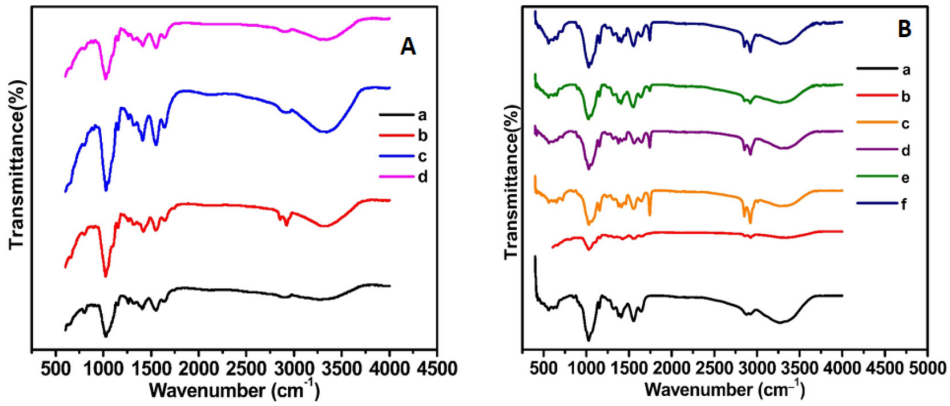

Fig. 6. (A) FTIR spectra of films of sample NC/CH with (a) 0.5 g, (b) 1 g, (c) 1.5 g, and (d) 2 g chitosan, respectively and (B) FTIR spectra of samples with (a) 1 g chitosan only, (b) sample NC/CH with 1 g chitosan and then spectra of samples NC/CH/V with (c) 0.25 ml, (d) 0.35 ml, (e) 0.5 ml, and (f) 2.5 ml *Aloe vera*, respectively

Aloe vera, these bands become narrower. A clear assignment of characteristic modes in this spectral range is not trivial because the hydroxyl stretching vibration bands overlap with the vibrations of N–H stretching of chitosan. This band can also be assigned to –OH stretching groups of *Aloe vera* constituents (e. g. uronic acid, mannonse or galactruonic acid) or phenolic groups in traquinones such as aloinand emodin present in *Aloe vera* (Torres-Giner et al., 2017). Such a wide range may also indicate the formation of intermolecular hydrogen bonds caused by dipole – dipole attraction forces. It can be assumed that in the studied systems, this type of bonds may be formed between the same (i. e., chitosan-chitosan) or various (*Aloe vera*-chitosan) molecule interactions.

Spectral region between 900 and 1200 cm^{-1} has an intense absorption band. This band is predominantly visible in the case of composites with *Aloe vera* and in the plain chitosan sample. These are present due to the C–O–C bond (in anhydrase glucose ring) stretching vibration of polysaccharide in *Aloe vera* gel but also in chitosan. This moiety, called «saccharide band», is sensitive to some conformational changes and is directly related to the crystal and amorphous phase in samples. It has been reported that a small band at ~ 1200 cm^{-1} is assigned to C–O stretching vibration and intramolecular hydrogen bonding of OH groups in chitosan (Arias et al., 2018; Anicuta et al., 2010; Pawlak, Mucha, 2003). The band at 1200 cm^{-1} in plain chitosan sample is shifted to higher frequencies (1210 cm^{-1}) in the spectra of the sample with 0.25 ml, 0.35 ml, 0.5 ml, and 2.5 ml *Aloe vera* addition. It is probably due to some interactions between chitosan and glycerol with *Aloe vera* macromolecules through H-bonding, which facilitates the mutual intercalation of substrates. This characteristic band is also sensitive to water content, and it shifts into higher frequencies when water content increases (Bajer et al., 2020, El Fawal et al., 2019).

UV–Vis adsorption spectra were recorded to determine the optical properties of chitosan-nanocellulose films as shown in Fig. 7A. Film opacity is one of the important factors that determine the quality of nanocomposite films. Transparency/light transmittance of composite films was measured between 200 and 800 nm, using a UV–Vis recording spectrophotometer. The films obviously showed transmittance values in the range of both visible light (400–800 nm) and ultraviolet light (200–400 nm) (Salari et al., 2018). As we increased the molecular weight of chitosan, the films showed an increase in absorbance and therefore a decrease in transmittance (Fig. 7A) (Valencia-Chamorro et al., 2011; Kaya et al., 2018).

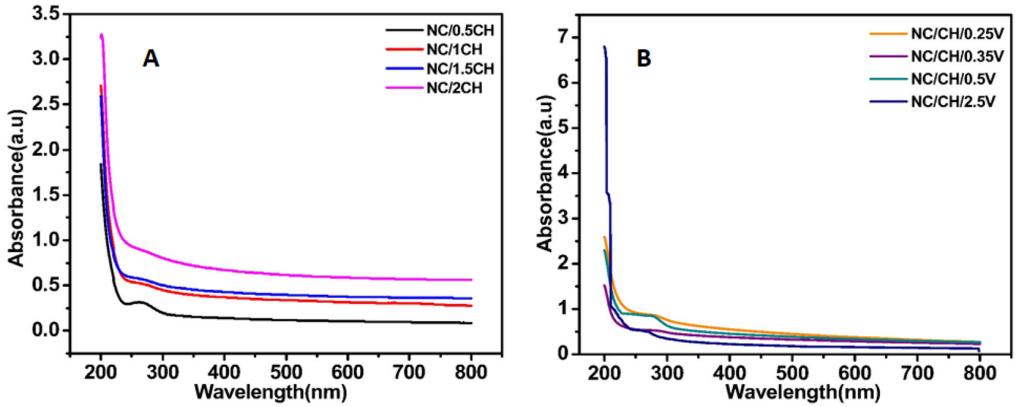

Fig. 7. UV–Visible spectra of (A) samples NC/CH and (B) samples NC/CH/V

Fig. 7B shows the UV–Vis absorption spectra of chitosan-nanocellulose films with different quantities of *Aloe vera* extract. An adsorption band between 250 and 350 nm is shown for the films containing *Aloe vera*. However, no such band was seen in the given range for chitosan-nanocellulose films without *Aloe vera*. The absorbance of nanocomposites near UV region of 250 nm to 350 nm increases with an increase in *Aloe vera* content (Fig. 7B). This absorbance is notably higher in the case of 0.5 ml *Aloe vera* incorporated film. In this region, the transmittance decreases significantly. This reduction in the light transmittance value in the UV region compared to the chitosan-nanocellulose films without *Aloe vera* confirms the UV absorption potential of *Aloe vera* incorporated in the matrix. This will certainly help to protect the food items from UV degradation (Nieto-Suaza et al., 2019; Sánchez et al., 2020a).

Contact angle measurements give the information about hydrophobicity or hydrophilicity of materials. This property is very important for their application as edible coating materials, especially in food industry, where the use of limited water permeability is crucial to maintaining the durability of food products (Noorbakhsh-Soltani et al., 2018). In this work, wetting characteristics of chitosan based nanocellulose composite films with different compositions were studied. Wetting characteristics such as work of adhesion, total surface free energy, and spreading coefficient were studied in detail.

Fig. 8 shows the contact angle images of 0.5 g, 1 g, 1.5 g, and 2 g chitosan films. All the samples show contact angle less than 90 degrees, indicating its hydrophilic nature. The contact angles increase with an increase in chitosan concentration up to 1.5 wt.% and after that, they are reduced. This may be due to better interaction between nanocellulose and chitosan through hydrogen bonding. However, at a higher concentration of nanocellulose, the presence of OH groups in nanocellulose makes it more hydrophilic. A detailed analysis of the

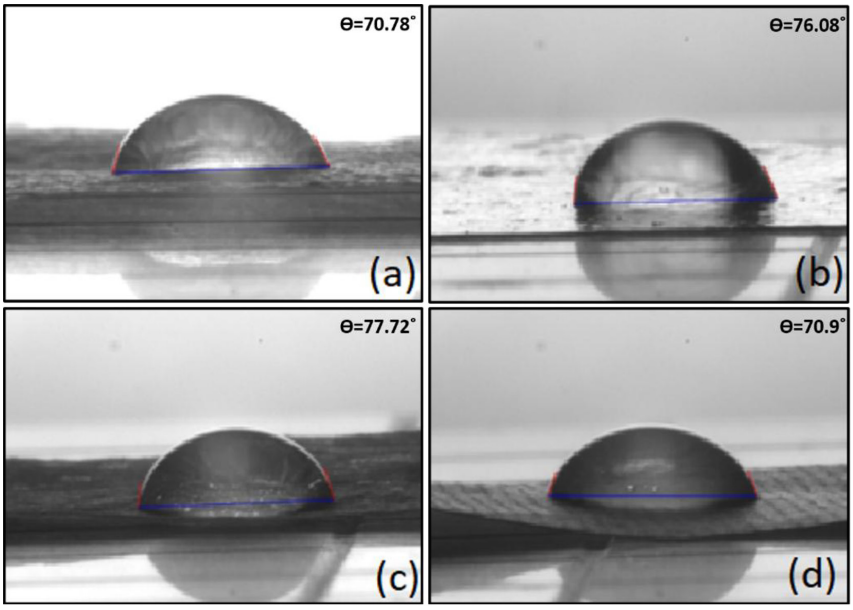

Fig. 8. Contact angle images of films of sample NC/CH with (a) 0.5 g, (b) 1 g, (c) 1.5 g, and (d) 2 g chitosan, respectively

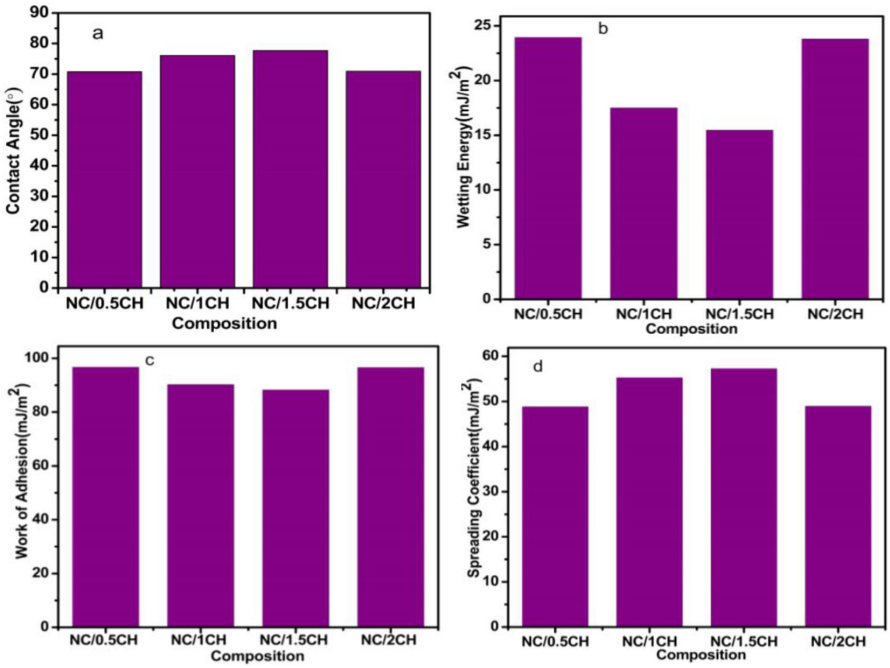

Fig. 9. Graph shows (a) contact angle v/s composition, (b) wetting energy v/s composition, (c) work of adhesion v/s composition, and (d) spreading coefficient v/s composition of sample NC/CH

films was done by plotting other parameters like wetting energy, work of adhesion, and spreading coefficient (Fig. 9). It is evident that the maximum contact angle is observed in the case of 1.5 g chitosan composite and, thus, this composition will have the highest hydrophobicity and lowest surface energy.

According to the theory of wetting process, if the solid–vapour interfacial energy is low, the tendency of liquid for spreading will be less and, thus, the system will be more hydrophobic. The solid surface is rich in hydrocarbon molecules. The forces that hold hydrocarbons together are much weaker than the force that acts between water molecules. A higher value for wetting energy means the liquid will spread over the surface. So, the film with the lowest wetting energy is less hydrophilic in nature. This is a favourable characteristic for edible coating application. The lowest wetting energy is shown by 1.5 wt.% of chitosan, indicating more hydrophobic nature as explained.

The work of adhesion (WA) is the work required to separate the composite surface and the liquid droplet. It is evident that film with 1.5 g of chitosan will have the lowest value for work of adhesion. Generally, the work of adhesion is found to decrease with an increase in the complexity of the composite and with a decrease in interfacial bonding. The polar and non-polar interactions across interface are a measure of adhesion between the test liquid and composite surface. Work of adhesion can be correlated to the nanocellulose-chitosan interaction. The effective dispersion of nanocellulose into the chitosan matrix decreases the work of adhesion, and, thus, an increment in the hydrophobic nature of the composite can be seen. Spreading coefficient gives the idea about the wetting and spreading of a liquid on the surface of a solid. A positive value of spreading coefficient indicates spontaneous wetting and spreading of the liquid on the surface of a solid, and a negative value indicates poor

wetting. It also depends on the surface tension of the test liquid: a liquid with high surface tension would not spread much. Spreading coefficient (Sc) values indicate that a liquid will spontaneously wet and spread on the solid surface if the value is positive, whereas a negative value of spreading coefficient implies the lack of spontaneous wetting. This means that there is a finite contact angle (i. e., u>0). The polar–polar interactions across the interface are a measure of wetting. Spreading coefficient increases with the amount of chitosan and, thus, hydrophobicity of nanocomposites will be enhanced.

Fig. 10 presents the contact angle images of chitosan-nanocellulose composite film with 0.25 ml, 0.35 ml, 0.5 ml, and 2.5 ml *Aloe vera*, respectively. The contact angle shows an initial increase, and above 0.5 ml of *Aloe vera*, it is reduced. The quantified data of contact angle, wetting energy, work of adhesion, and spreading coefficient for Sample NC/CH/V are given in Fig. 11. The data suggest that film containing 0.5 ml *Aloe vera* has favourable properties for edible film such as high contact angle, low wetting energy, low work of adhesion, and high spreading coefficient, which results in hydrophobic nature. It is evident from the analysis that addition of *Aloe vera* oil enhanced hydrophobic nature of films.

Fig. 12 shows the stress-strain graph of chitosan-nanocellulose films with 0.5 g, 1 g, 1.5 g, and 2 g chitosan. From the graph, it is clear that film containing 1 g chitosan has the maximum strength, which indicates that this particular composition has good dispersion of nanocellulose.

Successful coating should provide adequate mechanical strength to fruit and should be free from minor defects. This attribute can be accomplished by having a flexible coating that is resistant to breakage and abrasion. Tensile strength and elongation at break are parameters that affect this property. Factors that are critical to mechanical properties include polymer structure, type of plasticizer, concentration of plasticizer, molecular weight of coating forming materials, types of solvent, and thickness of coating. The tensile strength of chitosan-based bio composite increased with molecular weight of chitosan (Fig. 13). The increase in the TS

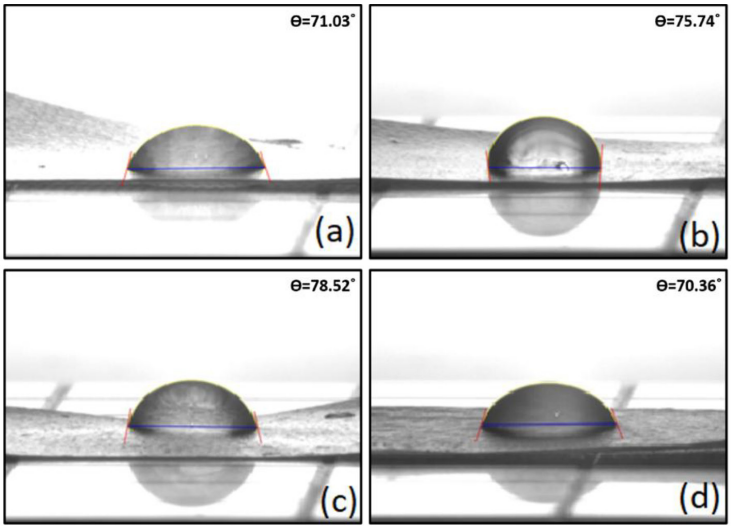

Fig. 10. Contact angle images of films of sample NC/CH/V with (a) 0.25 ml, (b) 0.35 ml, (c) 0.5 ml, and (d) 2.5 ml *Aloe vera*, respectively

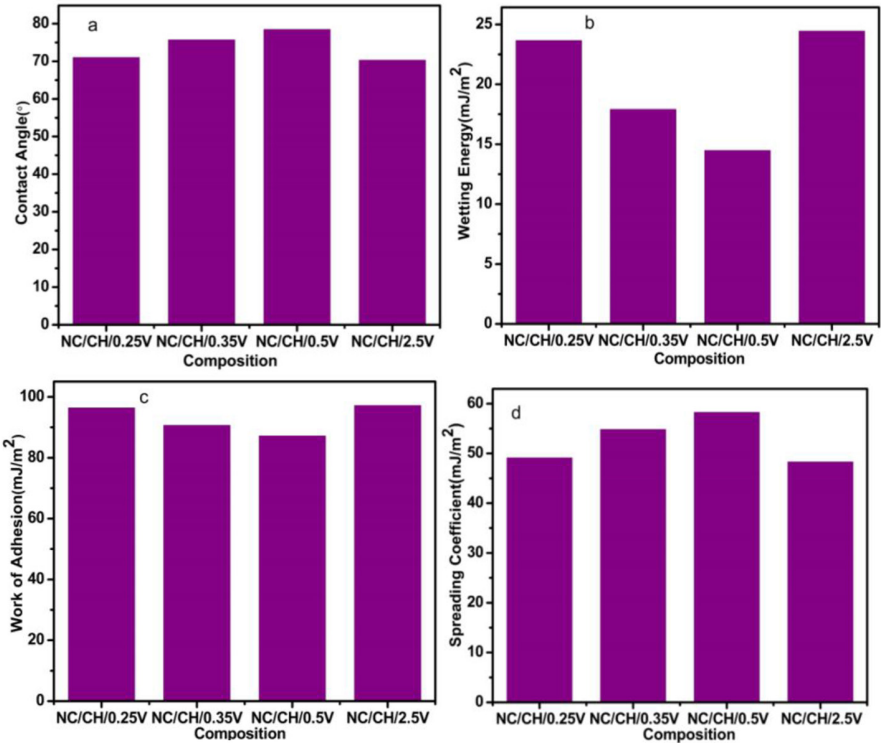

Fig. 11. Graph shows: (a) contact angle v/s composition, (b) wetting energy v/s composition, (c) work of adhesion v/s composition, and (d) spreading coefficient v/s composition for sample with *Aloe vera* (sample NC/CH/V)

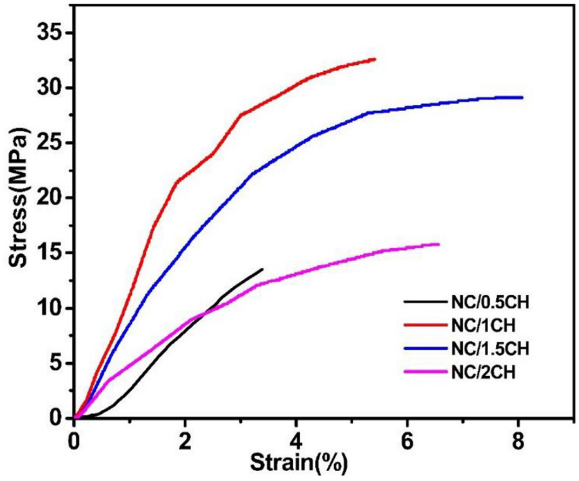

Fig. 12. Stress v/s Strain graph of films of sample NC/CH

values of the nanocellulose reinforced chitosan films can be attributed to two factors such as (1) the favourable nanofiber-chitosan interactions and (2) the reinforcing effect occurring through effective stress transfer at the nanofiber–chitosan interface (Valencia-Chamorro et al., 2011). The interaction between the anionic sulphate groups of nanocellulose and the cationic amine groups of

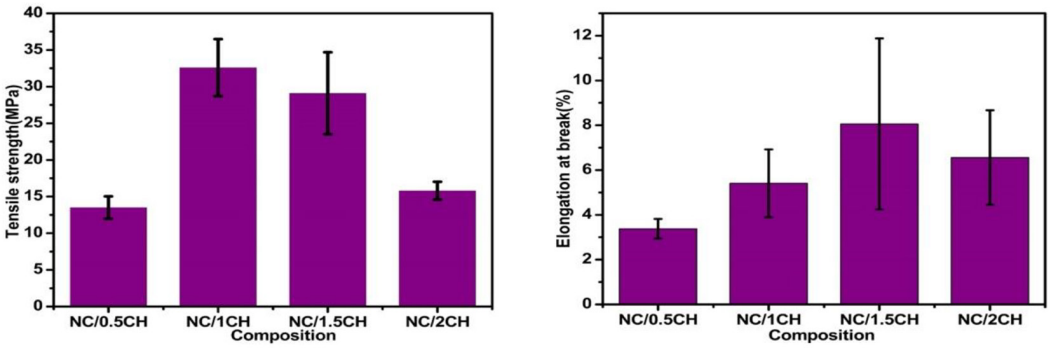

Fig. 13. Tensile strength vs composition, elongation at break vs composition of NC/CH

chitosan might favour a good interface between the matrix and the filler. This may lead to high tensile strength values of the nanocomposite films.

The elongation at break of chitosan-based bio composite increased with molecular weight of chitosan (Fig. 13). Elasticity of composite films is influenced by interaction of plasticizer with chitosan matrix. Thus, as molecular weight of chitosan increases, the interaction of chitosan with glycerol and water increases, which will result in increased elasticity or elongation at break with increasing molecular weight of chitosan.

Fig. 14 shows the stress-strain curve of composite film with 0.25 ml, 0.35 ml, 0.5 ml, and 2.5 ml *Aloe vera* and pure chitosan film (1-CH). The mechanical properties were enhanced by the addition of *Aloe vera* into the composite. Maximum ultimate stress is exhibited by the film with 0.25 ml *Aloe vera* (Fig. 14). The curve of this particular composition is ideal and film with this particular composition will have better strength for the application of edible coating.

For further clarification plots of composition v/s modulus, elongation at break, and tensile strength graphs were analysed (Fig. 15). Tensile strength (TS, in MPa) indicates the maximum tensile stress that the film can sustain; elongation at break (E, in%) is the maximum change in the length of a test film before being broken; and elastic modulus (EM, in MPa) is a measure of the stiffness of the film as a function of *Aloe vera* incorporation. These mechanical

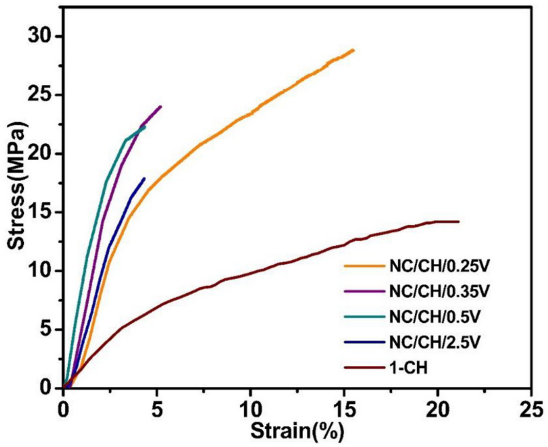

Fig. 14. Stress v/s Strain graph of films of sample NC/CH/V

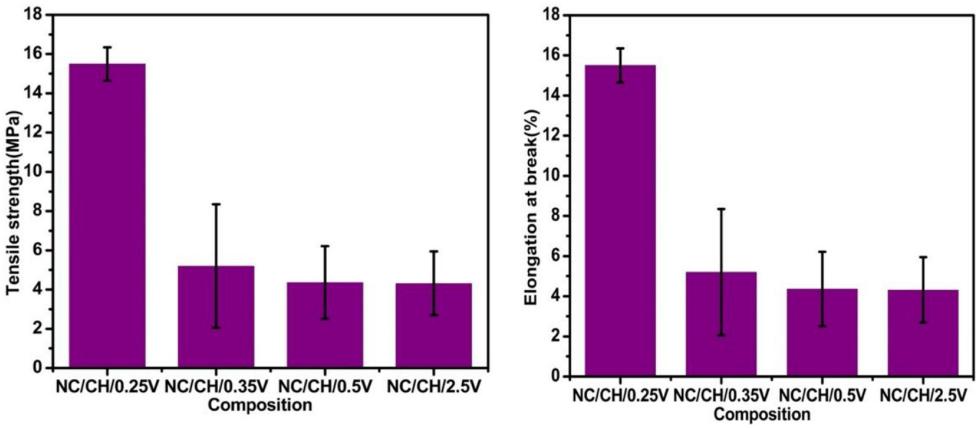

Fig. 15. The graphs of composition v/s tensile strength and elongation at break of composites with different compositions of *Aloe vera*

characteristics showed that by the addition of *Aloe vera* when compared to the plain composite film, a decrease in tensile strength was observed. However, it is quite clear from the graph (Fig. 14) that the modulus of the material is enhanced initially and tends to decrease with further addition. The tensile strength and elongation at break decrease with an increase in the amount of *Aloe vera* added. But data of plain composite films reveal that the tensile strength increases with the addition of *Aloe vera*. Results suggest that the optimum amount of *Aloe vera* needed to get an ideal film with maximum strength and elasticity is 0.25 ml.

The water content of fruits and vegetables is a major factor in maintaining quality of horticultural products. Low weight loss is important in maintaining the fruit quality over longer time. Weight loss is associated with respiration and transpiration of moisture. According to Lin et al. (2002), water loss in longan fruit was mainly from the pericarp rather than the aril (pulp). The water loss was also known to positively correlate with the pericarp browning of longan fruit (Lin et al., 2002; 2005). In this study, weight loss of nanocellulose (NC)/chitosan (CH)/ *Aloe vera* coated samples and uncoated chillies was determined for a period of three days (Fig. 16).

NC/CH/0.25 V treated chillies were noted to have relatively lower weight loss throughout storage days, as compared to standard chillies without any treatment and chillies treated with NC/CH/0.35V. By Day 3, the weight loss of uncoated chillies was 43.7 % and that of NC/ CH/0.25V coated chillies was 39.1 %. The weight loss of chillies coated with NC/CH/0.35 V was 40.3 %. Incorporation of nanocellulose and *Aloe vera* in the coating solutions shows a decrease in the weight loss percent. The barrier properties of coating film formed on the surface could be increased by the addition of nanocellulose, chitosan, and *Aloe vera* to coating solutions. Chitosan/nanocellulose/*Aloe vera* coated chillies show that the prepared film is effective, and it helps to enhance the storage life of chillies under humid condition.

Conclusions

An environmentally friendly bio nanocomposite edible coating material was successfully fabricated utilizing chitosan and nanocellulose with the addition of *Aloe vera* as an antimicrobial agent, via solvent casting

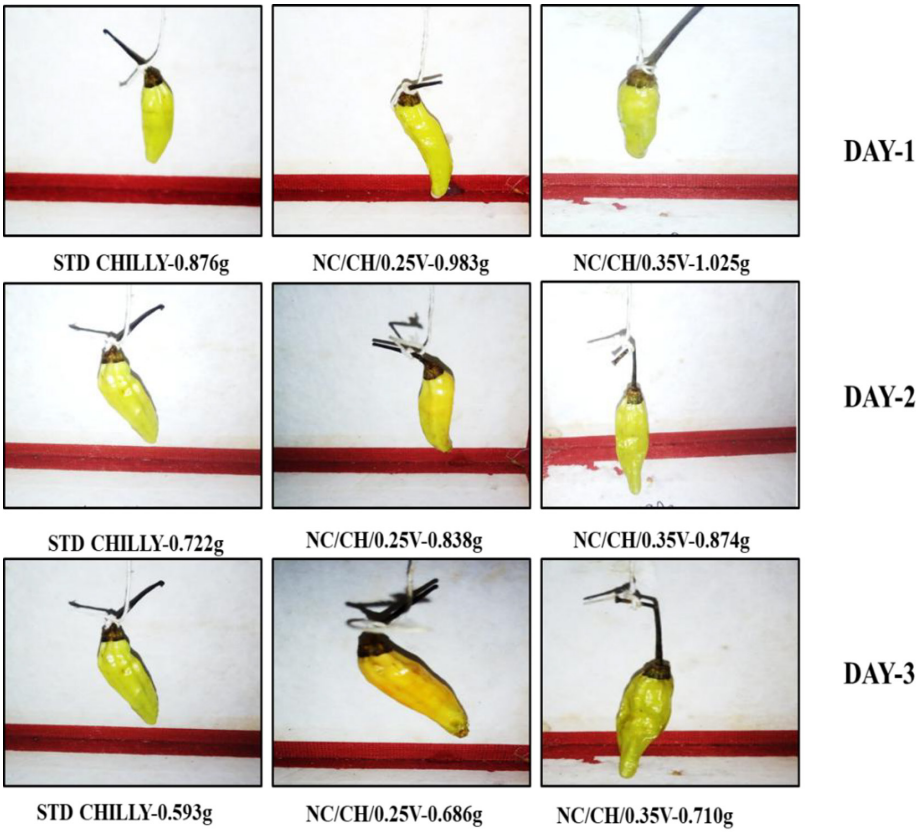

Fig. 16. Weight loss studies of uncoated and NC/CH/*Aloe vera* coated chillies for 3 days

technique. Due to the fibrous structure and fine dispersion of nanofibers over the chitosan matrix, there is an enhancement in properties of nanocomposites after reinforcement. But at higher filler loading, the properties decrease probably due to agglomeration of these nanofibers. Dispersion of nanocomposite is visible from the SEM images. Also, optical studies and UV visible studies show a nanoscale dispersion in the composite. Mechanical analysis guarantees the strength of the composite. Contact angle analysis demonstrates that the material is water repellent, which is a favourable property of edible coating materials. Transparency of the film is a great advantage, as we can provide a natural appearance to the fruits or vegetables to be coated. Coating application study using chilli gives a satisfying result, but further modifications are needed to prepare a better and promising material.

Chitosan based nanocellulose composite can be effectively used as an alternative to synthetic fruit coating. It can be used to increase the shelf life and freshness of fruit as well. Moreover, biodegradability is the main advantage of edible over polymer traditional synthetics, as they can be consumed with the products. Even if the films are not consumed, they are completely biodegradable and will not produce any detrimental effect on the environment.

References

Abraham E., Deepa B., Pothan L. A., Jacob M., Thomas S., Cvelbar U., Anandjiwala R. (2011) Extraction of nanocellulose fibrils from lignocellulosic fibres: a novel approach. *Carbohydrate Polymers*, 86(4): 1468–1475

Aloui H., Khwaldia K. (2016) Natural antimicrobial edible coatings for microbial safety and food quality enhancement. *Comprehensive Reviews in Food Science and Food Safety*, 15(6): 1080–1103

Amirabad L. M., Jonoobi M., Mousavi N. S., Oksman K., Kaboorani A., Yousefi H. (2018) Improved antifungal activity and stability of chitosan nanofibers using cellulose nanocrystal on banknote papers. *Carbohydrate Polymers*, 189: 229–237

Anicuta S. G., Dobre L., Stroescu M., Jipa I. (2010) Fourier transform infrared (FTIR) spectroscopy for characterization of antimicrobial films containing chitosan. *Analele UniversităŃii din Oradea Fascicula: Ecotoxicologie, Zootehnie* şi *Tehnologii de Industrie Alimentară*, 1234–1240

Arias L. D., Montaño D. L.N., Velasco S. M.A., Martínez G. J. (2018) Alimentos funcionales: avances de aplicación en agroindustria. *Tecnura*, 22(57): 55–68 (in Spanish)

Arvanitoyannis I. S. (1999) Totally and partially biodegradable polymer blends based on natural and synthetic macromolecules: preparation, physical properties, and potential as food packaging materials. *Journal of Macromolecular Science-Reviews in Macromolecular Chemistry and Physics*, C39(2): 205–271

Asrofi M., Abral H., Kasim A., Pratoto A. (2017) Characterization of the microfibrillated cellulose from water hyacinth pulp after alkali treatment and wet blending. *IOP Conference Series: Materials Science and Engineering*, 204(1): 012018

Azeredo H. M.C., Rosa M. F., Mattoso L. H.C. (2017) Nanocellulose in bio-based food packaging applications. *Industrial Crops and Products*, 97: 664–671

Bajer D., Janczak K., Bajer K. (2020) Novel starch/chitosan/Aloe vera composites as promising biopackaging materials. *Journal of Polymers and the Environment*, 28(3): 1021–1039

Balti R., Mansour M. B., Sayari N., Yacoubi L., Rabaoui L., Brodu N., Massé A. (2017) Development and characterization of bioactive edible films from spider crab (Maja crispata) chitosan incorporated with Spirulina extract. *International Journal of Biological Macromolecules*, 105: 1464–1472

Cazón P., Vázquez M., Velazquez G (2018) Composite films of regenerate cellulose with chitosan and polyvinyl alcohol: Evaluation of water adsorption, mechanical and optical properties. *International Journal of Biological Macromolecules*, 117: 235–246

Chandra C. S.J., George N., Narayanankutty S. K. (2016) Isolation and characterization of cellulose nanofibrils from arecanut husk fibre. *Carbohydrate Polymers*, 142: 158–166

Cherian B. M., Leão A. L., de Souza S. F., Thomas S., Pothan L. A., Kottaisamy M. (2010) Isolation of nanocellulose from pineapple leaf fibres by steam explosion. *Carbohydrate Polymers*, 81(3): 720–725

Cherian B. M., Leão A. L., de Souza S. F., Costa L. M.M., De Olyveira G. M., Kottaisamy M., Nagarajan E. R., Thomas S. (2011) Cellulose nanocomposites with nanofibres isolated from pineapple leaf fibers for medical applications. *Carbohydrate Polymers*, 86(4): 1790–1798

Cherpinski A., Torres-Giner S., Vartiainen J., Peresin M. S., Lahtinen P., Lagaron J. M. (2018) Improving the water resistance of nanocellulose-based films with polyhydroxyalkanoates processed by the electrospinning coating technique. *Cellulose*, 25(2): 1291–1307

Corsello F. A., Bolla P. A., Anbinder P. S., Serradell M. A., Amalvy J. I., Peruzzo P. J. (2017) Morphology and properties of neutralized chitosan-cellulose nanocrystals biocomposite films. *Carbohydrate Polymers*, 156: 452–459

Dutta T., Ghosh N. N., Chattopadhyay A. P., Das M. (2019) Chitosan encapsulated water-soluble silver bionanocomposite for size-dependent antibacterial activity. *Nano-Structures & Nano-Objects*, 20: 100393

El Fawal G. F., Omer A. M., Tamer T. M. (2019) Evaluation of antimicrobial and antioxidant activities for cellulose acetate films incorporated with Rosemary and Aloe vera essential oils. *Journal of Food Science and Technology*, 56(3): 1510–1518

Eshun K., He Q. (2004) Aloe vera: a valuable ingredient for the food, pharmaceutical and cosmetic industries – a review. *Critical Reviews in Food Science and Nutrition*, 44(2): 91–96

Fahma F., Iwamoto S., Hori N., Iwata T., Takemura A. (2011) Effect of pre-acid-hydrolysis treatment on morphology and properties of cellulose nanowhiskers from coconut husk. *Cellulose*, 18(2): 443–450

Fitch-Vargas P.R., Aguilar-Palazuelos E., de Jesús Zazueta-Morales J., Vega-García M.O., Valdez-Morales J.E., Martínez-Bustos F., Jacobo-Valenzuela N. (2016) Physicochemical and microstructural characterization of corn starch edible films obtained by a combination of extrusion technology and casting technique. *Journal of Food Science*, 81(9): E2224–E2232

Geueke B., Groh K., Muncke J. (2018) Food packaging in the circular economy: overview of chemical safety aspects for commonly used materials. *Journal of Cleaner Production*, 193: 491–505

Habeeb F., Shakir E., Bradbury F., Cameron P., Taravati M. R., Drummond A. J., Gray A. I., Ferro V. A. (2007) Screening methods used to determine the anti-microbial properties of Aloe vera inner gel. *Methods*, 42(4): 315–320

Hazrati S., Beyraghdar Kashkooli A., Habibzadeh F., Tahmasebi-Sarvestani Z., Sadeghi A. R. (2017) Evaluation of Aloe vera gel as an alternative edible coating for peach fruits during cold storage period. *Gesunde Pflanzen*, 69(3): 131–137

Iwamoto S., Kai W., Isogai A., Iwata T. (2009) Elastic modulus of single cellulose microfibrils from tunicate measured by atomic force microscopy. *Biomacromolecules*, 10(9): 2571–2576

Joseph B., Maria H. J., Thomas S., Kalarikkal N., Gopakumar D. A., James J., Grohens Y., Khalil H. P.S.A. (2019) Nanocellulose: health care applications. *Encyclopedia of polymer applications*. Mishra M. (Ed.) Boca Raton, CRC Press, p. 1829–1852

Joseph B., Sagarika V. K., Sabu C., Kalarikkal N., Thomas S. (2020a) Cellulose nanocomposites: fabrication and biomedical applications. *Journal of Bioresources and Bioproducts*, 5(4): 223–237

Joseph B., Sam R. M., Balakrishnan P., Maria H. J., Gopi S., Volova T., Fernandes S. C.M., Thomas S. (2020b) Extraction of nanochitin from marine resources and fabrication of polymer nanocomposites: recent advances. *Polymers*, 12(8): 1664

Joshy K. S., Augustine R., Li T., Snigdha S., Hasan A., Komalan C., Kalarikkal N., Thomas S. (2020a) Carboxymethylcellulose hybrid nanodispersions for edible coatings with potential anti-cancer properties. *International Journal of Biological Macromolecules*, 157: 350–358

Joshy K. S., Jose J., Li T., Thomas M., Shankregowda A. M., Sreekumaran S., Kalarikkal N., Thomas S. (2020b) Application of novel zinc oxide reinforced xanthan gum hybrid system for edible coatings. *International Journal of Biological Macromolecules*, 151: 806–813

Ju J., Xie Y., Guo Y., Cheng Y., Qian H., Yao W. (2019) Application of edible coating with essential oil in food preservation. *Critical Reviews in Food Science and Nutrition*, 59(15): 2467–2480

Kaya M., Ravikumar P., Ilk S., Mujtaba M., Akyuz L., Labidi J., Salaberria A.M., Cakmak Y.S., Erkul S.K. (2018) Production and characterization of chitosan based edible films from berberis crataegina's fruit extract and seed oil. *Innovative Food Science and Emerging Technologies*, 45: 287–297

Khan A., Khan R.A., Salmieri S., Le Tien C., Riedl B., Bouchard J., Chauve G., Tan V., Kamal M.R., Lacroix M. (2012) Mechanical and barrier properties of nanocrystalline cellulose reinforced chitosan based nanocomposite films. *Carbohydrate Polymers*, 90(4): 1601–1608

Khwaldia K., Perez C., Banon S., Desobry S., Hardy J. (2004) Milk proteins for edible films and coatings. *Critical Reviews in Food Science and Nutrition*, 44(4): 239–251

Kuila B.K., Nandi A.K. (2004) Physical, mechanical, and conductivity properties of poly(3-hexylthiophene) -montmorillonite clay nanocomposites produced by the solvent casting method. *Macromolecules*, 37(23): 8577–8584

Kumar S., Mukherjee A., Dutta J. (2020) Chitosan based nanocomposite films and coatings: emerging antimicrobial food packaging alternatives. *Trends in Food Science & Technology*, 97: 196–209

Lin H., Chen S., Guo Y.S., Xi Y., Guo S. (2002) Observation on pericarp ultrastructure by scanning electron microscope and its relation to keeping quality of longan fruit. *Nongye Gongcheng Xuebao/Transactions of the Chinese Society of Agricultural Engineering*, 18(3): 95–99

Lin H.T., Xi Y.F., Chen S.J. (2005) The relationship between the desiccation-induced browning and the metabolism of active oxygen and phenolics in pericarp of postharvest longan fruit. *Journal of Plant Physiology and Molecular Biology*, 31(3): 287–297

Lin N., Dufresne A. (2014) Nanocellulose in biomedicine: current status and future prospect. *European Polymer Journal*, 59: 302–325

Mahardika M., Abral H., Kasim A., Arief S., Asrofi M. (2018) Production of nanocellulose from pineapple leaf fibers via high-shear homogenization and ultrasonication. *Fibers*, 6(2): 28

Marpudi S.L., Abirami L.S.S., Pushkala R., Srividya N. (2011) Enhancement of storage life and quality maintenance of papaya fruits using Aloe vera based antimicrobial coating. *Indian Journal of Biotechnology*, 10(1): 83–89

Misir J., Brishti F.H., Hoque M.M. (2014) Aloe vera gel as a novel edible coating for fresh fruits: a review. *American Journal of Food Science and Technology*, 2(3): 93–97

Mohammadi R., Mohammadifar M.A., Rouhi M., Kariminejad M., Mortazavian A.M., Sadeghi E., Hasanvand S. (2018) Physico-mechanical and structural properties of eggshell membrane gelatin – chitosan blend edible films. *International Journal of Biological Macromolecules*, 107 (Part A): 406–412

Naseri N., Mathew A.P., Girandon L., Froehlich M., Oksman K. (2015) Porous electrospun nanocomposite mats based on chitosan – cellulose nanocrystals for wound dressing: effect of surface characteristics of nanocrystals. *Cellulose*, 22(1): 521–534

Nieto-Suaza L., Acevedo-Guevara L., Sánchez L.T., Pinzón M.I., Villa C.C. (2019) Characterization of Aloe vera-banana starch composite films reinforced with curcumin-loaded starch nanoparticles. *Food Structure*, 22: 100131

Noorbakhsh-Soltani S.M., Zerafat M.M., Sabbaghi S. (2018) Comparative study of gelatin and starch-based nano-composite films modified by nano-cellulose and chitosan for food packaging applications. *Carbohydrate Polymers*, 189: 48–55

Pawlak A., Mucha M. (2003) Thermogravimetric and FTIR studies of chitosan blends. *Thermochimica Acta*, 396(1–2): 153–166

Pinzon M. I., Sanchez L. T., Garcia O. R., Gutierrez R., Luna J. C., Villa C. C. (2020) Increasing shelf life of strawberries (Fragaria ssp) by using a banana starch-chitosan-Aloe vera gel composite edible coating. *International Journal of Food Science and Technology*, 55(1): 92–98

Ramadan M. A., Sharawy S., Elbisi M. K., Ghosal K. (2020) Eco-friendly packaging composite fabrics based on in situ synthesized silver nanoparticles (AgNPs) & treatment with chitosan and/or date seed extract. *Nano-Structures & Nano-Objects*, 22: 100425

Rhim J. W., Mohanty A. K., Singh S. P., Ng P. K.W. (2006) Effect of the processing methods on the performance of polylactide films: thermocompression versus solvent casting. *Journal of Applied Polymer Science*, 101(6): 3736–3742

Ribeiro A. M., Estevinho B. N., Rocha F. (2020) Preparation and incorporation of functional ingredients in edible films and coatings. *Food and Bioprocess Technology*, 14(2): 209–231

Rubentheren V., Ward T. A., Chee C. Y., Nair P. (2015) Physical and chemical reinforcement of chitosan film using nanocrystalline cellulose and tannic acid. *Cellulose*, 22(4): 2529–2541

Salari M., Sowti Khiabani M., Rezaei Mokarram R., Ghanbarzadeh B., Samadi Kafil H. (2018) Development and evaluation of chitosan based active nanocomposite films containing bacterial cellulose nanocrystals and silver nanoparticles. *Food Hydrocolloids*, 84: 414–423

Saldanha J. M., Kyu T. (1987) Influence of solvent casting on the evolution of phase morphology of PC/PMMA blends. *Macromolecules*, 20(11): 2840–2847

Sánchez J. T., García A. V., Martínez-Abad A., Vilaplana F., Jiménez A., Garrigós M. C. (2020a) Physicochemical and functional properties of active fish gelatin-based edible films added with vera gel. *Foods*, 9(9): 9091248

Sánchez M., González-Burgos E., Iglesias I., Gómez-Serranillos M.P. (2020b) Pharmacological update properties of Aloe vera and its major active constituents. *Molecules*, 25(6): 1324

Santos R. M.D., Flauzino Neto W. P., Silvério H. A., Martins D. F., Dantas N. O., Pasquini D. (2013) Cellulose nanocrystals from pineapple leaf, a new approach for the reuse of this agro-waste. *Industrial Crops and Products*, 50: 707–714

Sogut E., Seydim A. C. (2019) The effects of chitosan- and polycaprolactone-based bilayer films incorporated with grape seed extract and nanocellulose on the quality of chicken breast fillets. *LWT-Food Science and Technology*, 101: 799–805

Suh S. W., Shin J. Y., Kim J., Kim J., Beak C. H., Kim D.-I., Kim H., Jeon S. S., Choo I.-W. (2002) Effect of different particles on cell proliferation in polymer scaffolds using a solvent-casting and particulate leaching technique. *ASAIO Journal*, 48(5): 460–464

Sultana T., Sultana S., Nur H. P., Khan M. W. (2020) Studies on mechanical, thermal and morphological properties of betel nut husk nano cellulose reinforced biodegradable polymer composites. *Journal of Composites Science*, 4(3): 83

Sundaram J., Pant J., Goudie M. J., Mani S., Handa H. (2016) Antimicrobial and physicochemical characterization of biodegradable, nitric oxide-releasing nanocellulose – chitosan packaging membranes. *Journal of Agricultural and Food Chemistry*, 64(25): 5260–5266

Torres-Giner S., Wilkanowicz S., Melendez-Rodriguez B., Lagaron J. M. (2017) Nanoencapsulation of Aloe vera in synthetic and naturally occurring polymers by electrohydrodynamic processing of

interest in food technology and bioactive packaging. *Journal of Agricultural and Food Chemistry*, 65(22): 4439–4448

Valencia-Chamorro S.A., Palou L., Delŕio M. A., Pérez-Gago M.B. (2011) Antimicrobial edible films and coatings for fresh and minimally processed fruits and vegetables: a review. *Critical Reviews in Food Science and Nutrition*, 51(9): 872–900

Valverde J. M., Valero D., Martínez-Romero D., Guillén F., Castillo S., Serrano M. (2005) Novel edible coating based on Aloe vera gel to maintain table grape quality and safety. *Journal of Agricultural and Food Chemistry*, 53(20): 7807–7813

Vieira J. M., Flores-López M.L., de Rodríguez D. J., Sousa M. C., Vicente A. A., Martins J. T. (2016) Effect of chitosan-Aloe vera coating on postharvest quality of blueberry (Vaccinium corymbosum) fruit. *Postharvest Biology and Technology*, 116: 88–97

Vu K. D., Hollingsworth R. G., Leroux E., Salmieri S., Lacroix M. (2011) Development of edible bioactive coating based on modified chitosan for increasing the shelf life of strawberries. *Food Research International*, 44(1): 198–203

Wang S. Y., Gao H. (2013) Effect of chitosan-based edible coating on antioxidants, antioxidant enzyme system, and postharvest fruit quality of strawberries (Fragaria x Aranassa Duch.). *LWT-Food Science and Technology*, 52(2): 71–79

Xu J., Xia R., Zheng L., Yuan T., Sun R. (2019) Plasticized hemicelluloses/chitosan-based edible films reinforced by cellulose nanofiber with enhanced mechanical properties. *Carbohydrate Polymers*, 224: 115164

Journal of Siberian Federal University. Biology 2021 14(4): 498–509
~ ~ ~

DOI 10.17516/1997-1389-0367

УДК 581.143.5:57.085

Casein Stabilized Metal and Metal Oxide Nanoparticles for the Efficient *In Vitro* Culturing of *Scoparia dulcis* L.

Kalathil Rajan Rakhimol, Sabu Thomas, Nandakumar Kalarikkal and Kochupurakkal Jayachandran*
Mahatma Gandhi University
Kottayam, India

Received 14.06.2021, received in revised form 21.07.2021, accepted 23.08.2021

Abstract. Unique physicochemical properties of nanoparticles make them a novel candidate in agriculture and related areas. In the present work, we have studied the effect of casein stabilized metal and metal oxide nanoparticles, viz. AgNPs, AuNPs, and CuONPs, on *in vitro* propagation of *Scoparia dulcis* L. We have examined the effect of these nanoparticles on the callus induction, shoot regeneration, and root regeneration capacity. It was observed that Ag, Au, and CuO nanoparticles had interacted with the tissues differently and produced calluses with difference in color, nature, and texture. Nanoparticles also affected shoot regeneration, root regeneration, phenolic compound production, and chlorophyll content. Explants showed a very good response when treated with CuONPs. The formed callus underwent shoot and root regeneration without changing the medium.

Keywords: AgNPs, AuNPs, CuONPs, *Scoparia dulcis*, callus induction.

Acknowledgements. The authors would like to express their gratitude to School of Biosciences, M. G. University for providing tissue culture facility for the successful completion of the work.

Citation: Rakhimol K. R., Thomas S., Kalarikkal N., Jayachandran K. Casein stabilized metal and metal oxide nanoparticles for the efficient *in vitro* culturing of *Scoparia dulcis* L.. J. Sib. Fed. Univ. Biol., 2021, 14(4), 498–509. DOI: 10.17516/1997-1389-0367

* Corresponding author E-mail address: jayachandrank@mgu.ac.in
ORCID: 0000-0001-5002-4084 (Thomas S.); 0000-0002-4595-6466 (Kalarikkal N.); 0000-0001-6019-7261 (Jayachandran K.)

Использование стабилизированных казеином наночастиц металлов и оксидов металлов для эффективного культивирования *in vitro Scoparia dulcis* L.

К. Р. Рахимол, С. Томас,
Н. Каларикkал, К. Джаячандран
Университет Махатмы Ганди
Индия, Коттаям

Аннотация. Уникальные физико-химические свойства наночастиц делают их перспективными кандидатами для использования в сельском хозяйстве и смежных областях. В настоящей работе исследовано влияние стабилизированных казеином наночастиц металлов и оксидов металлов (AgNP, AuNP и CuONP) на рост *in vitro Scoparia dulcis* L. Исследовано влияние этих наночастиц на индукцию каллуса, регенерацию побегов и корней. Показано, что наночастицы Ag, Au и CuO по-разному взаимодействовали с тканями и образовавшиеся каллусы отличались по цвету, природе и текстуре. Наночастицы также оказывали влияние на регенерацию побегов и корней, продукцию фенольных соединений и содержание хлорофилла. Экспланты показали хороший отклик на применение наночастиц CuO. Образовавшиеся каллусы были способны к регенерации побегов и корней без смены среды.

Ключевые слова: наночастицы, Ag, Au, CuO, *Scoparia dulcis*, индукция каллуса.

Благодарности. Авторы хотели бы выразить свою благодарность Школе биологических наук Университета М. Г. за предоставление средства для культивирования тканей для успешного завершения работы.

Цитирование: Рахимол, К. Р. Использование стабилизированных казеином наночастиц металлов и оксидов металлов для эффективного культивирования *in vitro Scoparia dulcis* L. / К. Р. Рахимол, С. Томас, Н. Каларикkал, К. Джаячандран // Журн. Сиб. федер. ун-та. Биология, 2021. 14(4). С. 498–509. DOI: 10.17516/1997-1389-0367

Introduction

Scoparia dulcis L. is an important plant, which is used as herbal medicine to treat various diseases like cancer, bronchitis, hypertension, etc. Most of these biological properties are attributed to the phytochemicals present in the plant. Because of the high potential of *S. dulcis* in traditional medicine, its large-scale production through tissue culture is very important (Annie, Jayachandran, 2008).

Establishment of the totipotency of plant tissue, differentiation of callus, and vegetative multiplication under controlled *in vitro* conditions have opened a novel approach in the plant science. Plant tissue culture is a versatile technique for the development of plantlets in laboratory under controlled conditions. The basis of the plant tissue culture is the ability of plant cells to regenerate into a whole plant. Plant tissue culture is mainly used for the large-scale production of rare and endangered

species. It can also be used to produce virus-free plants from the shoot tip culture of virus infected plants (Dagla, 2012).

Metal nanoparticles have their application in various fields including medicine because of their unique physicochemical properties. In agriculture, the nanoparticles are commonly used as fertilizers. Application of nanoparticles in tissue culture is very limited (Sarkar et al., 2012). In our study, we try to investigate the influence of synthesized metal and metal oxide nanoparticles (Ag, Au, and CuO NPs) on the callus formation in the tissue culture of *S. dulcis*.

Previous studies revealed that the plants could produce mineralized nanoparticles naturally and these are required for growth. The study of artificially engineered nanoparticles in plant growth and development is a novel field of research and yet to be explored. Large surface to volume ratio and electron exchange engineering ability help them form favorable interactions with biomolecules present inside the cell (Sharma et al., 2012). Nanoparticles have received tremendous attention as the material for the improvement of crop yield (Jain et al., 2018). Engineered nanoparticles are also used to deliver agrochemicals and nutrients in a controlled manner, which is essential for the growth improvement, facilitating efficient utilization of nutrients and disease resistance (Athanassiou et al., 2018).

Materials and Methods

Materials

S. dulcis, MS tissue culture medium, indole-3-butyric acid (IBA), butyric acid (BA), mercuric chloride, 70 % ethanol, NaOH, agar, distilled water, casein stabilized nanoparticles [silver (AgNPs), gold (AuNPs), and copper oxide (CuONPs)] were used for the study.

Synthesis of nanoparticles

All the three types of nanoparticles were synthesized by casein reduction method (Rakhimol et al., 2020). Casein was used as the reducing agent. 10ml 1M NaOH was prepared and stirred well. 0.1 g of casein and 0.01 g of precursors ($AgNO_3$, $AuCl_3$, and $CuSO_4$) were added, and the stirring was continued for 5 minutes. The solution was then incubated for 12 hours at room temperature. It was then centrifuged, and the supernatant was collected. Then, it was lyophilized and suspended in distilled water.

Characterization of nanoparticles

Nanoparticle synthesis was confirmed using UV–Vis spectroscopy, and morphology of the synthesized nanoparticles was analyzed using transmission electron microscopy.

Source of explants

Fresh, healthy, young twigs of *S. dulcis* were collected from Athirampuzha, Kottayam, Kerala and Kottarakkara, Kollam, Kerala. The plant herbarium was prepared and deposited to Regional Herbarium Kerala, Department of Botany, SB College, Changanassery; it acquired the accession number 7639.

Surface sterilization of the explants

Healthy twigs of *S. dulcis* were washed thoroughly under tap water for three to four times to remove the dust and dirt from the surfaces. Then, they were washed with 1 % soap solution for 1 minute and, finally, with water to remove the soap completely. After that, the twigs were surface sterilized using 0.1 % mercuric chloride for one minute. To remove the mercuric chloride from the surface, they were rinsed with double distilled water several times. All the glassware, forceps, and blade holders were cleaned and kept in hot air oven for preliminary sterilization followed by the sterilization under ultraviolet radiation for 20 minutes in the laminar air flow chamber.

The medium was sterilized in the autoclave and the growth hormones were added to the medium after sterilization. Hands were wiped with 70 % ethanol before the experiments (Ahloowalia et al., 2004).

Inoculation and incubation of the explants

After the surface sterilization, the twigs were transferred to a Petri dish containing filter paper, where the stems were cut into 1 cm long explants and transferred into the tubes with sterile medium containing growth hormones, using sterile forceps. The tubes were then sealed with cotton plugs and labeled. The tubes with explants were then incubated under cool white fluorescent light (1000 lux) (Annie, Jayachandran, 2008).

The phytohormones, auxin and cytokinin, were used separately and in combination for the callus, shoot, and root regeneration. Various combinations of IBA and BA were used to identify the combination of phytohormone that gave the best result. During the experiment, time taken for the callus initiation, percentage of response, and nature, color, and texture of callus were determined. The experiment was carried out with ten replicates. Fresh growth index (FGI), callus frequency, and callus index were also calculated (Kittipongpatana et al., 1998) using the following equations.

$$\text{Fresh Growth Index (FGI)} = \frac{\text{Final fresh wt} - \text{initial fresh wt}}{\text{Initial fresh wt}}$$

Callus index = Fresh growth index ×% of response

Subculture

The calluses were cut in sterile environment, sub cultured in the same medium for callus multiplication, and sub cultured in higher concentrations of IBA and BA (10–15 mg/L) for the shoot and root regenerations through indirect organogenesis.

Treatment of tissue culture medium with metal and metal oxide nanoparticles

Effects of Ag, Au, and CuO NPs in tissue culture of *S. dulcis* were determined by adding different concentrations of nanoparticles (2, 4, 6, 8, and 10 mg/L) into the tissue culture medium containing the optimum concentrations of IBA and BA for callus induction. Time taken for the callus initiation, percentage of response, nature, color and texture of callus, FGI, and callus index were determined, and the values were compared with control (callus in medium without nanoparticles). Endophytic contamination in the tissue culture medium was also detected in the nanoparticle-treated and non-treated medium within two weeks of inoculation (Khodakovskaya et al., 2013).

Statistical analysis

The values expressed are mean ±standard error. ANOVA (analysis of variance) and SPSS (statistical package for the social sciences) 10th edition software were used for the analysis of data.

Results and discussion

Even though the same casein based reduction method was used for the synthesis of AgNPs, AuNPs, and CuONPs, the three types of nanoparticles formed differed in size and shape. AgNPs and AuNPs had a spherical shape with 13.5 and 3.5 nm diameters, respectively. CuONPs were spindle shaped with 25 nm thickness (Fig. 1). Different concentrations of auxins and cytokinins were used for the callus formation of explants. Callus formation showed a good response to IBA and BA concentration of 4 mg/L, which was used in all subsequent experiments (Table 1).

The tissue culture media (MS media) containing optimum concentrations of hormones for callus formation were supplemented with different concentrations, viz. 2 mg/L, 4 mg/L,

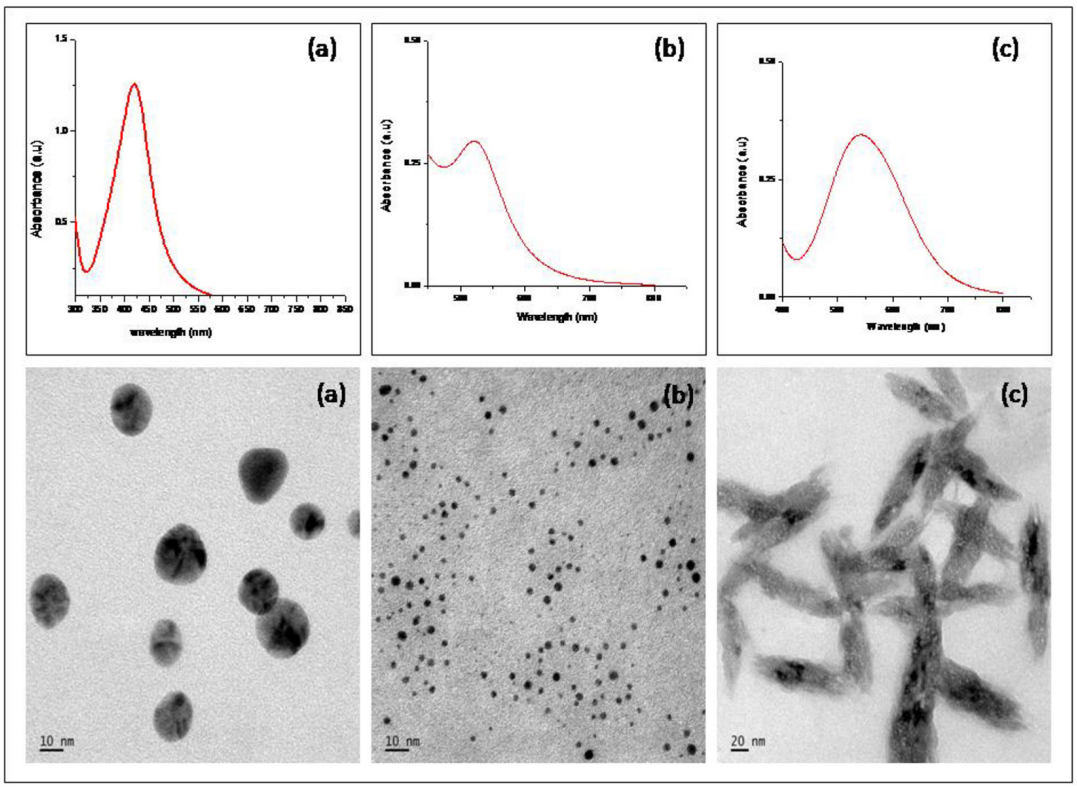

Fig. 1. UV-vis spectroscopy and TEM images of Ag NPs (a), Au NPs (b), and CuO NPs (c)

Table 1. Effect of IBA/BA on callus induction of *Scoparia dulcis* L. (CD value 5, $p<0.01$)

IBA (mg/L)	BA (mg/L)	Minimum no. of days for callus induction	% of response	FGI	Callus index	Nature of callus
1	1	20	50	9.076	453.8	Brownish green, soft, friable
1.5	1.5	20	50	26.111	1305.5	Brownish green, soft, friable
2	2	17	62	21.062	1305.8	Brownish green, soft, friable
2.5	2.5	14	60	31.666	1899.9	Brownish green, soft, friable
3	3	11	76	43.428	3300.5	Brownish green, soft, friable
3.5	3.5	11	93	44.000	4092.0	Brownish green, soft, friable
4	4	7	100	52.529	5252.9	Brownish green, soft, friable
4.5	4.5	9	100	39.309	3930.9	Brownish green, soft, friable
5	5	9	100	25.857	2585.7	Brownish green, soft, friable

and 6 mg/L, of Ag, Au and CuO nanoparticles and were kept for 30 days of incubation. The nanoparticles played a major role in the formation of callus, affecting the nature, color, and texture of callus. Of the three concentrations of nanoparticles, the 4 mg/L concentration was found to give the best results (Table 2).

The addition of the AgNPs to the tissue culture medium resulted in the formation of small, creamy, yellow callus around the explants. The callus formed was not very friable or compact. AuNPs lead to the formation of brown friable callus. However, the treatment with CuONPs resulted in the formation of embryogenic callus, which was compact and whitish green (Table 3, Fig. 2).

We found that after 45 days of incubation, the callus treated with 4 mg/L CuONPs started to form micro shoots from the embryogenic callus. It was an advantage, as the callus did not need to be transferred to a shooting medium for regeneration. 4 mg/L concentration of Ag, Au, and CuO NP showed the optimum influence on callus initiation. Callus showed a delayed and weaker response to 2 mg/L concentration of nanoparticles. At that concentration of nanoparticles, the chance of contamination was higher compared to other concentrations. The contamination was reduced as the concentration of nanoparticles was increased. However, higher concentration of nanoparticles reduced callus regeneration capacity.

Incubation of callus in the medium containing 4 mg/L of Ag, Au, and CuONPs showed that the CuONPs accelerated the shoot regeneration process, and multiple shoots were regenerated on

Table 2. Effect of Ag NPs, Au NPs, and CuO NPs on the callus formation

Nanoparticles (mg/L)		IBA/BA (mg/L)	Minimum number of days for callus induction	% of response
AgNPs	2	4/4	7	94
	4	4/4	7	100
	6	4/4	7	96
AuNPs	2	4/4	9	91
	4	4/4	7	100
	6	4/4	7	99
CuONPs	2	4/4	8	100
	4	4/4	7	100
	6	4/4	7	98

Table 3. Difference in color, texture, and nature of the callus after the treatment with nanoparticles

Treatment	Texture of callus	Color of callus	Nature of callus
Control (without nanoparticles)	Friable	Brownish green	Soft
AgNPs	Moderately friable	Creamy yellow	Soft
AuNPs	Friable	Brown	Soft
CuONPs	Compact	Whitish green	Hard

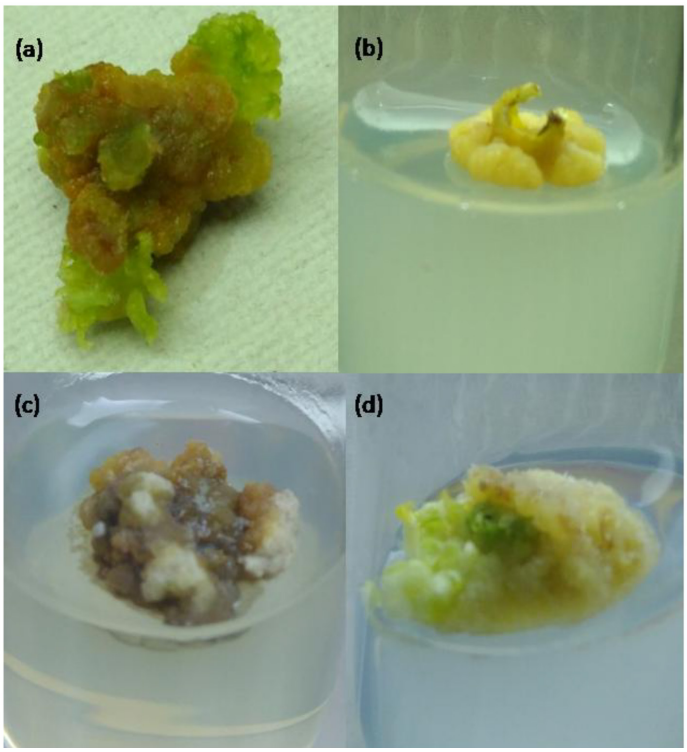

Fig. 2. Effect of Ag, Au, and CuO NPs on callus regeneration of *Scoparia dulcis* L. (a) callus formed in the medium with 4 mg/L IBA and 4 mg/L BA (control). (b) callus formed in the medium treated with AgNPs, (c) callus in the medium treated with AuNPs, (d) callus in the medium treated with CuONPs

the callus after 45 days of incubation. Initiation of root regeneration could be observed after 50 days of incubation on the same medium. 4 mg/L AgNPs also induced regeneration of shoots after 45 days of incubation. But only 2 or 3 shoots were regenerated and the shoots were not healthy. Root regeneration did not occur in these calluses. However, the callus treated with 4 mg/L Au NPs did not show any change even after 60 days of incubation (Fig. 3). It was observed that young leaflets formed from the calluses treated with both AgNPs and CuONPs showed a reduction in green color as compared to the untreated plantlets (Fig. 4). It might be due to the reduction in chlorophyll content of the nanoparticle-treated calluses. But as the plantlets were growing, they turned green. These observations suggested that the nanoparticle treatment could reduce the chlorophyll content of younger leaves only (Fig. 5).

We examined the effect of higher concentrations (8 & 10 mg/L) of synthesized nanoparticles on callus formation of *S. dulcis* explants. We found that the callus formation was low compared to 4 and 6 mg/L concentrations of nanoparticles. After 25 days of incubation, regeneration of callus stopped and blackening of callus occurred (Fig. 6). It might be because of the effect of nanoparticles on cellular metabolism of the callus.

In our study, we observed that casein stabilized metal and metal oxide nanoparticles could tune the color, texture, and nature of callus. There were many studies addressing the effect of Ag and Au NPs on seed germination (El-Temsah, Joner, 2012; Arora et al., 2012; Kumar et al., 2013) but no study was devoted to the effect of these nanoparticles on the regeneration of calluses and their morphology. The mechanism behind

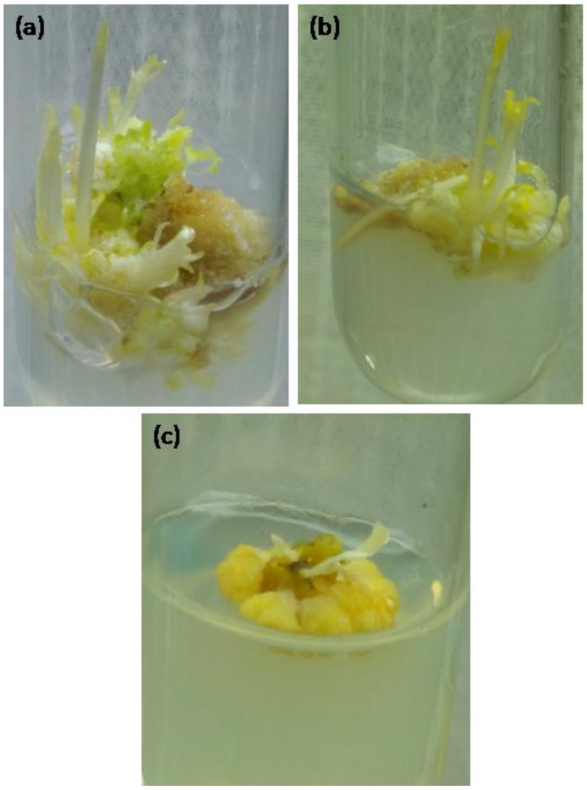

Fig. 3. Shoot and root regeneration of callus treated with nanoparticles. (a) multiple shoot regeneration of the callus treated with 4 mg/L CuONPs after 45 days of incubation, (b) root initiation of the shoots grown in the medium containing 4 mg/L CuONPs after 50 days of incubation, (c) shoot regeneration on the callus grown in medium containing 4 mg/L of AgNPs after 45 days of incubation

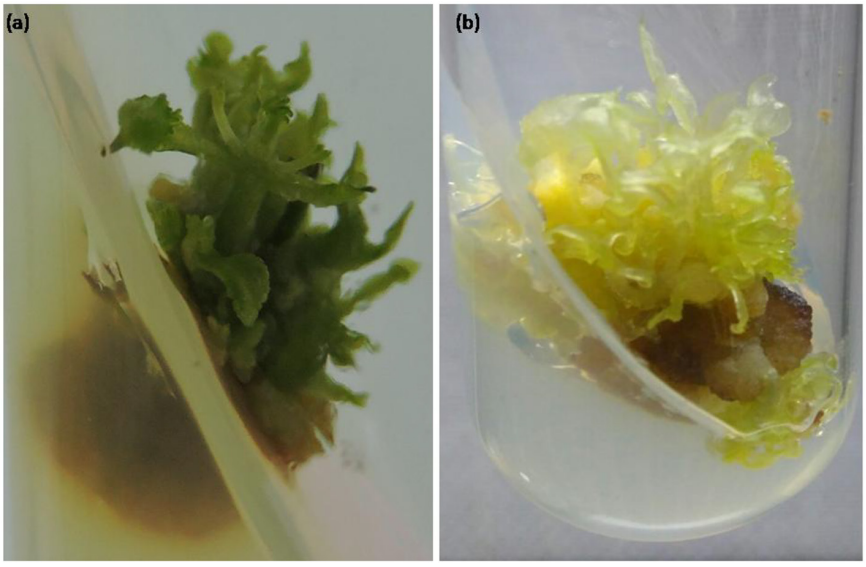

Fig. 4. Difference in the color of the shoots developed from (a) callus grown on medium without nanoparticles; (b) callus grown on medium with CuONPs

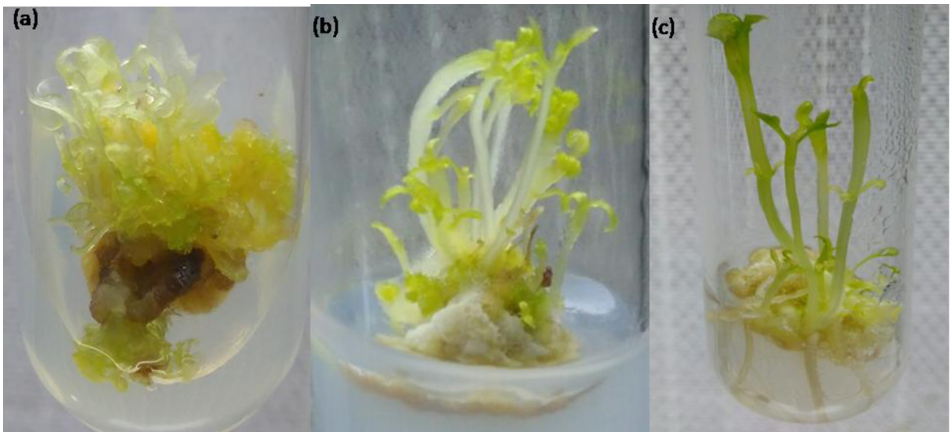

Fig. 5. (a) Reduction in the green color of plantlets grown on medium containing CuONPs (after 40 days); (b, c) Regaining of green color of the leaflet as it gets older (after 45 and 50 days, respectively)

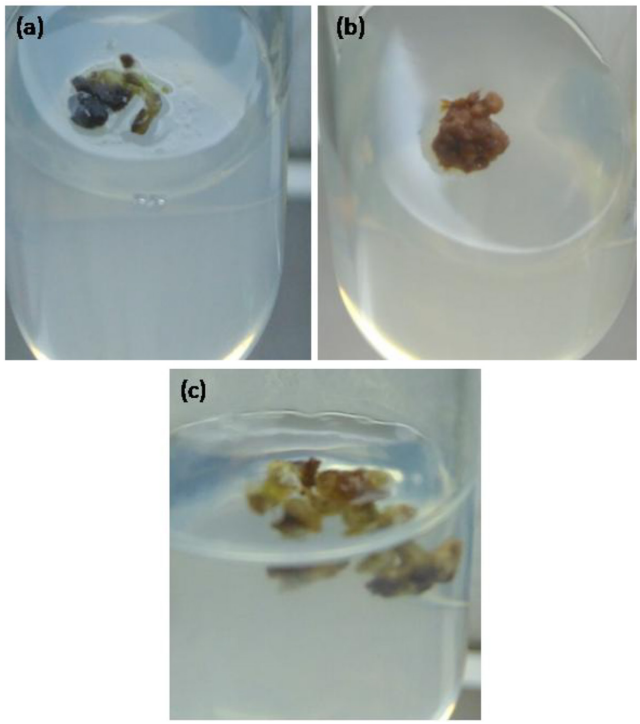

Fig. 6. Blackening of the callus grown on the medium containing 8 mg/L AgNPs (a), AuNPs (b), and CuONPs (c) after 15 days of incubation

the interaction of these metal nanoparticles with the plant tissue is unknown. Of these metal nanoparticles, CuONPs showed the greatest positive effect on the callus, shoot, and root regeneration.

Interaction of copper with plants was studied by many research teams, showing that lower concentration of copper was beneficial or essential for the growth of plants. But higher concentration of copper inhibited the growth and

metabolism of plants by the production of a large amount of oxygen free radicals, which interfered in the important cellular metabolic pathways. There was only a small difference between the minimum, optimum, and lethal concentrations of copper in the plants (Mocquot et al., 1996). Our results were also comparable with this. At 2 mg/L CuONPs, the callus formation was slow and less responsive. However, the treatment with 4 mg/L of CuONPs showed fast and productive results. At this concentration, we observed the formation of embryogenic callus within 30 days of incubation, shoot regeneration within 45 days of incubation, and root initiation within 50 days of incubation in the same medium. However, at a concentration above 4 mg/L, the response was delayed and blackening of the callus occurred at a concentration of CuONPs above 8 mg/L. Thus, the minimum concentration of the CuONPs for the response in the tissue culture medium was 2 mg/L, and the optimum and lethal concentrations were 4 mg/L and 8 mg/L, respectively. When compared with the shoots that developed in the standard tissue culture medium, the shoots grown on the medium containing CuONPs were less green. Earlier studies revealed that the chlorophyll pigment of the younger leaves may be affected by copper (Ouzounidou, 1994; Caspi et al., 1999; Zengin, Kirbag, 2007; Shakya et al., 2008; Ke et al., 2017). That might be the reason for reduction in green color in younger leaves. However, the increase in green color of the leaflets indicated that they could regain the chlorophyll content as they were growing. Higher concentration of copper had an inhibitory effect on the root elongation (Nair, Chung, 2015) but most of the studies revealed that lower concentration of copper had no effect on the rooting of shoots (Yuan et al., 2013). However, our observation clearly demonstrated that CuONPs had an important role in the rooting of the shoots by allowing the root formation without changing the auxin and cytokinin concentrations in the tissue culture medium. That was due to the unique physical and chemical properties of the CuONPs. Recent studies on Cu and CuO NPs showed an increase in the callus regeneration of the plants after the treatment with optimum concentrations (Abdel-Wahab et al., 2019; Ibrahim et al., 2019). Our findings also showed good agreement with these results. The size and shape of nanoparticles play a great role in their biological properties (Albanese et al., 2012). Spindle shape of the synthesized CuONPs may be also a reason for their excellent plantlet regeneration capacity.

The color of the callus grown on the nanoparticles changed because of the effect of nanoparticles on phenolic secretion of the callus. Studies revealed that at the higher phenolic secretion, the tissue will be browner, and the callus growth is inversely proportional to the phenolic secretion (Ozyigit, 2008; Reis et al., 2008). Our results showed a good agreement with these findings. Callus formed on the medium containing AuNPs was brownish in color with reduction in the regeneration capacity. Callus treated with CuONPs showed a very good regeneration capacity and it was whitish green in color.

All the three nanoparticles showed a dose and time dependent effect. A concentration of 4 mg/L was found to be the optimum concentration of the nanoparticles for their maximum effect. Above a particular concentration, all the nanoparticles showed a dose and time dependent toxicity on the callus. The higher concentration of nanoparticles allowed the explants to regenerate the callus for a limited period of time, but after that, they inhibited the growth and caused the blackening of the callus. Nanoparticles, along with their effect on callus formation, decreased the extent of contamination in the tissue culture medium. Explants on the tissue culture medium without nanoparticles were prone to fungal and bacterial contamination to a greater extent. Contamination

occurred after 10–15 days of inoculation of explants, confirming the presence of endophytic fungi and bacteria. However, treatment with all the three types of nanoparticles (AgNPs, AuNPs, and CuONPs) tremendously reduced the bacterial contamination, proving that the metal and metal oxide nanoparticles are also promising candidates to prevent the endophytic contamination.

Conclusion

The effect of nanoparticles on *in vitro* micro propagation of plants is a novel area of research. To the best of our knowledge, this is the first attempt to study the effect of nanoparticles on callus regeneration. Our study confirmed that the metal nanoparticles could affect the size, texture, and nature of callus. All the metal nanoparticles lead to the formation of calluses with different color, nature, and texture. Treatment of the tissue culture medium with CuONPs resulted in the shoot and root regeneration in the callus inducing medium. It will be also beneficial in the tissue culture of other plants. The action of nanoparticles depends on the size and shape of the nanoparticles used as well as the type of the plant. So, the mechanism of action of nanoparticles will vary with all these parameters. A systematic study is necessary to find out the mechanism of action of these nanoparticles on callus in the tissue culture medium.

References

Abdel-Wahab D.A., Othman N.A.R.M., Hamada A.M. (2019) Effects of copper oxide nanoparticles to Solanum nigrum and its potential for phytoremediation. *Plant Cell, Tissue and Organ Culture*, 137(3): 525–539

Ahloowalia B.S., Prakash J., Savangikar V.A., Savangikar C. (2004) Plant tissue culture. *Low cost options for tissue culture technology in developing countries. Proceedings of a Technical Meeting organized by the Joint FAO/IAEA Division of Nuclear Techniques in Food and Agriculture and held in Vienna, 26–30 August 2002*. Vienna, IAEA, p. 3–10

Albanese A., Tang P.S., Chan W.C.W. (2012) The effect of nanoparticle size, shape, and surface chemistry on biological systems. *Annual Review of Biomedical Engineering*, 14: 1–16

Annie M.J., Jayachandran K. (2008) Rapid propagation of Scoparia dulcis Linn. through leaf culture. *Research Journal of Biotechnology*, 3(2): 31–35

Arora S., Sharma P., Kumar S., Nayan R., Khanna P.K., Zaidi M.G.H. (2012) Gold-nanoparticle induced enhancement in growth and seed yield of Brassica juncea. *Plant Growth Regulation*, 66(3): 303–310

Athanassiou C.G., Kavallieratos N.G., Benelli G., Losic D., Usha Rani P., Desneux N. (2018) Nanoparticles for pest control: current status and future perspectives. *Journal of Pest Science*, 91(1): 1–15

Caspi V., Droppa M., Horváth G., Malkin S., Marder J.B., Raskin V.I. (1999) The effect of copper on chlorophyll organization during greening of barley leaves. *Photosynthesis Research*, 62(2–3): 165–174

Dagla H.R. (2012) Plant tissue culture: Historical developments and applied aspects. *Resonance*, 17(8): 759–767

El-Temsah Y.S., Joner E.J. (2012) Impact of Fe and Ag nanoparticles on seed germination and differences in bioavailability during exposure in aqueous suspension and soil. *Environmental Toxicology*, 27(1): 42–49

Ibrahim A.S., Fahmy A.H., Ahmed S.S. (2019) Copper nanoparticles elevate regeneration capacity of (Ocimum basilicum L.) plant via somatic embryogenesis. *Plant Cell, Tissue and Organ Culture*, 136(1): 41–50

Jain A., Ranjan S., Dasgupta N., Ramalingam C. (2018) Nanomaterials in food and agriculture: an overview on their safety concerns and regulatory issues. *Critical Reviews in Food Science and Nutrition*, 58(2): 297–317

Ke M., Zhu Y., Zhang M., Gumai H., Zhang Z., Xu J., Qian H. (2017) Physiological and molecular response of Arabidopsis thaliana to CuO nanoparticle (nCuO) exposure. *Bulletin of Environmental Contamination and Toxicology*, 99(6): 713–718

Khodakovskaya M. V., Kim B.-S., Kim J. N., Alimohammadi M., Dervishi E., Mustafa T., Cernigla C. E. (2013) Carbon nanotubes as plant growth regulators: effects on tomato growth, reproductive system, and soil microbial community. *Small*, 9(1): 115–123

Kittipongpatana N., Hock R. S., Porter J. R. (1998) Production of solasodine by hairy root, callus, and cell suspension cultures of Solanum aviculare Forst. *Plant Cell, Tissue and Organ Culture*, 52(3): 133–143

Kumar V., Guleria P., Kumar V., Yadav S. K. (2013) Gold nanoparticle exposure induces growth and yield enhancement in Arabidopsis thaliana. *Science of the Total Environment*, 461–462: 462–468

Mocquot B., Vangronsveld J., Clijsters H., Mench M. (1996) Copper toxicity in young maize (Zea mays L.) plants: effects on growth, mineral and chlorophyll contents, and enzyme activities. *Plant and Soil*, 182(2): 287–300

Nair P. M.G., Chung I. M. (2015) Study on the correlation between copper oxide nanoparticles induced growth suppression and enhanced lignification in Indian mustard (Brassica juncea L.). *Ecotoxicology and Environmental Safety*, 113: 302–313

Ouzounidou G. (1994) Copper-induced changes on growth, metal content and photosynthetic function of Alyssum montanum L. plants. *Environmental and Experimental Botany*, 34(2): 165–172

Ozyigit I. I. (2008) Phenolic changes during in vitro organogenesis of cotton (Gossypium hirsutum L.) shoot tips. *African Journal of Biotechnology*, 7(8): 1145–1150

Rakhimol K. R., Thomas S., Kalarikkal N., Jayachandran K. (2020) Casein mediated synthesis of stabilized metal/metal-oxide nanoparticles with varied surface morphology through pH alteration. *Materials Chemistry and Physics*, 246: 122803

Reis E., Batista M. T., Canhoto J. M. (2008) Effect and analysis of phenolic compounds during somatic embryogenesis induction in Feijoa sellowiana Berg. *Protoplasma*, 232(3–4): 193–202

Sarkar S., Guibal E., Quignard F., SenGupta A.K. (2012) Polymer-supported metals and metal oxide nanoparticles: synthesis, characterization, and applications. *Journal of Nanoparticle Research*, 14(2): 715

Shakya K., Chettri M. K., Sawidis T. (2008) Impact of heavy metals (copper, zinc, and lead) on the chlorophyll content of some mosses. *Archives of Environmental Contamination and Toxicology*, 54(3): 412–421

Sharma P., Bhatt D., Zaidi M. G.H., Saradhi P. P., Khanna P. K., Arora S. (2012) Silver nanoparticle-mediated enhancement in growth and antioxidant status of Brassica juncea. *Applied Biochemistry and Biotechnology*, 167(8): 2225–2233

Yuan H.-M., Xu H.-H., Liu W.-C., Lu Y.-T. (2013) Copper regulates primary root elongation through PIN1-mediated auxin redistribution. *Plant and Cell Physiology*, 54(5): 766–778

Zengin F. K., Kirbag S. (2007) Effects of copper on chlorophyll, proline, protein and abscisic acid level of sunflower (Helianthus annuus L.) seedlings. *Journal of Environmental Biology*, 28(3): 561–566

Journal of Siberian Federal University. Biology 2021 14(4): 510–525
~ ~ ~

DOI 10.17516/1997-1389-0368

УДК 615.46

Modern Methods and Materials for Modeling Brain Tissue and Blood-Brain Barrier *In Vitro*

Alla B. Salmina[a, b]*, Natalia A. Malinovskaya[b], Vladimir V. Salmin[b], Elena D. Khilazheva[b], Elena A. Teplyashina[b], Angelina I. Mosyagina[b] and Andrey V. Morgun[b]

[a]Research Center of Neurology
Moscow, Russian Federation
[b]Prof. V.F. Voino-Yasenetsky
Krasnoyarsk State Medical University
Krasnoyarsk, Russian Federation

Received 12.06.2021, received in revised form 20.07.2021, accepted 23.08.2021

Abstract. Neurovascular unit (NVU) is an ensemble of brain cells (cerebral endothelial cells, astrocytes, pericytes, neurons, and microglia), which regulates processes of transport through the blood-brain barrier (BBB) and controls local microcirculation and intercellular metabolic coupling. Dysfunction of NVU contributes to numerous types of central nervous system pathology. NVU pathophysiology has been extensively studied in various animal models of brain disorders, and there is growing evidence that modern approaches utilizing in vitro models are very promising for the assessment of intercellular communications within the NVU. Development of NVU-on-chip or BBB-on-chip as well as 3D NVU and brain tissue models suggests novel clues to understanding cell-to-cell interactions critical for brain functional activity, being therefore very important for translational studies, drug discovery, and development of novel analytical platforms. One of the mechanisms controlled by NVU activity is neurogenesis in highly specialized areas of brain (neurogenic niches, NNs), which are well-equipped for the maintenance of stem/progenitor cell pool and proliferation, differentiation, and migration of newly formed neuronal and glial cells. Specific properties of brain microvascular endothelial cells, particularly, high content of mitochondria, are important for establishment of vascular support in NVU and NNs. Metabolic activity of cells within NNs and NVU contributes to maintaining intercellular communications critical for the multicellular module integrity. We will discuss modern approaches to

* Corresponding author E-mail address: allasalmina@mail.ru
ORCID: 0000-0003-4012-6348 (Salmina A.); 0000-0002-0033-3804 (Malinovskaya N.); 0000-0003-4441-9025 (Salmin V.); 0000-0002-9718-1260 (Khilazheva E.); 0000-0001-7544-3779 (Teplyashina E.); 0000-0002-9644-5500 (Morgun A.)

development of optimal microenvironment for in vitro BBB, NVU and NN models with the special focus on neuroengineering and bioprinting potentials.

Keywords: brain, in vitro blood-brain barrier model, brain-on-chip models, scaffold.

Acknowledgements. The work was supported by Grant No. НШ-2547.2020.7, awarded by the President of Russian Federation for Russian Leading Research Teams, by the State Assignment for Research (Ministry of Public Health, Russian Federation, 2018–2020), and by Grant No. МД-3923.2019.7, awarded by the President of Russian Federation for Young Doctors of Sciences.

Citation: Salmina A. B., Malinovskaya N. A., Salmin V. V., Khilazheva E. D., Teplyashina E. A., Mosyagina A. I., Morgun A. V. Modern methods and materials for modeling brain tissue and blood-brain barrier *in vitro*. J. Sib. Fed. Univ. Biol., 2021, 14(4), 510–525. DOI: 10.17516/1997-1389-0368

Современные методы и материалы моделирования тканей мозга и гематоэнцефалического барьера *in vitro*

А. Б. Салмина[а, б], Н. А. Малиновская[б], В. В. Салмин [б], Е. Д. Хилажева[б], Е. А. Тепляшина[б], А. И. Мосягина[б], А. В. Моргун[б]

[а]Научный центр неврологии
Российская Федерация, Москва
[б]Красноярский государственный медицинский университет им. проф. В. Ф. Войно-Ясенецкого
Российская Федерация, Красноярск

Аннотация. Нейроваскулярная единица (НВЕ) – это совокупность клеток головного мозга (церебральные эндотелиальные клетки, астроциты, перициты, нейроны, микроглия), которые регулируют процессы транспорта через гематоэнцефалический барьер (ГЭБ), контролируют местную микроциркуляцию, межклеточную метаболическую связь. Дисфункция НВЕ способствует возникновению многих типов патологии центральной нервной системы. Патофизиология НВЕ широко изучена на различных моделях заболеваний мозга на животных. В настоящее время появляется все больше свидетельств того, что современные подходы с использованием моделей in vitro наиболее перспективны для оценки межклеточных коммуникаций внутри НВЕ. Разработка сосудисто-нервных единиц на чипе или ГЭБ на чипе, а также 3D НВЕ и модели ткани мозга обеспечивают новые подходы к пониманию межклеточных взаимодействий, критических для функциональной активности мозга, поэтому они очень важны для трансляционных исследований, открытия лекарств и создания новых аналитических платформ. Одним из механизмов, который контролируется активностью НВЕ, является нейрогенез в узкоспециализированных областях

мозга (нейрогенные ниши, НН), которые служат источником для поддержания пула стволовых/прогениторных клеток, пролиферации, дифференциации и миграции новообразованных нейронов и глиальных клеток. Специфические свойства эндотелиальных клеток микрососудов головного мозга, в частности высокое содержание митохондрий, важны для создания сосудистой поддержки при НВЕ и НН. Метаболическая активность клеток внутри НН и НВЕ способствует поддержанию межклеточных коммуникаций, критически важных для целостности многоклеточного модуля. В работе обсуждаются современные подходы к разработке оптимальной микросреды для in vitro моделей ГЭБ, НВЕ и НН. Особое внимание уделено перспективам нейроинженерии и биопечати.

Ключевые слова: мозг, модель гематоэнцефалического барьера in vitro, модели «мозг на чипе», каркас.

Благодарности. Работа была поддержана Грантом № НШ-2547.2020.7, присужденным Президентом Российской Федерации Ведущим научным коллективам России, Государственным заданием на исследования (Министерство здравоохранения Российской Федерации, 2018–2020) и Грантом № МД-3923.2019.7, присужденным Президентом Российской Федерации молодым докторам наук.

Цитирование: Салмина, А. Б. Современные методы и материалы моделирования тканей мозга и гематоэнцефалического барьера *in vitro* / А. Б. Салмина, Н. А. Малиновская, В. В. Салмин, Е. Д. Хилажева, Е. А. Тепляшина, А. И. Мосягина, А. В. Моргун // Журн. Сиб. федер. ун-та.Биология, 2021. 14(4). С. 510–525. DOI: 10.17516/1997-1389-0368

Introduction

Current achievements in neurobiology and biotechnology brought us novel approaches to deciphering the mechanisms underlying brain activity. Growing evidence indicates that application of new protocols of brain tissue reconstruction in vitro might shed light on molecular and cellular events determining the phenomenon of brain plasticity. Development of in vitro brain-on-chip models, in vitro blood-brain barrier models, or cerebral organoids leads to significant progress in basic, translational, and clinical neurosciences (Kilic et al., 2016; Bang et al., 2019).

In vitro brain tissue models suitable for application in pharmacology, toxicology, stem cell research, etc., should be based on the minimally acceptable functionally competent brain unit called the neurovascular unit (NVU) (Muoio et al., 2014). The NVU is an ensemble of brain cells (cerebral endothelial cells, astrocytes, pericytes, neurons, and microglia), which regulates processes of transport through the blood-brain barrier (BBB) and controls local microcirculation and intercellular metabolic coupling. It is commonly accepted that dysfunction of NVU contributes to numerous types of central nervous system pathology including brain ischemia, neurodegeneration, neurodevelopmental disorders, depression, epilepsy, etc. (Iadecola, 2017; McConnell et al., 2017). Such changes are usually associated with the impairment of astroglia-driven metabolic regulation of neuronal and endothelial cells, cell-to-cell communications, development of neuroinflammation, and BBB breakdown (Tohidpour et al., 2017; Salmina et al., 2021). NVU pathophysiology has been extensively studied in various animal models of brain disorders, and there is growing evidence that modern approaches utilizing in vitro models are very promising in the assessment of intercellular communications within the NVU.

Multiple in vitro NVU and BBB models are currently available in 2D format (NVU on a dish or plate), 3D format (transwell system with inserts covered with permeable membranes; hydrogel-embedded models, etc.), or in microfluidic format (systems with more or less complex architecture of the chip allowing establishment of cell perfusion and reproduction of changes in BBB cells induced by fluid rheology, i. e. shear stress or reactive oxygen species production in endothelial cells) (Salmina et al., 2021). For example, microfluidic/microphysiological systems have been created to reproduce different brain tissue compartments: blood, brain, and cerebral spinal fluid (Alcendor et al., 2013). Moreover, recent years brought us new models based on cerebral organoids obtained from induced pluripotent cells (Jeong et al., 2020), which offer new approaches to constructing brain-on-chip or neurogenic niche-on-chip models.

Development of NVU-on-chip or BBB-on-chip and 3D NVU and brain tissue models suggests novel clues to understanding cell-to-cell interactions critical for brain functional activity, being therefore very important for translational studies, drug discovery, and development of novel analytical platforms (Alcendor et al., 2013; Maoz et al., 2018; Bhalerao et al., 2020). The chips used for NVU and BBB modeling are made from polydimethylsiloxane (PDMS), collagen, gelatin, fibrin, polycarbonate, polypropylene, polycaprolactone/graphene, polylactic acid, etc. (Osipova et al., 2018; Bhalerao et al., 2020; Mantecón-Oria et al., 2020). The main idea of choosing the material for a model is to mimic the extracellular matrix properties critical for NVU functions (basement membrane in the case of BBB), that is why numerous materials have been already tested for their compatibility with NVU/BBB cells. For instance, porous polycaprolactone/poly (D, L-lactide-co-glycolide) (PCL/PLGA) microfluidic perfusion system was shown to serve as a vasculature network, and other types of NVU cells were co-cultured in a collagen matrix wrapping the vasculature network to produce the vascularized neural construct (Yue et al., 2020). Some models allow reproducing the gradient of molecules regulating cell development or proliferation, i. e. lactate embedded into photopolymerized gelatin scaffolds, as we showed before (Salmin et al., 2017). In other cases, microarchitecture of channels within the chip allows separating different parts of cells, i. e. neuronal soma and axon; therefore, more accurate modulation of cell activity can be performed (Bang et al., 2019).

The past decade opened new opportunities in modeling the brain tissue in vitro. Development of isogenic NVU/BBB models from induced pluripotent stem cells (iPSCs) might be useful for the generation of personalized brain tissue models suitable for diagnostic and therapeutic properties (Canfield et al., 2019). Application of 4D bioprinting promises novel approaches to reconstructing some elements of activity-dependent or stimuli-induced brain plasticity in vitro (Esworthy et al., 2019; Warren et al., 2021). However, modern in vitro NVU/BBB models have some technical difficulties that should be overcome. For example, obvious advantages of microfluidic in vitro NVU/BBB models like reproduction of «blood and cerebrospinal fluid flow» or achievement of higher integrity of the brain microvascular endothelial cells (BMECs) monolayer are diminished by another problem: culturing of NVU cell types on microfluidic chips changes their gene expression profiles caused by aberrant surface-to-volume ratios and substrate materials, as it was shown recently (Middelkamp et al., 2021). iPSCs-derived endothelial cells exhibited compromised expression pattern (Lu et al., 2021) and might be not applicable for the current BBB studies. Thus, to study the mechanisms that control functional competence

of NVU/BBB cells is of great importance for neurobioengineering and neurobiotechnology.

In general, placement of BBB cells in a transwell, hydrogel-based, or microfluidic platforms results in the formation of cell layers whose functional competence would depend on the combination of various factors: availability of nutrients and oxygen, preserved expression pattern of ion channels, transporters, enzymes, transcription factors and other signaling molecules, and the presence of regulatory growth factors and cytokines in the medium. Structural and functional integrity of the BBB could be further assessed using different approaches like measurement of the transendothelial electric resistance (to ensure establishment of integral barrier), analysis of metabolite levels in the extracellular space in different compartments of the model, and evaluation of the barrier permeability with easily identified compounds or complexes (i. e. Lucifer yellow, dextrans, liposomes, fluoresceins, and labeled xenobiotics) (Alcendor et al., 2013).

General characterization of functional and metabolic status of NVU

Identification of NVU as a self-supporting module in the brain means the association of all events recorded in it with changes in local microcirculation or permeability of the BBB (Fig. 1). In modern neurobiology, this is interpreted as the occurrence of several important (patho) physiological phenomena:

1) neuron-astroglial metabolic coupling: activated neurons stimulate astrocytes as glycolytically active cells that produce lactate, which is utilized by neurons, converted into pyruvate, and used in the Krebs' cycle to further ensure the operation of the mitochondrial electron transport chain (Mangia et al., 2009; Descalzi et al., 2019);

2) gliovascular control: an increase in the local concentration of extracellular lactate as a product of astrocytic metabolic activity leads to vasodilation needed for efficient oxygen supply in active brain regions (Mendrinos et al., 2008);

3) metabolic control of cerebral endothelial cells by pericytes and perivascular astroglia, enabling a change in the permeability (paracellular and transcellular) of the BBB, for the formation of a microenvironment in the tissue, which promotes the functional activity of neurons (Salmina et al., 2019);

4) mechanisms implying a local increase in the BBB permeability in the brain tissue, for instance, in neuroinflammation (associated

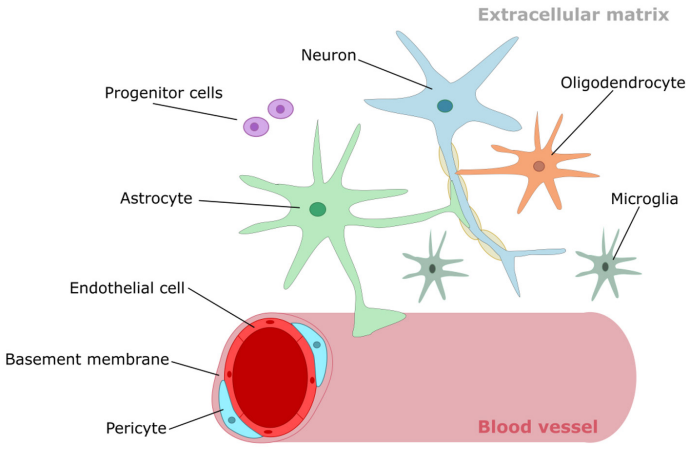

Fig. 1. Structure and composition of the neurovascular unit and the blood-brain barrier

with glial cells polarization), in neurogenesis (in neurogenic niches supporting the survival of neuronal stem and progenitor cells, or their activation followed by proliferation, differentiation, and migration), or in cerebral angiogenesis (based on the recruitment of endothelial progenitor cells and development of new vessels in active or affected brain regions) (Salmina et al., 2014; Tohidpour et al., 2017).

All of the above phenomena are based on quick and significant changes in the metabolic status of NVU/BBB cells, which are not studied in detail; however, the most critical characteristics of NVU cells should be taken into consideration when multicellular ensembles are going to be established in vitro.

BMECs are characterized by a higher content of mitochondria compared with endothelial cells in extra-brain localization; however, in a «resting» state, the main source of energy for them is glycolysis. Both glycolysis and oxidative phosphorylation (OXPHOS) are activated by pro-angiogenic stimuli in reparative cerebral angiogenesis or in activity-mediated cerebral angiogenesis (Malinovskaya et al., 2016). In addition, enhanced utilization of fatty acids further increases energy production in activated BMECs to support cell proliferation (Potente, Carmeliet, 2017). Disturbances in the glycolytic and mitochondrial activity of endothelial cells in cerebral microvessels lead to suppression of the angiogenic program and BBB breakdown and, presumably, disrupt the mechanisms of gliovascular control in the NVU (Chaitanya et al., 2014; Yetkin-Arik et al., 2019). Endothelial cells can respond to extracellular lactate of astroglial or peripheral origin due to expression of receptors for cell-derived lactate (GPR81 receptors) and monocarboxylate transporters (MCT), which ensure the uptake and release of lactate through the cell membrane. Alterations in GPR81 or MCT expression are usually associated with BBB leakage and aberrant astrocyte-endothelial interactions, for instance, in neuroinflammation (Boitsova et al., 2018). Furthermore, disturbances in mitochondrial dynamics in endothelial cells (fusion and fission of mitochondria, mitochondrial biogenesis, and mitophagy) contribute to diminished angiogenesis and development of endothelial dysfunction (Shenouda et al., 2011; Xiang et al., 2021). In addition to excessive energy-producing metabolism, mitochondria in BMECs contribute substantially to generation of reactive oxygen species, which are considered now not only as inducers of oxidative stress, but also as cell signaling species (Itoh et al., 2006; Zhang, Gutterman, 2007). Moreover, endothelial cells are equipped with NADPH-oxidases (NOX), including dual oxidases (DUOX), which are the major sources of hydrogen peroxide and reactive oxygen species negatively affecting BBB permeability, but which might be also required in low concentrations to maintain the resistance of cerebral endothelium to the harmful effects of bacteria and viruses (Cahill-Smith, Li, 2014; Carvalho, Moreira, 2018; Anasooya Shaji et al., 2019). Another population of NOX-expressing cells in the NVU/BBB is represented by pericytes: their NOX4 plays an important role in supporting proliferative activity, which is necessary for angiogenesis and barriergenesis (Kuroda et al., 2014). In general, pericytes largely depend on their own glycolytic activity rather than on mitochondrial respiration. However, during hypoxia, pericytes can become glucose donors or even mitochondria donors for damaged perivascular astroglia (Trudeau et al., 2011; Salmina et al., 2019).

Perivascular astroglia, which is in close contact with BMECs and pericytes and with NVU neurons, is characterized by extremely high glycolytic activity and lactate production needed for efficient neuron-astrocyte metabolic coupling (Salmina et al., 2015). Release of lactate from

astrocytes ensures local hyperemia in active brain regions and supports neuronal ATP production via rapid conversion of lactate to pyruvate and acetyl-CoA in activated neurons. It is generally accepted that astrocytes are able to accumulate glycogen to quickly provide themselves and other NVU cells with glucose in the event of an insufficient supply of glucose from the blood (Matsui et al., 2017). Lactate produced by astrocytes is captured by neurons and utilized for mitochondrial activity; this is ensured by expression of MCTs for lactate and pyruvate in almost all of NVU cells, which support the influx and efflux of metabolites depending in the current needs of cells (Salmina et al., 2015). In addition to glycolytic activity, astrocytes can maintain their OXPHOS for a long time, even under unfavorable conditions, and even serve as donors of mitochondria for damaged neurons, for instance, in severe brain ischemia (Hayakawa et al., 2016). Suppression of mitochondrial activity in astrocytes leads to disruption of the mechanism of capture of excess glutamate supplied to the extracellular space by activated neurons, resulting in the development of excitotoxicity and neuronal death (Volobouеva et al., 2007).

Neurons have been traditionally considered as cells whose activity is mainly determined by mitochondrial energy production. The maximum number of mitochondria are concentrated in neurons in the perisynaptic zone, thereby reflecting the high demand of ATP and mitochondria-provided Ca2+ handling for synaptic neurotransmission and plasticity (Lee et al., 2018). Disruption of mitochondrial activity in neurons is an essential component of ischemia, brain damage, and chronic neurodegeneration, and modulation of mitochondrial dynamics is rather beneficial for the restoration of neurological deficits (Motori et al., 2020). Being stimulated, neurons are able to increase the production of ATP due to glycolysis and even to transfer excess lactate to other NVU cells (Díaz-García et al., 2017).

Microglia are characterized by complex metabolism affected by glia polarization: activated microglial cells depend on glycolytic ATP production rather than mitochondrial respiration. Activation of microglia promotes the assembly of intracellular inflammasomes and the expression of redox enzymes (NOX) involved in the generation of reactive oxygen species. Therefore, conversion of resting microglia to activated ones is accompanied by fragmentation of mitochondria followed by release of fragmented mitochondria to trigger astroglial activation and propagation of inflammation (Joshi et al., 2019). However, excessive production of reactive oxygen species facilitates elongation of mitochondria and might significantly affect mitochondrial dynamics (Katoh et al., 2017).

Oligodendrocytes are predominantly glycolytically active cells. They consume glucose and lactate during myelination, and glycolysis begins to dominate over the mitochondrial respiration soon after completion of the myelination program, probably to prevent excessive generation of reactive oxygen species in active mitochondria (Fünfschilling et al., 2012). Expression of the MCT in oligodendrocytes is necessary for axonal maintenance, therefore oligodendroglia-derived lactate is important for preventing axonal dystrophy (Fünfschilling et al., 2012).

Metabolic plasticity of NVU cells depends on extracellular matrix (ECM), particularly, in the case of BBB, and the basement membrane (BM) composition and porosity affect energy metabolism of cells. BM consists of several types of ECM proteins: collagen IV, laminin, nidogen, collagen XVIII, matrix metalloproteinases (MMPs), growth factors (i. e. VEGF) and cytokines, thrombospondins, fibronectins, lectins, etc. It has a thickness up to 200 nm and

numerous pores with the diameter from 5 nm to 8 μm (McConnell et al., 2017; Logsdon et al., 2021). In the parts of BMECs non-covered with pericytes, the BM contacts directly with perivascular astroglia and endothelial monolayer (McConnell et al., 2017). NVU cells are sensitive to BM and ECM composition, but the sensitivity mechanisms differ from each other. Very recent findings suggest that ECM may affect mitochondrial dynamics in adjacent cells: ECM stiffening promotes mitochondrial fusion and suppresses mitochondrial fission in a DRP1-dependent manner (Chen et al., 2021). This might be due to sensing of ECM composition by intracellular mitochondria connected via cytoskeletal proteins (De Cavanagh et al., 2009). Another type of functional coupling between ECM/BM and NVU cell metabolism is based on CD147 activity. CD147 (basigin) is expressed in neuronal, glial, and endothelial cells, and it promotes MMPs activation and amyloid precursor protein (APP) proteolysis due to functional association with gamma-secretase (Uspenskaya et al., 2018). Therefore, it is not surprising that aberrant expression of CD147 in NVU cells accompanies pathologically enhanced cerebral angiogenesis, development of neuroinflammation, and BBB breakdown in experimental Alzheimer's disease (Morgun et al., 2020). At the same time, CD147 regulates lactate transport associated with MCT transporters in the NVU (Uspenskaya et al., 2018). Therefore, activation of CD147 would result either in MMPs-mediated degradation of ECV/BM and loss of BBB integrity or in the activation of MCT1-, MCT4-mediated lactate and H+ efflux from glycolytically active cells (Kirk et al., 2000), presumably leading to prevention of intracellular accumulation of lactate and H+. The latter might be important either for lactate-driven changes in local microcirculation or for maintaining high level of glycolysis and NVU cell proliferation. It should be taken into consideration that ECM and BM composition is greatly affected in brain diseases, i. e. in Alzheimer's type neurodegeneration (Thomsen et al., 2017). Therefore, application of BM analogues in the in vitro models of NVU/BBB/neurogenic niches (NN) could be inaccurate in reconstructing the impairments specific for the brain pathology.

Thus, in NVU/BBB in vitro models, cell metabolic activity should be supported with the optimal microenvironment, including soluble factors in media, and composition of ECM/BM or their analogues. Are these conditions fulfilled in the current in vitro models? It has now become clear that reproduction of the microenvironment supportive for efficient metabolic interactions between NVU/BBB cells could be achieved in rather complex systems like those based on 2 or more compartments, or in microfluidic chambers. For instance, in 3 coupled chips developed by (Maoz et al., 2018), mechanisms of influx across the blood–brain barrier (BBB) and to the brain parenchymal compartment and efflux across the BBB have been successfully reproduced. In that system, the BBB chip contained BMECs and pericytes, the brain chip contained mixed population of primary neural cells (dopaminergic, serotoninergic, GABAergic etc.), and in the coupled NVU chip, an endothelial medium (artificial blood) was placed to flow across the BBB chip, while neuronal medium (artificial cerebral spinal fluid) flowed through the perivascular compartment. The authors were able to develop functionally competent BBB and to preserve some parts (glycolysis, TCA, synthesis of GABA) of the linked metabolism of NVU cells, as it was confirmed by metabolomics (Maoz et al., 2018). Another approach was reported in (Huang et al., 2020), where a simpler system, made of primary astrocytes and BMECs, was used to get metabolomic profiling of endothelial cells in hypoxia. The authors demonstrated that astrocytes have greater capacity to rapidly

respond to the environmental stress whereas BMECs keep their metabolic activity at the baseline level and do not activate anaerobic ATP production, presumably to maintain the barrier intact. Therefore, BMECs appear to be more «metabolically rigid» compared to astrocytes in the NVU (Huang et al., 2020).

Cerebral organoids, which in recent years have been widely used to study brain activity and development, can be also considered as an in vitro NVU model. Development of brain region-specific cerebral organoids and assembloids (complex of various organoids) is a new step in the advancement of this technology (Jeong et al., 2020). However, there are some significant problems in the application of organoid models into translational studies. Actually, metabolism of cells within organoids is greatly compromised due to the absence of vessels (endothelial progenitor cells are not produced simultaneously with neuronal and glial cells because of their different origin). Therefore, the core cells within the organoids undergo hypoxic alterations leading to mitochondrial dysfunction, apoptosis, and necrosis. Recent attempts at the development of vascularized organoids, i. e. based on iPSCs-derived BMECs, offer new opportunities in the construction of personalized BBB-on-chip models since these cells show some characteristics of BBB cells (Cakir et al., 2019; Kumarasamy, Sosnik, 2021).

Angiogenesis and neurogenesis at the NVU

As we have shown above, NVU cells effectively cooperate and support each other in their metabolic needs, particularly when they are activated. Two general plastic processes in the developing and adult brain – neurogenesis and angiogenesis – closely associate at the level of NVU (Sawada et al., 2014), and their efficacy depends on the integrity of NVU metabolism (Fig. 2).

It is well-known that in rodents, development of BBB begins at E10–17, the controlled permeability is formed by E21, but the development of tight junction machinery in BMECs continues even in the postnatal period.

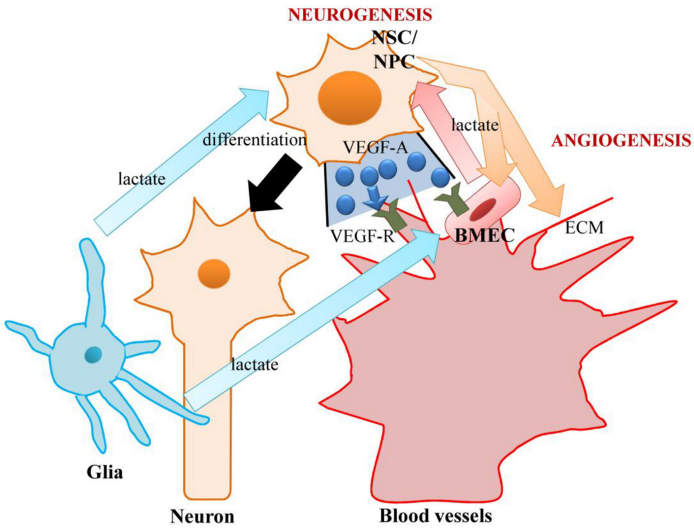

Fig. 2. Association of neurogenesis and angiogenesis at the level of neurovascular unit. Abbreviations: BMEC – brain microvessel endothelial cell, NSC – neural stem cell, NPC – neural progenitor cell, VEGF-A – vascular endothelial growth factor, VEGFR – VEGF receptor, ECM – extracellular matrix

In humans, BBB markers appear at the 8th week of embryogenesis, however, barriergenesis lasts up to 2–3 weeks of postnatal development (Malaeb et al., 2012). The most important point is that prenatal and early postnatal barriergenesis begins only after the establishment of the pool of neural stem cells (NSCs)/neural progenitor cells (NPCs) in the developing brain, and vascular and neural structures develop and mature simultaneously (Paredes et al., 2018). Molecules produced by developing immature neural cells stimulate specific patterning of sprouting capillaries and induce BBB characteristics in early BMECs (James, Mukouyama, 2011). Within the NVU, neuronal and astroglial cells affect angiogenesis in different modes. Specifically, loss of astroglial coverage results in excessive angiogenesis in the early postnatal brain (Ma et al., 2012). Thus, cerebral angiogenesis at the earliest stages of brain development tightly couples to synaptic activity and remodeling (Su et al., 2020). And vice versa, the germinal zone vasculature in the embryonic brain controls the balance between NPC self-renewal and production of new neurons irrespective of the oxygen-supplying ability of vessels (Tata et al., 2016). So, it is not surprising that the similar phenomenon is – at least partially – reproduced in the adult brain: functional activity of cells within the neurogenic niches (subventricular zone, SVZ, and subgranular zone, SGZ) depends on the preservation of vascular scaffold and local BBB permeability (high in the SVZ and low in the SGZ) (Pozhilenkova et al., 2017). In brain ischemia, loci with enhanced BBB permeability serve as multiple newly-established neurogenic niches along the ventricular system of the brain (Lin et al., 2015). The same outcome might be achieved by treatments affecting BBB integrity, i. e. transcranial focused ultrasound-induced reversible BBB breakdown stimulates hippocampal neurogenesis (Mooney et al., 2016).

How can the concept of tightly coupled neurogenesis and angiogenesis/barriergenesis be implemented in NVU modeling? Actually, the basic idea is to construct the reliable in vitro model of the neurogenic niche with the vascular support (Winkelman et al., 2021). In this context, appropriate ECM would greatly affect the reliability of the model since it was demonstrated that ECM composition controls self-renewal and prologeration of stem cells (Guilak et al., 2009). Application of various materials in the microfluidic models allowed identifying the most suitable conditions for integrating neurogenesis and angiogenesis: matrigel mixed gel promoted NSC differentiation into neurons, whereas capillary-like structures were formed in the fibrin-matrigel mixed gel by co-culturing BMECs and human mesenchymal stem cells (MSCs); then, a 3D NVU model, as a triculture system made of NSCs, BMECs, and MSCs, was constructed from neural and vascular compartments in the microfluidic device (Uwamori et al., 2017). Another approach was demonstrated in the spheroid BBB model: chitosan- or gelatin-based substrates were used to generate the 3D NSC/BMEC co-spheroids with pro-angiogenic potential (Han et al., 2019). We demonstrated that neurogenic activity of NSCs co-cultured with astrocytes and BMECs within the NN in vitro model implanted into hippocampus could be efficiently regulated by optogenetic stimulation of ChR2-expressing astroglia (Morgun et al., 2021).

The next step in the development of in vitro NN models is their application in regenerative neurology. Thus, considerable research has focused on bioprinting potential of NVU/NN models and cerebral organoids. One of the biggest challenges in this field is to create the «building blocks» that would resemble the structure of the real NVU or NN, and this depends on the availability of new materials as substituents of the ECM/BM (Potjewyd et al., 2018). The

following biomaterials are now tested for NVU/NN scaffolds in the context of 3D bioprinting technology: collagen, gelatin, fibrin, hyaluronan, and PEG (Potjewyd et al., 2018). Their physical and chemical properties can be modified via cross-linking, introduction of some modifying agents, or changing the porosity and stiffness. For instance, the presence of specific amino acid sequences (Arg–Gly–Asp (RGD) and Ile–Lys–Val–Ala–Val (IKVAV)) is important for integrin and laminin functions within the NVU ECM or BBB BM (Potjewyd et al., 2018). Decellularized natural ECM can be used for in vitro NVU and BBB modeling, particularly, for the development of vascular support of stem cell differentiation (Hoshiba et al., 2016), whereas poly-lactic acid-based scaffolds provide metabolic support of cells, particularly, for astrocytes (Pavia et al., 2019). Anyway, the technology of 3D and 4D bioprinting is a promising tool for NVU/BBB/NN and whole brain tissue modeling (Fantini et al., 2019).

Conclusion

Despite the huge number of in vitro NVU/BBB models available at present, no physiologically realistic one has been constructed yet. All the models that are currently in use have significant limitations, mainly associated with the apparent difficulties in achieving the controlled and tunable microenvironmental conditions that could support the activity of NVU cells and mimic brain plasticity. Once this issue has been resolved, there will be considerable progress in the development of in vitro models suitable for personalized testing of drug candidates, studying the molecular mechanisms of brain development and function, developing neuromorphic systems, and using 3D bioprinting protocols in basic, translational, and clinical studies.

References

Alcendor D. J., Block Iii F. E., Cliffel D. E., Daniels J. S., Ellacott K. L. J., Goodwin C. R., Hofmeister L. H., Li D., Markov D. A., May J. C., McCawley L. J., McLaughlin B., McLean J. A., Niswender K. D., Pensabene V., Seale K. T., Sherrod S. D., Sung H.-J., Tabb D. L., Webb D. J., Wikswo J. P. (2013) Neurovascular unit on a chip: implications for translational applications. *Stem Cell Research & Therapy*, 4(1): S18

Anasooya Shaji C., Robinson B. D., Yeager A., Beeram M. R., Davis M. L., Isbell C. L., Huang J. H., Tharakan B. (2019) The tri-phasic role of hydrogen peroxide in blood-brain barrier endothelial cells. *Scientific Reports*, 9(1): 133

Bang S., Jeong S., Choi N., Kim H. N. (2019) Brain-on-a-chip: A history of development and future perspective. *Biomicrofluidics*, 13(5): 051301

Bhalerao A., Sivandzade F., Archie S. R., Chowdhury E. A., Noorani B., Cucullo L. (2020) In vitro modeling of the neurovascular unit: advances in the field. *Fluids and Barriers of the CNS*, 17(1): 22

Boitsova E. B., Morgun A. V., Osipova E. D., Pozhilenkova E. A., Martinova G. P., Frolova O. V., Olovannikova R. Y., Tohidpour A., Gorina Y. V., Panina Y. A., Salmina A. B. (2018) The inhibitory effect of LPS on the expression of GPR81 lactate receptor in blood-brain barrier model in vitro. *Journal of Neuroinflammation*, 15(1): 196

Cahill-Smith S., Li J.-M. (2014) Oxidative stress, redox signalling and endothelial dysfunction in ageing-related neurodegenerative diseases: a role of NADPH oxidase 2. *British Journal of Clinical Pharmacology*, 78(3): 441–453

Cakir B., Xiang Y., Tanaka Y., Kural M. H., Parent M., Kang Y.-J., Chapeton K., Patterson B., Yuan Y., He C.-S., Raredon M. S.B., Dengelegi J. (2019) Engineering of human brain organoids with a functional vascular-like system. *Nature Methods*, 16(11): 1169–1175

Canfield S. G., Stebbins M. J., Faubion M. G., Gastfriend B. D., Palecek S. P., Shusta E. V. (2019) An isogenic neurovascular unit model comprised of human induced pluripotent stem cell-derived brain microvascular endothelial cells, pericytes, astrocytes, and neurons. *Fluids and Barriers of the CNS*, 16(1): 25

Carvalho C., Moreira P. I. (2018) Oxidative stress: a major player in cerebrovascular alterations associated to neurodegenerative events. *Frontiers in Physiology*, 9: 806

Chaitanya G. V., Minagar A., Alexander J. S. (2014) Neuronal and astrocytic interactions modulate brain endothelial properties during metabolic stresses of in vitro cerebral ischemia. *Cell Communication and Signaling*, 12(1): 7

Chen K., Wang Y., Deng X., Guo L., Wu C. (2021) Extracellular matrix stiffness regulates mitochondrial dynamics through PINCH-1- and kindlin-2-mediated signalling. *Current Research in Cell Biology*, 2: 100008

De Cavanagh E. M., Ferder M., Inserra F., Ferder L. (2009) Angiotensin II, mitochondria, cytoskeletal, and extracellular matrix connections: an integrating viewpoint. *American Journal of Physiology-Heart and Circulatory Physiology*, 296(3): H550-H558

Descalzi G., Gao V., Steinman M. Q., Suzuki A., Alberini C. M. (2019) Lactate from astrocytes fuels learning-induced mRNA translation in excitatory and inhibitory neurons. *Communications Biology*, 2(1): 247

Díaz-García C.M., Mongeon R., Lahmann C., Koveal D., Zucker H., Yellen G. (2017) Neuronal stimulation triggers neuronal glycolysis and not lactate uptake. *Cell Metabolism*, 26(2): 361–374.e4

Esworthy T. J., Miao S., Lee S.-J., Zhou X., Cui H., Zuo Y. Y., Zhang L. G. (2019) Advanced 4D-bioprinting technologies for brain tissue modeling and study. *International Journal of Smart and Nano Materials*, 10(3): 177–204

Fantini V., Bordoni M., Scocozza F., Conti M., Scarian E., Carelli S., Di Giulio A. M., Marconi S., Pansarasa O., Auricchio F., Cereda C. (2019) Bioink composition and printing parameters for 3D modeling neural tissue. *Cells*, 8(8): 830

Fünfschilling U., Supplie L. M., Mahad D., Boretius S., Saab A. S., Edgar J., Brinkmann B. G., Kassmann C. M., Tzvetanova I. D., Möbius W., Diaz F., Meijer D. (2012) Glycolytic oligodendrocytes maintain myelin and long-term axonal integrity. *Nature*, 485(7399): 517–521

Guilak F., Cohen D. M., Estes B. T., Gimble J. M., Liedtke W., Chen C. S. (2009) Control of stem cell fate by physical interactions with the extracellular matrix. *Cell Stem Cell*, 5(1): 17–26

Han H.-W., Hou Y.-T., Hsu S.-H. (2019) Angiogenic potential of co-spheroids of neural stem cells and endothelial cells in injectable gelatin-based hydrogel. *Materials Science and Engineering C*, 99: 140–149

Hayakawa K., Esposito E., Wang X., Terasaki Y., Liu Y., Xing C., Ji X., Lo E. H. (2016) Transfer of mitochondria from astrocytes to neurons after stroke. *Nature*, 535(7613): 551–555

Hoshiba T., Chen G., Endo C., Maruyama H., Wakui M., Nemoto E., Kawazoe N., Tanaka M. (2016) Decellularized extracellular matrix as an in vitro model to study the comprehensive roles of the ECM in stem cell differentiation. *Stem Cells International*, 2016: 6397820

Huang S.-F., Fischer S., Koshkin A., Laczko E., Fischer D., Ogunshola O. O. (2020) Cell-specific metabolomic responses to injury: novel insights into blood-brain barrier modulation. *Scientific Reports*, 10(1): 7760

Iadecola C. (2017) The neurovascular unit coming of age: a journey through neurovascular coupling in health and disease. *Neuron*, 96(1): 17–42

Itoh Y., Takaoka R., Ohira M., Abe T., Tanahashi N., Suzuki N. (2006) Reactive oxygen species generated by mitochondrial injury in human brain microvessel endothelial cells. *Clinical Hemorheology and Microcirculation*, 34(1–2): 163–168

James J. M., Mukouyama Y.-S. (2011) Neuronal action on the developing blood vessel pattern. *Seminars in Cell & Developmental Biology*, 22(9): 1019–1027

Jeong H.-J., Jimenez Z., Mukhambetiyar K., Seo M., Choi J.-W., Park T.-E. (2020) Engineering human brain organoids: from basic research to tissue regeneration. *Tissue Engineering and Regenerative Medicine*, 17(6): 747–757

Joshi A. U., Minhas P. S., Liddelow S. A., Haileselassie B., Andreasson K. I., Dorn G. W., II, Mochly-Rosen D. (2019) Fragmented mitochondria released from microglia trigger A1 astrocytic response and propagate inflammatory neurodegeneration. *Nature Neuroscience*, 22(10): 1635–1648

Katoh M., Wu B., Nguyen H. B., Thai T. Q., Yamasaki R., Lu H., Rietsch A. M., Zorlu M. M., Shinozaki Y., Saitoh Y., Saitoh S., Sakoh T. (2017) Polymorphic regulation of mitochondrial fission and fusion modifies phenotypes of microglia in neuroinflammation. *Scientific Reports*, 7(1): 4942

Kilic O., Pamies D., Lavell E., Schiapparelli P., Feng Y., Hartung T., Bal-Price A., Hogberg H. T., Quinones-Hinojosa A., Guerrero-Cazares H., Levchenko A. (2016) Brain-on-a-chip model enables analysis of human neuronal differentiation and chemotaxis. *Lab on a Chip*, 16(21): 4152–4162

Kirk P., Wilson M. C., Heddle C., Brown M. H., Barclay A. N., Halestrap A. P. (2000) CD147 is tightly associated with lactate transporters MCT1 and MCT4 and facilitates their cell surface expression. *EMBO Journal*, 19(15): 3896–3904

Kumarasamy M., Sosnik A. (2021) Heterocellular spheroids of the neurovascular blood-brain barrier as a platform for personalized nanoneuromedicine. *iScience*, 24(3): 102183

Kuroda J., Ago T., Nishimura A., Nakamura K., Matsuo R., Wakisaka Y., Kamouchi M., Kitazono T. (2014) Nox4 is a major source of superoxide production in human brain pericytes. *Journal of Vascular Research*, 51(6): 429–438

Lee A., Hirabayashi Y., Kwon S.-K., Lewis T. L. Jr, Polleux F. (2018) Emerging roles of mitochondria in synaptic transmission and neurodegeneration. *Current Opinion in Physiology*, 3: 82–93

Lin R., Cai J., Nathan C., Wei X., Schleidt S., Rosenwasser R., Iacovitti L. (2015) Neurogenesis is enhanced by stroke in multiple new stem cell niches along the ventricular system at sites of high BBB permeability. *Neurobiology of Disease*, 74: 229–239

Logsdon A. F., Rhea E. M., Reed M., Banks W. A., Erickson M. A. (2021) The neurovascular extracellular matrix in health and disease. *Experimental Biology and Medicine*, 246(7): 835–844

Lu T. M., Houghton S., Magdeldin T., Barcia Durán J. G., Minotti A. P., Snead A., Sproul A., Nguyen D.-H.T., Xiang J., Fine H. A., Rosenwaks Z., Studer L. (2021) Pluripotent stem cell-derived epithelium misidentified as brain microvascular endothelium requires ETS factors to acquire vascular fate. *Proceedings of the National Academy of Sciences of the United States of America*, 118(8): e2016950118

Ma S., Kwon H. J., Huang Z. (2012) A functional requirement for astroglia in promoting blood vessel development in the early postnatal brain. *PLoS One*, 7(10): e48001

Malaeb S. N., Cohen S. S., Virgintino D., Stonestreet B. S. (2012) Core concepts: Development of the blood-brain barrier. *NeoReviews*, 13(4): e241-e250

Malinovskaya N. A., Komleva Y. K., Salmin V. V., Morgun A. V., Shuvaev A. N., Panina Y. A., Boitsova E. B., Salmina A. B. (2016) Endothelial progenitor cells physiology and metabolic plasticity in brain angiogenesis and blood-brain barrier modeling. *Frontiers in Physiology*, 7: 599

Mangia S., Simpson I. A., Vannucci S. J., Carruthers A. (2009) The in vivo neuron-to-astrocyte lactate shuttle in human brain: Evidence from modeling of measured lactate levels during visual stimulation. *Journal of Neurochemistry*, 109(Suppl. 1): 55–62

Mantecón-Oria M., Diban N., Berciano M. T., Rivero M. J., David O., Lafarga M., Tapia O., Urtiaga A. (2020) Hollow fiber membranes of PCL and PCL/graphene as scaffolds with potential to develop in vitro blood – brain barrier models. *Membranes*, 10(8): 161

Maoz B. M., Herland A., Fitzgerald E. A., Grevesse T., Vidoudez C., Pacheco A. R., Sheehy S. P., Park T.-E., Dauth S., Mannix R., Budnik N., Shores K. (2018) A linked organ-on-chip model of the human neurovascular unit reveals the metabolic coupling of endothelial and neuronal cells. *Nature Biotechnology*, 36(9): 865–877

Matsui T., Omuro H., Liu Y.-F., Soya M., Shima T., Mcewen B. S., Soya H. (2017) Astrocytic glycogen-derived lactate fuels the brain during exhaustive exercise to maintain endurance capacity. *Proceedings of the National Academy of Sciences of the United States of America*, 114(24): 6358–6363

McConnell H.L., Kersch C. N., Woltjer R. L., Neuwelt E. A. (2017) The translational significance of the neurovascular unit. *Journal of Biological Chemistry*, 292(3): 762–770

Mendrinos E., Petropoulos I. K., Mangioris G., Papadopoulou D. N., Stangos A. N., Pournaras C. J. (2008) Lactate-induced retinal arteriolar vasodilation implicates neuronal nitric oxide synthesis in minipigs. *Investigative Ophthalmology & Visual Science*, 49(11): 5060–5066

Middelkamp H. H.T., Verboven A. H.A., De Sá Vivas A. G., Schoenmaker C., Klein Gunnewiek T. M., Passier R., Albers C. A., 't Hoen P. A.C., Nadif Kasri N., van der Meer A. D. (2021) Cell type-specific changes in transcriptomic profiles of endothelial cells, iPSC-derived neurons and astrocytes cultured on microfluidic chips. *Scientific Reports*, 11(1): 2281

Mooney S. J., Shah K., Yeung S., Burgess A., Aubert I., Hynynen K. (2016) Focused ultrasound-induced neurogenesis requires an increase in blood-brain barrier permeability. *PLoS One*, 11(7): e0159892

Morgun A. V., Osipova E. D., Boitsova E. B., Lopatina O. L., Gorina Y. V., Pozhilenkova E. A., Salmina A. B. (2020) Vascular component of neuroinflammation in experimental alzheimer's disease in mice. *Cell and Tissue Biology*, 14(4): 256–262

Morgun A. V., Osipova E. D., Boitsova E. B., Shuvaev A. N., Malinovskaya N. A., Mosiagina A. I., Salmina A. B. (2021) Neurogenic potential of implanted neurospheres is regulated by optogenetic stimulation of hippocampal astrocytes ex vivo. *Bulletin of Experimental Biology and Medicine*, 170(6): 693–698

Motori E., Atanassov I., Kochan S. M.V., Folz-Donahue K., Sakthivelu V., Giavalisco P., Toni N., Puyal J., Larsson N.-G. (2020) Neuronal metabolic rewiring promotes resilience to neurodegeneration caused by mitochondrial dysfunction. *Science Advances*, 6(35): eaba8271

Muoio V., Persson P. B., Sendeski M. M. (2014) The neurovascular unit – concept review. *Acta Physiologica*, 210(4): 790–798

Osipova E. D., Komleva Y. K., Morgun A. V., Lopatina O. L., Panina Y. A., Olovyannikova R. Y., Vais E. F., Salmin V. V., Salmina A. B. (2018) Designing in vitro blood-brain barrier models reproducing alterations in brain aging. *Frontiers in Aging Neuroscience*, 10: 234

Paredes I., Himmels P., Ruiz de Almodóvar C. (2018) Neurovascular communication during CNS development. *Developmental Cell*, 45(1): 10–32

Pavia F. C., Di Bella M. A., Brucato V., Blanda V., Zummo F., Vitrano I., Di Liegro C. M., Ghersi G., Di Liegro I., Schiera G. (2019) A 3D-scaffold of PLLA induces the morphological differentiation and migration of primary astrocytes and promotes the production of extracellular vesicles. *Molecular Medicine Reports*, 20(2): 1288–1296

Potente M., Carmeliet P. (2017) The link between angiogenesis and endothelial metabolism. *Annual Review of Physiology*, 79: 43–66

Potjewyd G., Moxon S., Wang T., Domingos M., Hooper N. M. (2018) Tissue engineering 3d neurovascular units: a biomaterials and bioprinting perspective. *Trends in Biotechnology*, 36(4): 457–472

Pozhilenkova E. A., Lopatina O. L., Komleva Y. K., Salmin V. V., Salmina A. B. (2017) Blood-brain barrier-supported neurogenesis in healthy and diseased brain. *Reviews in the Neurosciences*, 28(4): 397–415

Salmin V., Morgun A., Khilazheva E., Pisareva N., Boitsova E., Lavrentiev P., Sadovsky M., Salmina A. (2017) Secret life of tiny blood vessels: lactate, scaffold and beyond. *Bioinformatics and biomedical engineering*. Cham, Springer International Publishing, p. 591–601

Salmina A. B., Morgun A. V., Kuvacheva N. V., Lopatina O. L., Komleva Y. K., Malinovskaya N. A., Pozhilenkova E. A. (2014) Establishment of neurogenic microenvironment in the neurovascular unit: The connexin 43 story. *Reviews in the Neurosciences*, 25(1): 97–111

Salmina A. B., Kuvacheva N. V., Morgun A. V., Komleva Y. K., Pozhilenkova E. A., Lopatina O. L., Gorina Y. V., Taranushenko T. E., Petrova L. L. (2015) Glycolysis-mediated control of blood-brain barrier development and function. *International Journal of Biochemistry and Cell Biology*, 64: 174–184

Salmina A. B., Komleva Y. K., Lopatina O. L., Birbrair A. (2019) Pericytes in Alzheimer's disease: novel clues to cerebral amyloid angiopathy pathogenesis. *Advances in Experimental Medicine and Biology*, 1147: 147–166

Salmina A. B., Kharitonova E. V., Gorina Y. V., Teplyashina E. A., Malinovskaya N. A., Khilazheva E. D., Mosyagina A. I., Morgun A. V., Shuvaev A. N., Salmin V. V., Lopatina O. L., Komleva Y. K. (2021) Blood–brain barrier and neurovascular unit in vitro models for studying mitochondria-driven molecular mechanisms of neurodegeneration. *International Journal of Molecular Sciences*, 22(9): 4661

Sawada M., Matsumoto M., Sawamoto K. (2014) Vascular regulation of adult neurogenesis under physiological and pathological conditions. *Frontiers in Neuroscience*, 8: 53

Shenouda S. M., Widlansky M. E., Chen K., Xu G., Holbrook M., Tabit C. E., Hamburg N. M., Frame A. A., Caiano T. L., Kluge M. A., Duess M.-A., Levit A. (2011) Altered mitochondrial dynamics contributes to endothelial dysfunction in diabetes mellitus. *Circulation*, 124(4): 444–453

Su L., Lei X., Ma H., Feng C., Jiang J., Jiao J. (2020) PRDM16 orchestrates angiogenesis via neural differentiation in the developing brain. *Cell Death & Differentiation*, 27(8): 2313–2329

Tata M., Wall I., Joyce A., Vieira J. M., Kessaris N., Ruhrberg C. (2016) Regulation of embryonic neurogenesis by germinal zone vasculature. *Proceedings of the National Academy of Sciences of the United States of America*, 113(47): 13414–13419

Thomsen M. S., Routhe L. J., Moos T. (2017) The vascular basement membrane in the healthy and pathological brain. *Journal of Cerebral Blood Flow and Metabolism*, 37(10): 3300–3317

Tohidpour A., Morgun A. V., Boitsova E. B., Malinovskaya N. A., Martynova G. P., Khilazheva E. D., Kopylevich N. V., Gertsog G. E., Salmina A. B. (2017) Neuroinflammation and infection: molecular mechanisms associated with dysfunction of neurovascular unit. *Frontiers in Cellular and Infection Microbiology*, 7: 276

Trudeau K., Molina A. J.A., Roy S. (2011) High glucose induces mitochondrial morphology and metabolic changes in retinal pericytes. *Investigative Ophthalmology and Visual Science*, 52(12): 8657–8664

Uspenskaya Y. A., Komleva Y. K., Gorina Y. V., Pozhilenkova E. A., Belova O. A., Salmina A. B. (2018) CD147 polyfunctionality and new diagnostic and therapy opportunities. *Siberian Medical Review*, 4: 22–30 (in Russian)

Uwamori H., Higuchi T., Arai K., Sudo R. (2017) Integration of neurogenesis and angiogenesis models for constructing a neurovascular tissue. *Scientific Reports*, 7(1): 17349

Volobouеva L. A., Suh S. W., Swanson R. A., Giffard R. G. (2007) Inhibition of mitochondrial function in astrocytes: implications for neuroprotection. *Journal of Neurochemistry*, 102(4): 1383–1394

Warren D., Tomaskovic-Crook E., Wallace G. G., Crook J. M. (2021) Engineering in vitro human neural tissue analogs by 3D bioprinting and electrostimulation. *APL Bioengineering*, 5(2): 020901

Winkelman M. A., Koppes A. N., Koppes R. A., Dai G. (2021) Bioengineering the neurovascular niche to study the interaction of neural stem cells and endothelial cells. *APL Bioengineering*, 5(1): 011507

Xiang H., Song R., Ouyang J., Zhu R., Shu Z., Liu Y., Wang X., Zhang D., Zhao J., Lu H. (2021) Organelle dynamics of endothelial mitochondria in diabetic angiopathy. *European Journal of Pharmacology*, 895: 173865

Yetkin-Arik B., Vogels I. M.C., Neyazi N., van Duinen V., Houtkooper R. H., van Noorden C. J.F., Klaassen I., Schlingemann R. O. (2019) Endothelial tip cells in vitro are less glycolytic and have a more flexible response to metabolic stress than non-tip cells. *Scientific Reports*, 9(1): 10414

Yue H., Xie K., Ji X., Xu B., Wang C., Shi P. (2020) Vascularized neural constructs for ex-vivo reconstitution of blood-brain barrier function. *Biomaterials*, 245: 119980

Zhang D. X., Gutterman D. D. (2007) Mitochondrial reactive oxygen species-mediated signaling in endothelial cells. *American Journal of Physiology-Heart and Circulatory Physiology*, 292(5): H2023-H2031

Journal of Siberian Federal University. Biology 2021 14(4): 526–532
~ ~ ~

DOI 10.17516/1997-1389-0369

УДК 615.46.015

Treatment of Non-Healing Trophic Ulcers in Patients with Chronic Venous Insufficiency Using Wound Coatings Based on Bacterial Cellulose Loaded with Silver Nanoparticles

Nadezhda M. Tyukhteva*,
Yuri S. Vinnik, Natalia S. Solovyeva,
Andrey P. Zuev and Leonid A. Polezhaev
Prof. V. F. Voino-Yasenetsky Krasnoyarsk State Medical University
Krasnoyarsk, Russian Federation

Received 15.08.2021, received in revised form 05.10.2021, accepted 12.11.2021

Abstract. Chronic venous insufficiency is a common condition that affects people of different ages. Trophic ulcers are a complication of venous insufficiency which is difficult to treat. Therefore, development of new, combined methods of treatment using coatings that have both antibacterial and wound healing properties is a topical issue. The article presents a comparative analysis of clinical trials of wound coatings based on bacterial cellulose (experimental group 1), cellulose loaded with silver (experimental group 2), and «Hydrocall» (control group) in treatment of trophic ulcers in patients with chronic venous insufficiency. Application of all types of wound coatings demonstrated a positive dynamics of healing. Complete epithelialization was observed in experimental group 2 by the 42nd day, whereas in patients of the control group, epithelialisation was not complete by the 45th day. Thus, application of wound coatings based on cellulose loaded with silver shortened the epithelialisation process and trophic ulcers healing, which justifies to their efficiency and practicality.

Keywords: wound coating, trophic ulcer, cellulose, nanosilver.

Citation: Tyukhteva N.M., Vinnik Yu.S., Solovyeva N.S., Zuev A.P., Polezhaev L.A. Treatment of non-healing trophic ulcers in patients with chronic venous insufficiency using wound coatings based on bacterial cellulose loaded with silver nanoparticles. J. Sib. Fed. Univ. Biol., 2021, 14(4), 526–532. DOI: 10.17516/1997-1389-0369

* Corresponding author E-mail address: markelova_nadya@mail.ru
ORCID: 0000-0002-3773-8741 (Tyukhteva N.M.); 0000-0002-8995-2862 (Vinnik Yu.S.)

Результаты применения раневых покрытий на основе бактериальной целлюлозы, нагруженной наночастицами серебра, у больных с длительно незаживающими трофическими язвами на фоне хронической венозной недостаточности

Н. М. Тюхтева, Ю. С. Винник,
Н. С. Соловьева, А. П. Зуев, Л. А. Полежаев
Красноярский государственный медицинский университет им. проф. В. Ф. Войно-Ясенецкого
Российская Федерация, Красноярск

Аннотация. Распространенной патологией среди населения различного возраста является хроническая венозная недостаточность. Трофические язвы – осложнение венозной недостаточности, лечение которых сопряжено с большими трудностями. В связи с этим актуальной остается разработка новых, комбинированных методов лечения с применением перевязочных средств, обладающих одновременно антибактериальными и ранозаживляющими свойствами. В статье представлен сравнительный анализ результатов клинических испытаний раневых покрытий, основой которых является целлюлоза биологического происхождения (исследуемая группа 1) и целлюлоза, нагруженная серебром (исследуемая группа 2), в сравнении с раневым покрытием «Гидроколл» у больных с длительно незаживающими трофическими язвами на фоне хронической венозной недостаточности. В результате применения различных раневых покрытий во всех случаях отмечена положительная динамика течения раневого процесса, однако в группе сравнения к 45-м суткам эпителизация не завершилась, в то же время в исследуемой группе 2 к 42-м суткам наступила полная эпителизация длительно незаживающих трофических язв. Таким образом, раневые покрытия на основе целлюлозы, нагруженной серебром, позволяют добиться сокращения сроков заживления и эпителизации трофических язв, что свидетельствует об эффективности и целесообразности их применения.

Ключевые слова: раневое покрытие, трофическая язва, целлюлоза, наносеребро.

Цитирование: Тюхтева, Н. М. Результаты применения раневых покрытий на основе бактериальной целлюлозы, нагруженной наночастицами серебра, у больных с длительно незаживающими трофическими язвами на фоне хронической венозной недостаточности / Н. М. Тюхтева, Ю. С. Винник, Н. С. Соловьева, А. П. Зуев, Л. А. Полежаев // Журн. Сиб. федер. ун-та. Биология, 2021. 14(4). С. 526–532. DOI: 10.17516/1997-1389-0369

Введение

Одна из серьезных проблем медицины – поиск эффективных методов лечения осложнений у больных с хронической венозной недостаточностью. Трофические язвы нижних конечностей, обусловленные нару-

шением в работе венозной системы, обрекают таких пациентов на длительный период лечения, а следовательно, страдает качество жизни. Вышеуказанная патология достаточно распространена среди населения различного возраста (Благитко и др., 2004; Bogdanets et al., 2007; Bogomolov, Slobodianiuk, 2013).

Лечение венозных трофических язв – длительный и трудоемкий процесс, поскольку явления, вызванные трофическими нарушениями, крайне тяжело поддаются лечению (Гостищев, 2007; Olson et al., 2002). В связи со сложным и длительным лечением продолжаются научно-исследовательские и практические работы, направленные на поиск оптимального метода, позволяющего снизить сроки фаз раневого процесса и уменьшить длительность стационарного и амбулаторного лечения. Для достижения желаемого эффекта применяемые раневые покрытия, перевязочные средства должны обладать одновременно несколькими свойствами, поскольку в ином случае динамика в лечении слабоположительная (Дибиров, 2008; Cappugi et al., 2014). Фармацевтические компании представляют множество раневых покрытий, таких как гели, губки, пленки, пленкообразующие композиции, гидроколлоиды, порошки, пасты, комбинации различных материалов, обладающих рядом преимуществ, в отличие от традиционной марли, сетки, нетканого полотна (Лечиев и др., 2015; Robson et al., 2006).

Оптимальными средствами в лечении длительно незаживающих трофических язв на фоне хронической венозной недостаточности являются раневые покрытия, представляющие собой своеобразную лекарственную форму. Применение таких покрытий позволяет значительно повысить эффективность лечения. Разработаны и разрабатываются новые материалы, активно применяются полимеры биологического и целлюлоза микробного происхождения, что позволяет улучшить результаты и прогнозы лечения за счет воздействия одновременно нескольких свойств (Будневский и др., 2017; Ambrozy et al., 2013; Volova et al., 2018).

Комбинация раневых покрытий с различными препаратами достаточно перспективное направление научной деятельности, поскольку положительных результатов лечения больных с длительно незаживающими трофическими язвами на фоне хронической венозной недостаточности удается достичь в разы быстрее по сравнению с классическими методами лечения.

Цель работы – улучшить результаты лечения больных с инфицированными трофическими язвами на фоне хронической венозной недостаточности с помощью высокотехнологичных раневых покрытий биологического происхождения. Были проведены клинические испытания раневых покрытий, основой которых служит целлюлоза биологического происхождения и целлюлоза, нагруженная серебром, в сравнении с раневым покрытием «Гидроколл» у больных с длительно незаживающими трофическими язвами на фоне хронической венозной недостаточности.

Материалы и методы

Работа носит клинический характер, выполнена на клинической базе кафедры общей хирургии имени проф. М.И. Гульмана в хирургическом отделении № 2 ЧУЗ «КБ «РЖД-Медицина» город Красноярск» совместно с кафедрой медицинской биологии Института фундаментальной биологии и биотехнологии СФУ.

В исследование были включены пациенты с длительно незаживающими трофическими язвами нижних конечностей на фоне хронической венозной недостаточности (n=45). Группу сравнения состави-

ли больные (n=15), у которых в качестве раневого покрытия были использованы повязки «Гидроколл», исследуемая группа 1 (n=15) – с применением целлюлозы микробного происхождения, исследуемая группа 2 (n=15) – с применением комбинации серебра и целлюлозы микробного происхождения. Образцы бактериальной целлюлозы (БЦ) получены в Сибирском федеральном университете (патент РФ на изобретение № 2568605 «Штамм бактерий *Komagataeibacter xylinus* – продуцент бактериальной целлюлозы»).

Группы больных были сопоставимы по возрасту, полу, фазе раневого процесса и площади ран. Сроки наблюдения за пациентами колебались от 14 до 42 сут. Методы исследования включали клиническую оценку раневого процесса, планиметрию ран, pH-метрию. Статистическая обработка результатов проведена с помощью пакета программ Statistica 6.1. Для оценки нормальности распределения использовали критерий Шапиро-Уилка. Для описания использовали среднее и стандартное отклонение (M±σ), сравнение проводили с помощью параметрических методов статистики, предварительно оценивая равенство дисперсии с помощью критерия Левена. Значимыми считали различия при $p<0,05$.

Результаты и обсуждение

Применение комбинации целлюлозы микробного происхождения и серебра позволяет оптимизировать раневой процесс, сократить время появления и заполнения ран зрелой грануляционной тканью на 3 и 3–14 суток соответственно, повысить частоту эпителизации на 28,7 % по сравнению с традиционной терапией. У всех больных при поступлении в стационар отмечался высокий уровень эндогенной интоксикации. Согласно анализу результатов клинико-лабораторных показателей больных исследуемой группы 2 на вторые сутки с начала лечения отмечалось снижение температуры тела, а к 6–7-м суткам показатели приближались к норме. Достоверное снижение показателей эндотоксикоза отмечено уже на третьи сутки наблюдения. Количество лейкоцитов в крови у больных исследуемой группы 2 до лечения составило $18,5±1,2×10^9$/л, а к 10-м суткам лечения этот показатель не превышал нормального уровня – $8,7±1,2×10^9$/л ($p<0,05$). В первые сутки лечения лейкоцитарный индекс интоксикации составлял 5,22±2,10 ед., на фоне проводимого лечения достоверное ($p<0,05$) снижение этого показателя до 2,97±0,41 ед. происходило к пятым суткам.

Динамика показателей pH на фоне применения различных способов местного воздействия на раневой процесс была различной (табл. 1). Благодаря комбинированному методу лечения с применением раневого покрытия на основе бактериальной целлюлозы в сочетании с наносеребром, к 6-м суткам показатель pH становился нейтральным, а к 14-м суткам среда становилась слабокислой, приближаясь в течение раневого процесса к наиболее оптимальным значениям.

Планиметрия трофических язв, расчет индекса Л. Н. Поповой, pH-метрия позволяли оценить клиническое течение процесса. Система оценки динамики раневого процесса представлена в табл. 2. При клинической оценке течения раневого процесса учитывались такие критерии, как сроки исчезновения отека, появление единичных грануляций, заполнение трофических язв зрелой грануляционной тканью, начало эпителизации и наступление полной эпителизации.

Результаты лечения показали, что в группе сравнения переход раневого процесса во вторую фазу был длительным,

Таблица 1. Динамика pH ран у больных в группе сравнения (ГС) и исследуемых группах (ИГ)

Table 1. Dynamics of wound pH in patients of control and experimental groups

Сроки регистрации pH	Группы больных		
	ГС	ИГ 1	ИГ 2
До лечения	8,43±0,12	8,71±0,10*	8,77±0,09*
6-е сутки	8,02±0,28	7,74±0,24*	7,73±0,24*
14-е сутки	7,11±0,31	6,63±0,22*	6,33±0,36*
21-е сутки	6,80±0,25	5,42±0,45*	5,27±0,44*

* – достоверность различия между исследуемой группой и группой сравнения ($p \leq 0,05$).

Таблица 2. Методика оценки результатов лечения

Table 2. Evaluation criteria for treatment results

Критерии оценки	Результаты лечения		
	Хорошие	Удовлетвори-тельные	Неудовлетво-рительные
Исчезновение перифокального отека, сут.	< 4	5–8	> 9
Появление единичных грануляций, сут.	< 6	7–10	> 10
Заполнение ран зрелой грануляционной тканью, сут.	< 10	11–16	>16
Появление краевой эпителизации, сут.	< 11	12–17	> 17
Полная эпителизация, сут.	< 30	31–35	> 35
Индекс Л. Н. Поповой во II и III фазах раневого процесса,%	> 4	3–4	< 3

Таблица 3. Оценка результатов лечения в группе сравнения (ГС) и исследуемой группе 2 (ИГ2)

Table 3. Treatment results in the control and experimental group 2

Критерии оценки динамики	Результаты лечения (% пациентов)					
	Хорошие		Удовлетворительные		Неудовлетворительные	
	ГС	ИГ2	ГС	ИГ2	ГС	ИГ2
Исчезновение перифокального отека	-	7 (46,7 %)	4 (26,6 %)	5 (33,3 %)	11 (73,4 %)	3 (20 %)
Появление единичных грануляций	-	7 (46,7 %)	4 (26,6 %)	8 (53,3 %)	11 (73,4 %)	-
Заполнение ран зрелой грануляционной тканью	-	5 (33,3 %)	5 (33,3 %)	10 (66,7 %)	10 (66,7 %)	-
Появление краевой эпителизации	-	5 (33,3 %)	3 (20 %)	8 (53,3 %)	12 (80 %)	2 (13,3 %)
Полная эпителизация	4 (26,6 %)	5 (33,3 %)	5 (33,3 %)	8 (53,3 %)	6 (40,1 %)	2 (13,3 %)

у 6 (40,1 %) больных к 45-м суткам эпителизация не завершилась (табл. 3). Оценка скорости заживления ран в исследуемой группе 2 свидетельствовала о достижении хороших и удовлетворительных результатов – к 42-м суткам у 13 (86,7 %) пациентов наступила

1 2 3

Рис. Клинические примеры применения раневых повязок: 1 – больная Е., 56 лет. Длительно незаживающая трофическая язва на левой голени, 5-е сутки – очищение дна язвы, намечены процессы краевой эпителизации; 2 – больной Ф., 66 лет. Длительно незаживающая трофическая язва на правой голени, 6-е сутки – очищение дна язвы, намечены процессы краевой эпителизации; 3 – больной И., 45 лет. Длительно незаживающая трофическая язва, 9-е сутки – зрелые розовые грануляции, активная краевая эпителизация

Fig. Clinical examples of the use of wound coatings: 1 – Patient E., 56 years. Long-term non-healing trophic ulcer of the lower third of the left leg, 5th day – cleansing of the bottom of the ulcer, marginal epithelialisation is outlined; 2 – Patient F., 66 years. Long-term non-healing trophic ulcer of the lower third of the right leg, 6th day – cleansing of the bottom of the ulcer, marginal epithelialisation is outlined; 3 – Patient I., 45 years. Long-term non-healing trophic ulcer, 9th day – mature pink granulation, active marginal epithelialisation

полная эпителизация длительно незаживающих трофических язв. На рисунке представлены клинические примеры.

Заключение

Применение комбинированного метода лечения, включающее раневое покрытие на основе целлюлозы микробного происхождения и серебра, позволяет достичь больших успехов в лечении больных с длительно незаживающими трофическими язвами на фоне хронической венозной недостаточности в сравнении с другими вышепредставленными методами. Происходит более быстрое и интенсивное очищение и эпителизация трофических язв, покрытие является подобием матрицы для образования новых тканей. Смена повязки менее болезненна для пациента, на поверхности целлюлозы удаляются некрозы и фрагменты разрушенных клеток. Целлюлоза микробного происхождения в комбинации с серебром обладает рядом важных функций: служит барьером против возникновения вторичных инфекций, ограничивает потерю жидкости и одновременно с этим обеспечивает необходимую аэрацию раны, а следовательно, и ускорение процессов заживления таких ран.

Список литературы / References

Благитко Е. М., Бурмистров В. А., Колесников А. П., Михайлов Ю. И., Родионов П. П. (2004) *Серебро в медицине*. Новосибирск, Наука-Центр, 254 с. [Blagitko E. M., Burmistrov V. A., Kolesnikov A. P., Mikhailov Yu.I., Rodionov P. P. (2004) *Silver in medicine*. Novosibirsk, Nauka-Centr, 254 p. (in Russian)]

Будневский А. В., Цветикова Л. Н., Андреев А. А., Карапитьян А. Р., Чуян А. О. (2017) Опыт применения мобильного приложения «+WoundDesk» для оценки динамики репарации экспериментальных ран. *Моделирование, оптимизация и информационные технологии*, 5(1) [Budnevskiy A. V., Andreev A. A., Tsvetikova L. N., Karapityan A. R., Chuyan A. O. (2017) The

practice of use of +WoundDesk mobile application for evaluation of experimental wound repair dynamics. *Modeling, Optimization and Information Technology* [Modelirovanie, optimizaciya i informacionnye tekhnologii], 5(1) (in Russian)]

Гостищев В.К. (2007) *Инфекции в хирургии: руководство для врачей*. Москва, ГЭОТАР-Медиа, 761 с. [Gostishchev V.K. (2007) *Infections in surgery: a guide for physicians*. Moscow, GEOTAR-Media, 761 p. (in Russian)]

Дибиров М.Д. (2008) Хроническая венозная недостаточность и трофические язвы у пациентов пожилого и старческого возраста. *Справочник поликлинического врача*, 6: 39–42 [Dibirov M.D. (2008) Chronic venous insufficiency and trophic ulcers in elderly and senile patients. *Outpatient Doctor's Guide* [Spravochnik poliklinicheskogo vracha], 6: 39–42 (in Russian)]

Лечиев И.У., Берсанов Р.У., Сипова М.М. (2015) Майодил и Аевит – этиопатогенетические предпосылки применения в комплексном лечении трофических язв. *Вестник МАНЭБ*, 20(3): 34–39 [Lechiev I.U., Bersanov R.U., Sipova M.M. (2015) Mayodil and Aevitum – etiopathogenetical background application in treatment of venous ulcers. *Bulletin of the International Academy of Ecology and Life Safety* [Vestnik MANEB], 20(3): 34–39 (in Russian)]

Ambrozy E., Waczulikova I., Willfort A., Boehler K., Cauza K., Ehringer H., Heinz G., Koppensteiner R., Maric S., Gschwandtner M.E. (2013) Healing process of venous ulcers: the role of microcirculation. *International Wound Journal*, 10(1): 57–64

Bogdanets L.I., Berezina S.S., Kirienko A.I. (2007) Conception of «humid» healing of venous ulcers. *Khirurgiia*, 5: 60–63

Bogomolov M.S., Slobodianiuk V.V. (2013) Treatment of trophic ulsers of different etiology. *Vestnik khirurgii imeni I.I. Grekova*, 172(5): 34–40

Cappugi P., Comacchi C., Torchia D. (2014) Photodynamic therapy for chronic venous ulcers. *Acta Dermatovenerologica Croatica*, 22(2): 129–131

Olson M.E., Ceri H., Morck D.W., Buret A.G., Read R.R. (2002) Biofilm bacteria: formation and comparative susceptibility of antibiotics. *Canadian Journal of Veterinary Research*, 66(2): 86–92

Robson M.C., Cooper D.M., Aslam R., Gould L.J., Harding K.G., Margolis D.J., Ochs D.E., Serena T.E., Snyder R.J., Steed D.L., Thomas D.R., Wiersma-Bryant L. (2006) Guidelines for the treatment of venous ulcers. *Wound Repair and Regeneration*, 14(6): 649–662

Volova T.G., Prudnikova S.V., Sukovatyi A.G., Shishatskaya E.I. (2018) Production and properties of bacterial cellulose by the strain Komagataeibacter xylinus B-12068. *Applied Microbiology and Biotechnology*, 102(17): 7417–7428

Journal of Siberian Federal University. Biology 2021 14(4): 533–540
~ ~ ~

DOI 10.17516/1997-1389-0370

УДК 577.121.2:628.47

Microbiological Degradation of Poly(3-Hydroxybutyrate) Films in Different Edaphoclimatic Zones of Siberia

Svetlana V. Prudnikova*
Siberian Federal University
Krasnoyarsk, Russian Federation

Received 10.08.2021, received in revised form 25.09.2021, accepted 12.11.2021

Abstract. The urgency of handling plastic waste is escalating every year and the problem can be only solved using an integrated approach. Replacing non-degradable materials synthesised from fossil fuels with carbon-neutral biopolymers can reduce non-biodegradable waste, CO_2 emissions and energy use. However, even completely biodegradable biopolymer materials will stay in the environment for a long time since the rate of their biodegradation depends on many factors. The paper evaluates the influence of edaphoclimatic and microbiological factors on the biodegradation rate of biopolymer films from the poly(3-hydroxybutyrate) [P(3HB)] when exposed to soddy-carbonate, cryogenic, and agrogenically transformed Siberian soils. A principal component analysis showed that in different soils, characterised by specific temperature, moisture content, pH values, biogenicity and abundance of microorganisms, the kinetics of mass loss of P(3HB)-films were primarily determined by the temperature- precipitation ratio and it increased as the content of humus in soil increased. The maximum rates of film mass loss of 0.63 ± 0.09 and 0.93 ± 0.01 mg $\cdot$ day^{-1} were detected in agrogenic soils. No correlation between mass loss of the films and the total number of microorganisms was found. A phylogenetic analysis revealed differences in the composition of primary P(3HB)-degrading microorganisms in different soil types.

Keywords: poly-3-hydroxybutyrate, biopolymers, biodegradation, soil conditions, soil microbiology, P(3HB)-degrading microorganisms.

Acknowledgements. The research was carried out in accordance with the State Assignment by the Ministry of Science and Higher Education of Russian Federation to Siberian Federal University in 2020 (Project № FSRZ-2020-0006 “Biologically active substances in ecological, biotechnological and medical systems”).

* Corresponding author E-mail address: sprudnikova@sfu-kras.ru
ORCID: 0000-0001-8990-3043

Citation: Prudnikova S. V. Microbiological degradation of poly(3-hydroxybutyrate) films in different edaphoclimatic zones of Siberia.J. Sib. Fed. Univ. Biol., 2021, 14(4), 533–540. DOI: 10.17516/1997-1389-0370

Микробиологическая деградация пленок из поли(3-гидроксибутирата) в различных почвенно-климатических зонах Сибири

С. В. Прудникова
Сибирский федеральный университет
Российская Федерация, Красноярск

Аннотация. Проблема обращения с пластиковыми отходами ежегодно обостряется и требует комплексного подхода к ее решению. Замена синтетических материалов, полученных из ископаемого топлива, на углеродно-нейтральные биополимеры позволит уменьшить объем стойких к биоразложению отходов, снизить выбросы CO_2 и количество потребляемой энергии. Однако темпы биодеградации изделий из биополимеров в окружающей среде зависят от многих факторов, поэтому в природных условиях даже полностью биоразлагаемые материалы могут сохраняться длительное время. В работе проведена оценка влияния почвенно-климатических и микробиологических характеристик на темпы биодеградации пленок из биополимера поли(3-гидроксибутирата) [П(3ГБ)] при экспозиции в сибирских почвах: дерново-карбонатной, криогенной и агрогенно-преобразованной. Анализ, проведенный методом главных компонент, показал, что в почвах разного типа, характеризующихся определенной температурой, увлажненностью, значениями pH, биогенностью и обилием микроорганизмов, скорость убыли массы пленок из П(3ГБ) в первую очередь определялась соотношением температуры и количества осадков и увеличивалась при повышении содержания гумуса в почве. Максимальные темпы убыли массы пленок – 0,63±0,09 и 0,93±0,013 мг·сут$^{-1}$ – были зарегистрированы в агрогенных почвах. Показано отсутствие корреляции убыли массы пленок с общей численностью микроорганизмов. Филогенетический анализ выявил отличия в наборе первичных деструкторов в разных типах почв.

Ключевые слова: поли-3-гидроксибутират, биополимеры, биодеградация, почвенные условия, микробиология почвы, П(3ГБ)-разрушающие микроорганизмы.

Благодарности. Работа выполнена в рамках Государственного задания Министерства науки и высшего образования Российской Федерации Сибирскому федеральному университету на 2020 год (проект № FSRZ-2020–0006, тема проекта «Биологически активные вещества в экологических, биотехнологических и медицинских системах»).

Цитирование: Прудникова, С. В. Микробиологическая деградация пленок из поли(3-гидроксибутирата) в различных почвенно-климатических зонах Сибири / С. В. Прудникова // Журн. Сиб. федер. ун-та. Биология, 2021. 14(4). С. 533–540. DOI: 10.17516/1997-1389-0370

Введение

Высокие темпы роста количества полимерных отходов, получаемых из невозобновляемого сырья и стойких к биоразложению, побуждают исследователей искать новые экологически чистые и безопасные материалы – биополимеры, произведенные биологическим путем и способные к биодеградации. Использование биополимеров уменьшает зависимость от ископаемого топлива, сокращает выбросы углекислого газа и, таким образом, снижает углеродный след (Meereboer et al., 2020).

Полигидроксиалканоаты (ПГА), в том числе поли(3-гидроксибутират) [П(3ГБ)], – это уникальный класс химических соединений, в полной мере соответствующий определению «биополимеры» (Koller, Mukherjee, 2020; Nandakumar et al., 2021). Несмотря на то что П(3ГБ) активно продвигается в качестве заменителя синтетических пластмасс, его биодеградация в окружающей среде зависит от многих факторов и требует определенных условий (Meereboer et al., 2020). Время разложения изделий из биополимеров может зависеть от их морфологии, пористости, степени кристалличности полимера, температуры окружающей среды, pH, концентрации солей, микробной плотности, биоразнообразия и пр. (Fernandes et al., 2020; Koller, Mukherjee, 2020). Анализ литературы показывает, что идеальные условия для естественного разложения ПГА очень ограничены, что затрудняет выделение ключевых факторов, определяющих скорость биоразложения полимерных изделий.

Цель работы – оценка влияния условий экспозиции на темпы биодеградации пленок из П(3ГБ) в сибирских почвах разного типа.

Материалы и методы

Образцы П(3ГБ) в виде пленок помещали в сетчатые пакеты из органзы и размещали в охарактеризованную почву. Общую численность микроорганизмов в исходной почве (ОМЧ) учитывали на мясопептонном агаре общепринятыми методами почвенной микробиологии, бактерии-деструкторы П(3ГБ) выделяли из изолированных колоний методом прозрачных зон на минеральном агаре с добавлением порошкообразного полимера (Mergaert et al., 1993). Полимерные пленки экспонировали в почвах разного типа: лесная дерново-карбонатная (два участка с разной кислотностью почвы в районе г. Красноярска), криогенная почва (пос. Тура, Центральная Эвенкия), полевая почва агрочернозем криогенно-мицеллярный (пос. Минино, Красноярский край) и огородная сильно агрогенно-преобразованная почва (с. Субботино, Красноярский край). Срок экспозиции зависел от интенсивности деградации и степени разложения пленок: в контролируемых условиях опыта с агрогенными почвами в теплице эксперимент длился 1 месяц, в естественных условиях натурного эксперимента – от 3 до 15 месяцев. В ходе эксперимента регистрировали среднесуточную температуру, суммарное количество осадков, pH почвенного раствора (по ГОСТ 26423–85), содержание гумуса (по ГОСТ 26213–9); убыль массы пленок определяли на аналитических весах 4-го класса точности Adventurer AR2140 (Ohaus, США) и рассчитывали по разности исходной и конечной массы за время экспозиции (мг·сут$^{-1}$). Идентификацию видов бактерий-деструкторов проводили методом секвенирования гена 16S рРНК по Сэнгеру и используя программу поиска гомологичных последовательностей BLAST (https://blast.ncbi.nlm.nih.gov). Филогенетический анализ бактерий-деструкторов П(3ГБ) выполнен методом ближайших соседей (Saitou, Nei, 1987) в пакете программ MEGA версии X (Kumar et al., 2018). Статистическую обработку ре-

зультатов проводили с применением пакетов программ Excel MS Office 2019, R версия 4.0.3 и RStudio версия 1.3.1093.

Результаты и обсуждение

Предыдущие исследования показали, что биоразрушение ПГА зависит от почвенно-климатических условии среды, микробной составляющей почвы, а также типа полимера и формы полимерного изделия (Boyandin et al., 2012). Биодеградация ПГА в почвах Средней Сибири может значительно варьироваться, что обусловлено резко континентальным климатом региона и большими амплитудами температуры и количества осадков в разные годы. Даже при высокой среднесуточной температуре воздуха дефицит влаги может существенно снижать скорость биодеградации. Так, в дерново-карбонатной почве, характеризующейся невысоким содержанием гумуса (2,6 %), при благоприятных для роста микроорганизмов условиях и достаточной увлажненности почвы (20–25 %) численность бактерий была высокой – от 10^8до 10^9 КОЕ· $г^{-1}$ почвы (табл. 1). Это привело к быстрой убыли массы пленок П(3ГБ) – от 0,17 до 0,36 мг·$сут^{-1}$. Если температура была выше среднемноголетних значений, а количество осадков меньше нормы, это приводило к снижению численности бактерий на 2–3 порядка и медленному разрушению полимерных пленок – 0,06–0,07 мг·$сут^{-1}$ (табл. 1). Следовательно, характер биодеградации полимерных изделий в природных условиях отличается от теоретически возможного.

Другая ситуация складывается в контролируемых условиях: в агрочерноземах, богатых гумусом и с доступными формами азота, при стабилизированной температуре

Таблица 1. Характеристика условий экспозиции полимерных пленок в сибирских почвах

Table 1. Characteristics of exposure conditions of polymer films in Siberian soils

Район/ тип почвы	Содержание гумуса, %	Срок экспозиции	Количество осадков, мм	Среднемесячная температура, °С	pH	ОМЧ[a], млн КОЕ·$г^{-1}$ почвы (n=5)	Убыль массы П(3ГБ)-пленок, мг·$сут^{-1}$ (n=6)
г. Красноярск / дерново-карбонатная	2,6	3 месяца (2010 г.)	190	17,0±1,3	6,9 7,5	0,27±0,02 3,2±0,2	0,06±0,01 0,07±0,02
		3 месяца (2007 г.)	231	15,8±3,4	6,1 7,3	133,0±47,0 1470,0±80,0	0,17±0,03 0,36±0,06
пос. Минино / агрочернозем криогенно-мицеллярный	8,7	1 месяц (2016 г.)	750	21,0±1,0	7,5	16,3±5,2	0,63±0,09
с. Субботино / сильно агрогенно-преобразованная	17,4	1 месяц (2016 г.)	750	21,0±1,0	6,6	66,3±29,5	0,93±0,01
пос. Тура / криогенная	8,8	15 месяцев (2017–2018 гг.)	288[b]	9,5±5,7[b]	5,1	1,9±0,2[c]	0,004±0,001[c]
						2,4±0,3[d]	0,008±0,001[d]

[a] ОМЧ – общее микробное число.
[b] Учитывается за летний период (июнь-август).
[c] Северный склон экспозиции.
[d] Южный склон экспозиции

21 °C и влажности почвы около 50 % (дополнительный полив почвы) активность микробных деполимераз возрастала и П(3ГБ) пленки быстро разрушались – в 1,7–14,7 раза быстрее по сравнению с биодеградацией в естественных условиях в дерново-карбонатных почвах. Становится вполне ожидаемым, что в почвах в районе пос. Тура при низкой среднемесячной температуре в летний период даже в условиях достаточного увлажнения почвы и обеспеченности микроорганизмов азотом ферментативная активность оставалась на низком уровне и убыль массы пленок за два вегетационных сезона была крайне малозначительна – 4–8 мкг·сут$^{-1}$.

Анализ биоразрушения пленок П(3ГБ), проведенный методом главных компонент, показал, что две первые главные компоненты в сумме покрывают 83,8 % дисперсии. Наибольший вклад в первую компоненту вносят переменные убыль массы пленок, температура и количество осадков (табл. 2). Во вторую главную компоненту вносит вклад содержание гумуса в почве и значение pH. Общая численность микроорганизмов (ОМЧ) вносит максимальный вклад в третью компоненту. На графике главных компонент (рис. 1) показано, что проекции почв разного типа распределяются на разных участках графика. Направление стрелки убыли массы образцов П(3ГБ) совпадает с проекцией точек, соответствующих агрогенно-трансформированным почвам. Дерново-карбонатные почвы в районе г. Красноярска формируют общий кластер; зона криогенных почв располагается обособленно. Ряд авторов подтверждают, что тип почвы влияет на деградацию ПГА. Например, в песчаной почве с низкой влажностью и дефицитом органического вещества деградация биополимерных материалов протекает гораздо медленнее, чем в других почвенных тестах, тогда как в полевых почвах разложение ПГА может достигать 100 % (Meereboer et al., 2020).

Скорость ферментативных реакций почвенных микроорганизмов коррелирует с температурой, причем наилучшие показатели деполимеразной активности наблюдаются при оптимальных для микроорганизмов сочетаниях температуры и влажности (Mtibe et al., 2021). Расчет коэффициентов корреляции показал, что убыль массы пленок коррелировала ($p<0,001$) с температурой ($r=0,80$), количеством осадков ($r=0,89$) и содержанием гумуса ($r=0,75$). Корреляция с pH была слабой ($r=0,40$; $p=0,02$). Несмотря на то что деградация образцов П(3ГБ) пленок в почве происходит под действием

Таблица 2. Вклад переменных в главные компоненты

Table 2. Contribution of variables to the principal components

Переменные	Вклад,%			
	Dim.1	Dim.2	Dim.3	Dim.4
pH	7.87	35.43	7.57	8.27
Гумус	13.34	26.48	6.41	5.80
Температура	22.47	9.85	9.81	20.64
Осадки	26.71	5.27	0.20	56.08
ОМЧ	0.07	22.96	70.09	0.19
Убыль массы	29.54	0.004	5.91	9.01

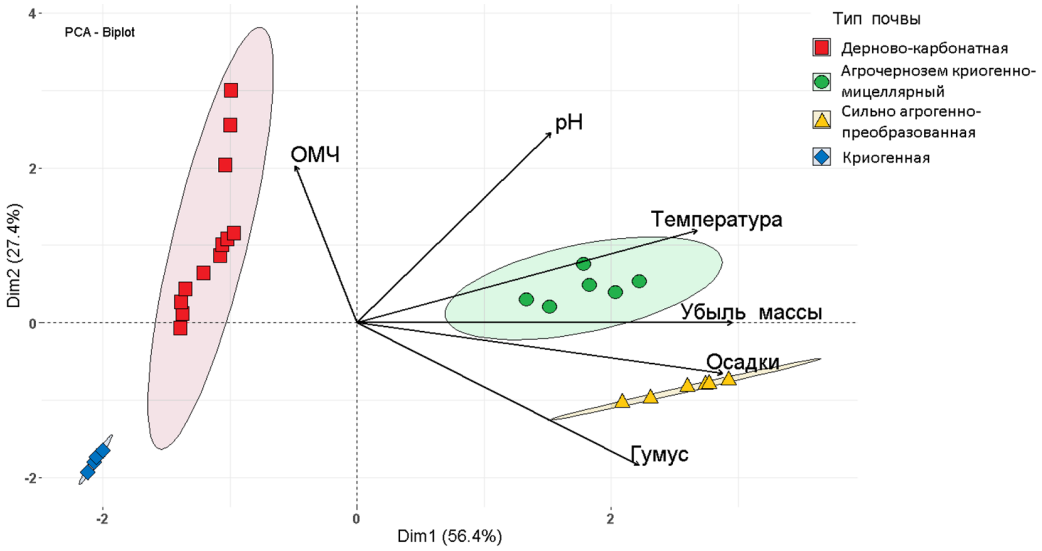

Рис. 1. Анализ физико-химических свойств почвы и убыли массы образцов П(3ГБ) в разных районах Сибири методом главных компонент

Fig. 1. Principal component analysis of soil physical and chemical properties and mass loss of P(3HB)-samples in different soil types in Siberia

микробных ферментов, интенсивность разрушения пленок не показала корреляцию с численностью микроорганизмов (r=0,01; p=0,95). Это указывает на необходимость принимать во внимание не только численность, но и активность микроорганизмов, а также наличие в микробном сообществе первичных деструкторов, продуцирующих ПГА-деполимеразы. Проведенный филогенетический анализ выявил отличия в наборе первичных деструкторов в разных почвах (рис. 2).

Наиболее разнообразным был состав деструкторов в агрогенных почвах, он включал представителей классов *Actinobacteria*, *Bacilli*, *β-Proteobacteria*, *γ-Proteobacteria*. В дерново-карбонатных почвах преобладали протеобактерии и представители рода *Bacillus*. Следует отметить, что видовой состав деструкторов в криогенных почвах также был разнообразным и включал представителей из разных классов. Это указывает на высокий микробный потенциал криогенных почв к биодеградации изделий из П(3ГБ).

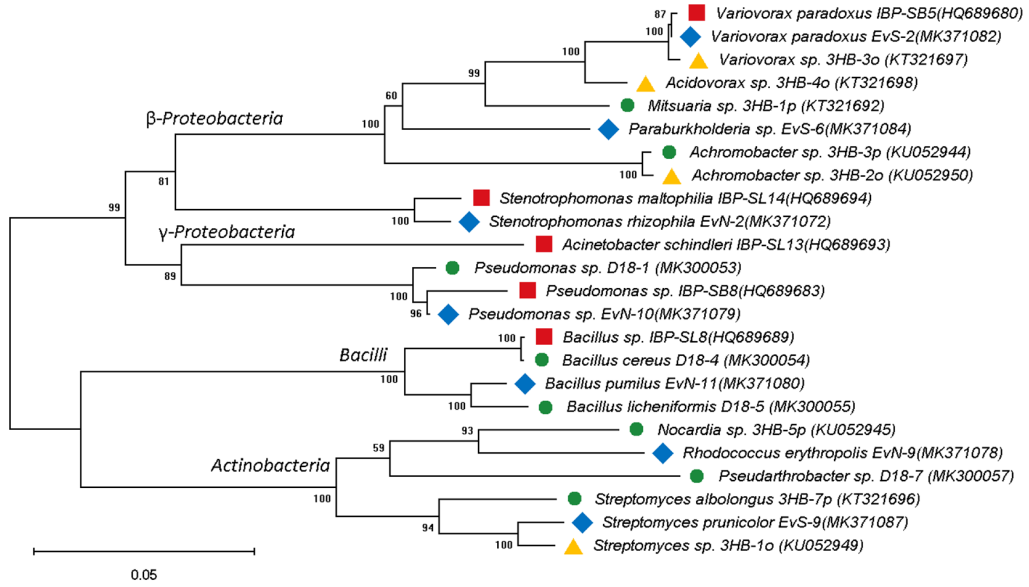

Рис. 2. Филогенетическое дерево, построенное на основе последовательностей 16S рРНК бактерий-деструкторов П(3ГБ), распространенных в разных типах почв в Сибири; масштаб указывает количество замен нуклеотидов на сайт; цифры показывают достоверность ветвления, установленную с помощью бутстреп-анализа; обозначение маркеров для типа почвы как на рис. 1

Fig. 2. Phylogenetic tree based on 16S rRNA sequences of P(3HB)-degrading bacteria common in different types of soils in Siberia; the scale bar indicates the number of nucleotide substitutions per site; the numbers show the branching accuracy determined using bootstrap analysis; markers for soil types as in Fig. 1

Заключение

Результаты исследований показали, что наиболее благоприятные условия для деградации П(3ГБ) складываются в агрогенных почвах, характеризующихся достаточным увлажнением, высокой биогенностью и широким спектром бактерий-деструкторов П(3ГБ). Несмотря на крайне незначительную убыль массы пленок в криогенной почве, таксономическое разнообразие видов, обладающих деполимеразной активностью, указывает на наличие потенциала криогенных почв к биодеградации П(3ГБ).

Список литературы / References

Boyandin A. N., Rudnev V. P., Ivonin V. N., Prudnikova S. V., Korobikhina K. I., Filipenko M. L., Volova T. G., Sinskey A. J. (2012) Biodegradation of polyhydroxyalkanoate films in natural environments. *Macromolecular Symposia*, 320(1): 38–42

Fernandes M., Salvador A., Alves M. M., Vicente A. A. (2020) Factors affecting polyhydroxyalkanoates biodegradation in soil. *Polymer Degradation and Stability*, 182: 109408

Koller M., Mukherjee A. (2020) Polyhydroxyalkanoates-linking properties, applications, and end-of-life options. *Chemical and Biochemical Engineering Quarterly*, 34(3): 115–129

Kumar S., Stecher G., Li M., Knyaz C., Tamura K. (2018) MEGA X: Molecular Evolutionary Genetics Analysis across computing platforms. *Molecular Biology and Evolution*, 35(6): 1547–1549

Meereboer K. W., Misra M., Mohanty A. K. (2020) Review of recent advances in the biodegradability of polyhydroxyalkanoate (PHA) bioplastics and their composites. *Green Chemistry*, 22(17): 5519–5558

Mergaert J., Webb A., Anderson C., Wouters A., Swings J. (1993) Microbial degradation of poly(3-hydroxybutyrate) and poly(3-hydroxybutyrate-co-3-hydroxyvalerate) in soils. *Applied and Environmental Microbiology*, 59(10): 3233–3238

Mtibe A., Motloung M. P., Bandyopadhyay J., Ray S. S. (2021) Synthetic biopolymers and their composites: advantages and limitations – an overview. *Macromolecular Rapid Communications*, 42(15): 2100130

Nandakumar A., Chuah J. A., Sudesh K. (2021) Bioplastics: A boon or bane? *Renewable and Sustainable Energy Reviews*, 147: 111237

Saitou N., Nei M. (1987) The neighbor-joining method: A new method for reconstructing phylogenetic trees. *Molecular Biology and Evolution*, 4(4): 406–425

Journal of Siberian Federal University. Biology 2021 14(4): 541–549
~ ~ ~

DOI 10.17516/1997-1389-0371

УДК 632.93

Global Crop Protection Industry

Oleg N. Shishatskiy*
Institute of Economics and Industrial Engineering SB RAS
Novosibirsk, Russian Federation
Institute of Biophysics SB RAS,
FRC «Krasnoyarsk Science Center SB RAS»
Krasnoyarsk, Russian Federation
Siberian Federal University
Krasnoyarsk, Russian Federation

Received 14.06.2021, received in revised form 23.07.2021, accepted 23.08.2021

Abstract. The problem of the steady food supply to the population is becoming particularly pressing in the face of a projected decrease in the specific area of agricultural land per resident. In an effort to increase crop yields, agriculture depends mainly on chemical plant protection agents (PPAs), which produce strong negative effects. The research activities need to be concentrated on developing the alternative plant protection technologies that will ensure a sufficient crop yield increase. Based on statistical data of the Food and Agriculture Organization of the United Nations (FAO) and studies and analytical reviews on protection of agricultural crops, the present work describes current market trends in the global crop protection industry: the volume and dynamics of the global PPA market, the regional distribution of this market, and the consolidation of key producers. Recent years have seen a decrease in the number of new chemical PPAs entering the market due to the greater research effort devoted to novel crop protection technologies, in particular genetically modified crops (GM crops), biological PPAs, and other alternative technologies, which are being developed and put on the market in response to increasingly stringent regulations in agrochemistry and ecology. Recommendations are made to producers of agrochemicals that will allow them to remain competitive and contribute to satisfaction of the growing demand for agricultural products.

Keywords: pesticides, global markets for plant protection, R & D, new technologies for plant protection.

Acknowledgements. This work was supported by Project «Agropreparations of the new generation: a strategy of construction and realization» (Agreement No 074–02–2018–328) in accordance with

* Corresponding author E-mail address: shishatskiy@mail.ru

Resolution No 220 of the Government of the Russian Federation of April 9, 2010, «On measures designed to attract leading scientists to the Russian institutions of higher learning».

Citation: Shishatskiy O. N. Global crop protection industry. J. Sib. Fed. Univ. Biol., 2021, 14(4), 541–549. DOI: 10.17516/1997-1389-0371

Глобальная индустрия защиты растений

О. Н. Шишацкий
Институт экономики и организации промышленного производства СО РАН
Российская Федерация, Новосибирск
Институт биофизики ФИЦ КНЦ СО РАН
Российская Федерация, Красноярск
Сибирский федеральный университет
Российская Федерация, Красноярск

Аннотация. Проблема устойчивого обеспечения продовольствием населения становится особенно актуальной в условиях прогнозируемого уменьшения удельной площади сельскохозяйственных земель на одного жителя. Для повышения урожайности в растениеводстве широко используются в основном химические средства защиты растений (СЗР), имеющие серьезные негативные эффекты. Перед научным сообществом стоит задача разработать альтернативные технологии защиты растений, которые обеспечат адекватный рост урожайности. На основе статистических данных FAO (Food and Agriculture Organization of the United Nations – Продовольственная и сельскохозяйственная организация Объединенных Наций), публикаций и аналитических обзоров по теме защиты сельскохозяйственных растений в работе описываются текущие рыночные тенденции в глобальной отрасли СЗР: объем и динамика мирового рынка СЗР, региональное распределение объемов этого рынка, консолидация ключевых производителей. Установлено, что в последние годы сократилось число поступающих на рынок новых химических СЗР вследствие того, что более интенсивно стали разрабатываться новые технологии защиты сельскохозяйственных культур, в частности генно-модифицированные культуры, биологические СЗР и другие альтернативные технологии, которые разрабатываются и выводятся на рынок в ответ на все более жесткие нормы регулирования в области агрохимии и экологии. Приведены рекомендации производителям СЗР, которые позволят им оставаться конкурентоспособными и участвовать в удовлетворении растущего спроса на сельскохозяйственную продукцию.

Ключевые слова: пестициды, глобальные рынки средств зашиты растений, НИОКР, новые технологии защиты растений.

Благодарности. Работа выполнена за счет средств мегагранта «Агропрепараты нового поколения: стратегия конструирования и реализация» (Соглашение № 074–02–2018–328) по Постановлению Правительства РФ № 220 от 9 апреля 20210 г. «О мерах по привлечению ведущих ученых в вузы России».

Цитирование: Шишацкий, О.Н. Глобальная индустрия защиты растений / О.Н. Шишацкий // Журн. Сиб. федер. ун-та. Биология, 2021. 14(4). С. 541–549. DOI: 10.17516/1997-1389-0371

Введение

Прогнозируемый дефицит посевных площадей для производства продовольствия, достаточного для пропитания большего количества людей (ожидается, что к 2050 г. численность населения мира достигнет почти 10 млрд человек), определяет необходимость повышения эффективности технологий растениеводства. Предполагается, что решение этой продовольственной проблемы дополнительно осложнит изменение климата, которое угрожает растениеводству в целом. Во всем мире потери урожая в 2050 г. по сравнению с 2000 г., как ожидается, составят 24 % для кукурузы, 11 % для риса, 9 % для картофеля и 3 % для пшеницы (nationalgeographic.com). При современных темпах производства сельскохозяйственной продукции невозможно сохранять баланс спроса и предложения на нее. Для решения этих проблем необходимо применять более эффективные сельскохозяйственные технологии и новые средства защиты растений (СЗР).

Цель работы – анализ текущего состояния мирового рынка СЗР, его динамики и тенденций в области новых технологий защиты растений и выработка конкурентоспособных рекомендаций.

Динамика, ключевые тенденции глобального рынка средств защиты растений

Современный уровень сельскохозяйственного производства невозможен без применения химических СЗР (Oerke, 2006). Мировой рынок СЗР в целом растет, несмотря на локальные периоды снижения (рис. 1). На рис. 2 показано распределение долей региональных рынков СЗР в 1998 и 2018 гг. На Северную Америку в 1998 г. приходилось 26,2 % мирового рынка СЗР; к 2018 г. эта доля снизилась до 16,7 %. Доля Европейского рынка снизилась с 25,9 до 23,4 %, но в рамках этих цифр потеря доли на зрелых рынках ЕС-15 была более значительной. Этот показатель был частично компенсирован за счет роста на рынках более поздних новых членов ЕС.

Доля Азии на мировом рынке увеличилась благодаря развивающимся странам, а доли рынков Японии, Южной Кореи и Австралии снизились. Наиболее значительное увеличение доли приходится на Латинскую Америку. На рис. 3 крупнейшие национальные рынки СЗР отсортированы по величине совокупного годового прироста в местных валютах за 5 лет (с 2013 по 2018 г.). Наибольший рост показали развивающиеся рынки Аргентины, России и Румынии. При этом для зрелых рынков положительные показатели зафиксированы только для Испании, Италии, Австралии, США и Великобритании.

Основная причина того, что на развивающихся рынках наблюдается более значительный рост, заключается в том, что во многих из этих стран СЗР применяются в количестве ниже оптимального уровня, необходимого для достижения полного потенциала урожайности. По мере улучшения экономики этих

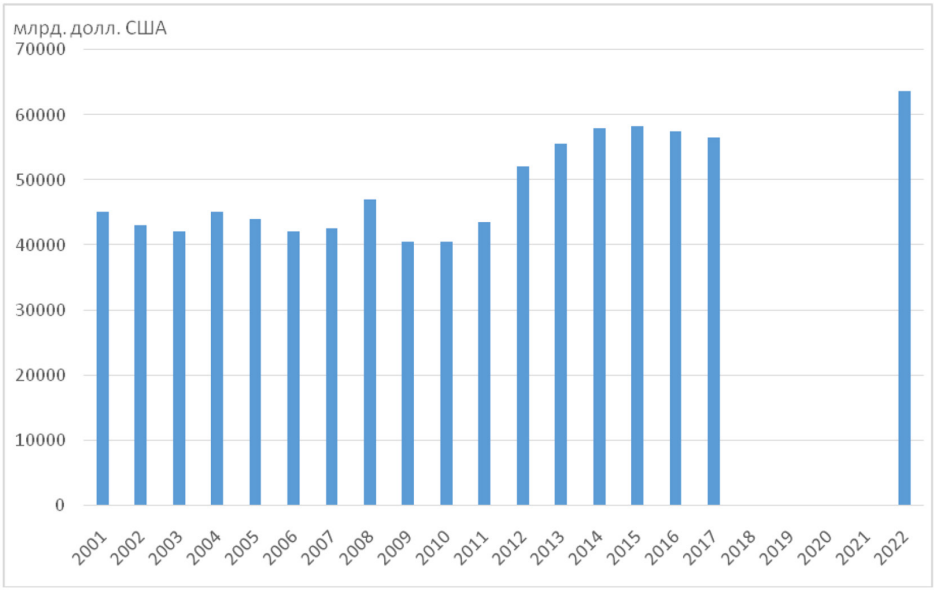

Рис 1. Рынок СЗР: исторические данные 2001–2017 гг. и рыночный прогноз 2022 г. (FAOSTAT; Phillips, 2020)

Fig. 1. 2001–2017 crop protection history and 2022 market forecast (FAOSTAT; Phillips, 2020).

Рис. 2. Распределение рынка СЗР (%) между регионами в 1998 и 2018 гг. (FAOSTAT)

Fig. 2. Crop protection regional market development from 1998 to 2018 (% share) (FAOSTAT)

стран растет объем применений, что приводит к росту рынка. Многие из развивающихся рынков ориентируются на более дешевые химические препараты. На зрелых рынках оптимальные уровни СЗР уже используются и, следовательно, имеется мало возможностей для дальнейшего роста. Эти рынки, как правило, растут только вследствие замены старых препаратов новыми. Защита полезной биоты, человека и окружающей среды в целом от негативного воздействия химических препаратов является ключевой задачей нормативного регулирования в области современной агрохимии. Правила, регулирующие оборот хи-

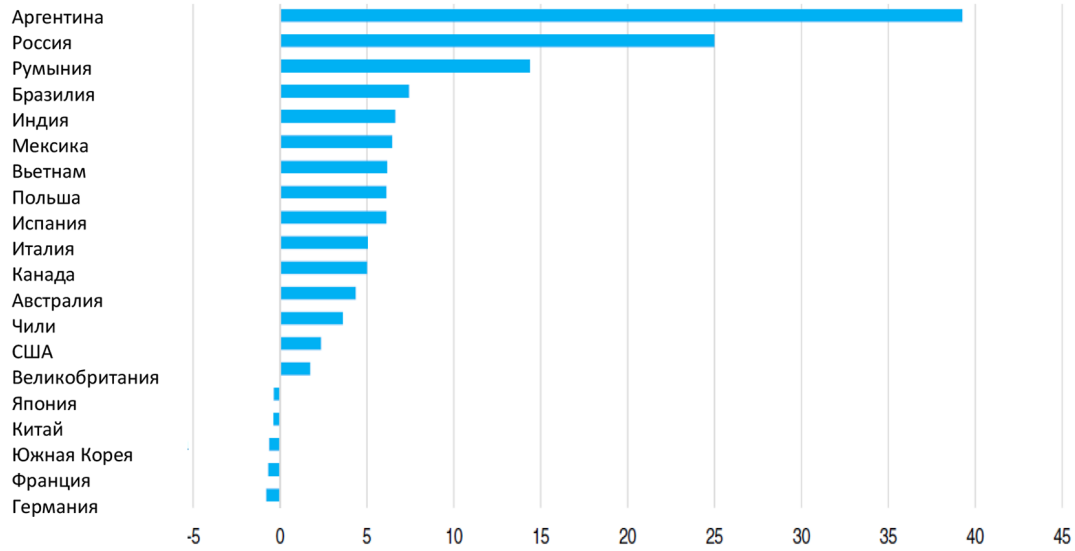

Рис. 3. Топ-20 страновых рынков: процентное изменение рынков СЗР 2018/2013 в локальной валюте (FAOSTAT)

Fig. 3. Top 20 country markets: 2018/2013 local currency change (FAOSTAT)

мических СЗР во многих регионах, включая США и европейские страны, с каждым годом становятся все более строгими. Результат влияния норм регулирования на эволюцию СЗР демонстрируют следующие данные. Если в 1950-х гг. средние нормы внесения химических СЗР составляли 1200, 1700 и 2400 г действующего вещества на гектар (г/га) соответственно для фунгицидов, инсектицидов и гербицидов, то к 2000-м гг. средние нормы внесения этих пестицидов были снижены до 100, 40, и 75 г/га. Эта технологическая эволюция означает, что количество соответствующих действующих веществ, используемых в растениеводстве сегодня, примерно на 95 % ниже, чем в 1950-х гг. (McDougall, 2018). Эти данные демонстрируют значительный прогресс в разработке и выведении на рынок новых и более эффективных химических препаратов для защиты растений. Для разработки и выведения на рынок любого нового препарата обычно необходимо более десяти лет, и это требует значительных затрат на НИР и ОКР, которые оцениваются порядка 100–350 млн долл. США на один препарат. Вероятность доведения нового действующего вещества до регистрации оценивается как одно из примерно 160 тыс. соединений. Таким образом, каждой компании, разрабатывающей новые препараты, приходится ежегодно инвестировать сумму средств эквивалентную 7–10 % от объема своих продаж в НИОКР. К примеру, в 1995 г. расходы на разработку новых препаратов для защиты растений составили 152 млн долл. США, а затраты времени на НИОКР – 8,3 года. Более поздние оценки, согласно опросу 2010–2014 гг., отразили рост показателей до 286 млн долларов США и 11,3 года соответственно (McDougall, 2016).

С середины 2000-х гг. более 50 % совокупного объема рыночных продаж приходится на пять-семь компаний – лидеров в отраслевых сегментах селекции семян и производства агропрепаратов (Fuglie, 2012). В 2013 г. «большая шестерка» компаний контролировала свыше 75 % мирового агрохи-

мического рынка, 63 % рынка семян, а также инвестировала приблизительно 2/3 от общей суммы затрат на исследования и разработки семян и пестицидов. Затраты «большой шестерки» компаний на исследования и разработки в 15 раз превышали бюджет Министерства сельского хозяйства США на проведение аналогичных научных исследований (ETC Group, 2015).

Инновационные разработки в области защиты растений

Анализ публикаций в предметной области позволил выявить прорывные направления разработки новых средств и технологий защиты растений, соответствующие современным требованиям агрохимического регулирования, в которых наиболее активно в настоящее время проводятся научные исследования.

Биологические средства защиты растений

Значимым трендом рынка является рост сегмента СЗР биологического происхождения, которые в отличие от химических средств защиты представляют собой живые объекты или естественные биологически активные соединения, синтезируемые живыми организмами. Преимущества биологических СЗР – высокая длительность действия; отсутствие аккумуляции в растениях; отсутствие привыкания к ним вредителей; обладание способностью расщеплять растительные остатки; повышение иммунитета. Однако биологические СЗР не свободны от недостатков, которые влияют на их рыночный успех. Как правило, они не способны уничтожить популяцию вредителя или патогена полностью, а только снижают их вредоносность; скорость действия биологических СЗР, как правило, ниже химических; биологическая эффективность применения зависит от условий среды (температуры, влажности); их применение требует повторных обработок, которые необходимо повторять часто – из-за дожей, высокой освещенности, колебаний температуры. Размер рынка биологических СЗР пока относительно невелик. В 2016 г. он составлял всего 5,6 % рынка СЗР, показывая скромные продажи отдельных препаратов (Nishimoto, 2019). Согласно отчету маркетингового агентства BCC Research (BCC Research, 2018), мировой рынок биологических СЗР в 2016 г. оценивался в 3,42 млрд долл. США, и по прогнозам, достигнет 14,62 млрд долл. США к 2025 г.

Препараты с медленным и контролируемым высвобождением действующих веществ

Еще одна альтернативная технология защиты растений – это применение препаратов с контролируемым высвобождением действующего вещества. Технология СЗР контролируемого высвобождения: «комбинация биологически активных действующих веществ и наполнителя, обычно полимера, которая позволяет доставлять препарат к мишени с контролируемыми скоростями в течение определенного периода времени» (Rajan et al., 2020). Для контролируемого высвобождения широко используют технику микроинкапсулирования, полимерные микрокапсулы и гидрогели. Основное преимущество СЗР контролируемого высвобождения заключается в том, что они позволяют медленно дозировать действующие вещества, обеспечивая длительность их действия в количествах, необходимых для достижения нужного эффекта, не загрязняя окружающую среду.

Для создания экономически привлекательных СЗР контролируемого высвобождения необходимо решение ряда проблем. Первое, стоимость систем контролируемого

высвобождения обычно высока по сравнению с традиционными химическими препаратами, что обусловлено технологией и материалами, используемыми для их конструирования. Поэтому для крупномасштабного производства СЗР контролируемого высвобождения требуются экономически приемлемые биоразлагаемые в природных условиях материалы. Второе, в настоящее время в основном для разработки СЗР контролируемого высвобождения используют инертные полимеры, которые не являются биоразлагаемыми. Вместо таких материалов следует использовать биоразлагаемые полимеры, поскольку продукты их разложения не только предотвращают загрязнение, но и повышают плодородие почвы и сельскохозяйственных культур, однако ассортимент и доступность таких материалов пока низки. В обзоре маркетингового агентства Market Data Forecast (Market Data Forecast, 2020) показано, что в 2019 г. размер мирового рынка СЗР с контролируемым высвобождением составил порядка 1,83 млрд долл. США. К 2025 г. прогнозируется рост до 2,78 млрд долл. США с ежегодным темпом 7,4 %. Текущая рыночная доля этих продуктов пока составляет менее 3 % от размера рынка химических СЗР (68,6 млрд долл. США (BCC Research, 2020). Согласно материалам исследования маркетингового агентства Market Data Forecast, производством и продажей СЗР контролируемого высвобождения занимаются следующие компании: BASFSE, Bayer AG, The Dow Chemical Company, DuPont, Monsanto Company, Syngenta, ADAMA Agricultural Solutions Ltd, Arysta Life Science Corporation, Sumitomo Chemical Co. Ltd. Это свидетельствует о том, что практически все крупнейшие агрохимические компании вовлечены в продвижение данных инновационных препаратов.

Рекомендации производителям средств защиты растений

За последние 70 лет инновации в агротехнологиях изменили сельскохозяйственный рынок и жизнь миллиардов людей во всем мире. За указанный период в целом глобальная производительность сельского хозяйства более чем удвоилась (Kurth et al., 2020). При этом в последние годы темпы инноваций среди крупных агрохимических компаний, производящих СЗР, значительно замедлились. Некоторые аналитики рынка прогнозируют, что через десять лет только одна из пяти крупнейших агрохимических компаний останется в числе ведущих игроков рынка. Если крупные производители СЗР хотят избежать этой участи, они должны преобразовать свои НИОКР модели сейчас в следующих направлениях:

Первое, ориентироваться на решение реальных проблем клиентов. Компании должны ставить потребности клиентов на первое место, расширить свои портфели продуктов с помощью услуг, которые могут быть адаптированы к индивидуальным потребностям клиентов и которые обеспечивают наглядные положительные результаты. Компании должны выпускать и продвигать продукты, услуги и методы, которые поддерживают устойчивое сельское хозяйство, которые могут еще больше сократить использование химических действующих веществ, и они должны продавать интегрированные пакеты продуктов, предназначенных для конкретных потребностей клиентов. Агрохимическим компаниям следует напрямую взаимодействовать с реальным сектором растениеводства и сотрудничать в разработке новых СЗР и технологий их применения. При этом компаниям необходимо найти правильный баланс между удовлетворением требований индивидуальных заказчиков и необходимостью разработ-

ки продуктов и решений, которые могут быть стандартизированы в рамках широкой клиентской базы для получения максимальной ценности.

Второе, следует сконцентрироваться на разработке решений с наибольшей потенциальной ценностью. Агрохимические компании должны научиться правильно расставлять приоритеты в своих НИОКР, а затем распределять необходимые финансовые и кадровые ресурсы для достижения наиболее выгодных возможностей. Ресурсы НИОКР должны быть сосредоточены на решении самых больших проблем, с которыми сталкиваются растениеводы, а не на сохранении наследия компаний. Это, вероятно, потребует смещения значительных ресурсов от некоторых внутренних ранее популярных программ, в рамках которых больше не разрабатываются новые продукты с высокой ценностью и внесения изменений в действующие механизмы управления НИОКР и процессы принятия решений.

Третье, целесообразно балансировать внутренние НИОКР с внешними инновациями. Крупные агрохимические компании, помимо продолжения своих собственных разработок внутри компании, также должны инвестировать в перспективные молодые компании с помощью специфичных для открытых инноваций моделей финансирования, таких как внутренние подразделения корпоративного венчурного капитала. Для этого потребуется выделение ресурсов, необходимых для эффективного поиска внешних возможностей и новых технологий, а также для быстрого продвижения процессов с тем, чтобы воспользоваться ими. Компаниям следует рассмотреть несколько вариантов: равные партнерские отношения; сделки, ориентированные на помощь небольшим компаниям финансировать свои исследования в конкретных областях; сотрудничать с университетами, государственными учреждениями и неправительственными организациями.

Заключение

На основе анализа текущего состояния мирового рынка СЗР, его динамики и тенденций в области новых технологий защиты растений показано, что глобальный рынок химических СЗР увеличивается, что сопровождается негативным воздействием на нецелевые биообъекты и окружающую среду в целом. Ключевые тенденции глобальной отрасли производства СЗР включают усиливающееся регулирование, рост расходов на НИОКР и борьбу за добавленную стоимость между ведущими компаниями-производителями, что приводит к консолидации крупнейших участников. Параллельно с выпуском традиционных химических пестицидов актуализируется разработка новых средств и технологий защиты растений, включая разработку биопестицидов и биоудобрений, конструирование препаратов нового поколения с медленным и контролируемым высвобождением действующих веществ. Сделан вывод о том, что для обеспечения конкурентоспособности новых средств и технологий защиты растений и удовлетворения растущего спроса на сельскохозяйственную продукцию необходимо ориентироваться на решение реальных проблем потребителей, разрабатывать решения с высокой потенциальной ценностью, балансировать внутренние НИОКР с внешними инновациями.

Список литературы / References

BCC Research (2018) Global biopesticides market. URL: https://www.bccresearch.com/partners/verified-market-research/global-biopesticides-market.html

BCC Research (2020) Global markets for agrochemicals. URL: https://www.bccresearch.com/market-research/chemicals/agrochemicals-global-markets-report.html

ETC Group (2015) Breaking Bad: Big Ag Mega-Mergers in Play Dow + DuPont in the Pocket? Next: Demonsanto? URL: http://www.etcgroup.org/files/files/etc_breakbad_23dec15.pdf

FAOSTAT. Food and agriculture data. URL: https://www.fao.org/faostat/en/#data

Fuglie K., Heisey P., King J., Schimmelpfennig D. (2012) Rising concentration in agricultural input industries influences new farm technologies. URL: https://www.ers.usda.gov/amber-waves/2012/december/rising-concentration-in-agricultural-input-industries-influences-new-technologies/

Kurth T., Möller C., Jerratsch J.-F., Adolphs B., Wübbels G., Walker D. (2020) Reviving agricultural innovation in seeds and crop protection. URL: https://www.bcg.com/publications/2020/reviving-agricultural-innovation-seeds-crop-protection

Market Data Forecast (2020) Slow and controlled release pesticides market. URL: https://www.marketdataforecast.com/market-reports/slow-and-controlled-release-pesticides-market

Nishimoto R. (2019) Global trends in the crop protection industry. *Journal of Pesticide Science*, 44(3–4): 141–147

Nationalgeographic.com. Climate change. How to live with it. Crops. URL: https://www.nationalgeographic.com/climate-change/how-to-live-with-it/crops.html

Oerke E.-C. (2006) Crop losses to pests. *Journal of Agricultural Science*, 144(1): 31–43

Phillips M. W.A. (2020) Agrochemical industry development, trends in R&D and the impact of regulation. *Pest Management Science*, 76(10): 3348–3356

McDougall P. (2016) The cost of new agrochemical product discovery, development and registration in 1995, 2000, 2005–8 and 2010–2014. URL: https://croplife.org/wp-content/uploads/2016/04/Cost-of-CP-report-FINAL.pdf

McDougall P. (2018) Evolution of the crop protection industry since 1960. URL: https://croplife.org/wp-content/uploads/2018/11/Phillips-McDougall-Evolution-of-the-Crop-Protection-Industry-since-1960-FINAL.pdf

Rajan M., Chandran V., Shahena S., Mathew L. (2020) Controlled release pesticides as a route to sustainable crop production. *Controlled release of pesticides for sustainable agriculture*. Rakhimol K. R., Thomas S., VolovaT., Jayachandran K. (eds.) Springer, Cham, p. 111–125

Journal of Siberian Federal University. Biology 2021 14(4): 550–559
~ ~ ~

DOI 10.17516/1997-1389-0372

УДК 615.46.015

A Feasibility Study of New Generation Pesticides Application

Anastasia V. Sharopatova[a, b], Elena A. Bryukhanova[c, d] and Oleg N. Shishatskiy*[b, c, d]
[a]Krasnoyarsk State Agrarian University
Krasnoyarsk, Russian Federation
[b]Institute of Biophysics SB RAS
FRC «Krasnoyarsk Science Center SB RAS»
«Krasnoyarsk Science Center SB RAS»
Krasnoyarsk, Russian Federation
[c] Institute of Economics and Industrial Engineering SB RAS
Novosibirsk, Russian Federation
[d]Siberian Federal University
Krasnoyarsk, Russian Federation

Received 05.08.2021, received in revised form 16.09.2021, accepted 31.10.2021

Abstract. The paper presents the results of a feasibility study of long-term herbicidal and fungicidal preparations deposited with a degradable microbial poly-3-hydroxybutyrate polymer base. Deposited pesticides, tribenuron-methyl and tebuconazole, were introduced into soil simultaneously with seeds of spring wheat Novosibirskaya 15. The control included a pre-sowing treatment of grain with the commercial fungicide «Bunker» and spraying the crops in the tillering phase with the herbicide «Mortira». The feasibility studies have shown that pre-emergence soil application of deposited pesticide preparations ensured cost savings in wheat production of 327.34 roubles per 1 ha, decreased the cost price of the product and increased the profitability of production by 66.1 % as compared with the traditional use of commercial pesticide preparations. Thus, elimination of pre-sowing seed treatment and spraying crops with herbicides during the growing season accompanied by a wheat yield increase resulted in reduced costs of production. Additionally, application of deposited pesticides may reduce the risk of uncontrolled spread and accumulation of xenobiotics in the biosphere.

Keywords: feasibility study, deposited pesticide preparations, field trials, spring wheat crops.

* Corresponding author E-mail address: shishatskiy@mail.ru
ORCID: 0000-0003-0763-974X (Sharopatova A. V.); 0000-0002-0768-4770 (Bryukhanova E. A.)

Acknowledgements. This study was supported by the Project «Agropreparations of new generation: a strategy of construction and realization» (Agreement No 074–02–2018–328) in accordance with Resolution No 220 of the Government of the Russian Federation of April 9, 2010, «On measures to attract leading scientists to Russian institutions of higher education».

Citation: Sharopatova A. V., Bryukhanova E. A., Shishatskiy O. N. A feasibility study of new generation pesticides application. J. Sib. Fed. Univ. Biol., 2021, 14(4), 550–559. DOI: 10.17516/1997-1389-0372

Технико-экономическая оценка эффективности применения пестицидных препаратов нового поколения

А. В. Шаропатова[а, б], Е. А. Брюханова[в, г], О. Н. Шишацкий[б, в, г]

[а]Красноярский государственный аграрный университет
Российская Федерация, Красноярск
[б]Институт биофизики ФИЦ «КНЦ СО РАН»
Российская Федерация, Красноярск
[в]Институт экономики и организации промышленного производства СО РАН
Российская Федерация, Новосибирск
[г]Сибирский федеральный университет
Российская Федерация, Красноярск

Аннотация. Проведен технико-экономический анализ результатов пионерных полевых испытаний долговременных пестицидных препаратов гербицидного и фунгицидного действия, депонированных в полимерную основу с использованием разрушаемого микробного полимера поли-3-гидроксибутирата. Депонированные гербицид трибенурон-метил и фунгицид тебуконазол были внесены в почву одновременно с семенами яровой пшеницы Новосибирская 15. Контролем служило предпосевное протравливание зерна коммерческим фунгицидом «Бункер» и опрыскивание посевов в фазу кущения гербицидом «Мортира». Технико-экономические исследования показали, что довсходовое грунтовое применение депонированных пестицидных препаратов обеспечивает экономию затрат при ее производстве на 327,34 руб. на 1 га и снижение себестоимости продукции, повышая рентабельность производства на 66,1 % по сравнению с традиционным применением коммерческих пестицидных препаратов. Это связано с исключением затрат на операции по протравливанию семян и опрыскиванию растений в период вегетации, а также увеличением урожайности пшеницы. Внедрение в практику депонированных пестицидов направлено на снижение риска неконтролируемого распространения и аккумуляции ксенобиотиков в биосфере.

Ключевые слова: технико-экономический анализ, депонированные пестицидные препараты, полевые испытания, посевы яровой пшеницы.

Благодарности. Работа выполнена за счет средств мега гранта «Агропрепараты нового поколения: стратегия конструирования и реализация» (Соглашение № 074–02–2018–328) по Постановлению Правительства РФ № 220 от 9 апреля 2010 г. «О мерах по привлечению ведущих ученых в вузы России».

Цитирование: Шаропатова, А. В. Технико-экономическая оценка эффективности применения пестицидных препаратов нового поколения / А. В. Шаропатова, Е. А. Брюханова, О. Н. Шишацкий // Журн.Сиб. федер. ун-та. Биология, 2021. 14(4). С. 550–559. DOI: 10.17516/1997-1389-0372

Введение

Необходимость наращивания объемов растениеводства, в первую очередь производства зерновых культур, диктуется ростом населения, для которого зерно является одним из главных источников продуктов питания, а также расширением потребительской базы животноводства и птицеводства, где зерно один из основных компонентов кормов. Современная практика в основном базируется на применении химических средств защиты культивируемых растений, включающем предпосевное протравливание посадочного материала и обработку растений опрыскиванием растворами пестицидов в период вегетации. Интенсивные технологии ведения сельского хозяйства требуют применения огромного количества разнообразных химических веществ для борьбы с вредителями, сорняками и возбудителями болезней культивируемых видов. Масштабы производства и применения пестицидов возрастают во всем мире. Темпы роста объема производства пестицидов составляют 6,9 % в год (http://agropravda.com/news/chimiya-dla-pochvy/1473-mirovoj-rynok-pesticidov-k-2019-g-sostavit-759-mlrd). При этом не более 10 % применяемых и вносимых в окружающую среду пестицидов достигают цели; основная масса этих веществ аккумулируется в биологических объектах, загрязняет почвы, водоемы, вызывает гибель полезных организмов, что нарушает равновесие в природных экосистемах (Hansen et al., 2004; Damalas, Eleftherohorinos, 2011; Mineau, Whiteside, 2013). Химические пестициды не специфичны, вызывают гибель нецелевых организмов, часто токсичны для животных и человека, а также способствуют формированию устойчивых популяций сорняков и фитопатогенов, что приводит к необходимости увеличения кратности обработок и норм расхода препаратов. Указанные обстоятельства и высокая экономическая затратность химической защиты вызывают необходимость разработки экологически безопасных средств и способов их применения для снижения пестицидного пресса на природные экосистемы и окружающую среду в целом.

Новейшим направлением исследований является разработка препаратов нового поколения с контролируемым выходом активного начала за счет использования в качестве матрикса (основы) биоразрушаемых материалов, которые разрушаются в почве под воздействием почвенной микрофлоры до безвредных продуктов и обеспечивают постепенный и длительный выход пестицидов в почву. Преимущества таких форм включают: пролонгированное действие препаратов, что приводит к сокращению количества обработок посевов; продление активности

нестабильных пестицидов; снижение токсичности для биоты и накопления пестицидов в трофических цепях; преобразование жидких форм в твердую, что делает безопасным их применение и облегчает транспортировку (Controlled release of pesticides…, 2020; Nanopesticides…, 2020).

Перспективность новых препаратов для зашиты растений и возможность их практического использования не только определяются биологической эффективностью в сравнении с традиционными средствами и технологиями применения, но в значительной мере зависят от технико-экономических показателей их производства и применения.

Цель настоящей работы – технико-экономическая оценка результатов пионерных полевых испытаний долговременных пестицидных препаратов, депонированных в разрушаемую полимерную основу, которые однократно вносят в почву с семенным материалом, в сравнении с традиционными технологиями защиты сельскохозяйственных культур.

Материалы и методы

Технико-экономический анализ выполнен по результатам полевых испытаний (вегетационный сезон 2020 г.) согласно нормативной документации (Миньков, 2014; Марченко и др., 2016; Руководство по проведению…, 2018). Полевые испытания включали пестицидные средства в двух формах – свободные коммерческие препараты (контроль) и экспериментальные формы в виде гранул, депонированные в основу из разрушаемого поли-3-гидроксибутирата, синтезированного согласно (Патент РФ № 2439143) по разработанной и запатентованной технологии (Патент РФ № 2733295).

Испытаны разработанные формы системного гербицида трибенурон-метил (ТРИБ) и системного фунгицида тебуконазол (ТЭБ), который испытывали в комплексе с гербицидом в (ТРИБ+ТЭБ); пестициды произведены в Китае (фирма Xi'anTai Cheng Chem Co., Ltd). В контроле использовали коммерческие аналоги (гербицидный препарат «Мортира» и фунгицидный препарат «Бункер», производство фирмы «Август», Россия). Полевые испытания проведены в пригороде Красноярска на базе учебного хозяйства «Миндерлинское» ФГБОУ ВО «Красноярский государственный аграрный университет» на яровой пшенице сорта Новосибирская 15. В экспериментальных группах депонированные пестициды вносили в подготовленную и охарактеризованную почву однократно, одновременно с семенами пшеницы. В контроле посевной материал за сутки до посева был протравлен раствором препарата «Бункер»; посевы пшеницы в фазу кущения были обработаны раствором гербицидного препарата «Мортира».

Результаты и обсуждение

Технико-экономический анализ включал: технологические карты структуры затрат при производстве пшеницы в зависимости от формы и способа применения пестицидных препаратов; характеристику затрат на производственные операции при производстве пшеницы с использованием коммерческих и депонированных препаратов; показатели экономической эффективности применения депонированных пестицидных препаратов.

Технологические карты структуры затрат при производстве пшеницы в зависимости от формы и способа применения пестицидных препаратов

Определение экономической эффективности применения депонированных пестицидных препаратов включает сравнение

производственных затрат по всем технологическим операциям, используемым при производстве зерновых культур в агросекторе РФ. Расчет экономической эффективности базируется на определении материальных и производственных затрат на единицу площади и единицу сельскохозяйственной продукции, сравнение урожайности и себестоимости полученной продукции, рентабельности. Производственные затраты при возделывании испытуемых сельскохозяйственных культур определены по составленным технологическим картам, которые включают прямые затраты, состоящие из затрат на основную обработку почвы, предпосевную обработку (культивация, обработка семян, посев), применения химикатов в течение вегетации, уборку урожая.

Для расчета технологических карт по производству зерна пшеницы в качестве показателя взята посевная площадь в 1 га и данные по урожайности, полученные в полевых испытаниях (табл. 1). Основными статьями затрат при производстве продукции растениеводства являются оплата труда с отчислениями на социальные нужды, материальные затраты, в том числе затраты на семена, горюче-смазочные материалы, химические средства защиты растений, электроэнергию и др., амортизация, затраты на текущий ремонт сельхозтехники и прочие затраты, включающие общепроизводственные и общехозяйственные расходы. Исходя из составленных технологических карт по возделыванию зерновых культур в табл. 2 приведены производственные затраты и себестоимость произведенной продукции. Наибольшие затраты при производстве пшеницы имели место в положительном контроле (в варианте с протравливанием семян препаратом «Бункер» и опрыскиванием посевов препаратом «Мортира») – 13013,32 руб. на 1 га. Самые низкие затраты получены в экспериментальном варианте при использовании гранул ТРИБ – 12482,11 руб. Самая низкая себестоимость зерна пшеницы получена в экспериментальном варианте, в котором получена самая высокая урожайность пшеницы при использовании комплексных гранул. Экономия затрат в экспериментальных группах относительно контролей составила от 180,92 до 327,43 руб. на 1 га.

Характеристика затрат на производственные операции при производстве пшеницы с использованием коммерческих и депонированных пестицидных препаратов

Определены затраты на 1 га посевов яровой пшеницы Новосибирская 15 (табл. 3). Расчет эксплуатационных затрат по выращиванию пшеницы произведен по каждой от-

Таблица 1. Урожайность яровой пшеницы Новосибирская 15 при различных формах и способах применения пестицидов в условиях полевых испытаний

Table 1. Yield of spring wheat Novosibirskaya 15 under different regimens of pesticide treatment in field trials

Вариант	Урожайность, ц/га
Контроль (опрыскивание посевов гербицидом «Мортира» в фазе кущения)	32,5±0,5
Контроль (протравливание семян фунгицидом «Бункер» и опрыскивание посевов гербицидом «Мортира» в фазе кущения)	31,1±0,4
Эксперимент (внесение гранул ТРИБ в почву при посеве)	33,6±0,5
Эксперимент (внесение гранул ТРИБ+ТЭБ в почву при посеве)	42,3±0,5

Таблица 2. Состав основных статей затрат на выращивание пшеницы и себестоимость 1 ц зерна, руб., при различных формах и способах применения пестицидов

Table 2. Main cost items for wheat production and cost price of 1 centner of grain under different regimens of pesticide application, roubles

Статьи затрат	Вариант			
	Контроль (опрыскивание посевов гербицидом «Мортира»)	Контроль (протравливание семян фунгицидом «Бункер» и опрыскивание посевов гербицидом «Мортира»)	Эксперимент (внесение гранул ТРИБ при посеве)	Эксперимент (внесение гранул ТРИБ+ТЭБ при посеве)
1. Оплата труда с отчислениями на социальные нужды	2104,3	2151,7	1880,6	1898,5
2. Материальные затраты – всего	4810,8	4888,0	4797,2	4922,8
в т. ч. семена	1350,0	1350,0	1350,0	1350,0
горюче-смазочные материалы	2211,3	2211,3	2120,5	2120,5
химические средства защиты растений (семенного материала)	280,0	362,8	-	-
электроэнергия	5,2	6,2	5,4	6,8
автотранспорт	161,1	154,5	166,4	207,8
вода на производственные нужды	3,2	3,3	-	-
мелкий инвентарь	800,0	800,0	800,0	800,0
депонированные пестицидные препараты	-	-	355,0	437,8
3. Амортизация	1549,4	1558,4	1524,9	1533,0
4. Текущий ремонт	1681,5	1688,1	1662,2	1666,2
5. Прочие затраты	772,7	783,1	761,8	776,0
6. Общепроизводственные и общехозяйственные расходы (20 %)	1913,7	1943,9	1855,3	1889,3
Всего затрат на 1 га посева пшеницы	12832,4	13013,3	12482,1	12685,9
Себестоимость 1 ц зерна	394,8	418,4	371,5	299,9

дельной технологической операции. Общая сумма эксплуатационных затрат на технологическую операцию «посев» в расчете на 1 га во всех вариантах исходя из вышеприведенных расчетов составила 901,18 руб. Эксплуатационные расходы на выполнение технологической операции «опрыскивание посевов гербицидами» в контрольном варианте равнялись 572,13 руб.

Стоимость депонированных форм пестицидов зависит от стоимости полимера (ПЗГБ), которая, в свою очередь, зависит от технологии синтеза, типа субстрата, степени очистки полимера и др. В приведенных расчетах использованы данные анализа мировых рынков. Для расчетов приняты данные по стоимости технического полимера (95 % чистоты) в 60 руб./кг (https://russian.alibaba.

Таблица 3. Структура затрат при возделывании пшеницы по основным технологическим операциям (руб. на 1 га) при различных формах и способах применения пестицидов

Table 3. Costs structure in wheat production under different regimens of pesticide application, roubles per 1 ha

Статьи затрат	Посев	Протравливание семян фунгицидом «Бункер»	Опрыскивание посевов гербицидом «Мортира»	Итого по трем операциям	Посев с одновременным внесением гранул	
					Гранулы ТРИБ	Гранулы ТРИБ+ТЭБ
1. Основная и дополнительная заработная плата с отчислениями на социальные нужды	272,85	39,33	165,15	477,33	272,85	272,85
2. Амортизация	146,21	10,38	11,65	168,24	146,21	146,21
3. Текущий ремонт агрегата	150,19	7,26	10,00	167,45	150,19	150,19
4. Горюче-смазочные материалы	289,02	-	74,86	363,88	289,02	289,02
5. Электроэнергия	-	1,26	-	1,26	-	-
6. Химикаты	-	82,83	283,23	366,06	355,00	437,80
7. Прочие прямые расходы	42,91	7,05	27,24	77,20	42,91	42,91
Всего затрат	901,18	148,11	572,13	1621,42	1256,18	1338,98

com/product-detail/polyhydroxyalkanoates-pha-resin-pha-granule-fully-biodegradable-materials-pha-60407456188). Расход полимера в составе гранулированных пестицидов составил 1,25 кг/га, стоимость соответственно: гранулы ТРИБ 355 руб./га; комплексные гранулы ТРИБ+ТЭБ 437,8 руб./га. Эксплуатационные затраты на операцию «посев» с одновременным внесением гранул ТРИБ в экспериментальной группе составили 1256,18 руб.; комплексных гранул ТРИБ+ТЭБ – 1338,98 руб.

Сопоставление затрат при двух исследованных способах химической защиты посевов пшеницы с применением коммерческих и экспериментальных форм пестицидов дано в табл. 3. Эксплуатационные затраты при выращивании пшеницы с учетом технологических операций «посев» и «протравливание семенного материала» в сумме равны 1049,29 руб. При применении операций по уходу за посевами (подвоз воды, приготовление раствора для опрыскивания и опрыскивание посевов гербицидами) общая сумма эксплуатационных затрат на 1 га составила 1621,42 руб. Таким образом, при использовании технологии химической защиты посевов пшеницы с применением депонированных пестицидных препаратов в сравнении с традиционными технологиями затраты сокращаются с 1621,42 до 1256,18 руб./га или 1338,98 руб./га в зависимости от состава гранул, соответственно, с одним гербицидным препаратом или в комплексе гербицид+фунгицид. Посев с одновременным внесением в почву депонированных пестицидов вместе с семенным материалом экономически выгоден, так как при этом происходит сокращение эксплуатационных затрат с 11,8 до 9,4 % по сравнению с затратами при осуществлении комплекса работ по посе-

ву, протравливанию семян и опрыскиванию посевов гербицидами.

Показатели экономической эффективности применения депонированных пестицидных препаратов

Для оценки экономической эффективности депонированных пестицидных препаратов произведен расчет экономических показателей производства продукции, включающий урожайность сельскохозяйственной культуры по обычной (общепринятой) и экспериментальной технологии химической защиты посевов яровой пшеницы с учетом: определения производственных затрат на единицу площади (1 гектар) и на себестоимость 1 ц произведенной продукции; полученной прибыли на 1 га и 1 ц продукции; уровня рентабельности производства продукции рассматриваемой сельскохозяйственной культуры.

Показатели экономической эффективности производства зерна пшеницы по традиционной и экспериментальной технологиям даны в табл. 4. Несмотря на то что в экспериментальном варианте с применением комплексных пестицидных препаратов в виде гранул их стоимость выше по сравнению с гранулами, содержащими только один гербицид, себестоимость 1 ц пшеницы в этом варианте снижена на 19,3 % с учетом полученной более высокой урожайности пшеницы.

Таблица 4. Показатели экономической эффективности производства зерна пшеницы при различных формах и способах применения пестицидов

Table 4. Indicators of economic efficiency of wheat grain production under different regimens of pesticide application

Показатели	Варианты			
	Контроль (опрыскивание посевов гербицидом «Мортира»)	Контроль (протравливание семян фунгицидом «Бункер» и опрыскивание посевов гербицидом «Мортира»)	Эксперимент	
			Внесение гранул ТРИБ при посеве	Внесение гранул ТРИБ + ТЭБ при посеве
Посевная площадь пшеницы, га	1,0	1,0	1,0	1,0
Урожайность пшеницы, ц с 1 га	32,5	31,1	33,6	42,3
Затраты средств на 1 га посева пшеницы, руб.	12832,40	13013,32	12482,11	12685,89
Себестоимость производства 1 ц зерна, руб.	394,8	418,4	371,5	299,9
Средняя цена реализации 1 ц зерна, руб.	700,0	700,0	700,0	700,0
Прибыль на 1 ц зерна, руб.	305,2	281,6	328,5	400,1
Доход на 1 га посева пшеницы, руб.	22750,0	21770,0	23520,0	29610,0
Получено прибыли на 1 га зерна, руб.	9919,00	8757,76	11037,60	16924,23
Уровень рентабельности производства пшеницы,%	77,3	67,3	88,4	133,4

В целом полученная прибыль на 1 ц зерна пшеницы и на 1 га посева пшеницы по данному варианту составила соответственно 400,1 и 16924,23 руб. при уровне рентабельности производства пшеницы 133,4 %. Это выше уровня рентабельности при производстве продукции в контрольном варианте с коммерческими препаратами и также при использовании гранул только с одним гербицидом. Таким образом, применение технологии выращивания пшеницы с использованием депонированных пестицидных препаратов, в особенности при комплексном содержании в них гербицида и фунгицида, является наиболее эффективным по сравнению с традиционными технологиями, а также технологией, при которой применяют гранулы только с одним гербицидом.

Заключение

Выполненные технико-экономические исследования показали, что довсходовое грунтовое применение депонированных пестицидных препаратов за счет исключения затрат на операции по протравливанию семян и опрыскиванию растений в период вегетации, сопровождающееся увеличением урожайности культуры яровой пшеницы сорта Новосибирская 15, обеспечивает экономию затрат при производстве пшеницы на 327,34 руб. на 1 га. Это снижает себестоимость продукции и повышает рентабельность производства пшеницы на 66,1 % по сравнению с применением коммерческих пестицидных препаратов по традиционным технологиям.

Список литературы / References

Марченко А. В., Меньщикова А. Ф., Светлакова Т. В., Юшкова М. К. (2016) *Методические рекомендации по разработке организационно-технологических карт в растениеводстве: методические рекомендации*. Пермь, ФГБОУ ВО Пермская ГСХА, 75 с. [Marchenko A. V., Men'shchikova A.F., Svetlakova T. V., Yushkova M. K. (2016) *Methodological recommendations for the development of organizational and technological maps in plant growing: methodological recommendations*. Perm, Perm State Agricultural Academy, 75 p.]

Миньков С. Л. (2014) *Технико-экономическое обоснование выполнения проекта: методическое пособие*. Томск, ТУСУР, 30 с. [Min'kov S.L. (2014) *Feasibility study of the project: methodological guide*. Tomsk, Tomsk State University of Control Systems and Radioelectronics, 30 p.]

Патент РФ на изобретение № 2439143 «Штамм бактерий ВКПМ B-10646 – продуцент полигидроксиалканоатов и способ их получения» (авторы Волова Т. Г. и Шишацкая Е.И) [Patent RU2439143 «Strain of bacteria *Cupriavidus eutrophus* VKPM B-10646 – producer of polyhydroxylcanoates and method for producing them» (Authors: Volova T. G., Shishatskaya E. I.)]

Патент РФ на изобретение № 2733295 «Пестицидное средство длительного действия для грунтового применения» (авторы Волова Т. Г., Барановский С. В., Демиденко А. В. и др.) [Patent RU2733295 «Long-acting pesticide agent for soil application» (Authors: Volova T. G., Demidenko A. V., Baranovsky S. V., et al.)]

Руководство по проведению регистрационных испытаний агрохимикатов в сельском хозяйстве: производственно-практическое издание (2018) Москва, ФГБНУ «Росинформагротех», 220 с. [*Guidelines for conducting registration tests of agrochemicals in agriculture: production and practical edition* (2018) Moscow, Rosinformagrotekh, 220 p.]

Controlled release of pesticides for sustainable agriculture (2020) Rakhimol K. R., Thomas S., Volova T., Jayachandran K. (eds.) Springer, Cham, 266 p.

Damalas C. A., Eleftherohorinos I. G. (2011) Pesticide exposure, safety issues, and risk assessment indicators. *International Journal of Environmental Research and Public Health*, 8(5): 1402–1419

Hansen L. J., Schwacke L. H., Mitchum G. B., Hohn A. A., Wells R. S., Zolman E. S., Fair P. A. (2004) Geographic variation in polychorinated biphenyl and organochlorine pesticide concentrations in the blubber of bottlenose dolphins from the US Atlantic coast. *Science of the Total Environment*, 319(1–3): 147–172

Mineau P., Whiteside M. (2013) Pesticide acute toxicity is a better correlate of US grassland bird declines than agricultural intensification. *PLoS One*, 8(2): e57457

Nanopesticides. From research and development to mechanisms of action and sustainable use in agriculture (2020) Fraceto L. F., de Castro V. L.S.S., Grillo R., Ávila D., Oliveira H. C., Lima R. (eds.) Springer, Cham, 360 p.